DEVELOPMENT OF DESIGN AND ANALYSIS METHOD FOR SLOPE STABILIZATION USING DRILLED SHAFTS

A Dissertation

Presented to

The Graduate Faculty of The University of Akron

In Partial Fulfillment

of the Requirements for the Degree

Doctor of Philosophy

Wassel Al Bodour

May, 2010

DEVELOPMENT OF DESIGN AND ANALYSIS METHOD FOR SLOPE STABILIZATION USING DRILLED SHAFTS

Wassel Al Bodour

Dissertation

Approved:

_____
Advisor
Dr. Robert Liang

_____
Committee Member
Dr. Craig Menzemer

_____
Committee Member
Dr. Ala Abbas

_____
Committee Member
Dr. Zhenhai Xia

_____
Committee Member
Dr. Kevin Kreider

Accepted:

_____
Department Chair
Dr. Wieslaw Binienda

_____
Dean of the College
Dr. George K. Haritos

_____
Dean of the Graduate School
Dr. George R. Newkome

_____
Date

ABSTRACT

A practical methodology for stability analysis and design of drilled shafts reinforced slopes was developed utilizing limiting equilibrium method of slices. Complex soil stratifications and general failure slip surfaces can be handled in the developed method. The effect of soil arching due to the presence of the drilled shafts was accounted for by using a load transfer factor. The numerical values of the load transfer factor were developed based on 3-D FEM parametric study results. Many of the design variables controlling the slope/shaft systems, such: drilled shafts size, shafts location, and the required spacing between the drilled shafts can be successfully determined from the developed method. The optimum location can be searched for and determined from the developed methodology. The global factor of safety for slope/shaft systems and the forces acting on the stabilizing drilled shafts due to the moving ground can be successfully estimated.

For the purpose of verifying the validity of the proposed design methodology, the results of a field load testing program on the fully instrumented drilled shafts installed on an existing failed slope together with the companion 3-D FEM simulations are presented. This real case was analyzed using the proposed analysis and design methodology, the analysis results were compared with the FEM results, and it is found that they are in good agreement.

In addition, Real-time instrumentation and monitoring were carried out for three landslide sites in the Southern part of Ohio. Various types of instruments were extensively installed inside the stabilizing shafts and the surrounding soils to monitor and better understand the behavior of slope/shaft systems. The field instrumentation and monitoring processes have provided excellent and unique information on the lateral responses of shafts undergoing slope movements. Also, the results of the instrumented cases have provided that the structural design (moments, shear, lateral deflection, and shaft tip fixity) of the shafts are overestimated (i.e., estimated forces acting on the shafts are high), and the geotechnical design (FS of slope/shaft system: movement and rate of movement) is achieved.

DEDICATION

To my parents

To my sisters and brothers

To my Uncle Shawkat

To my wife to be

To anyone who would read, improve, or add to this work

ACKNOWLEDGEMENTS

All thanks and praise is due to ALLAH (SWT), without ALLAH's help nothing could have ever been accomplished or come to existence.

I would like to thank my graduate advisor, Professor Robert Liang whose guidance, support, and patience, have allowed me to finish this work.

Also, I would like to thank my committee members: Dr. Ala Abbas, Dr. Craig Menzemer, Dr. Xia Zhenhe, and Dr. Keven Kreider for their insight, valuable suggestions, and time. I would also like to acknowledge the support I received from the personnel in our Department, particularly the department chair Dr. Wieslaw Binienda, Mrs. Kimberly Stone, Mrs. Christina and Ms. Jacelyn Lombardi.

I must also acknowledge my former advisor Professor Abdallah Malkawi for his guidance and valuable ideas, I am very grateful to have such a teacher and advisor.

There is a special group of friends and colleagues who have provided me with support, encouragement, valuable help and understanding without which I would have not made it past the first year of my graduate school. It's my pleasure to convey my gratitude and thanks to all of them, namely, Dr. Samer Rababa'h, Dr. Madhar Taamneh, Dr. Mohammad Khasawneh, Dr. Firas Hassan, Dr. Muhammad Yamin, Khalid Mustafa, Ayman Ali, and Osamah Alkhateeb.

Also, I would like to acknowledge Dr. Jamal Nusairat for his great ideas, fruitful suggestions, and his assistance in my field work.This work would have not been possible without the financial support provided by the Ohio Department of Transportation over the past years. Special thanks must go to Chris Merklin who has been very helpful and generous.

Finally, I am grateful to my parents, sisters, and brother who, although thousands of miles away, were always able to provide the emotional support and inspiration when needed.

TABLE OF CONTENTS

LIST OF TABLES

LIST OF FIGURES

CHAPTER I

INTRODUCTION

1.1 Overview

An increased popularity of using drilled shafts to stabilize an unstable slope in highway applications could be attributed to several factors: (1) various construction techniques are available for installing drilled shafts in almost any type of soil and rock conditions; (2) lateral load test can be performed to verify the lateral load-resistance capacity of the drilled shafts; (3) the use of drilled shafts avoids the need to address the right-of-way issues that may be needed for other types of slope stabilization methods; (4) the drilled shafts offer a reliable and economical solution compared to other slope stabilization methods; and (5) the drilled shafts are typically structurally capable of resisting long-term environmental effects. The most fundamental causes of slope instability are reduction of shear strength of the soil and increase in driving shear stresses. Installing a row of drilled shafts in a slope reduces the shear stresses required for equilibrium (i.e., driving shear stresses), which in turn, leads to satisfactory stabilization of a slope. There have been numerous documents in the literature regarding the successful utilization of drilled shafts to stabilize a slope (e.g., Fukumoto, 1972 and 1973; Sommer, 1977; Ito et al., 1981 and 1982; Nethero, 1982; Morgenstern, 1982; Gudehus

and Schwarz, 1985; Reese et al., 1992; Rollins and Rollins, 1992; Poulos, 1995 and 1999; Zeng and Liang, 2002; Christopher et al. 2007). Despite an increased usage of drilled shafts for slope stabilization in recent years, there still is a lack of coherent and widely accepted design method that could provide both safe and economic design outcomes.

1.2 Statement of the Problem

Landslide stabilization methods are varied and dependent upon specific site situation. Installing drilled shafts in a moving soil mass is considered one of the effective and reliable techniques in landslide stabilization. Arresting an unstable slope movements using a single row of spaced and rock-socketed drilled shafts as shown in Figure 1.1 requires the geotechnical and structural engineers to determine the following important key design parameters: (1) drilled shafts diameter; (2) spacing between the drilled shafts to ensure development of soil arching; (3) the necessary socket length of the drilled shafts in the non-yielding strata (e.g., rock layer) so that the shafts act as a relatively stable structural member against the moving soil; (4) location of the drilled shafts within the slope body so that the global factor of safety of the stabilized slope is optimized for the most economical configuration of the drilled shafts; (5) the forces imparted on the drilled shafts due to sliding mass so that structural design of drilled shafts can be performed to meet the capacity requirements. However, the existing available methods that deal with drilled shafts stabilized slopes do not provide enough information on how to stabilize landslides using drilled shafts especially because of the many idealized assumptions

made by several investigators trying to overcome the complexity and difficulties encountered. In addition, these idealized and simplifying assumptions have sometimes led to over designing the drilled shafts stabilized slopes with respect to geotechnical and structural aspects, which in turn, would increase the construction cost associated with the landslide repair. For these reasons, there is a compelling need to (a) develop a well defined and sensible design methodology that allows the geotechnical and structural engineers perform a complete design for landslide stabilization using a single row of spaced rock-socketed drilled shafts; (b) conduct instrumentation and monitoring on the performance of drilled shafts stabilized landslide repair projects to gain real cases for assessing the validity of the developed design method, and (c) develop a user friendly computer program, based on both theoretical findings and field monitoring results, for application by geotechnical and structural engineers.

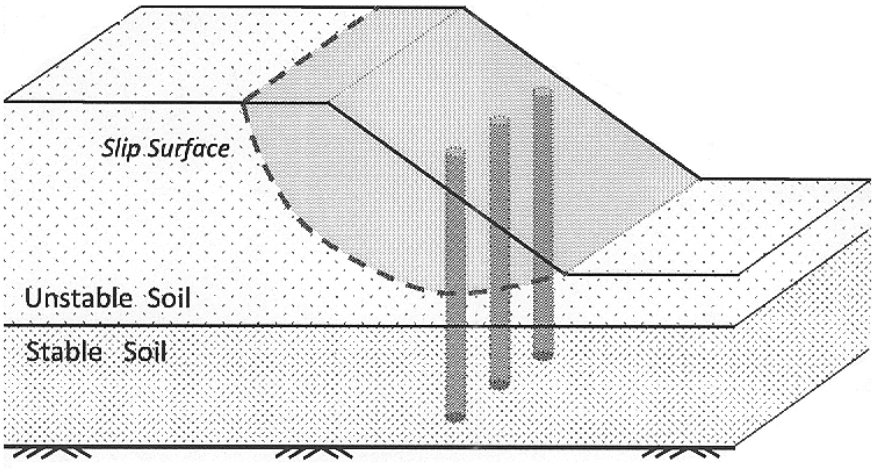

Figure 1.1: Statement of the problem

1.3 Objectives

The main objective of this research study is to verify and refine a previously developed design and analysis method and the accompanied computer program for the design of a row of drilled shafts to stabilize unstable slopes, in particular for highway related applications. Specific objectives are enumerated as follows:

- Plan and carry out field instrumentation and long-term monitoring program at ODOT landslide stabilization project sites to collect long-term field data on the structural responses (i.e., forces, bending moments, and deflections) of the drilled shafts, and the earth forces thrusting upon the drilled shafts, and ground movements
- Use the gathered field data and perform additional 3-D finite element modeling studies to verify and/or to refine (if necessary) the previous method documented in Liang (2002)
- Update and modify the PC based computer program to ensure accuracy, robustness, and user-friendliness for use by ODOT geotechnical and structural engineers
- Develop the final dissertation to provide detailed documentation of the following: (a) field monitoring data, (b) finite element based numerical study results, (c) the developed design method, and (d) the verification study results.

The design method should address the following two essential design issues

a) Geotechnical Design Issues: The geotechnical design requirements are considered to be satisfied when the global factor of safety for the repaired new slope/shaft system is met with the target factor of safety. In other words, the design entails evaluating the enhancement in the stability of the slope when a row of drilled shafts are installed with specific drilled shafts design configurations. Usually, a target factor of safety is determined based on the importance of the site, potential impact of slope failure on the adjacent properties, and the budget available for landslide repair.

b) Structural Design Issues: Structurally, the installed drilled shafts will start to act similar to cantilever beams if drilled shafts fixity was provided; therefore, shafts will require steel reinforcement in order to resist the shear and bending stresses developed in the shafts due to lateral earth pressures acting on the shafts. For that reason, the forces imparted on the drilled shafts need to be determined. After determination of shaft forces (i.e., shear forces and bending moments) and based on drilled shafts configurations and the surrounding soil materials; the shaft section is designed structurally to withstand these forces and prevent any excessive movement.

1.4 General Work Plan

The general framework to accomplish these stated objectives will consist of the following aspects of work: (a) three-dimensional finite element analysis to understand and quantify arching effects in a drilled shaft/slope system, (b) the general procedure of limiting equilibrium approach which incorporated the drilled shafts induced arching

effects in its formulation, and (c) the use of instrumentation and monitoring techniques for validation purpose of actual ODOT landslide repair projects.

On the theoretical side, three-dimensional finite element modeling using the strength reduction method will be conducted to simulate the real situation in the field (i.e., to give an idea on how the lateral earth pressures are transferred between soil and drilled shafts due to soil movement and arching phenomenon). This three-dimensional finite element simulation would contribute to the development of the design method for landslide stabilization using drilled shafts by considering the following aspects: (1) three-dimensional state of stresses (i.e., a real situation) rather than two-dimensional plane strain conditions; (2) the effects of drilled shaft modulus, total length, and location within the slope; (3) the effects of rock modulus and drilled shaft rock socket length; (4) the effects of the depth of slip surface in the slope; (5) the effects of soil cohesion and friction angle; (6) the effects of a composite slip surface other than simple circular or log spiral type of slip surface. In this research, the three-dimensional finite element modeling considers the elastic behavior of drilled shafts, the nonlinear elastic-perfectly plastic behavior of soils, and the elastic behavior of the firm rock where the drilled shafts will be socketed into (i.e., rock layer). Frictional interactions are considered among the three medium: soil, rock, and the drilled shaft. These finite element simulations provide much needed understanding and insight on the behavior of drilled shafts stabilized slopes. The finite element simulation results also provide numerous cases for validating the limiting equilibrium based analysis method.

A limiting equilibrium based analysis algorithm for a drilled shaft/slope system, incorporating the arching induced load transfer effects, will be formulated to provide

necessary tools for geotechnical and structural engineers to perform design tasks. This algorithm will be coded into a new PC based computer program UA SLOPE 2.0 for easy uses by practicing engineers.

A total of three ODOT landslide repair project sites where drilled shafts were used to stabilize the re-construct slope on highways will be instrumented and monitored. In addition, a special load testing program will be carried out to conduct surcharge loading on the constructed drilled shafts at the failed slope site to exam the performance of the drilled shafts and the slope movement at the load test site. These field testing programs will provide important field data for helping refine and validate the developed design method. Figure 1.2 illustrates the general work plan to achieve the stated objectives of this research.

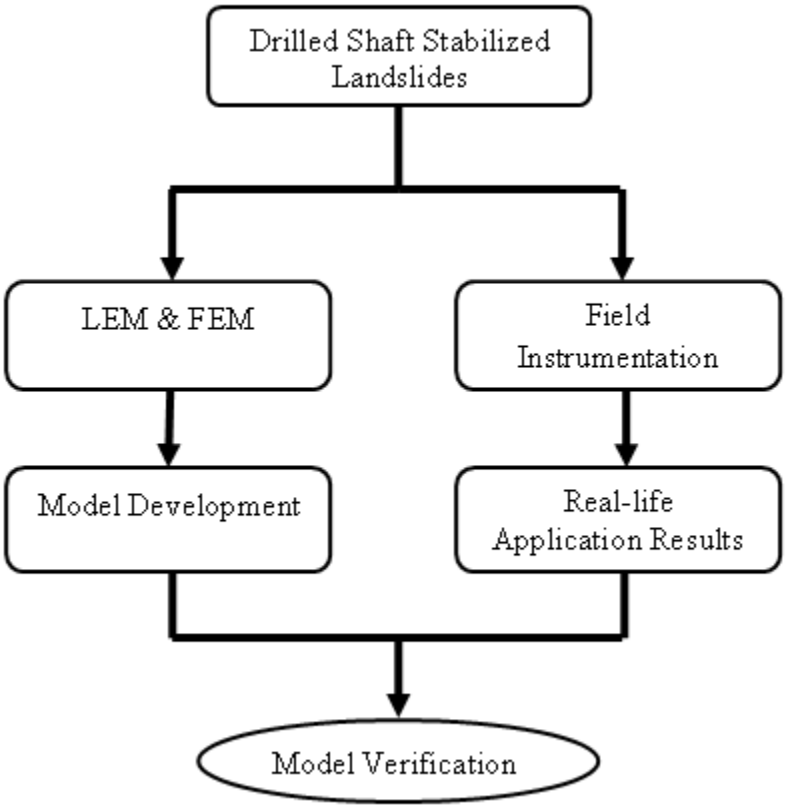

Figure 1.2: Flow Chart Depicting the General Work Plan

1.5 Dissertation Outlines

Chapter II presents pertinent review of relevant literature on the design methods for using the drilled shafts to stabilize an unstable slope.

Chapter III presents the three-dimensional finite element modeling performed using ABAQUS/CAE computer program and the strength reduction techniques for quantifying the drilled shafts induced load transfer phenomenon (arching behavior) in a drilled shaft/slope system.

Chapter IV introduces the developed pertinent design methodology of a single row of rock-socketed drilled shafts for stabilizing an unstable slope. The validation of the computer program UA SLOPE 2.0 based on both finite element simulation results and the special case study of the ATH-124 load testing program was presented in this chapter.

Chapter V presents the field instrumentation and monitoring results of three ODOT landslide repair projects where the row of drilled shafts was used as the primary means for enhancing the factor of safety of the restored slopes. The three project sites are: JEF-152, WAS-7, and MRG-376, respectively. The analysis results of the original slope failure and the drilled shafts stabilized new slope using the new computer program UA SLOPE 2.0 demonstrated the structural adequacy and geotechnical safety of the repaired slopes.

Chapter VI presents a summary of work done, conclusions, and recommendations for implementation.

CHAPTER II

LITERATURE REVIEW

This chapter presents a summary of literature review pertaining to the following aspects of using the drilled shafts to stabilize an unstable slope: (a) past field applications, (b) existing design/analysis methods, (c) past research on soil arching concept, and (d) recent work by the University of Akron research team. The essential ingredients for developing a successful design method will be elucidated in this chapter as well.

2.1 Past Field Applications

The use of drilled shafts or piles as a means to enhance the stability of an unstable slope or to arrest the movement of creeping slopes has been documented in the literature, such as Bulley (1965), Taniguchi (1967), De Beer et al (1970), Fukumoto (1972), Esu and D'Elia (1974), Ito and Matsui (1975), Sommer (1977), Fukuoka (1977), Offenberger (1981), Ito et al. (1981 and 1982), Morgenstern (1982), Nethero (1982), Gudehus and Schwarz (1985), Reese et al. (1992), Rollins and Rollins (1992, and 1999), Poulos (1995 and 1999), Zeng and Liang (2002), Christopher et al. (2007). The success of these documented successful cases of using drilled shafts to stabilize an unstable slope could be attributed to rather conservative design approaches and the large structural capacity

offered by the drilled shafts or the cast-in-place piles. Despite the success of these field applications, it is also clear that there is no universally accepted design method available for assessing the F.S. of a slope reinforced with a single row of spaced drilled shafts as well as for determining the earth thrusts on the drilled shafts for drilled shaft structural design.

With the advancement of drilled shaft construction technologies, a failed slope can generally be accessed by the construction equipment for constructing drilled shafts. Also, the drilled shafts can be installed in different types of soil and rock conditions, thus providing a means for installing drilled shafts with sufficient rock socket length in a slope stabilization project. Compared to some of other slope stabilization techniques, installation of the drilled shafts could be one of those techniques that may not further disturb the slope or causing additional distress or movement of the slope. Therefore, from both successful cases cited in the above and the advantages of the drilled shaft construction techniques, there is no doubt that the use of the drilled shafts should be continuously considered as a viable means to stabilize a stable slope.

2.2 Design Objectives

The design objectives of using the drilled shafts to stabilize an unstable slope should be twofold: (a) find an optimized configuration of drilled shafts, such as diameter and length of shaft, location and spacing of the shaft, and the necessary socket length, etc. to ensure that the target global factor of safety of the slope/shaft system is achieved with the least construction cost, and (b) find the internal forces and moments of the drilled

shaft on slope so that adequate structural capacity of the drilled shaft can be designed to support these internal forces.

To achieve the first design objective, typically one has to use the commonly available slope stability analysis methods, such as method of slice with the limiting equilibrium approach. Therefore, the effects of the drilled shafts within the framework of method of slices should be properly accounted for in the stability analysis of the slope/shaft system. Two schools of thoughts on the incorporation of the effects of drilled shaft have emerged. One is to consider that the drilled shafts provide additional resistance to slope sliding, which in turn, increases the F.S. of the slope/shaft system. The second approach is to view the drilled shafts as a way to provide soil arching in the slope, which in turn, reduces the driving stresses and thus resulting in an increased F.S. of the slope/shaft system.

The analysis of drilled shaft for ensuring the adequacy of its structural capacity is complicated as it is a truly soil-structure interaction problem. The essence of the problem is that the force applied to the drilled shaft is highly dependent upon the nature of the soil and drilled shaft interaction in the process of preventing the soil on the slope from moving further down-slope. Thus, the amount of soil thrust on the drilled shafts can be a function of the slope movement and the stress transfer due to arching. Once the earth thrust on the drilled shaft is determined, the analysis typically uses the beam on Winkler spring type of solution algorithm, such as those employed in the LPILE computer program, to compute the internal forces due to the prescribed external loads or displacement field. The amount of the earth thrust applied to the drilled shaft could be estimated from soil arching theory. However, there are many factors which may govern

the load transfer process in the slope-shaft system, including the soil basic strength properties, shaft dimensions (length and diameter), spacing between the adjacent drilled shafts, location of the drilled shafts on the slope, slope geometry and the location of the slip surface, among others. Thus, three-dimensional finite element simulations would be a necessary tool to investigate the complicated soil-shaft interaction in a slope/shaft system for determining the earth thrust on the drilled shaft.

Based on the above discussions, a suitable design method for using the drilled shafts to stabilize an unstable slope needs to provide a means for considering both geotechnical and structural related design issues. For geotechnical design issue, the geotechnical engineer is ultimately required to determine the final drilled shaft layout (i.e., location, size, length, shaft socket length, and shaft spacing) for a slope/shaft system that is not only adequate for the target safety factor but also most cost effective. For structural related design issue, the engineer is ultimately required to determine the reinforcement requirement to provide structural capacity for supporting the internal stresses and for maintaining structural serviceability (i.e., limiting shaft deflection to within a tolerable amount). The design should be iterative in nature so that both geotechnical and structural design outcome is optimized from safety and economy perspectives.

2.3 Existing Analysis and Design Methods

The analysis involved in determining the global factor of safety of a slope reinforced with a single row of drilled shafts is generally formulated using limiting equilibrium based method of slices. The main contribution of the drilled shafts in the slope/shaft system in the past was treated as an increased resistance force against the sliding soil mass. Examples of such approach include Ito, et al. (1981), Hassiotis et al. (1997), Reese et al (1992), and Poulos (1995, 1999), among others. Contrary to the existing methods of analysis, Liang (2002) proposed to incorporate the effects of drilled shafts in the factor of safety computation in terms of reducing the driving force for the portion of the soil on the down-slope side of the drilled shafts. This reduction in the driving force is attributed to the soil arching phenomenon in the slope/shaft system. Mathematically, the two analysis methods for global factor of safety can be expressed as follows:

$$FS = \frac{F_R + (\Delta F_R)_{shaft}}{F_D} \tag{2.1}$$

$$FS = \frac{F_R}{F_D - (\Delta F_D)_{arching}} \tag{2.2}$$

where

FS = global factor of safety of a slope/shaft system.

F_R = Resistance Force

$(\Delta F_D)_{shaft}$ = Additional Resistance due to Drilled Shaft

F_D = Driving Force

$(\Delta F_D)_{arching}$ = Drilled Shaft Induced Arching Effect on Driving Force

Regardless the difference in treating the effects of the drilled shafts on the slope, both approaches need to provide a means for calculating either the additional resistance provided by the drilled shafts or the driving force reduction factor due to arching. The methods of computing the additional resistance provided by the drilled shafts include the theory developed by Ito and Matsui (1975). Furthermore, Reese (1992) used the theory of Broms (1964) by assuming that the additional resistance can be estimated from the ultimate passive soil resistance on the down-slope side of the drilled shaft. The group effect was considered by means of group efficiency factor under lateral loading conditions. Finite element methods, presumably, could also be used to quantify the soil-drilled shaft interaction such that the additional resistance provided by the drilled shafts could be estimated. Up to now, for the specific purpose of determining the additional drilled shafts resistance; however, there was a lack of such study in the literature. In the approach proposed by Liang, the key issue is to develop the capability to compute the driving force reduction due to the drilled shafts induced arching. A more detailed review of past understanding of soil arching in the drilled shaft/slope system is presented in the next section.

2.4 Arching in Slope/shaft System

The soil arching concept was first noted by Terzaghi (1936, 1943). Initially, most studies on soil arching were focused on vertical stress re-distribution due to arching

through experimental study using a trap door device. The motivation of such early studies on soil arching was due to the need to better understand the earth pressure acting on the underground pipes or tunnel linings. A classic work by Bosscher and Gray (1986) examined the soil arching behavior experimentally using the trap door experiments. It is worth noting that there were research work on soil arching with focus on the zone and the shape of soil arching. Kellogg (1987) observed different shapes of soil arching for different situations, such as parabolic, hemispherical, domal, and corbelled. Recently, a renewed interest on soil arching was focused on applications related to pile supported embankment on soft ground, such as the work by Hewlett and Randolph (1988).

There has been some literature available regarding soil arching in the drilled slope/shaft system. For example, Chen & Martin, (2002) used the finite difference method to analyze the soil structure interaction for a slope reinforced with different types of piles. Some tactical assumptions were involved in their research, including two dimensional model for studying the three-dimensional problem, rigid piles, and relatively small soil movements in the modeling. Earlier, Wang and Yen (1974) also studied the soil arching in a slope, in which the slope was assumed an infinite slope while the soil was modeled as an elastic, perfectly plastic soil. Their numerical study was able to confirm that soil strength parameters played an important role in arching behavior, in addition to the spacing between the adjacent piles. Adachi et al. (1989) portrayed the arching zone as an equilateral triangular arch and defined the arching foot hold around the drilled shaft. Nevertheless, they did not provide any quantitative estimation for the load transfer behavior from the soil to the pile.

More recent studies on arching in the pile stabilized slope can be found in Bransby et al. (1999) and Jeong et al. (2003). Notably, the former used small-scale model tests along with finite element simulation techniques to study the effect of pile spacing and the soil constitutive law on the load transfer process in a slope reinforced with a row of drilled shafts. Their study revealed the link between the soil stress-strain law and the soil deformation mechanism and the load transfer curves. However, their work was limited to sandy soils. The latter performed a finite element study to analyze the response of a row of slope-stabilizing piles to the lateral loads. They defined the load transfer factor by the maximum moment generated in a pile in a row of reinforcing piles to the maximum moment developed in an isolated single pile. Their contributions were the validation of the group effect of a row of drilled shafts in stabilizing the slope.

2.5 Past Research by The University of Akron Group

In this section, some details about the research conducted by The University of Akron on the topic of slope stabilization using single row of drilled shafts are provided. This will include the research conducted by two former doctoral students under the guidance of Professor Liang: Zeng (2002) and Yamin (2007). Furthermore, an ODOT report by Liang (2002) also contains the work by Zeng (2002).

2.5.1 Research by Zeng

Zeng (2002) presented his original work in his doctoral dissertation. Subsequently, two journal articles were published in Liang and Zeng (2002) and Zeng

and Liang (2002). A succinct summary of their work is provided herein. Essentially, 2-dimensional finite element approach, as shown in Figure 2.1, was used to study soil arching behavior. In their finite element simulations, the soil was assumed as elastic, perfectly plastic material with Mohr-Coulomb failure criterion. The drilled shafts were modeled as rigid inclusions in a manner very similar to a trap door experiment. The formulation of soil arching was facilitated by applying a triangular displacement field occurring in the soil between the drilled shafts. It was found that soil arching is highly dependent on the prescribed soil movement, soil properties, and drilled shafts configurations.

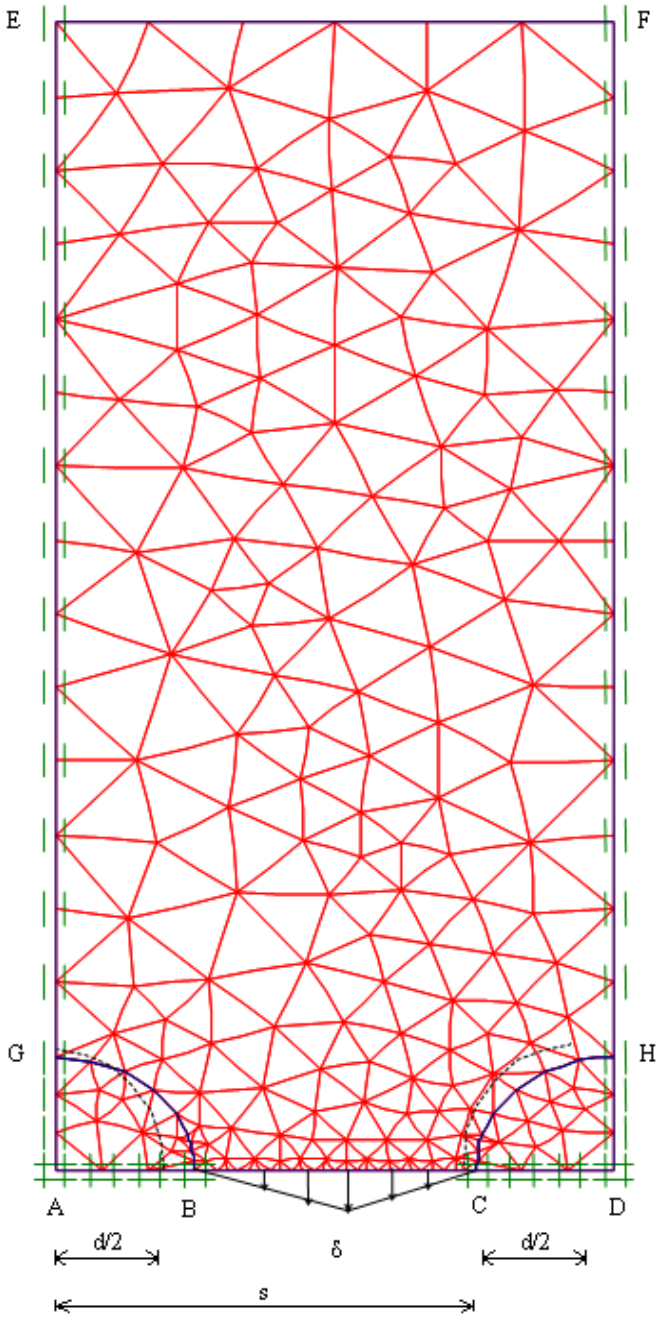

Figure 2.1: Finite Element Model for Slope/shaft System (after Liang and Zeng, 2002)

Based on a systematic parametric finite element simulation, the arching effect in the slope/shaft system was accounted for by the use of the load reduction factor and residual stresses. They defined the load reduction factor as the percent of the soil stresses remained in the soil between the adjacent drilled shafts when full arching in the drilled slope/shaft system was developed. Subsequently, a limiting equilibrium based method of slice for slope stability analysis was developed to incorporate the load reduction factor. The computer program, UA SLOPE 1.0, was developed based on Zeng's work and provided to ODOT for their trial uses. The work by Zeng was later enhanced by Yamin through three dimensional finite element simulations of the drilled slope/shaft system to better quantify the load reduction factor.

2.5.2 Research by Yamin

In Yamin's dissertation work (Yamin, 2007), the main focus was a comprehensive 3-dimensional finite element simulation of the effects of the drilled shafts in promoting the development of soil arching between the adjacent drilled shafts in a slope/shaft system. The representative finite element mesh used by Yamin is shown in Fig. 2.2. As can be seen, the model consists of one single drilled shaft due to the nature of symmetry. The slope movement was activated by incrementally increasing the intensity of the surcharge load placed at the top of the slope crest. When the numerical convergence problem occurs or when the drilled shaft had experienced excessive deflection, the state of the stresses surrounding the drilled shaft were integrated to obtain the inter-slice forces on the up-slope side and down-slope sides of the drilled shaft. The

load transfer factor was then defined as the ratio of these two forces and used in formulating the stability analysis equations of the slope/shaft system.

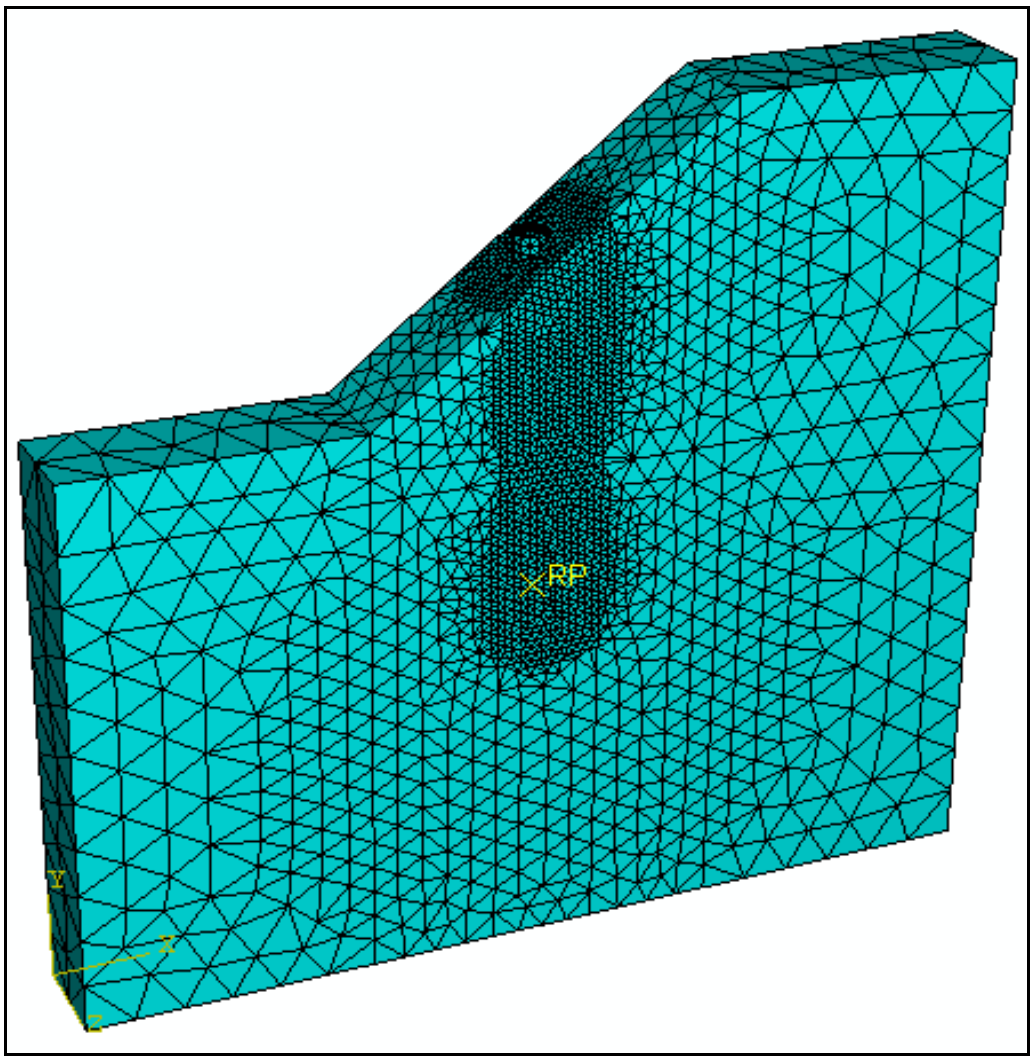

Figure 2.2: 3D Finite Element Model Developed by Yamin (2007)

According to the sensitivity analysis done by Yamin, eleven parameters were found to have controlling influences on the load transfer factor. These parameters include: soil cohesion, soil angle of internal friction, shaft diameter, shaft length, shaft elastic modulus, shaft location, spacing to diameter ratio, rock socket length of the shaft,

and failure surface depth. Liang and Yamin (2010) presented a series of design charts to allow for the determination of the load transfer factor for specific conditions.

Yamin and Liang (2010) presented a closed form solution for determining the factor of safety of a slope/shaft system using the load transfer concept. The closed form solution is given in Equation 2.3, where FS needs to be determined in an iterative manner to satisfy the force equilibrium requirement. This closed form solution can be used to gain insight on the interrelationship between the location of the drilled shafts, shaft diameter and spacing, and soil properties for a given prescribed slope geometry and slip surface location.

$$\eta_m = \frac{\left[L_n - A_n - \left(\sum_{i=m+2}^{n} A_{i-1} \prod_{j=i}^{n} B_j \right) \right]}{\left[\left(B_{m+1} \sum_{i=2}^{m+1} A_{i-1} \prod_{\substack{j=i; \\ j \neq m+1}}^{n} B_j \right) + \left(B_n B_m \prod_{\substack{i=1; \\ i \neq m}}^{n-1} B_i \right) R_1 \right]} \qquad ; 0 < \eta_m \leq 1.0 \tag{2.3}$$

$$\begin{aligned} A_i = & \left[W_i \sin(\alpha_i) + Q_i \sin(\beta_i - \alpha_i) - \frac{C_i b_i \sec(\alpha_i)}{FS} \right] \frac{\tan(\phi_i)}{FS} \\ & - \left[W_i \cos(\alpha_i) + Q_i \cos(\beta_i - \alpha_i) - U_i \right] \frac{\tan(\phi_i)}{FS} \end{aligned} \tag{2.4}$$

$$B_i = \left[\cos(\alpha_{i-1} - \alpha_i) - \sin(\alpha_{i-1} - \alpha_i) \frac{\tan(\phi_i)}{FS} \right] \tag{2.5}$$

η_m= is the required load transfer factor

W_i = weight of slice i

N_i = force normal to the base of slice i

T_i = force parallel to the base of slice i

Q_i = external surcharge applied at slice i

R_i = right-interslice force of slice i

L_i = left-interslice force of slice i

α_i = inclination of slice i base

α_{i-1} = inclination of slice i-1 base

β_i = inclination of the external surcharge applied at slice i

c_i = soil cohesion at the base of slice i

ϕ_i = soil friction angle at the base of slice i

2.6 Concluding Remarks

Despite a long history of successful uses of drilled shafts to stabilize an unstable slope, there is still a lack of unified and widely accepted design method for use by practicing geotechnical and structural engineers. An integrated, but easily applied, method needs to be developed to allow for accurate calculation of the global geotechnical factor of safety of a slope/ shaft system as well as for structural design of the drilled shaft for its structural adequacy. It is also recognized that the design process should be iterative to allow for optimization for best economy and constructability.

The existing approaches to estimating FS of a slope/ shaft system are essentially cast within the method of slice for slope stability analysis, with the effects of drilled shafts treated as additional resistance against driving force. The methods available for estimating this drilled shaft enabled additional resistance varied from theoretical theory of plasticity to more simplified approach using passive pile resistance theory. The main drawback of such approach is that the estimated additional resistance tends to be at the

limiting state, thus providing in general fairly high estimated global F.S. of the drilled Slope/shaft system. In addition, the structural design of drilled shafts tends to be over-conservative due to the extremely large earth thrust at the ultimate state. Ideally, one could perform finite element simulation to determine the suitable empirical equations for estimating the additional resistance provided by the drilled shafts in a slope/shaft system, but this has not been reported in the literature.

The approach taken by Liang (2002) differs from the common approach in that the effect of the drilled shaft was incorporated in the method of slice analysis by a reduction factor of the inter-slice force at the location of the drilled shafts. The load transfer factor was quantified through an evolution of series of finite element simulation studies, from original 2-D modeling to subsequent 3-D modeling. Since the inter-slice reduction (or the load transfer) factor was evaluated through a series of 3-D finite element analysis, the drawbacks of the former approach are avoided. The study by Yamin provided empirical charts for estimating the load transfer factor for prescribed conditions. However, the FEM simulations in the Yamin's study could not provide data for validating the method by Liang. A new series of finite element simulation study using the strength reduction technique was recently carried out in this research work, from which a new set of semi-empirical equations were obtained for the load transfer factor. More importantly, though, the results of the series of finite element simulation cases provided the F.S. of the slope/shaft system, thus allowing for validating the Liang approach. The main focus of this research work is on the finite element simulation approach and the accompanied method of slice analysis method in the framework of Liang (2002). Based on the findings from this study, a new computer program UA SLOPE 2.0 was developed for analyzing a

realistic slope/shaft system. The accuracy of the UA SLOPE 2.0 program was validated by a case study of the ATH-124 project, where field testing of the drilled shafts at the existing failed slope site provided valuable data for necessary calibration and verification of a finite element model and comparison between FEM and UA SLOPE 2.0 predictions for the site.

CHAPTER III

FINITE ELEMENT STUDY OF SOIL ARCHING IN A SLOPE/SHAFT SYSTEM

This chapter presents succinct review of previous studies on arching, with particular focus on the relevant literature on slope/shaft systems. The research work by the UA research team, as documented in three doctoral dissertation (Zeng, 2002; Yamin, 2007; and this dissertation, will be briefly summarized. The main portion of this chapter, however, presents the work done in this research study with the strength reduction method applied to ABAQUS finite element simulation studies.

Semi-empirical equations developed for quantifying the arching-induced load transfer in a slope/shaft system are presented, together with semi-empirical equation for estimating net force on the drilled shaft.

3.1 Arching Phenomenon

As reviewed earlier in chapter II, arching is a well recognized phenomenon in soil mechanics. The arching effect in sands was first investigated by Terzaghi (1936, 1943) using an experimental set up consisting of a platform with a narrow strip of a trap door. As the trap door was slowly lowered, the soil weight induced gravitational stresses of the soil on top of the trap door was found to redistribute to the stationary portion of the soil

mass, thus resulting in reduced stresses in the moving part of the soil mass. This behavior can be attributed to the shear resistance developed between the stationary sand and the moving sand at the failure interface. However, it should be noted that the experiment conducted by Terzaghi was mainly for understanding arching in vertical soil movement. This experiment may not reflect the condition of a slope reinforced with a single row drilled shafts, where the soils in between the adjacent drilled shafts may move relative to the soils directly behind the drilled shafts. This type of relative movements of soil masses may result in arching as well. The past study of arching phenomenon observed in drilled shafts reinforced slope system is reviewed in the next section.

3.2 Past Research on Arching in a Slope/Shaft System

There exist relatively a few published studies on the arching phenomenon in the drilled Slope/shaft system. Notably, Chen and Martin (2002) demonstrated the use of the finite difference method to analyze the soil structure interaction in a slope with a row of piles. Although the findings from Chen and Martin provided useful understanding of the arching in a qualitative manner, their study nevertheless was limited due to 2-D modeling of the problem and the prescribed small velocity field for the soil deformation pattern.

In experimental work of the pile reinforced slope, Bosscher and Gray (1986) conducted small-scale experiment using sand to construct the slope model. They were able to show that arching indeed contributed to the observed stabilization effects of the model piles on the slope. Bransby et al (1999) conducted small-scale model tests to derive semi-theoretical equations for use for analyzing the load transfer process in a

drilled slope/shaft system. They related the load transfer process to passive earth pressure theory.

Study of arching in slopes reinforced with drilled shaft was also carried out by Wang and Yen (1974), in which several assumptions were made, including infinite slope, rigid-plastic soil, predefined failure plane (translational slip plane).

Jeong et al (2003) analyzed the response of a row of slope-stabilizing piles to the lateral load. They defined the load transfer factor by the maximum moment generated in a pile within a row of reinforcing piles to the maximum moment developed in an isolated single pile.

Liang and Zeng (2002) studied the soil arching in a drilled slope/ shaft system using FEM. Their study was based on a 2D FEM analysis of rigid inclusions representing drilled shafts. A prescribed triangular shape displacement field in between the two inclusions was used to introduce soil movement and to facilitate arching occurring in between the two rigid inclusions. Essentially, the finite element model created by Liang and Zeng represents a trap door-type of arching, rather than arching in a slope/shaft system. The arching induced stress transfer was quantified through a parametric study and the concept of load transfer was represented by the stress reduction factor. It should be noted that UA SLOPE version 1.0 computer program (Liang, 2002) developed for the Ohio Department of Transportation was based on the load transfer factor based on this simplified 2-D finite element study.

3.3 Study of Arching by Yamin (2007)

As part of this research, Yamin (2007) conducted three-dimensional finite element model simulations of the drilled slope/shaft system where surcharge load was applied at the crest area of the slope to facilitate soil movement. By gradually increasing the surcharge load, the soil in the slope and the reinforcing drilled shafts would experience deformation so that arching effect can be quantified from the numerical simulation results. In the FEM model, Yamin (2007) used elastic-perfectly plastic Mohr-Coulomb model for the soils on the slope. The drilled shafts were modeled as an elastic material. The non-yielding (or rock) stratum where the drilled shafts are socketed into was modeled as an elastic material. The interface between the shaft and the surrounding soil and rock was implicitly considered as a frictional model. The controlling factors which were considered in a comprehensive finite element parametric study include the following: 1) soil cohesion [c], 2) internal friction of the soil [ϕ], 3) shaft diameter [D], 4) shaft location [ξ_s], 5) shaft spacing to shaft diameter ratio [S/D], 6) shaft elastic modulus [E_p], 7) total shaft length [L_p], and 8) slope angle [β]. The FE simulation involved applying surcharge load at the slope crest area to facilitate slope movement until the ultimate state of the slope/shaft system was reached. The ultimate state was defined by the limiting shaft displacement. The arching induced load transfer factor was defined as the ratio of the earth thrust on the shaft on the up-slope side of the shaft and the earth thrust on the down-slope side of the drilled shaft. Among some of the limitations of Yamin's load transfer factor are noted below.

- The ultimate state of the slope/shaft system was obtained by incrementally increasing the surcharge load at the top of the slope. In this way, the true factor of safety of the slope/shaft system cannot be ascertained.
- The ultimate state was defined by the limiting shaft displacement. Most of the time, failure of slope/shaft system is due to excessive soil movement at small shaft displacement. The limiting shaft displacement in Yamin's study is greater than the shaft displacement at failure.
- Yamin's study indicated that the rock socket length could be an important factor in the load transfer process. However, in this study, based on 3-D FEM using strength reduction method, it was found that a rock-socket length 10% to 15% of the total shaft length for a wide range of rock properties (weak to very strong) should be enough for providing full shaft fixity. Therefore, rock socket length of a drilled shaft is not a controlling factor for the load transfer process in a slope/shaft system.
- In Yamin's work, the elastic modulus of a drilled was considered one of the most important factors which govern the load transfer process. However, since the typical diameter of the drilled shafts used in slope stabilization is between 2 ft to 4 ft; therefore, the large difference between the soil and the shaft modulus led to conclusions that modulus of the shaft needs not be considered in the design process.

3.4 Arching Study by Using Shear Strength Reduction Method

This study adopted a new approach using strength reduction method in the ABAQUS finite element computer code to address the main deficiency of Yamin's work. The strength reduction method used in conjunction with finite element method was recognized by Zienkiewicz (1973) and Duncan (1996). The essence of the strength reduction method is to reduce the soil strength parameters (c and ϕ) proportionally to bring the slope to the verge of failure (FS =1, Plastic flow). The factor of safety of the slope is equal to strength reduction factor, or in other words, the available soil strength divided by the reduced soil strength at slope failure. The strength reduction method is specifically suited for the soil behavior that obeys the elastic-perfectly plastic constitutive law with strength parameters of c and ϕ, such as Mohr-Coulomb model or Drucker-Prager model.

Some of the advantages of the shear strength reduction method used in slope stability analysis are as follows:

- The failure zone can be automatically generated; therefore, there is no need for an iterative process to search for the critical failure surfaces.
- Accounts for the soil constitutive model.
- Can solve 2D and 3D problems

The mathematical formulation which describes the strength reduction method is as follows. The soil strength (initial state) parameters [c, and tan(ϕ)] are reduced incrementally throughout the finite element simulation by dividing them by a Reduction

Factor (RF). Therefore, the reduced cohesion c_R and internal friction angle ϕ_R at each step of reduction are given by:

$$c_R = c/RF \quad (3.1)$$

$$[\tan(\phi)]_R = \tan(\phi)/RF \quad (3.2)$$

The smallest reduction factor which triggers the soil in a slope/shaft system to flow plastically is considered the factor of safety.

3.4.1 Failure Criteria of Shear Strength Reduction Method (SSRM)

In slope stability analysis using FEM and Shear Strength Reduction Method (SSRM) the ultimate state (Plastic flow) can be defined by one of the two following conditions:

1) A rapid increase of the nodal displacement occurs when the reduction factor exceeds a certain value (Griffiths and Lane 1999); or
2) FEM computations divergence (Ugai, 1989; Dawson et al, 1999).

3.4.2 Implementing Shear Strength Reduction Method in ABAQUS

In the past, the application of the shear strength reduction method in a FEM simulation was done manually in an incremental, iterative process until the minimum reduction factor was obtained. Recently, Hügel, et al. (2008) referred to the power of commercial FEM code ABAQUS (2006) for analyzing slope stability problems within the framework of SSRM by utilizing a temperature field. Qianjun, et al. (2009) developed a temperature-based method to reduce soil properties internally in ABAQUS.

Consequently, there is no need for the manual process to incrementally apply the strength reduction factor in FEM simulations.

In this study, the dimensionless horizontal displacement $\delta = U_{max}/H$, where U_{max} is the maximum horizontal displacement, and H is the slope height, is calculated in terms of the RF (Qianjun et al, 2009). The reduction factor RF, which corresponds to the point at which the dimensionless horizontal displacement begins to change rapidly, is the Factor of Safety of the slope or the slope/shaft system. The factor of safety (strength reduction factor) versus the dimensionless horizontal displacement for a typical case run is shown in Figure 3.1 to illustrate the point at which the slope failure occurs.

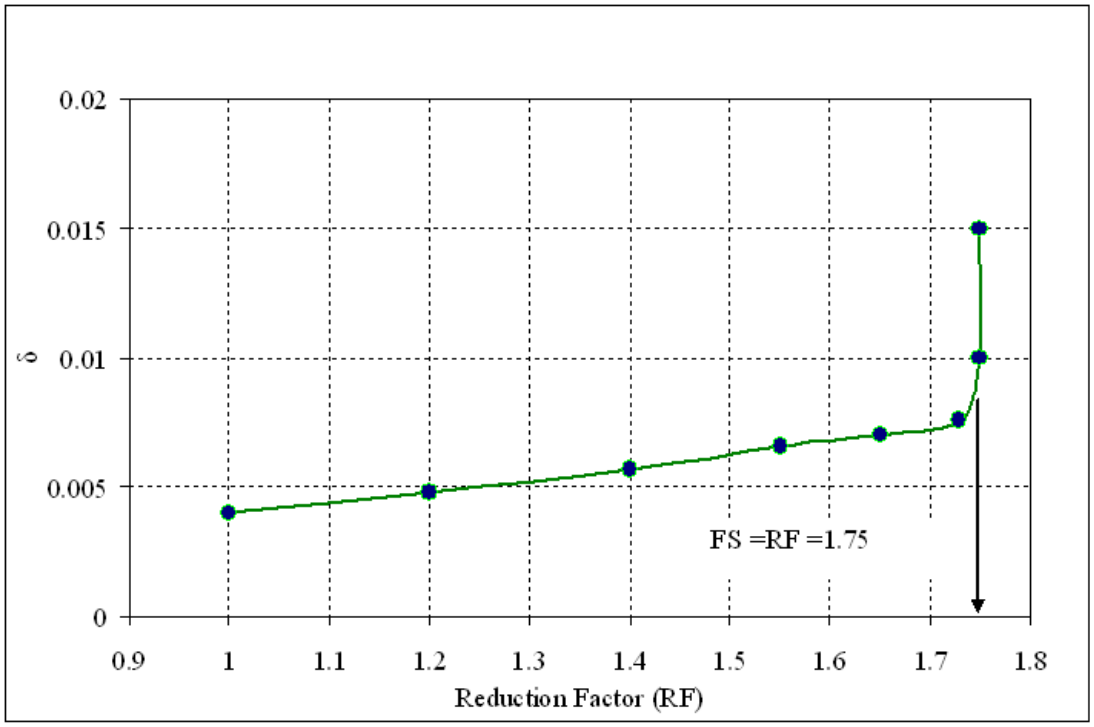

Figure 3.1: Dimensionless Maximum Horizontal Displacement (δ) vs the Reduction Factor (RF) for the Baseline Model

3.4.3 FEM Modeling

3D finite element model was constructed using ABAQUS program (version 6.7-1) for studying the soil structure interaction behavior of the drilled shafts on a slope under the effect of shear strength reduction. The baseline finite element model was constructed for a slope that is on the verge of failure (FS =1.0). The properties of this model are provided in Table 3.1. The baseline model was reinforced with a row of drilled shafts to improve the factor of safety. It is noted that nature of symmetry of the problem domain was taken into consideration in constructing the 3-D finite element model of the slope/shaft system, as depicted in Figure 3.2.

Table 3.1: Properties of the Baseline Model

Group	**Parameter**	**Parameter Value**
Soil Properties	Angle of internal friction (ϕ, degrees)	10
	Cohesion (c, psf)	400
	Soil Elastic Modulus (Es, psf)	$2x\ 10^5$
	Dry Soil Unit weight (γd, pcf)	115
Shaft Parameters	Pile Diameter (D, ft)	4
	Pile Length (Lp, ft)	50
	Pile Elastic Modulus(Ep, psf)	$4.2\ x\ 10^8$
	Pile Poisson's Ratio (υ_p)	0.2
	Rock Socket Length ratio(Lr/Lp)	0.2
Rock Properties	Rock Elastic Modulus (Er)	$5\ x\ 10^8$
	Rock Poisson's Ratio (υ_r)	0.2
Geometry and Arrangement	Slope Angle (β, degrees)	40
	S/D Ratio (S = c.t.c spacing)	3
	Pile Location (x_i/X) =ξ	0.5
Interaction	Soil-Pile Interaction (δ)	0.3

3.4.3.1 Material Models

Soil is modeled as a linear elastic-perfectly plastic material which obeys Mohr-Coulomb failure criterion. The model properties are: the angle of internal friction, cohesion, elastic modulus, and Poisson's ratio. The thermal expansion coefficient was set to equal to zero. The rock and the drilled shaft are modeled as a linear elastic material described by the elastic modulus and Poisson's ratio.

3.4.3.2 Modeling of Contact Interfaces

Three contact interfaces were defined to account for the contact boundaries in the model: 1) soil-shaft interface, 2) rock-shaft interface (which consists of two parts, the first one is the interface between the shaft perimeter area and the rock, and the other one is the interface between the bottom of the shaft and rock), and 3) soil-rock interface.

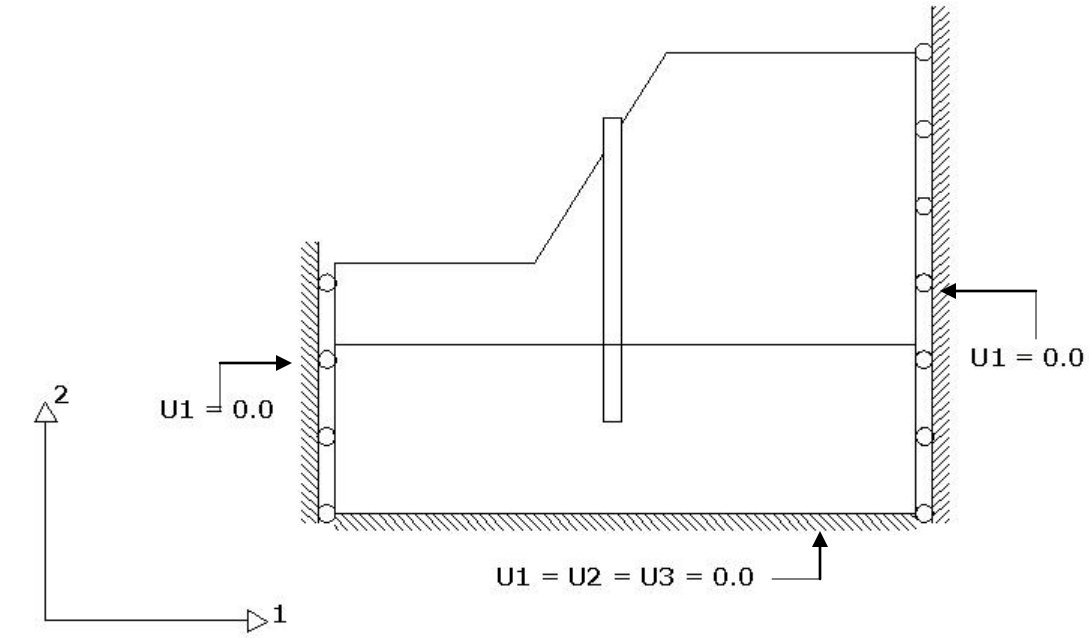

(a)

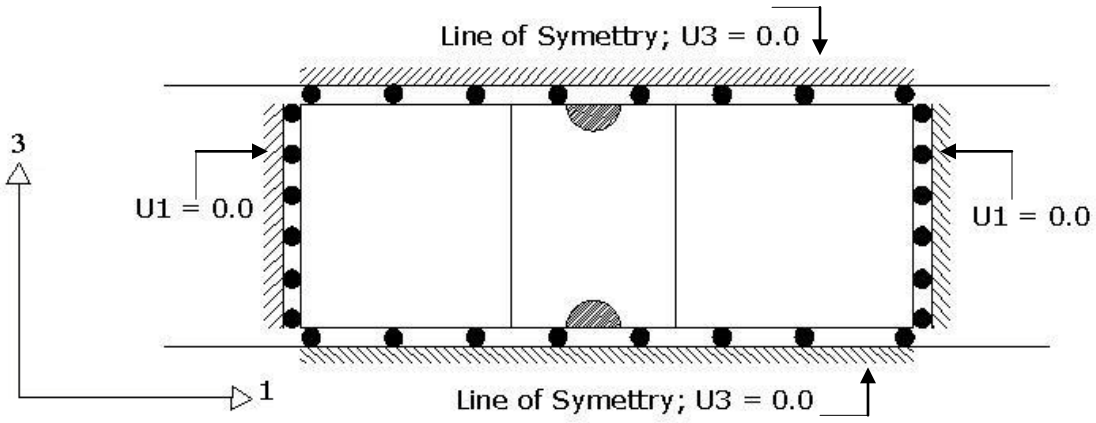

(b)

Figure 3.2: Boundary Conditions Used in the Finite Element Model (a) Elevation View (b) Top View

It should be noted that the normal contact is chosen as "Hard Contact" type, meaning that contact pressure will be generated only if there is a full over-closure between the contact surfaces. Furthermore, this type of contact minimizes the penetration of the slave nodes into the master surface, and it does not allow the transfer of the tensile stresses across the interface. If any separation takes place between the contact surfaces, no contact pressure will be generated.

3.4.3.3 Loads and Boundary Conditions

The only load used in this analysis is the gravity load. The boundary conditions are modeled as follows. The bottom of the rock is fixed in all directions. For all the vertical boundaries the soil movement is prohibited (fixed) in the horizontal direction. The left and right vertical boundaries are considered as lines of symmetry. All the boundary conditions are shown in Figure 3.2-a and 3.2-b for elevation view and top view, respectively.

3.4.3.4 FEM Mesh

The mesh generated for the problem is depicted in Figure 3.3. It consists of 7,696 hexahedral elements for soil body, and 23,600 similar hexahedral elements for rock. The drilled shaft was modeled using 420 similar hexahedral elements. The mesh of the shaft and the adjacent area was finer than the other zones because this region was expected to experience high stress concentration. The optimum mesh was selected based on the computed factor of safety. At the beginning, a trial mesh was made and the corresponding

factor of safety was found, then the mesh was refined incrementally and the factor of safety was obtained and compared to the factor of safety obtained from the previous one. When the newly obtained value of the factor of safety becomes stable compared to previous value, then the mesh with the minimum number of elements that gives this safety factor value is used. This process is illustrated for the base line model in Figure 3.4 by drawing the factor of safety against the relative mesh density, which is the number of mesh elements divided by 20,000 to avoid a large number in the graph. This procedure is repeated for all models conducted in the parametric study.

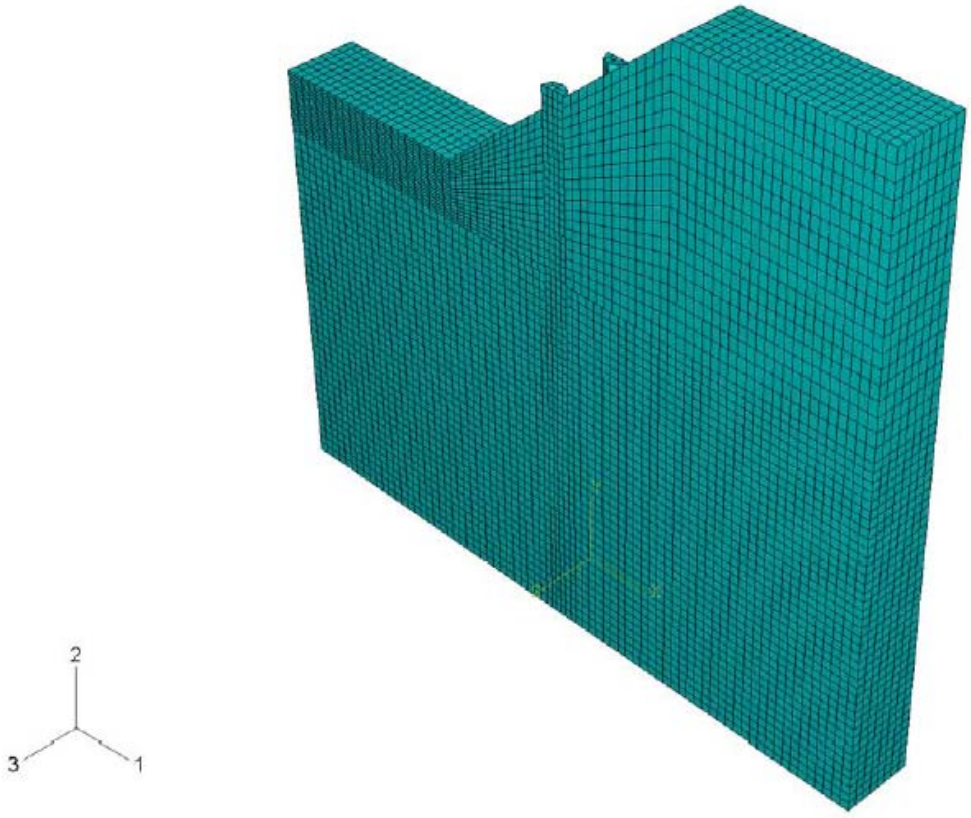

Figure 3.3: Finite Element Mesh

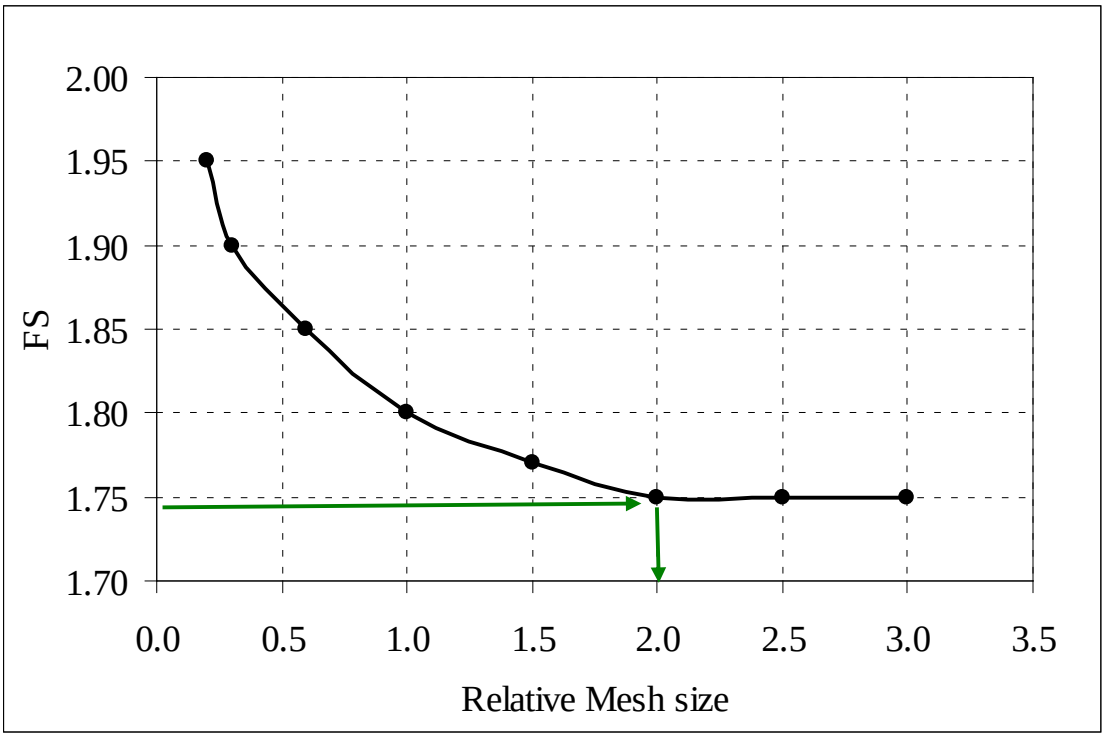

Figure 3.4: Mesh Refinement and Convergence for the Baseline Model

3.5 Parametric Study Using Shear Strength Reduction Method

Based on the above mentioned finite element model, the effect of fifteen parameters on the load transfer process was investigated. These parameters are classified into five groups: 1) Soil parameters (cohesion c, internal friction ϕ, elastic modulus E_s, and unit weight γ), 2) Rock properties (Elastic modulus E_r, and Poisson's ratio υ_r), 3) Shaft properties (total shaft length L_p, rock socket length L_r, diameter D, elastic modulus E_p, and Poisson's ratio υ_p), 4) Geometry (spacing to diameter ratio S/D, slope angle β, dimensionless shaft location $\xi = x_i/X$); and finally 5) The soil-shaft friction at the interface δ. The geometry of the slope is shown in Figure 3.5 with all the related terms defined.

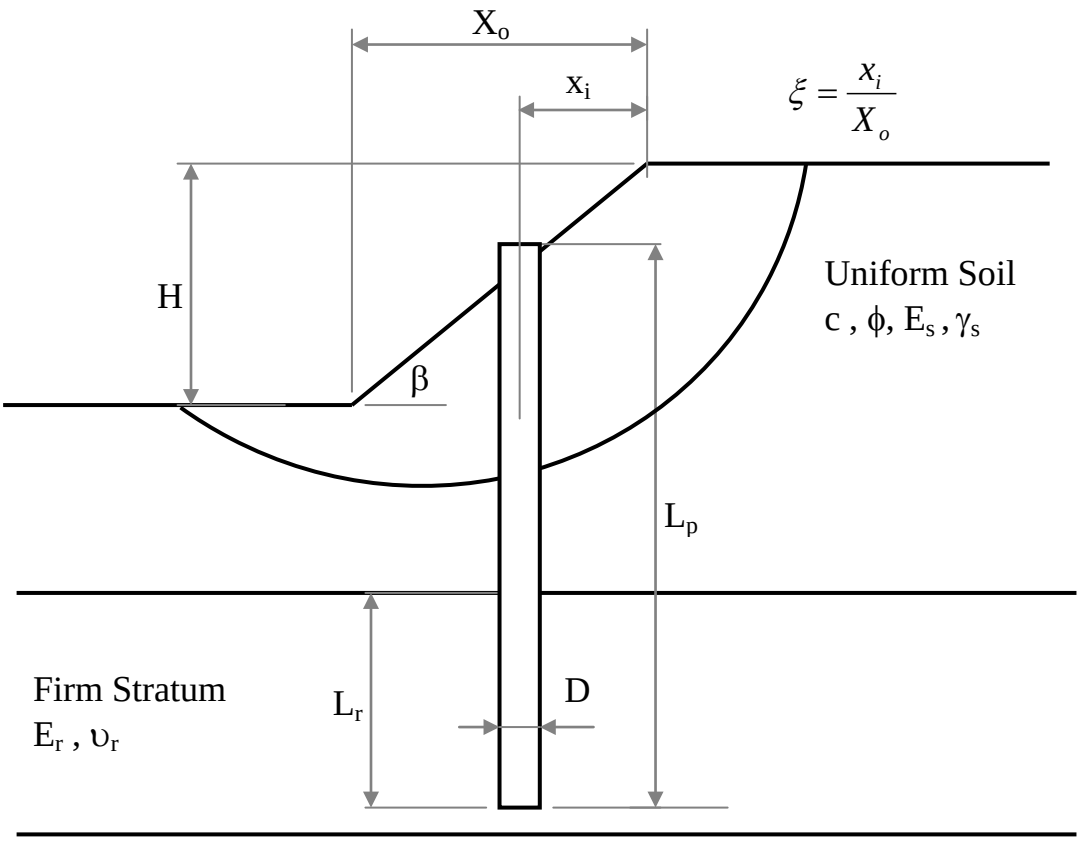

Figure 3.5: Illustration of the Terms Related to the Slope Geometry

The baseline model (will be explained in detail in the next section) geometry and parameters for this study was selected such that it has a factor of safety equal to unity. For the subsequent parametric study, the value of each parameter was varied over a reasonable range. For each value of each parameter, the model was analyzed using FEM and SSRM. At failure, the factor of safety of the slope/shaft system, the up-slope and down-slope horizontal soil stresses around the shaft perimeter, the location of the failure surface, and the depth of the failure surface at the drilled shaft location were obtained.

3.5.1 Baseline Model

The baseline model was constructed based on geometry and soil properties which define a slope on the verge of failure (FS = 1.0). The slope was reinforced with a single row of drilled shafts with a wide range of selected properties; these properties are listed in Table 3.1. The geometry and dimension of the baseline model are shown in Figure 3.6-a, and 3.6-b. In taking the advantage of symmetry of the problem domain, the drilled shafts reinforced slope model is represented by a slice of soil with a half drilled shaft at each side, wherein the center to center distance between the drilled shafts (i.e., the thickness of the soil slice) represents the center to center spacing between the shafts. As an illustration, the baseline model reinforced with drilled shafts (Diameter = 4 ft and S/D = 3.0) yields factor of safety of 1.75. The failure surface is obtained from the equivalent plastic strains (i.e., a measure of the amount of permanent strain) at failure. The bottom of this plastic zone (shown in Fig. 3.7-a) is considered to be the failure surface.

The parametric study was conducted by systematically changing the value of one parameter while keeping all the other parameters the same as baseline model. The range over which the values of each parameter are varied is listed in Table 3.2. For each case analyzed, the horizontal soil stresses around the shaft, the depth of failure surface at the drilled shaft location and the plastic zone, Figure 3.7-b, were obtained for subsequent computation of the load transfer factor.

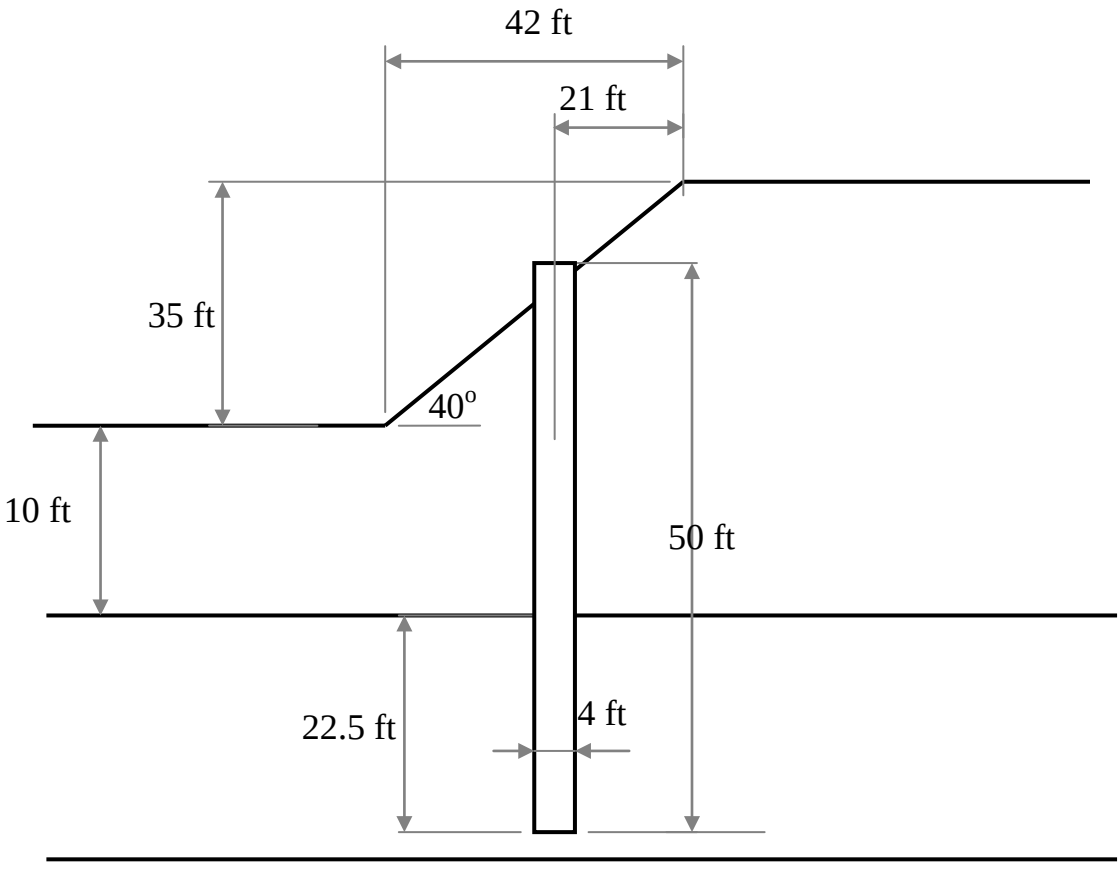

(a)

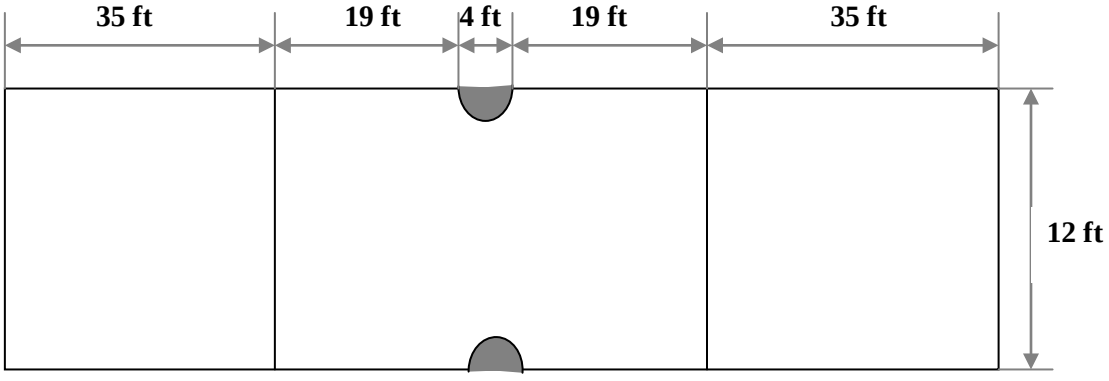

(b)

Figure 3.6: Geometry and Dimensions of the Baseline Model a) Cross-Section b) Top View

Table 3.2: The Ranges of the Parameters Used in the Parametric Study

Group	Parameter	Parameter Value	Range of Parameter
Soil Properties	Angle of internal friction (ϕ, degrees)	10	0,5,10,15,20,25,30,35,40,45, 50
	Cohesion (c, psf)	400	0,250,400,500,750,1000, 1250,1500,1750,2000
	Soil elastic modulus (E_s, psf)	$2x\ 10^5$	1,2,5,7.5,10,12.5,15,17.5, $20(x10^5)$
	Dry soil unit weight (γ_d, pcf)	115	100,105,110,115,120,125,13 0
Shaft Parameters	Pile diameter (D, ft)	4.0	2,3,4,5,6,8,9,10
	Pile length (Lp, ft)	50	30,40,45,50,60,65,70,75,80
	Pile elastic modulus(Ep, psf)	4.2×10^8	3.5, 4.2,4.8,5.6,6.8 ($x10^8$)
	Pile Poisson's ratio (υ_p)	0.2	0.12,0.15,0.18,0.22,0.25
	Rock socket length ratio(L_r/L_p)	0.2	0.15,0.2,0.25,0.35,0.45,0.5
Rock Properties	Rock elastic modulus (E_r)	5×10^8	0.5,1,3,5,5.5,7,8 ($x10^8$)
	Rock Poisson's ratio (υ_r)	0.2	0.15,0.2,0.18,0.23,0.25
Geometry and Arrangement	Slope angle (β, degrees)	40	25,30,35,40,45,50,55,60
	S/D Ratio	3.0	1.875,2,2.75,3.25,3.5,4,4.5,5
	Pile location (xi/X) =ξ	0.5	0.15,0.3,0.4,0.6,0.75,0.9
Interaction	Soil-Pile friction (δ)	0.3	0,0.1,0.2,0.3,0.4,0.5
20 random Runs			

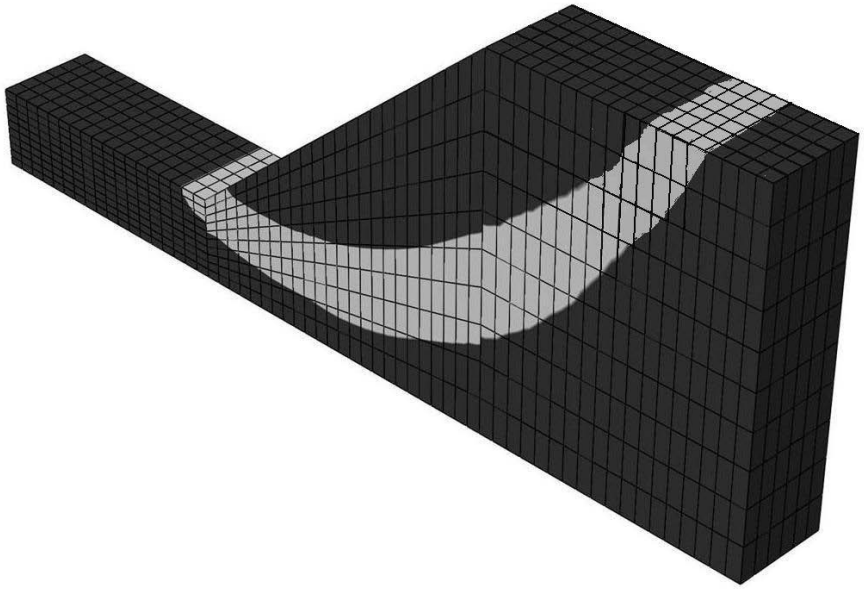

(a)

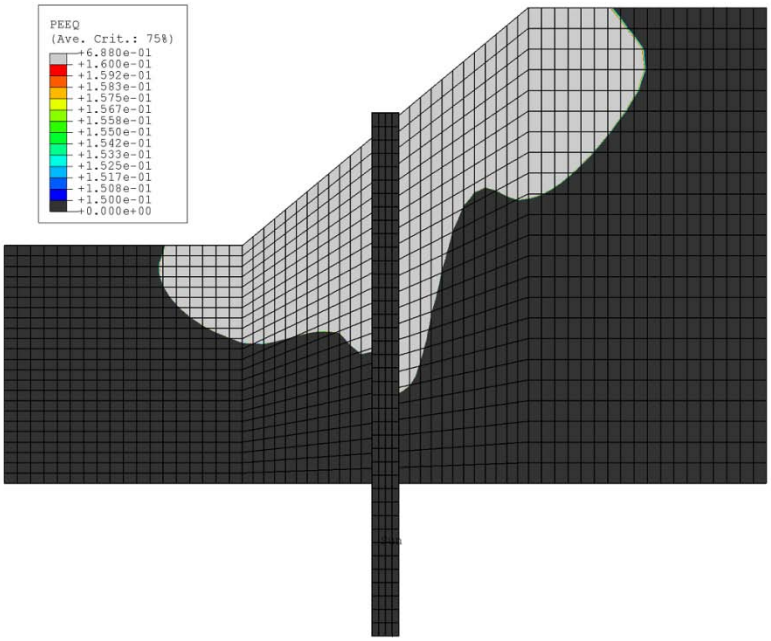

(b)

Figure 3.7: Plastic Zone a) Failure Surface from the Equivalent Plastic Strain for the Baseline Model b) Failure Surface for a Reinforced Model

3.5.2 Importance of the Parameters

One of the main purposes of the parametric study is to find out the major parameters which control the load transfer process under the effect of shear strength reduction in a slope reinforced with a single row of drilled shafts. To evaluate the importance of each factor used in this study, the effect of each parameter on the global factor of safety was evaluated by changing the target parameter while the other parameters remain the same as that used in the baseline model. The parameters which showed no significant effect on the factor of safety were further investigated by randomly changing them with other parameters to ensure the same conclusions remain. The seven parameters considered to be non-significant were based on the total importance percentage of less than 10%. The importance of each parameter was calculated from the following equation

$$I = \frac{FS_i^{max} - FS_i^{min}}{\sum FS_i^{max} - \sum FS_i^{min}} \quad (3.3)$$

where

I = importance of the parameter (i)

FS_i^{max} = the maximum factor of safety obtained from the parameter (i)

FS_i^{min} = the minimum factor of safety obtained from the parameter (i)

Finally, for more verification, a step-wise statistical analysis was performed using the software SPSS. In this analysis the parameter to be investigated is excluded from the analysis and influence of the exclusion of this parameter is examined by testing the significant level (α) and the R^2. If the exclusion of a parameter does not affect the value

of the R^2 (within the allowable tolerance) and the significant level (α) is greater than 5% then it is excluded totally from the analysis. The parameters which were found to be of controlling effect are set into three categories; a) the soil properties [cohesion(c), angle of internal friction (ϕ), and the modulus of elasticity (E_s)], b) the drilled shaft parameters [diameter (D), and the total shaft length (L_p)], and c) arrangement and geometry [spacing to diameter ratio(S/D), slope angle (β), location of the shaft (ξ)]. The order of importance of these parameters starting from the most important parameter is as follows: c, ϕ, S/D, ξ, D, β, E_s, L_p.

3.6 Load Transfer Factor

The single row of drilled shafts in a slope works to reduce the driving stresses in the soil. The effect of the shaft is observed in the changes occurred in the horizontal stresses in the soil mass in the up-slope and down-slope sides of the shafts. The variation of the horizontal soil stresses and the soil arching effects can be seen clearly in Figure 3.8, which represents a horizontal cross section of the drilled slope/ shaft system. Figure 3.9 shows the arching stresses variations a long a path up-slope the shafts starting from the centerline of the shaft (edge of the model) and ending at the centerline of the model. The results of arching shape shown in Figure 3.8 are comparable to the arching patterns described by Adachi (1989).

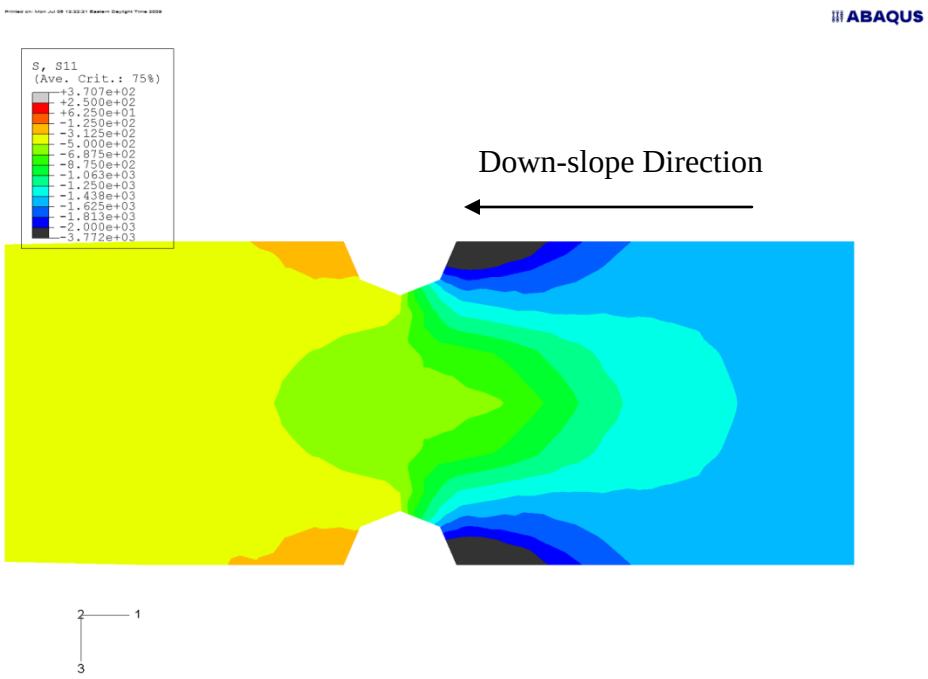

Figure 3.8: Soil Arching as Observed from the Horizontal Soil Stresses in the Direction of the Soil Movement (Horizontal Section)

Figure 3.10 shows 3D isometric stress contours. The horizontal stresses in the transverse direction usually cancel each other due to the symmetry. On the other hand, the changes in the vertical soil stresses, both on the up-slop and down-slope sides of the shaft, are usually not significant. These changes in vertical stresses usually work toward improving the geotechnical factor of safety of the system, and they might add some axial force to the shaft. Therefore, the focus of this study is to investigate the variations of the horizontal stresses in a slope reinforced with a single row of drilled shafts.

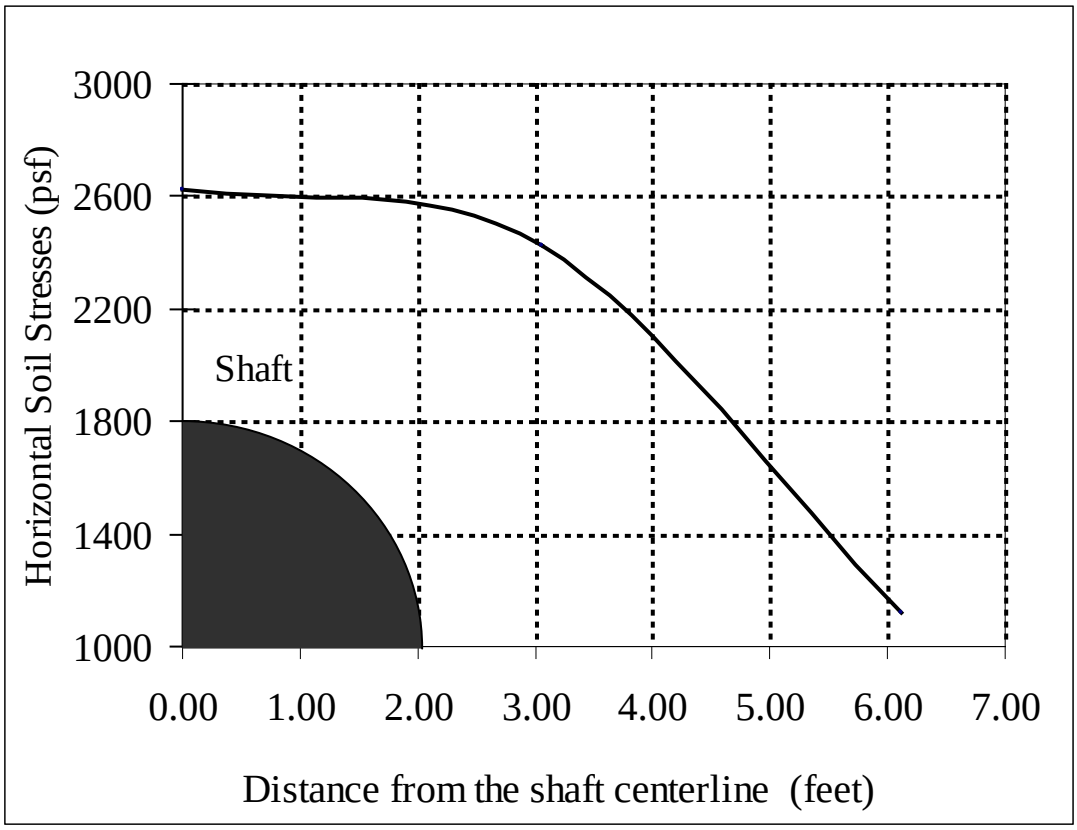

Figure 3.9: A Graph of Soil Arching between Two Shafts

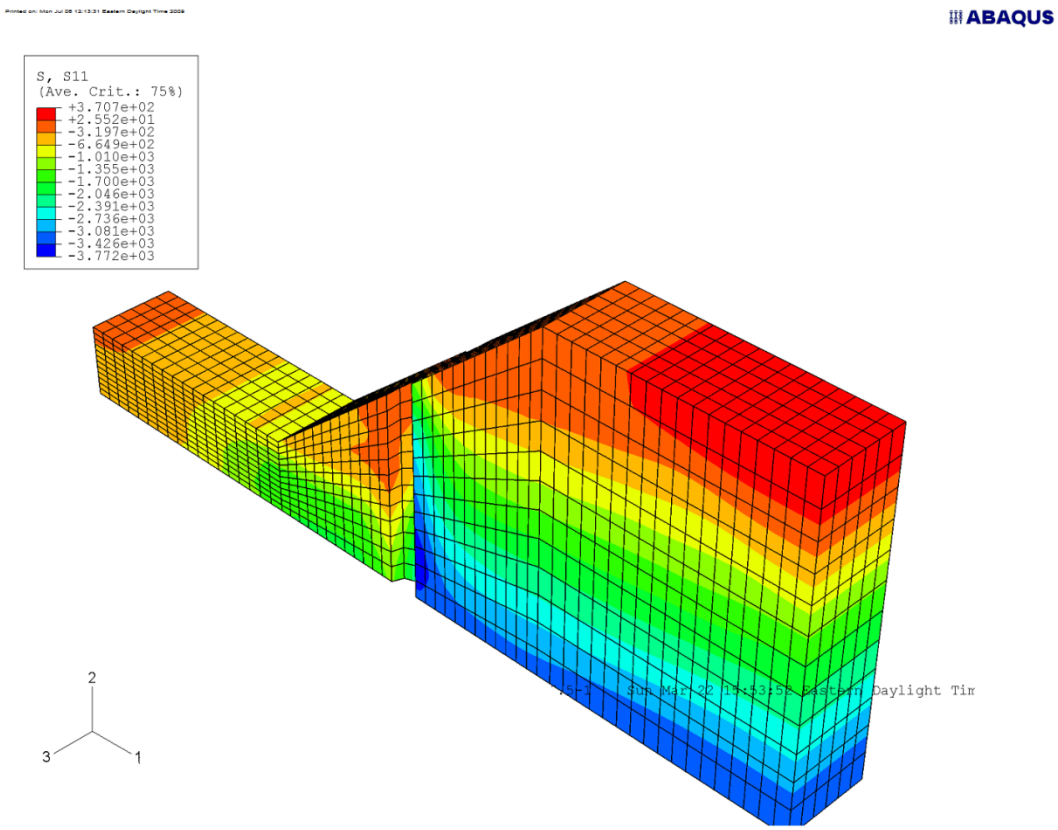

Figure 3.10: Horizontal Stresses at Failure (3D Isometric Stress Contours)

The load transfer factor is defined herein as the ratio between the horizontal force on the down-slope side of the shaft and the horizontal force on the up-slope side of the shaft. Mathematically, the load transfer factor is expressed as:

$$\eta = \frac{F_{Down}}{F_{up}} \qquad (3.4)$$

F_{up}= is the resultant horizontal force (in the direction of the soil movement) on the up-slope of the shaft

F_{down}= is the resultant horizontal force (in the direction of the soil movement) on the down-slope side of the shaft.

The resultant force in the soil up-slope and down-slope sides of the shaft is estimated by integrating the horizontal soil stresses around the perimeter of the shaft as shown in Figure 3.11-a and from the top of the shaft down to the failure surface as shown in Figure 3.11-b :

$$F_{up} = \int_0^{L_f} \int_0^{\pi D/2} \sigma_{xx} \, ds \, dz \qquad (3.5)$$

$$F_{Down} = \int_0^{L_f} \int_0^{\pi D/2} \sigma'_{xx} \, ds \, dz \qquad (3.6)$$

where

D = the diameter of the drilled shaft

L_f = the distance from the top of the shaft down to the failure surface

$\sigma_{xx} = S_{11}$ = the horizontal soil stresses on the up-slope side of the shaft

$\sigma'_{xx} = S'_{11}$ = the horizontal soil stresses on the down-slope side of the shaft.

The general characteristics of the load transfer factor as affected by three groups of variables were studied. These three groups are as follows. (a) Soil properties (c, ϕ, E_s), (b) shaft parameters (L_p, D), and (c) the geometry parameters (S/D, ξ, β). The software CurveExpert (1995, version 1.3) was used to establish best fit to data points.

The behavior of the load transfer factor with the variations of the slope/shaft parameters can be summarized as follows.

1. The load transfer factor variations with the parameters of the soil: this behavior can be seen from Figures 3.12-a, 3.12-b, and 3.12-c, and cab be summarized as below.
    - The load transfer factor increases proportionally with the soil cohesion, and c-η relationship is a power equation. This indicates that soils with

high cohesions are capable to carry major part of the driving stress. In such a case, the soil is coherent and its tendency to transfer stresses to the rigid boundaries is low.

- The load transfer factor increases linearly with the soil internal angle friction. Soil friction usually consists of five frictional components (basic, sliding, dilation, reorientation, and degradation), and for the soil which has high net internal friction usually the basic component of the internal friction is very high and independent of the soil conditions and failure. Therefore, even at failure condition, it is most likely for these types of soils to keep high internal frictions from the basic component. This friction prevents huge soil mass to move freely and to transfer its driving stresses to the drilled shaft.
- The load transfer factor is inversely proportional to soil elastic modulus based on a power equation. During the elastic stage, materials which have high stiffness have higher tendency to transfer stresses than these have small stiffness.

2. The load transfer factor variations with shaft layout and slope geometry. Figures 3.13-a, 3.13-b, and 3.13-c show the variations of the load transfer factor with S/D,ξ, and β. The effect of these parameters on the load transfer factor can be summarized as follows.
    - The load transfer factor increases with increasing S/D, based on logarithmic equation. As the distance between the shafts increases the

shafts tend to work as a single shaft and the soil loses its support (foothold) and its arching behavior.

- The load transfer factor decreases with increasing ξ based on a power equation. When the shaft location becomes closer to the toe of the slope, it is expected that a large amount of stresses could be transferred to the shaft due to the large moving soil block size.
- The load transfer factor decreases with increasing β. The relationship between η and $\tan\beta$ is a power equation. As the inclination of the slope increases, the driving component of the force increases in a high shaft load and small load transfer factor.

3. Figure 3.14 shows the relationship between the load transfer factor and the shaft parameters [L_p, D].
    - It can be seen that the load transfer factor decreases with the shaft length L_p based on the power equation.
    - The load transfer factor increases with the shaft diameter D up to a certain limit before reversing the trend, based on the modified power equation. Also, it can be seen that the load transfer factor is very sensitive to the shaft diameter when it is greater than 8 ft or smaller than 2.5 ft. In both cases, very small load transfer factors were obtained, which would result in very high and unrealistic shaft forces.

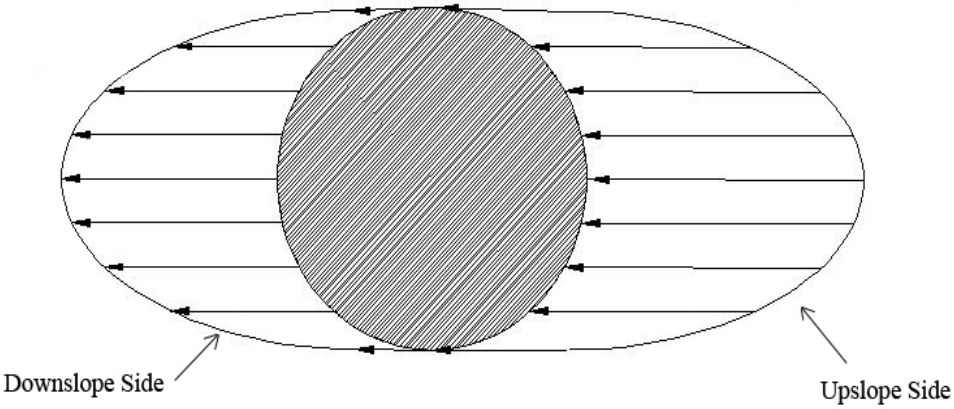

(a)

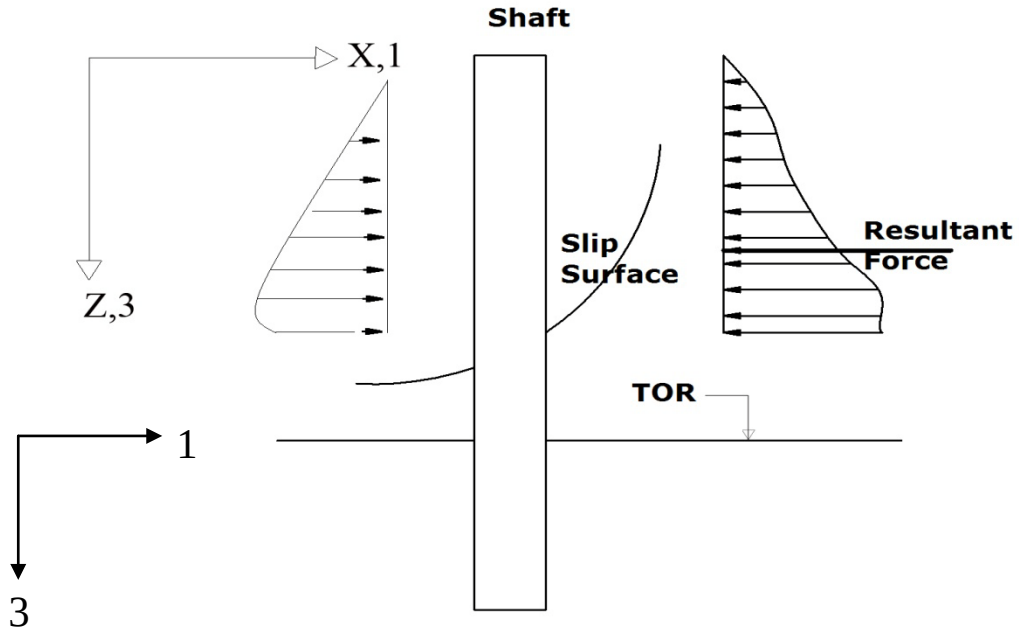

(b)

Figure 3.11: The Soil Stresses Distribution a) Around the Shaft Perimeter b) From the Top of the Shaft Down to the Failure Surface

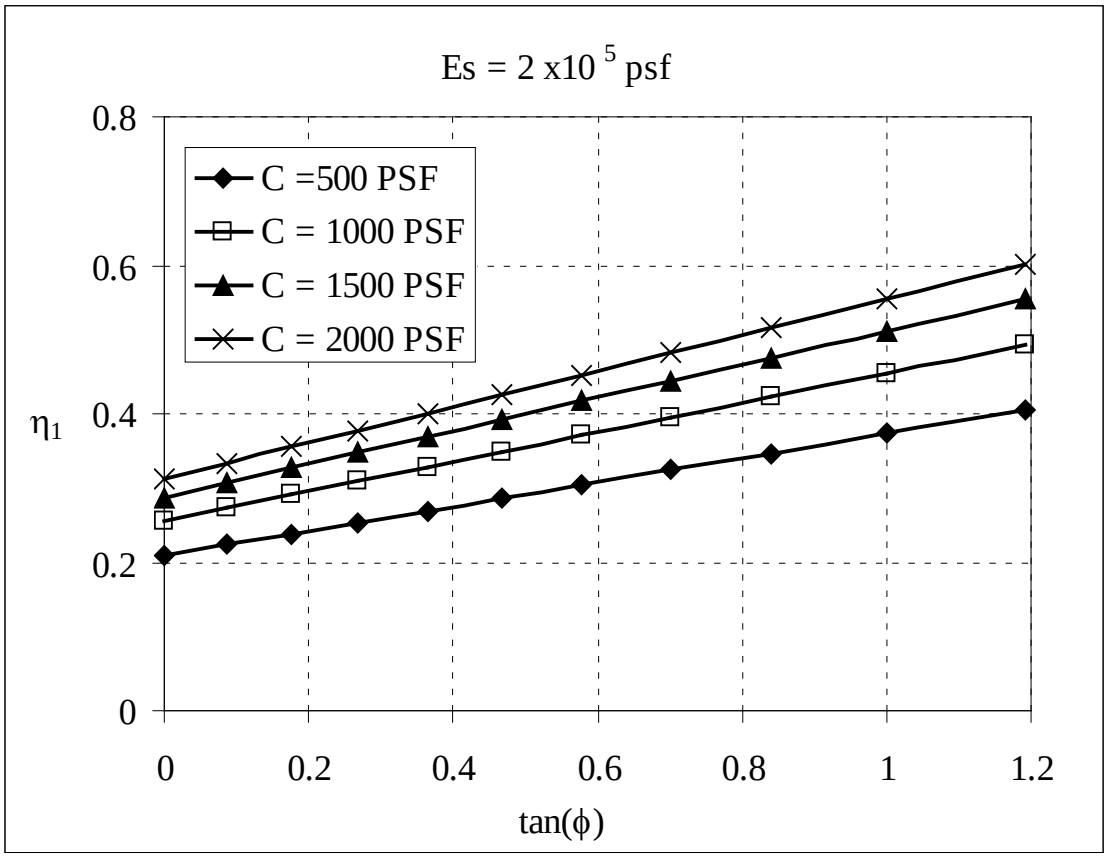

(a)

Figure 3.12: Variation of η versus c, and tan(ϕ) for Three Soil Modulus Values: (a) E_s = 2x 10^5 psf , (b) E_s = 8x 10^5 psf, (c) E_s = 15x 10^5 psf

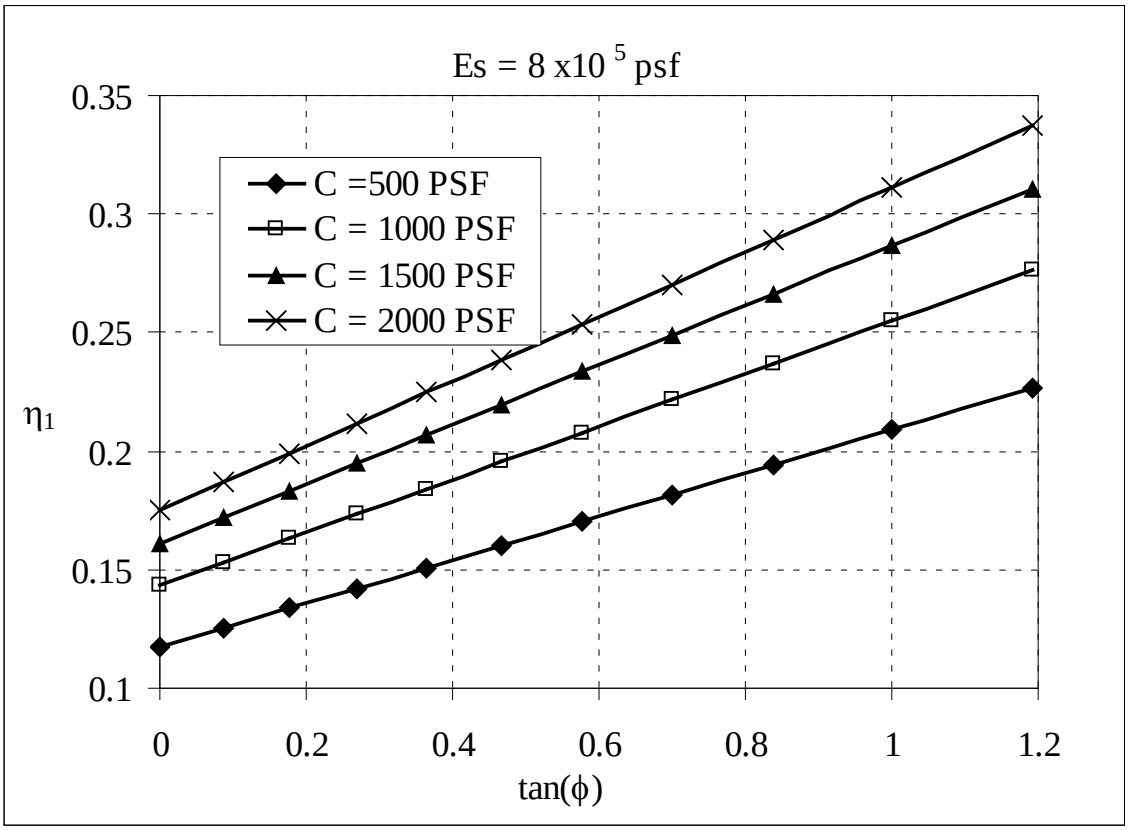

(b)

Figure 3.12: Variation of η versus c, and tan(ϕ) for Three Soil Modulus Values: (a) E_s = 2x 10^5 psf , (b) E_s = 8x 10^5 psf, (c) E_s = 15x 10^5 psf, Continued

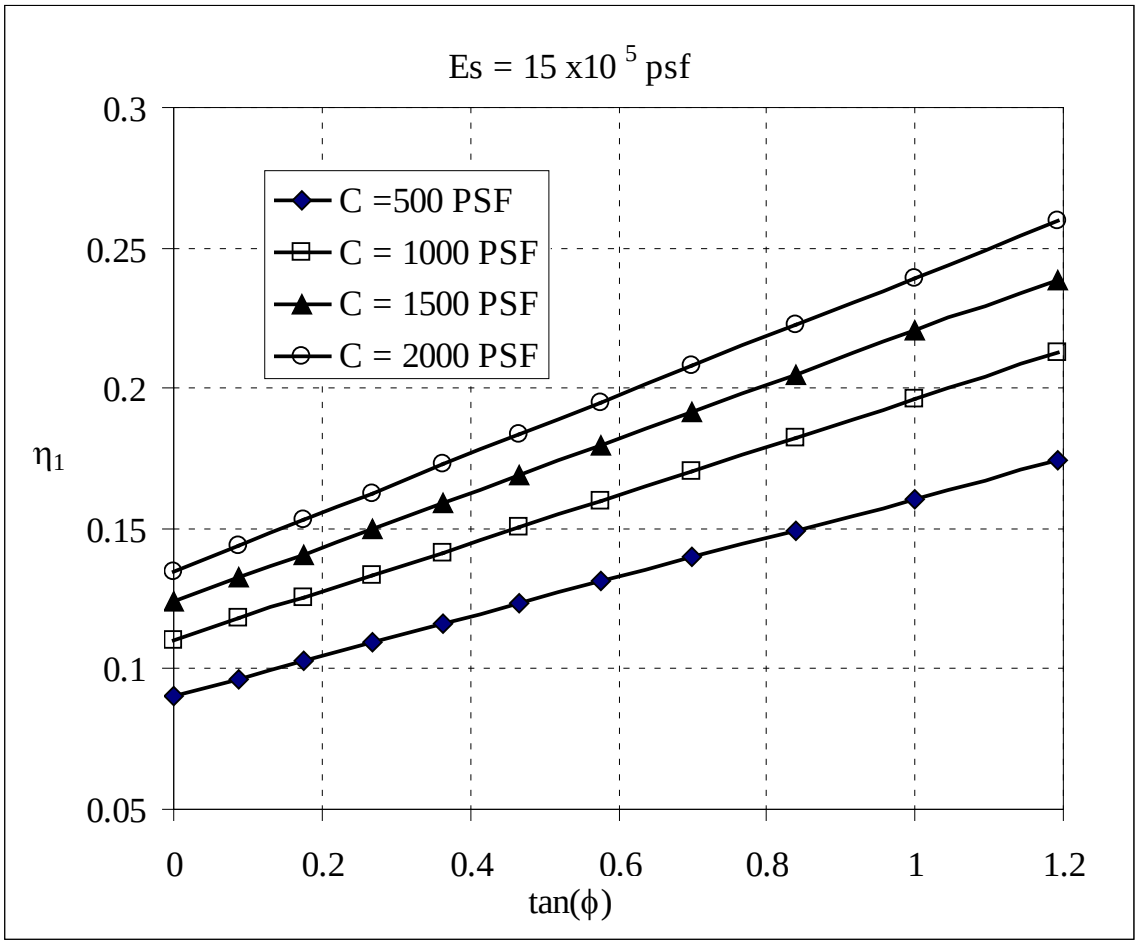

(c)

Figure 3.12: Variation of η versus c, and tan(ϕ) for Three Soil Modulus Values: (a) E_s = 2x 10^5 psf , (b) E_s = 8x 10^5 psf, (c) E_s = 15x 10^5 psf, Continued

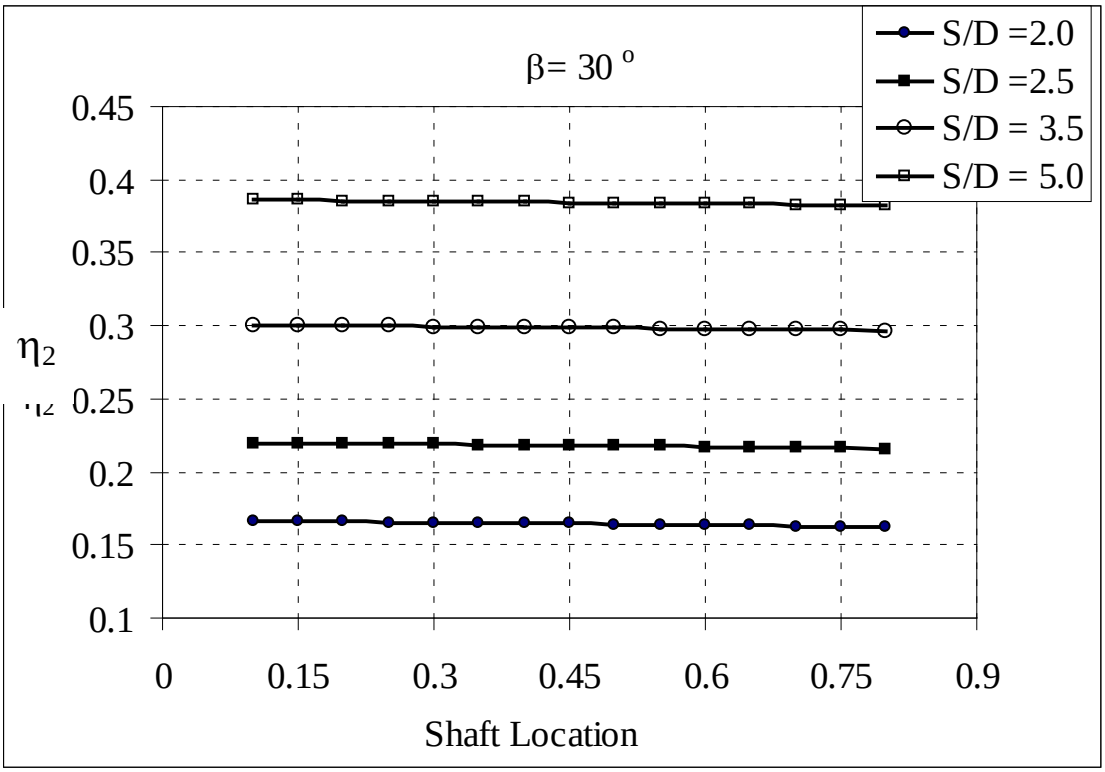

(a)

Figure 3.13: Variation of η versus Shaft Location and S/D for Three Slope Angles: (a) $\beta = 30^o$, (b) $\beta = 40^o$, (c) $\beta = 50^o$

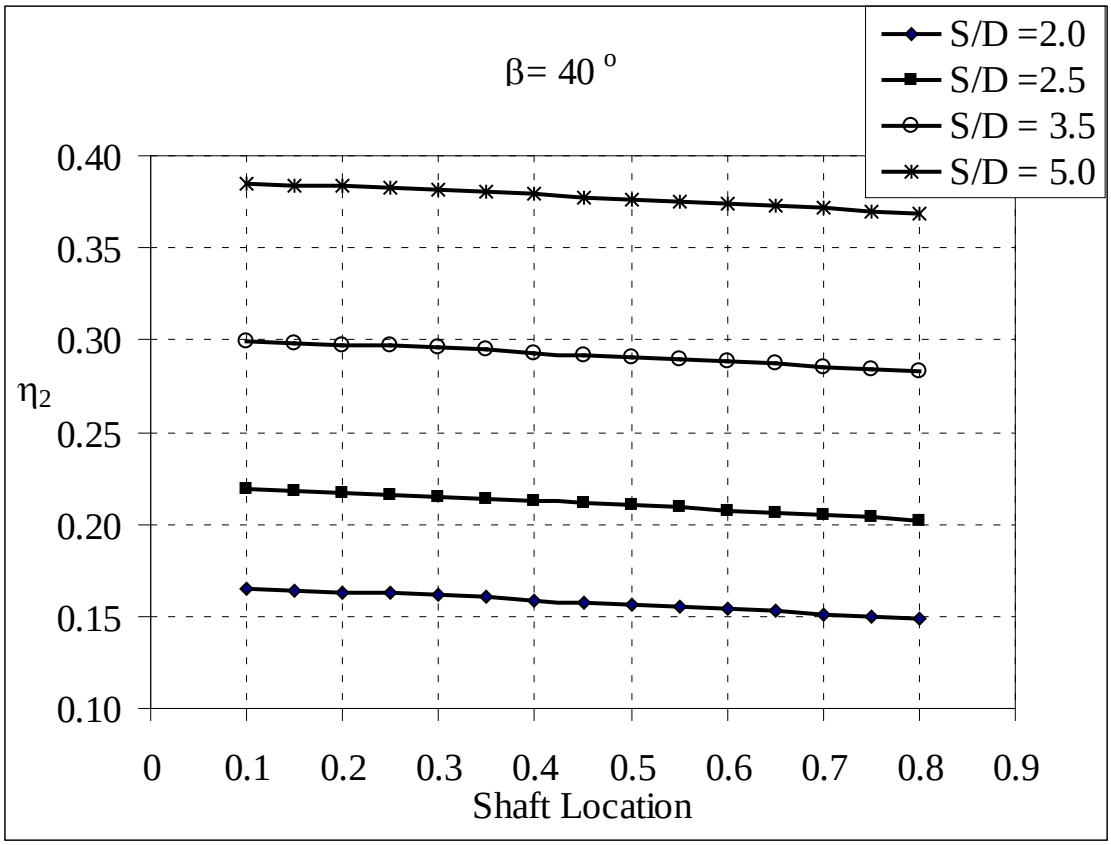

(b)

Figure 3.13: Variation of η versus Shaft Location and S/D for Three Slope Angles: (a) $\beta = 30^o$, (b) $\beta = 40^o$, (c) $\beta = 50^o$, Continued

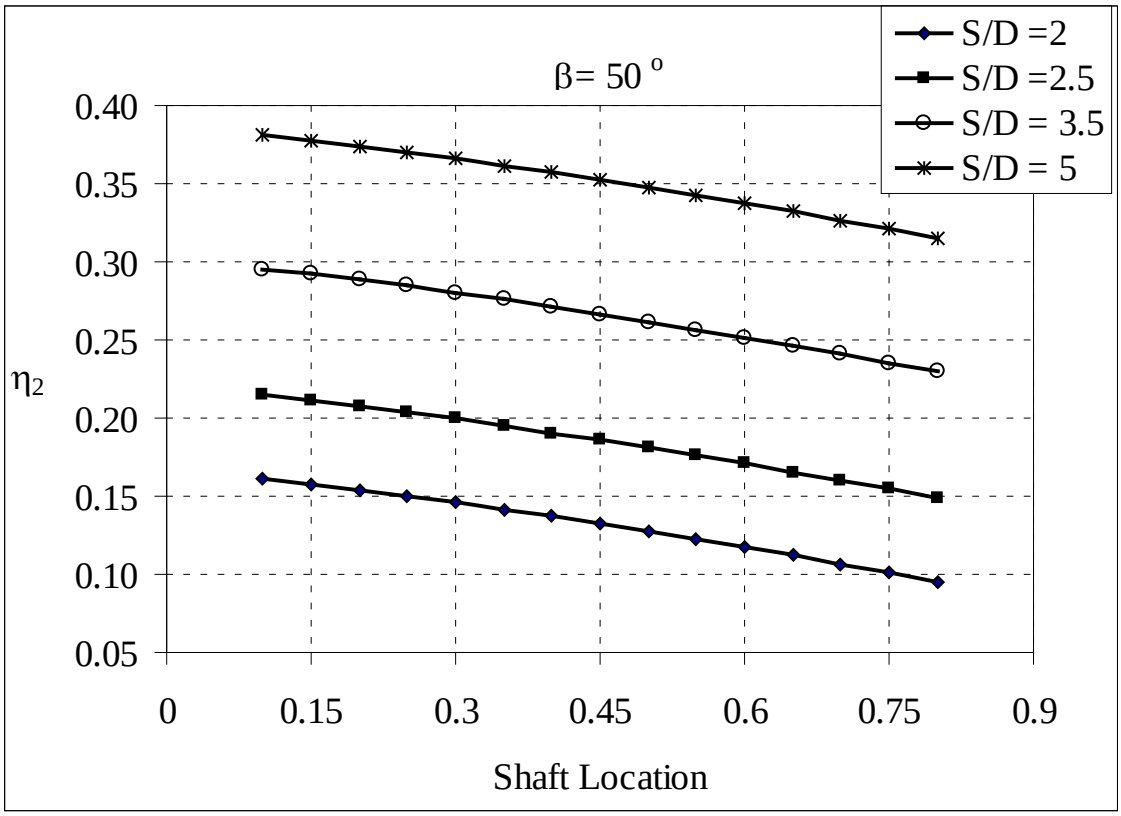

(c)

Figure 3.13: Variation of η versus Shaft Location and S/D for Three Slope Angles: (a) $\beta = 30^o$, (b) $\beta = 40^o$, (c) $\beta = 50^o$, Continued

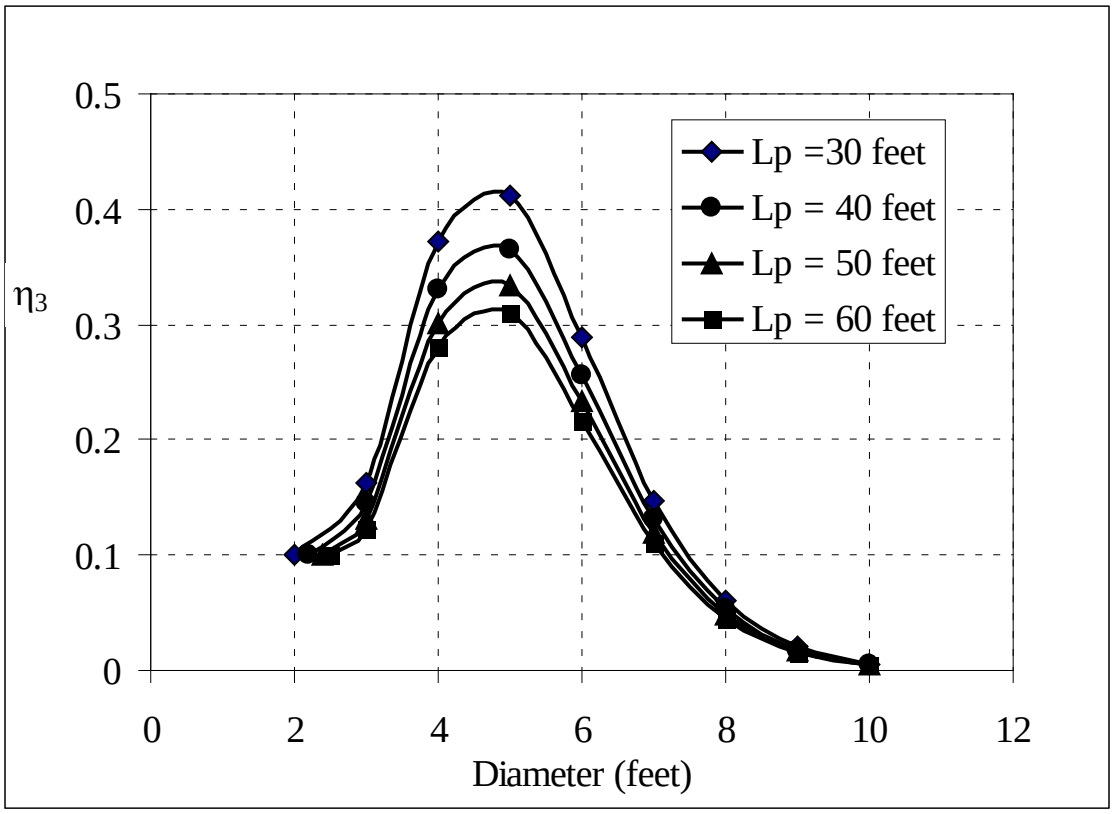

Figure 3.14: Variation of η versus Shaft Diameter and Shaft Length

All data set obtained from the finite element parametric study were utilized in the software SPSS to yield a set of mathematic equations for determining the load transfer factor. The equation of the load transfer factor η is given as follows:

$$\eta = \eta_1^{0.7}\eta_3^{0.76}\left(3.23 + 0.96\ln\eta_2\right) \tag{3. 7}$$

where

$$\eta_1 = \frac{c^{0.287}}{E^{0.418}}\left[0.018 + 0.256\tan\phi\right] \tag{3. 8}$$

$$E = \frac{E_s}{10^6} \tag{3. 9}$$

$$\eta_2 = 0.24\ln(S/D) - 0.047\xi^{3.95}\tan\beta \tag{3.10}$$

$$\xi = \frac{x_i}{X} \tag{3.11}$$

$$\eta_3 = \frac{0.004D^{11.2}}{L_p^{0.412}}(0.091)^D \tag{3.12}$$

$0 < \eta < 1.0$

$L_r > 0.15L_p$

The load transfer factor should be always greater than zero and less than one. The value of zero indicates that the drilled shafts would work as a wall and it takes all the earth thrust. On the other hand, when the load transfer factor equals to 1.0, it means that the drilled shafts exert no effect on arching.

η_1 represents the effects of the soil properties on the load transfer factor, regardless the values of the other parameters of the slope/ shaft system. The range of the values of η_1 can be as small as 0.05 (severe conditions) to 0.7 (good conditions). For average soil properties, it is about 0.25 to 0.3. It was also observed that the value of η_1 is inversely proportional to (E_s), meaning that when the soil has a high stiffness it could work effectively in stress transfer. As a result, a large amount of stresses could be transferred to the shaft, thus yielding a low load transfer factor. On the other hand, when the values of c, and ϕ increase, the soils have increased capability of carrying the stresses within the soil skeleton, reducing the amount of the load transferred to the drilled shaft, which in turn yields high values of load transfer factor.

η_2 represents the effect of the slope geometry and the layout (e.g., S/D) of drilled shafts. It ranges from 0.02 to 0.4, with a typical value of 0.25 for average slope angle. The load transfer factor increases with increasing S/D ratio due to the fact that the soil arching effect decreases with the increasing distance between the two adjacent drilled shafts. For a steep slope and drilled shaft located near the lower part of the slope, a large amount of soil thrust is to be transferred to the drilled shaft, thus giving a small value of load transfer factor.

The effect of the shaft length and shaft diameter is reflected by η_3. As the shaft diameter increases at a specific (S/D) ratio, the spacing between the drilled shafts increases. As a result, the soil loses some of its ability to transfer stresses and consequently the value of the load transfer factor will be high. However, when the drilled shaft diameter becomes exceedingly large, it works as a retaining wall and the load transfer factor begins to decrease. The effect of the shaft length is very small and it is inversely proportional to the load transfer factor. The possible range for η_3 is 0.015 to 0.5, with a value of 0.23 for typical S/D ratio and shaft locations.

For the purpose of checking the validity of the developed semi-empirical equations, the load transfer factor was calculated for all the considered FE models using Eq. 3.7. The results obtained from Eq. 3.7 were compared against the FE results as shown in Figure 3.15. It can be seen that there is a good agreement between the FE results and the results obtained from Eq. 3.7.

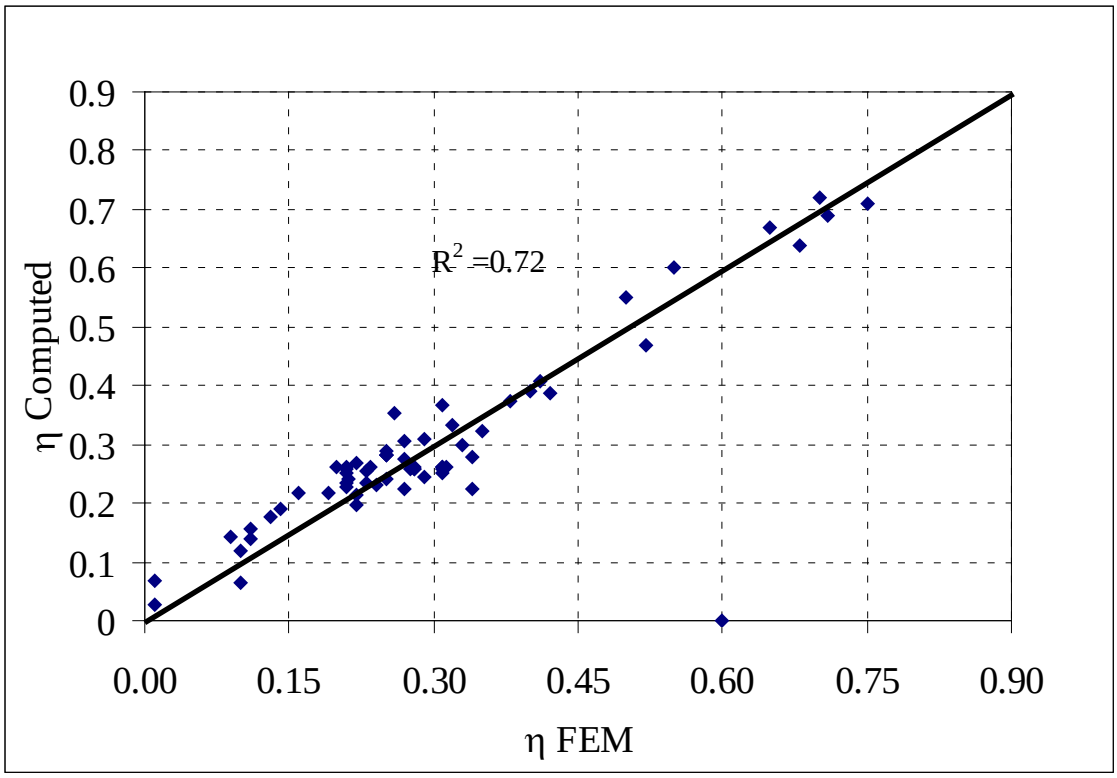

Figure 3.15: Comparison of Load Transfer Factor Computed by Semi-Empirical Equation and FEM

3.7 Resultant Net Force on Shaft

One of the objectives of this research work was to develop a simple equation that could be used to determine the amount and the distribution pattern of the horizontal force transferred from the moving soil to the drilled shaft in a slope/ shaft system. The effects of vertical stresses on the net resultant force on the shaft were not considered in this study because the difference between the vertical stresses on the up-slope and down-slope sides of the shaft is not significant. In addition, the axial force on the drilled shaft is not the controlling force for structural design of the drilled shaft.

The calculations of force distribution along the shaft were performed as follows. First, the failure surface in the slope was determined by tracking the zone of the plastic flow of the soil as shown in Figure 3.7. Next, the nodal horizontal soil stresses around the shaft on the up-slope and down-slope sides of the shaft were computed. The computed horizontal stress distribution on the up-slope and down-slope sides of the shaft are depicted in Figure 3.11-a. This process was repeated for every three feet of the shaft depth starting from the ground surface down to the determined failure surface. The up-slope side of stresses were integrated along the up-slope half of the shaft circumference to determine the up-slope side of force distribution. Similarly, the down-slope side of stresses were used to determine the down-slope side of force distribution along the shaft as shown in Figure 3.11-b. The mathematical equations for computing the net shaft force is as follows.

The up-slope side of force distribution can be obtained from the following integration

$$F(Z)_{up} = \int_0^{\pi D/2} \sigma_{xx} ds \tag{3.13}$$

Similarly, the down-slope side of force distribution is obtained as flows:

$$F(Z)_{Down} = \int_0^{\pi D/2} \sigma'_{xx} ds \tag{3.14}$$

Then net horizontal force distribution along the shaft is computed by subtracting the down-slope force distribution from the up-slope force distribution.

$$\mathrm{F(Z)_{net}} = \mathrm{F(Z)_{Up}} - \mathrm{F(Z)_{Down}} \tag{3.15}$$

$$\mathrm{F(Z)_{net}} = \int_0^{\pi D/2} \sigma_{XX} \mathrm{ds} - \int_0^{\pi D/2} \sigma'_{xx} \mathrm{ds} \tag{3.16}$$

For presenting the results in dimensionless terms, the net force distribution was normalized by $D\sigma'_V$, while the depth Z was normalized by the depth of the failure surface at the shaft location, L_f.

The statistical regression analysis was performed to explore the relationship between the normalized force and the normalized depth. It was found that the following equation can be used to describe the net normalized force distribution with the normalized depth.

$$\frac{F(\overline{Z})}{D\sigma'} = k_1 e^{k_2 \overline{Z}} \tag{3.17}$$

$$\overline{Z} = \frac{Z}{L_f}$$

The resultant shaft force (R) can be obtained by integrating $F(\overline{Z})$ from $\overline{Z} =$ 0.0 to 1.0

$$R = DL_f \gamma' \int_0^1 \overline{Z} k_1 e^{k_2 \overline{Z}} \tag{3.18}$$

By Integration by parts

$$R = L_f D\gamma' k_1 \left[e^{k_2} \left(\frac{1}{k_2} - \frac{1}{(k_2)^2} \right) + \frac{1}{k_2} \right] \tag{3.19}$$

D = the shaft diameter

σ' = the effective stress

K_1 and k_2 = constants to be discussed in detail later.

The coefficients K_1, K_2 of the exponential equation in Eq. 3.17 were analyzed via SPSS software. Semi-empirical equation of k_1 and k_2 are given below.

$$k_1 = \frac{2.3\overline{D}\exp\left(0.3\overline{E}_s + 0.3\xi\right)\left(S/\overline{D}\right)^{0.5}}{\overline{L}_p^{0.3}} \tag{3.20}$$

$$k_2 = \frac{\left(0.57 + 74\tan\varphi\right)\left(-1.24 + 0.74\xi\right)}{0.28 + 0.35\overline{c}} \tag{3.21}$$

where

$\overline{c} = \frac{c}{500}$ for the (pound-foot) units; $\overline{c} = \frac{c}{23.94}$ for (kN-M) units;

$\overline{D} = \frac{D}{4}$ for the (pound-foot) units; $\overline{D} = \frac{D}{1.2}$ for (kN-M) units;

$\overline{L}_p = \frac{L_p}{50}$ for the (pound-foot) units; $\overline{L}_p = \frac{L_p}{15.0}$ for (kN-M) units

The forces obtained from Eq. 3.19 were compared with finite element results in Figure 3.16. It can be seen that most points are banded around the equality line, indicating good agreement between the FE results and the empirical equation.

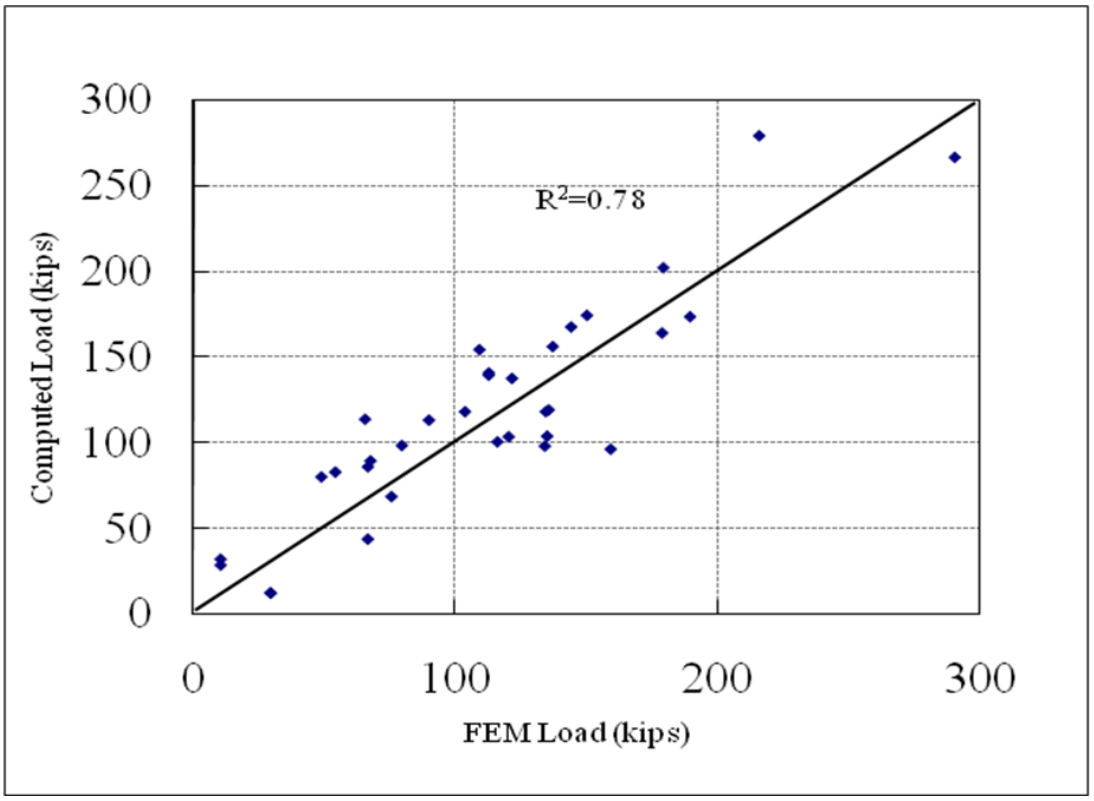

Figure 3.16: Comparison of Net Force on Shaft by Semi-empirical Equations and FEM

3.8 Summary and Conclusions

As a part of research to quantify the arching phenomenon in a drilled slope/ shaft system, a well designed and systematic 3-D finite element parametric study using ABAQUS commercial software was conducted. An innovative method of strength reduction technique together with the use of temperature field for automatic execution of strength reduction based on the prescribed temperature variation with time has helped in running the parametric study more efficiently. From the finite element parametric analysis results, semi-empirical mathematic expressions were developed for the load transfer factor for describing the drilled shaft induced soil arching effect in a slope/ shaft system, where the soil can be characterized as a c-ϕ material satisfying Mohr-Coulomb

strength criterion. This finite element study revealed the major factors controlling the load transfer process between the soil and the reinforcing drilled shafts in a drilled shaft stabilized slope under the effect of shear strength reduction. These influencing factors included the soil strength parameters (cohesion, angle of internal friction, and elastic soil modulus), drilled shaft dimensions (diameter, length), and geometry and arrangement (shaft location, the shaft spacing to diameter ratio, and the slope angle).

The load transfer factor was defined in this chapter, which was used to reflect the force transferred from the soil to the drilled shaft in a slope/ shaft system. The use of load transfer factor in a limiting equilibrium slope stability analysis framework will be discussed in Chapter IV. The values of the load transfer factor are bounded between 0.0 and 1.0. The zero value of the load transfer factor indicates that the row of drilled shafts work like a continuous wall and it takes all the earth thrust from the upslope soil movement. On the other hand, when the load transfer factor approaches 1.0, it means that the drilled shafts exert very little influences on arching in the slope/shaft system.

Semi-empirical equations based on regression analysis of finite element parametric analysis results were obtained to allow the computation of the load transfer factor. The load transfer factor obtained from the semi-empirical equations was shown to match quite well with the results obtained from the finite element analysis. However, it should be mentioned that the semi-empirical equations worked well for shaft diameter in the range of 2 ft to 6 ft and the shaft rock socket length is at least 15% of the total shaft length.

Based on analysis of finite element parametric study, semi-empirical equations were developed for estimating the net force on the drilled shaft and its distribution along

the shaft length. The resultant force obtained from the developed equations was compared quite well with the force obtained from the finite element analysis results.

CHAPTER IV

DESIGN METHOD BASED ON LIMITING EQUILIBRIUM AND ARCHING CONCEPT

In this chapter, the method of slice stability analysis method for a slope, with or without the presence of a single row of spaced drilled shafts, was developed to incorporate the arching induced load transfer effect in a slope/shaft system. A PC based, user friendly computer program, UA SLOPE 2.0, was developed from the modification of an earlier program, UA SLOPE (Liang, 2002). The modifications of the computer program involved the adoption of the newly developed load transfer factor through 3-D finite element simulation parametric studies wherein the strength reduction technique was used to facilitate reaching a failure state of a slope/shaft system. A step-by-step design procedure was outlined in this chapter, followed by a presentation of a design example. The validity of the developed method and the accompanied computer program, UA SLOPE 2.0, was established by excellent comparisons with 57 cases of 3-dimensional finite element simulation results using ABAQUS finite element program and the strength reduction technique. The validity of UA SLOPE 2.0 program was further ascertained by a comparison with test data from the ATH-124 load test program.

4.1 Problem Formulation

The analysis and design for using a single row of drilled shafts to stabilize an unstable slope, in general, needs to address both geotechnical as well as structural design issues. The geotechnical issues deal with assessing the geotechnical factor of safety of a repaired or re-constructed slope using the drilled shafts as the primary stabilization means. The structural design issues concern with assessing the structural capacity needs of the drilled shafts for carrying the developed internal forces and moments as well as for limiting the deflection of the drilled shafts subjected to the earth thrust from the soil mass of the slope.

An unstable slope or a failed slope can be stabilized or restored with the use of a single row of drilled shafts, due to the arching phenomenon presented in Chapter III. With the driving stresses of the moving soil mass in the slope partially transferred to the drilled shafts through the arching effects, the driving stresses on the down-slope side of the drilled shafts are reduced, thus resulting in increase of the geotechnical factor of safety of the slope/shaft system. The amount of this driving stress reduction due to arching phenomenon is influenced by the relative movement between the soil and the shaft as well as soil strength parameters and layout of drilled shafts. In the study presented in Chapter III, the arching induced load transfer factor in a slope/shaft system was determined at the stage of incipient failure of the slope/ shaft system, thus representing the ultimate state. Furthermore, the study presented in Chapter III showed that the arching induced load transfer factor in a drilled slope/ shaft system is dependent upon the factors such as: soil properties (ϕ, c, E_s), shaft parameters (D, L_p), and slope

geometry and shaft layout (β, ξ, S/D). Consequently, the design parameters of the slope/shaft system should include an optimization approach to determine the location, length, diameter, and spacing of the drilled shafts.

The structural capacity of the drilled shaft should satisfy the design requirements for the load transferred from the soil thrust. The structural analysis of a drilled shaft subjected to the arching induced loads can be carried out using the existing laterally loaded drilled shaft analysis approach such as LPILE computer program or its equivalent software. The key is to input appropriate loads and p-y curve representations in the LPILE analysis.

4.1.1 Overview of Chapter Organization

In this chapter, a method of slices analysis based on limiting equilibrium is developed for calculating global factor of safety (FS) of a slope with or without the presence of a row of drilled shafts. Force equilibrium was satisfied for each individual slice in the mathematic formulation, while the arching effect due to drilled shafts was accounted for by the load transfer factor. The newly developed UA SLOPE 2.0 computer program, incorporating the mathematic formulation of the limiting equilibrium method of slices, is presented. The design method using the UA SLOPE 2.0 program as a tool for optimization of the design of the drilled shafts stabilized slope is presented. The validation of the developed method and the accompanied UA SLOPE 2.0 program is provided by comparisons with the 3-D finite element simulation results and the special field load testing program at the ATH-124 project. Details of the ATH-124 load test

program and the measured results, in comparison with UA SLOPE 2.0 predictions, are presented. The comparisons with both theoretical finite element simulation results as well as with calibrated finite element simulations of the ATH-124 case provide strong evidence of the validity of the developed design method and the accompanied UA SLOPE 2.0 computer program.

4.2 Limiting Equilibrium Formulation Incorporating Load Transfer Factor Due To Soil Arching

The limiting equilibrium method developed by Zeng and Liang (2002) is modified herein by incorporating the newly developed load transfer factor discussed in Chapter III. Figure 4.1 provides a schematic illustration of the method of slices analysis for calculating the factor of safety of a slope. It is noted that the presence of the drilled shafts was treated in the analysis as a virtual drilled shaft without physically occupying the space; however, the drilled shaft effects were taken into account through the load transfer factor concept. The essence of the modifications made to the conventional limiting equilibrium method was that at the location of the drilled shafts, a significant portion of the driving forces on the up-slope side of the drilled shaft were transferred from the soil mass to the drilled shaft due to arching, thus reducing the driving force on the down-slope side of the drilled shaft.

The modified method of slice analysis method was developed based on the following assumptions:

(1) FS was assumed to be the same along the entire failure surface.

(2) The normal force on the base of the slice was applied at the midpoint of the slice base.

(3) The location of the thrust line of the inter-slice forces was placed at one-third of the average inter-slice height above the failure surface, as in Janbu (1973).

(4) The inclination of the inter-slice forces was assumed as depicted in Figure 4.2. The right-inter-slice force (P_{i-1}) was assumed to be parallel to the inclination of the preceding slice base (i.e., α_{i-1}), while the left-inter-slice force (P_i) was assumed to be parallel to the current slice base (i.e., α_i).

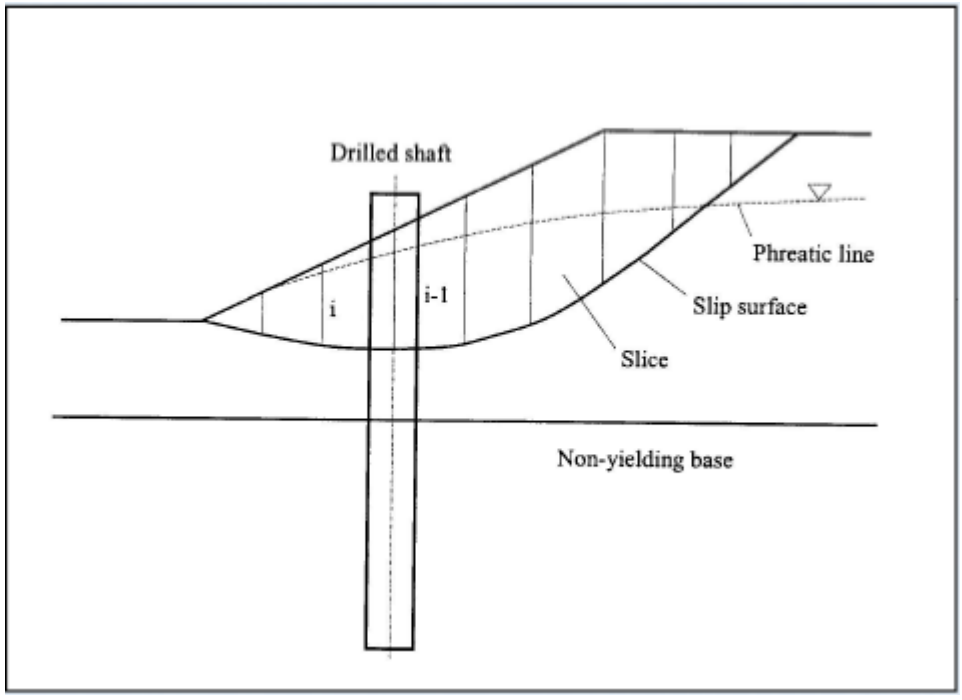

Figure 4.1: A Typical Cross-Section Divided into Slices for a Slope Reinforced with Single Row of Drilled Shafts

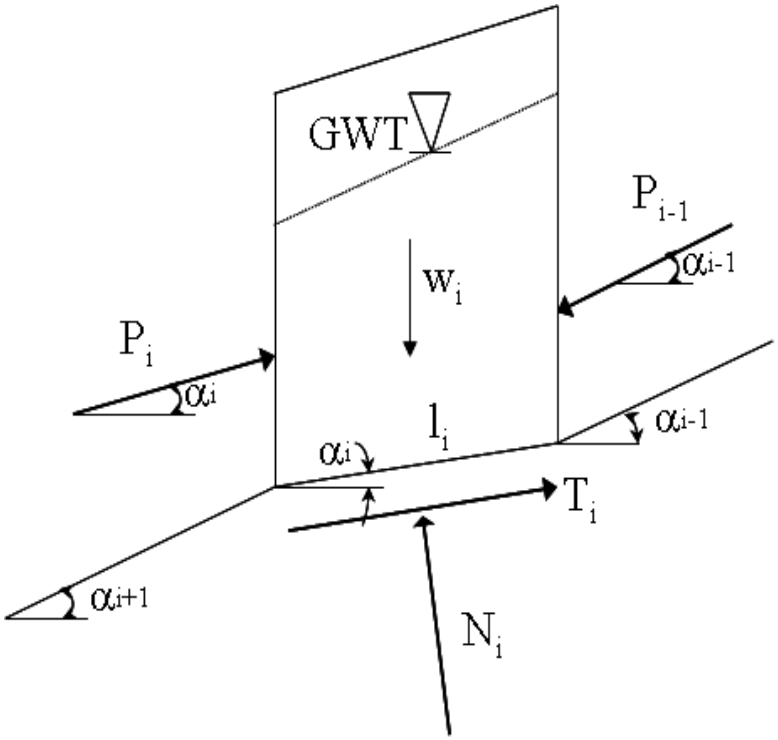

Figure 4.2: A Typical Slice Showing All Force Components

Referring to Figures 4.1 and 4.2 and applying the equilibrium method of slices for any slice i of the slope, the summation of the forces in the direction normal to the base of the slice and in the tangential direction yields the following two equations, respectively:

$$N_i - w_i \cos\alpha_i - P_{i-1} \sin(\alpha_{i-1} - \alpha_i) = 0 \quad (4.1)$$

$$T_i + P_i - w_i \sin\alpha_i - P_i \cos(\alpha_{i-1} - \alpha_i) = 0 \quad (4.2)$$

Applying Mohr-Coulomb equation

$$T_i = \frac{c_i l_i}{FS} + [N_i - u_i l_i] \frac{\tan\phi}{FS} \quad (4.3)$$

Substituting Eq.4.1 and Eq.4.2 into Eq.4.3 yields the following equation:

$$T_i = \frac{c_i l_i}{FS} + \left[w_i \cos\alpha_i + P_{i-1} \sin(\alpha_{i-1} - \alpha_i) - u_i l_i \right] \frac{\tan\phi}{FS} \quad (4.4)$$

Finally

$$P_i = w_i \sin\alpha_i - \left[\frac{c_i l_i}{FS} + (w_i \cos\alpha_{i-1} - u_i l_i) \frac{\tan\phi}{FS} \right] + k_i P_{i-1} \quad (4.5)$$

$$k_i = \cos(\alpha_{i-1} - \alpha_i) - \sin(\alpha_{i-1} - \alpha_i) \frac{\tan\phi}{FS} \quad (4.6)$$

P_i = the inter-slice force acting on the left side of slice

P_{i-1} = the inter-slice force acting on the right side of slice

α_i = the slope of the base of the slice i

Eq. 4.5 and Eq. 4.6 relate the inter-slice force P_i to the inter-slice force P_{i-1} for slice i. An iterative computational scheme is required to satisfy boundary load conditions and equilibrium requirements, along with Mohr-Coulomb strength criterion, to find the FS.

Eq. 4.5 is used for all slices except for the slice (i) which is right behind the drilled shafts. The inter-slice force acting on the interface (i-1), with respect to the boundary of slice (i), is reduced to $R_\eta P_{i-1}$, where η is the load transfer factor due to the soil arching arising from a row of drilled shafts installed on the slope, and R_η is the average load reduction factor along the spacing between the centers of two adjacent shafts. Replacing P_{i-1} with $R_\eta P_{i-1}$ in Eq. 4.5 results in

$$P_i = w_i \sin\alpha_i - \left[\frac{c_i l_i}{FS} + (w_i \cos\alpha_{i-1} - u_i l_i) \frac{\tan\phi}{FS} \right] + k_i R_\eta P_{i-1} \quad (4.7)$$

This equation should be used to calculate the P_i located just behind the drilled shaft. It should be noted that the physical existence of the drilled shaft was not

represented by a soil slice, but the effect of the drilled shaft was accounted for by the load transfer factor.

The reduction factor R_η is derived based on the method developed by Zeng and Liang (2002) as follows. The reduction factor was defined by Zeng and Liang (2002) as in Eq. 4. 8.

$$R_\eta = \frac{1}{s/d} + \left(1 - \frac{1}{s/d}\right) R_p \tag{4. 8 }$$

The force up-slope the shaft and the force down slope the shaft were defined by Eq. 4.9 and Eq. 4.10, respectively.

$$F_{shaft}^{up} = P_{i-1} d + (1 - R_p) P_{i-1} (s - d) \tag{4. 9}$$

$$F_{shaft}^{down} = P_{i-1} d \tag{4. 10}$$

In chapter III, the load transfer factor was defined by

$$\eta = \frac{F_{shaft}^{down}}{F_{shaft}^{up}} \tag{4. 11 }$$

From Eq. 4.9, Eq. 4.10, and Eq.4.11, a relationship between the factor R_p and the load transfer factor η can be derived.

$$\eta = \frac{d}{d + (1 - R_p)(s - d)} \tag{4. 12}$$

Finally, the factor R_p can be obtained from Eq. 4.13

$$R_p = \frac{\eta s - d}{\eta (s - d)} \tag{4. 13}$$

The factor R_p obtained from Eq. 4.13 can be used in Eq. 4.8 to calculate the reduction factor R_η; therefore, the reduction factor can be implemented in Eq. 4.7 for conducting the stability analysis for a slope-shaft system.

4.2.1 Drilled Shaft Force

Within the framework presented in the above section for determining the FS of a slope reinforced with a row of drilled shafts, the force imparted on the drilled shaft can be estimated by calculating the difference between the force on the up-slope side of the shaft and the force on the down-slope side of the shaft.

$$F_{shaft} = F_{up-slope} - F_{down-slope} \tag{4. 14}$$

Substituting Eq. 4.9 and Eq. 4.10 into Eq. 4.14, the following equation is obtained:

$$F_{shaft} = (1 - R_p) P_{i-1} (s - d) \tag{4. 15}$$

where

F_{shaft} = the total force imparted onto the shaft due to arching

s = center-to-center spacing between two adjacent drilled shafts

d = drilled shaft diameter

From Eq. 4.13 and Eq. 4.15, one can see that as the load transfer factor η increases, the total force imparted onto the shaft decreases. If η =1, this means that there is no arching. According to the proposed arching concept, then the global FS of the slope is not affected by the presence of the drilled shafts. This, of course, is not necessarily true and should be considered as one of the limitations of the method. For a case where small

values of η are present, then it implies that a large amount of force is transferred from the soil to the drilled shaft. When η = 0.0, this indicates that the shafts work as a wall unit so that the forces on the drilled shafts are derived from the driving stresses. Again, the present arching concept was not intended to apply for the two extreme cases: η = 0.0 and η =1.

Once the resultant shaft force is obtained from Eq. 4.15, the structural design of the drilled shaft can be conducted in a straightforward procedure by using the commercial program, such as LPILE or the equivalent laterally loaded pile analysis software. The structural design procedure for using LPILE program was detailed in Chris et al. (2007). This procedure suggested that a shear force equal to the net total force calculated from Eq. 4.15 and a moment equal to the shaft force multiplied by one-third of the distance between the top of the shaft and the slip surface be applied as the boundary forces to the drilled shaft at the location of the slip surface.

4.3 UA SLOPE 2.0 Computer Program

The computer program UA SLOPE 2.0 was developed based on the earlier computer program UA SLOPE 1.0 (Liang, 2002) with necessary modifications to incorporate the newly obtained load transfer factor presented in Chapter III of this dissertation. This computer code can be used in two different procedures. In the first approach, the user can input the load transfer factor and solve for FS for different locations of the drilled shafts. This approach is used for conducting an optimization analysis in which the optimum shaft location, the minimum shaft force, and the optimum

S/D can be determined from the computer runs. The second procedure is used when the parameters of the slope/shaft system are defined, which can be input to the computer code to obtain the shaft force and the factor of safety of the slope/shaft system directly. Essentially, in the first procedure, the input parameters are the load transfer factor and the location of the drilled shaft; whereas, along with slope geometry and relevant soil properties in the second procedure, the input parameters are the shaft diameter, the soil properties, the shaft diameter, the shaft location, the shaft length, spacing to diameter ratio, and the slope angle. The use of the later approval is intuitive and straightforward.

Some of the pointers in using the UA SLOPE 2.0 are provided herein. The UA SLOPE 2.0 set a limit of twenty (20) for the maximum number of soil layers that could be used to represent the soil layers of the slope. In computing factor of safety of the slope with or without the drilled shafts, the actual input soil layer information was used. However, for calculating the load transfer factor, the soil properties of different soil layers were averaged along the drilled shaft length to yield a single value from which the load transfer factor was computed. The slip surface location and the location of the ground water table are separately input in the UA SLOPE 2.0. However, it should be noted that the computer program is very sensitive to the shape of the slip surface. The near vertical segment of the slip surface should be avoided. If there was any vertical or near vertical segment (e.g., tension crack) of the slip surface, it should be judiciously flattened to avoid the computational run time error and divergence problems. In addition, irregularities and kinks in the slip surface should be smoothened to avoid computational errors. The UA SLOPE 2.0 program can perform both the total stress analysis and the effective stress analysis. If the load transfer factor is computed internally by the computer

program based on the equations provided in Chapter III, the effective stress method should be used.

4.4 Design Method

Design of a slope/shaft system implies that there is a set of the system parameters that should be determined and optimized, such that they would satisfy both the geotechnical and structural design requirements to assure safety of the slope and to reduce the construction cost as well. The geotechnical design parameters are as follows: shaft diameter (D), shaft location (ξ), shaft spacing to shaft diameter ratio (S/D). The shaft length is dictated by the geometry of the slope and the location of the slip surface to ensure that enough socket length in a firm stratum is achieved and to limit the drilled shaft deflection under service condition to be within the allowable deflections. In some situations, it is required to reconstruct the slope such that the slope angle (β) could also be part of design parameters. The above mentioned design parameters should be determined to satisfy the target factor of safety FS_{target} of the slope/shaft system. The design of the drilled shafts for stabilizing a slope could be conducted in two ways: 1) to determine the required load transfer factor η from the target factor of safety FS_{target}, then the design parameters of the slope/shaft system could be selected to return this required value of η, 2) to select the design parameters and find η corresponding to the selected parameters, then the factor of safety is determined and compared to the F_{target}. If the determined factor of safety is less than the target factor of safety, then the design parameters should be modified in a way to improve the stability (for example; increase D,

reduce S/D). Once the new set of the parameters is selected, the new load transfer factor and the new factor of safety, corresponding to the new design parameters, are determined from UA SLOPE 2.0 program. This procedure should be repeated until the target factor of safety is obtained and the structural design of the drilled shafts is optimized.

UA SLOPE 2.0 provides the computed force on the shaft. Once the shaft force is obtained, the LPILE program can be used to compute the following information for structural design: the lateral shaft displacement, bending moments, and shear forces.

4.4.1 Step-by Step Design Procedure

For the convenience of the design engineers to use the developed method easily in practice, the computer code UA SLOPE Version 2.0 was developed to handle the analysis and design procedure of a slope reinforced with a row of spaced drilled shafts. The step by step procedure described herein provides more in-depth elucidation of the design approach using the developed framework of analysis equations. In practice, with the availability of UA SLOPE 2.0 program, the design engineer needs not to follow precisely this step-by step procedure, as the computer program can be easily used to optimize the design parameters to meet both safety and economy requirements.

1. Determine FS_o of the existing slope. The location of the existing slip surface and the relevant soil properties, such as strength parameters and unit weight of each soil layer present at the site, need to be carefully determined and assessed by the experienced geotechnical engineers based on thorough and comprehensive site investigation results. Typically, the strength parameters of the slip surface of the existing slope may

need to be back analyzed to obtain F.S. of 1.0 in reproducing the failure condition of the existing failed slope.

2. Specify a target factor of safety (FS_{target}) to be achieved for the slope/shaft system.
3. Specify the possible locations of drilled shafts where they can be placed within the slope. The decision could be dictated by the practical issues such as equipment accessibility, the depth to the firm strata, the feasibility of drilled shafts construction, etc. If no other factors present, the most likely location of the stabilizing drilled shafts would be in the lower half of the slope.
4. Select an initial shaft diameter D and center to center spacing S; therefore, implying selection of a spacing-to-diameter ratio S/D. Do not use S/D less than two or above four.
5. Calculate FS using UA SLOPE 2.0 for the selected D, S and shaft locations defined by ξ
6. Determine the net force imparted onto the drilled shafts using UA SLOPE 2.0 output for each case analyzed.
7. Repeat Steps 4 – 6 for other possible shaft diameters and spacing.
8. For the results obtained from Step 5 to 7, create plots relating the net force versus shaft location and FS versus location for the range of D and S/D selected in the Steps 4 to 7.
9. From the generated relationships between Net force and FS versus shaft location for different D and S/D values, the design engineer can choose the optimum location of the drilled shafts which satisfies the required factor of safety and generates the

smallest net force on shaft. If the target FS cannot be achieved with the trial range of D, S/D, and shaft location, then larger D should be tried and the process be repeated.

10. From the selected design parameters, the design load on the drilled shaft can be determined.
11. From the steps mentioned above, one can choose appropriate set of (D, ξ, S/D, and F_{shaft}) for subsequent structural design of the drilled shafts.
12. Perform structural analysis to design the shaft for transverse shear, flexural moment, and fixity. The computer program LPILE can be used to determine the lateral shaft movement, shear, and moment diagrams. The structural analysis using LPILE can be performed by using the reduced shaft length, which means that only the portion of the shaft below the slip surface is modeled. The boundary conditions at the top of this portion of shaft are as follows: a shear force equal to the net shaft force computed from UA SLOPE 2.0 program, and a bending moment equal to one-third of the distance between the slip surface and the top of the shaft multiplied by the net shaft force. Once the un-factored forces and moments are calculated, they should be factored with a load factor of 1.7 to obtain the factored design loads.
13. If structural capacity of the drilled shaft cannot be met with the chosen combination of D, S/D, and shaft location, then a larger shaft diameter needs to be considered and the above process should be repeated.

4.4.2 General Remarks on Selection of Design Variables

- Shaft Location (ξ): if the selection of the shaft location is restricted to specific places due to right of ways or construction equipment accessibility issues, the designer should chose these permissible locations in the design and optimization process. If within the selected locations, the designer cannot achieve the target FS for the reinforced slope, then the designer should attempt to alter other design parameters, such as D and S/D. If there is no restriction on the specific location of the drilled shafts, then usually, the drilled shafts can be initially located near the lower half of the slope. Nevertheless, it is recommended that the value of ξ remains within the range of 0.2 to 0.8.
- Shaft Diameter (D): as a starting point, drilled shafts diameter can be initially taken as 4 ft. After that, the designer can increase or decrease the shaft size as needed and the results can be compared. ODOT has shown preference for 3 ft diameter shafts. The economic benefits of 3 ft diameter shafts need to be established on a case by case basis. Usually, both structural and geotechnical related design issues control the selection of the shaft diameter. In all cases, the shaft diameter should be within the range between 2.5 ft and 8.0 ft when UA Slope 2.0 program is used.
- Spacing-to-diameter ratio (S/D): usually this ratio can be taken between 2 and 4 to ensure the development of soil arching. In other words, this range of S/D values would allow for the row of drilled shafts to work effectively in offering the stabilization effects while economizing the required number of drilled shafts.

- Shaft Force (F_{shaft}): usually controls the structural design of the drilled shafts. If the required steel reinforcement cannot be fit into the selected diameter of the drilled shaft or the drilled shafts deflect beyond the allowable deflection under the working loads, the engineer can resolve this issue by taking one of the following actions: (a) select another shaft location where the inter-slice forces at that location are less, (b) decrease the spacing-to-diameter ratio, and (c) increase the shaft diameter.
- The methodology was developed based on the effective stress analysis; therefore, whenever UA SLOPE 2.0 was used for design analysis, the strength parameters and ground water conditions should be properly input into the computer program.
- The finite element parametric analysis performed in Chapter III included an implicit assumption in shaft rock socket length. Therefore, the designer should select the shaft socket length (L_r) to be equal or greater than 15% of the total shaft length (L_p).
- For slopes which have inclination angle greater than 60 degrees, there might be computational convergence problem. Therefore, UA SLOPE 2.0 program is not recommended for any slope with slope angle greater than 60 degree.
- It is unlikely for the soil in the slope to have an angle of internal friction greater than 55 degree, or it is even unlikely to have a failure in such a case. Therefore, no numerical convergence is expected to be obtained for soils that have angle of internal friction greater than 55 degrees.
- The value of cohesion of the soil should be less than 2500 psf, since this is the limit of parametric analysis in Chapter III.
- It should be pointed out that UA SLOPE 2.0 program is sensitive to the input of slip surface location. To obtain good results, some smoothening should be made to the

shape of the slip surface if it contains too many jagged shapes or kinks. The near vertical initial segment of the slip surface would usually yield un-reasonable factor of safety with UA SLOPE 2.0 program and should be judiciously modified to avoid this kind of numerical error.

- There is no limitation on the slope height in using UA SLOPE 2.0 program, as long as the slope angle is less than 60 degree.

4.4.3 Illustrative Example

This illustrative example uses the same site information as the ATH-124 project. Shown in Figure 4.3 is the plan view of the site, and in Figure 4.4 a representative cross-section of the slope. The soil properties of the simplified soil layers at the site based on several site investigation reports are tabulated in Table 4.1. The location of failure surface was determined based on on-site inclinometer readings available from several geotechnical reports for the ATH-124 project. The computer program UA SLOPE 2.0 and Gtable7 with STEDwin (2003) were used independently to conduct back analysis for the failed slope. The failure state (FS =1.03) was obtained from both computer programs with a residual angle of internal friction along the slip surface $\phi=15.5^{o}$.

Table 4.1: Summary of Material Parameters at ATH-124 Site

Zone	Material Description	c (psf)	ϕ^o	γ(pcf)
1	Cohesive fill(A-6b)	200	30	133.5
2	Granular fill (A-1-b)	0	40	135.6
3	Colluvium/Alluvium	100	28	125
4	Cohesive (A-7-6)	0	15	130
5	Bed Rock	q_u =10000 psi		150

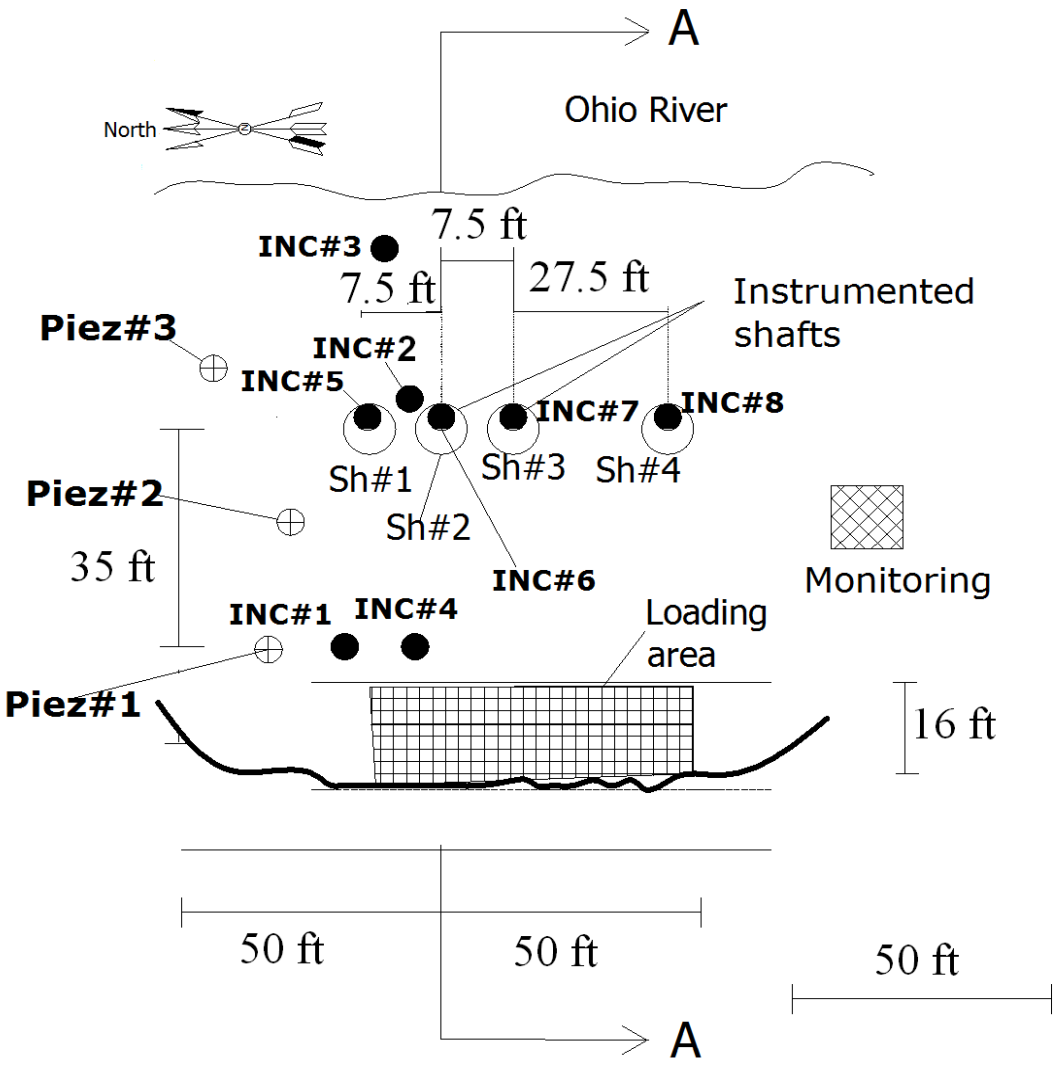

Figure 4.3: Plan View of ATH-124 Test Site and Instrumentation Layout

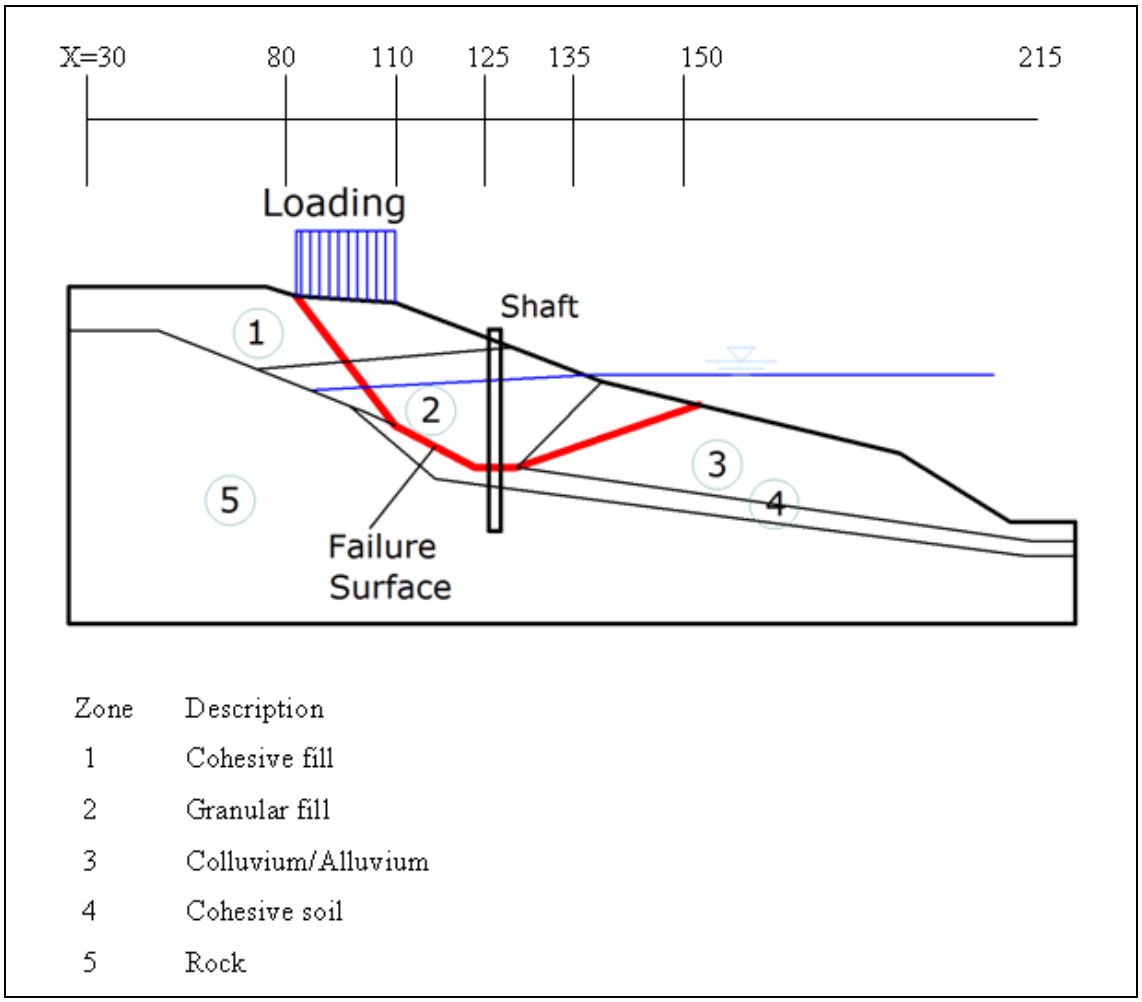

Zone	Description
1	Cohesive fill
2	Granular fill
3	Colluvium/Alluvium
4	Cohesive soil
5	Rock

Figure 4.4: Simplified Cross-Section of ATH-124 Landslide

The step-by step procedure for this illustrative example is given below.

1. Choose the target factor of safety FS_{target} of the slope/shaft system as 1.60
2. The allowable location for drilled shafts is between X = 110 ft to 135 ft as shown in Figure 4.4. The slope/shaft system will be analyzed for different shaft locations starting from X = 110 ft to X=135 ft with an increment equal to 5.0 ft.
3. Select different pairs of (S, D) combinations within the permissible range. Usually, this may depend on the site situations, local availability of drilled shaft construction

equipment. In this example, the following set of (S, D) combinations was selected: (7.5, 2.75), (5.54, 2.75), (8.25, 2.75), (6.75, 2.75), (6.0, 3.0), (7, 3.5), (6.0, 2.0), (10.0, 4.5), (13.5, 3.5), (12.0, 3.0). All units in the parenthesis are in feet.

4. For each (S, D) combination, use UA SLOPE 2.0 to determine the factor of safety for the above selected shaft locations.
5. For each (S, D) combination, use UA SLOPE 2.0 program to determine the shaft force for the above selected shaft locations
6. Plot the obtained force versus the shaft location for each (S, D) combination, as shown in Figure 4.5.
7. Plot the obtained FS versus the shaft location for each (S,D) point as shown in Figure 4.6
8. From Figures 4.5 and 4.6, it appears that the optimum location of the drilled shaft could be at X = 125 ft where the maximum net force on the shaft and the maximum factor of safety are attained.
9. From Figure 4.6, it can be seen that the target factor of safety can be satisfied from three different combinations of shaft locations, spacing and diameters. They are as follows: (a) X = 112 ft, S =5.5 ft, D =2.75 ft, (b) X = 113 ft, S =8.25 ft, D =2.75 ft, and (c) X = 125 ft, S =9.5 ft, D =2.75 ft.
10. The choice (a) and (b) in Step 9 provide satisfactory factor of safety with the net shaft force equal to 85 kips, while the choice (c) also satisfies the factor of safety but with the net force equal to 125 kips. From the structural reinforcement requirements, it may be better to select either option (a) or option (b). However, the length of the drilled shaft could be shorter in option (c) due to shorter distance from ground surface

to slip surface at that shaft location. Thus, option (c) is selected for subsequent structural design of the drilled shaft.

11. The software LPILE was used for the structural analysis of the shaft. Consider the shaft force equals to 125 kips. The depth of the slip surface at the shaft location is 30 ft. In LPILE analysis, the head of the shaft is considered to be coincide with the slip surface with an input of top boundary load as a combination of a shear force equal to 125 kips and a moment equal to 1250 foot-kip (125 kips x 10 ft of moment arm). The length of the analyzed segment of the shaft is 20 ft. The rock properties used were taken from the results of the field borings and lab testing results; these properties were used as input in the computer code LPILE. In such a case usually the p-y curves were internally generated in the computer code based on the input soil and rock properties. As suggested, the load factor of 1.7 would be applied to obtain the factored loading combination as follows: Shear = 212.5 kips and moment = 2,125 kips. Using these top boundary loading and free top boundary condition, the LPILE analysis results are as follows: the resulting maximum moment = 12,800 in-kip, maximum shear = 480 kips, maximum shaft deflection at the slip surface elevation = 0.15 in.

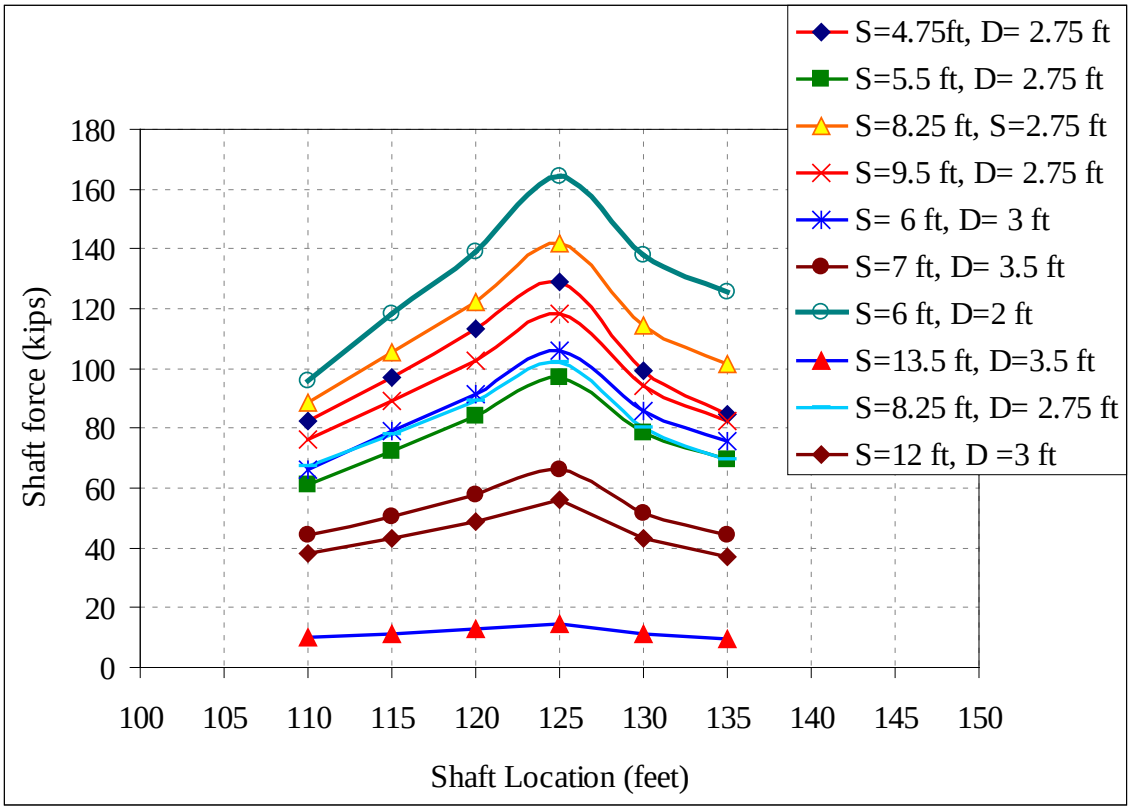

Figure 4.5: Shaft Force versus Shaft Location for Different (S, D) Combinations

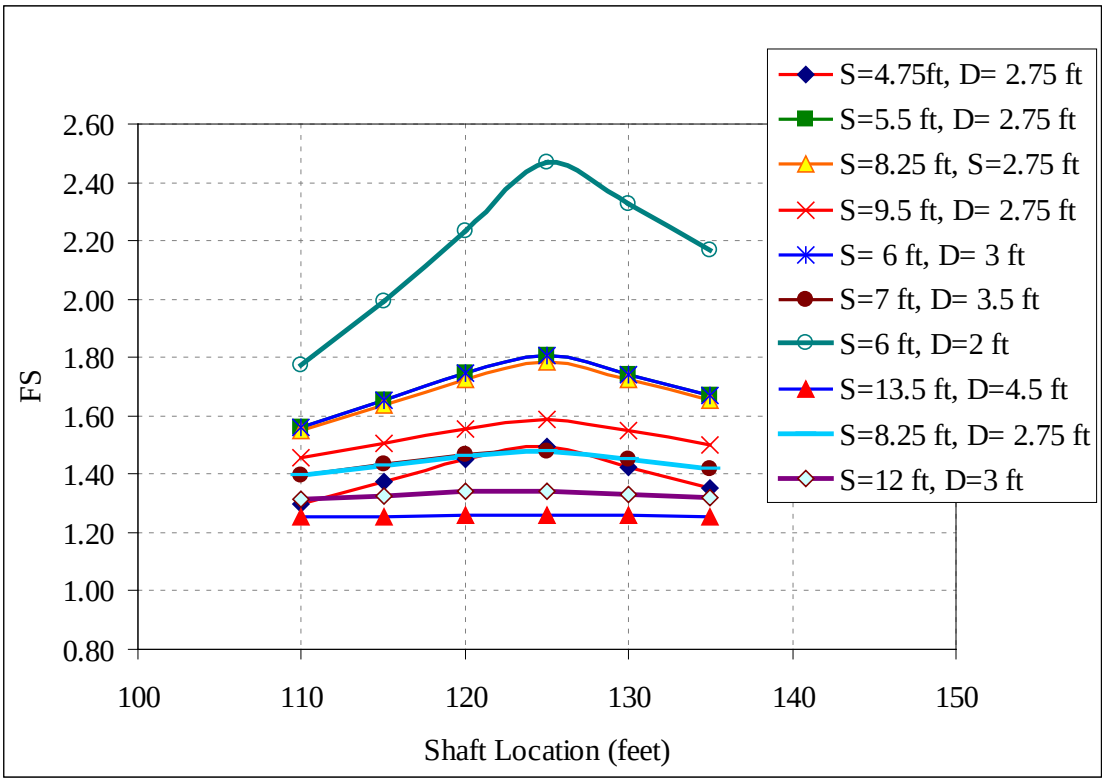

Figure 4.6: Factor of Safety of the Slope/Shaft System versus Shaft Location for Different (S, D) Combinations

4.5 Validation of UA SLOPE Results with FEM Results

As part of validating the UA SLOPE 2.0 program, which was coded on the basis of the developed limiting equilibrium based method of slices together with the load transfer factor, the factor of safety computed by the finite element simulations and the UA SLOPE 2.0 program are compared for a total of 57 different cases. Table 4.2 provides a summary of the FS computed by FEM simulations and UA SLOPE 2.0 for all 57 cases. The bias, defined by the ratio between UA SLOPE 2.0 predicted FS and FEM computed FS is also presented in Table 4.2. The mean, standard deviation, and the covariance of the bias for all 57 cases are 0.92, 0.19, and 0.35, respectively. Figure 4.7-a

shows a comparison between the FS obtained from UA SLOPE 2.0 and the FS obtained from FEM simulations. As can be seen, the correlation coefficient R^2 =0.77.

The differences between the factors of safety obtained from the two methods can be attributed to the following reasons:

1- The FEM analysis is 3D while the UA SLOPE 2.0 analysis is 2D, although the load transfer factor incorporated in UA SLOPE 2.0 was obtained from 3-D finite element simulation results.

2- The FEM analysis is based on continuum mechanics that treats the soils in the slope as deformable body, while the UA SLOPE is based on force equilibrium principle that treats the soil in the moving part of the soil to be a rigid body.

3- The constitutive law used in the FEM analysis is liner elastic- perfectly plastic material satisfying the Mohr-Coulomb strength criterion. In the UA SLOPE analysis, there is no constitutive law involved. The strength criterion is only specified for the soils in the slip surface.

Table 4.2: Summary of FS Computed by UA SLOPE 2.0 Program and FEM

Case no.	FS-FEM	FS-UA	Ratio(UA/FEM)
1	1.30	0.98	0.76
2	1.50	1.20	0.80
3	2.00	1.74	0.87
4	2.45	2.37	0.97
5	2.70	3.02	1.12
6	1.68	1.44	0.86
7	1.70	1.87	1.10
8	1.60	1.34	0.84
9	1.90	1.71	0.90
10	2.10	1.91	0.91
11	1.60	1.62	1.01
12	1.80	1.68	0.93
13	1.40	1.46	1.04
14	1.90	1.82	0.96
15	1.95	1.88	0.96
16	1.98	2.10	1.06
17	2.00	2.06	1.03
18	2.15	1.59	0.74
19	2.10	1.59	0.76
20	1.60	1.27	0.79
21	1.55	1.85	1.20
22	1.50	1.68	1.12
23	1.15	1.19	1.04
24	2.30	2.57	1.12
25	2.50	2.76	1.11
26	2.65	2.65	1.00
27	2.80	3.22	1.15

Table 4.2: Summary of FS Computed by UA SLOPE 2.0 Program and FEM, Continued

28	2.10	2.21	1.05
29	1.60	1.63	1.02
30	1.40	1.34	0.96
31	1.50	1.38	0.92
32	1.40	1.61	1.15
33	1.85	1.38	0.74
34	1.98	1.72	0.87
35	2.15	2.60	1.21
36	1.90	2.05	1.08
37	2.50	2.19	0.88
38	2.00	1.52	0.76
39	2.20	1.32	0.60
40	2.00	1.78	0.89
41	2.30	1.90	0.83
42	2.80	2.79	1.00
43	3.00	3.18	1.06
44	3.20	3.58	1.12
45	1.60	1.12	0.70
46	1.75	1.28	0.73
47	2.30	2.08	0.90
48	2.70	2.87	1.06
49	3.00	3.67	1.22
50	5.00	4.46	0.89
51	1.70	2.47	1.45
52	1.90	1.42	0.75
53	2.10	1.71	0.82
54	1.60	1.26	0.79
55	1.75	1.25	0.71

Table 4.2: Summary of FS Computed by UA SLOPE 2.0 Program and FEM, Continued

57	1.90	1.44	0.76
56	1.65	1.27	0.77
57	1.90	1.44	0.76
Statistical Summary			
Avg.			0.92
STD			0.19
COV	0.35		

The shaft force obtained from the computer code UA SLOPE 2.0 was also compared to the force obtained from the finite element analysis. The above mentioned 57 cases were investigated, and the bias, mean of the bias, and the standard deviation of the bias were calculated. The mean and standard deviation of the bias was found to be equal to 0.91 and 0.57, respectively. The average was very good, however the standard deviation indicate a wide scattering of bias. Since the comparison between the FE computed force and the UA SLOPE 2.0 computed force was very scattered, the bias was set into three intervals (1) the bias which lies within the range bounded by the mean plus and minus one-half of the standard deviation. (2) the bias which lies within the range bounded by the mean plus and minus a standard deviation and (3) all other bias points. The comparison between the results obtained from the FE analysis and UA SLOPE 2.0 analysis, and the above mentioned three categories are depicted in Figure 4.7-b.

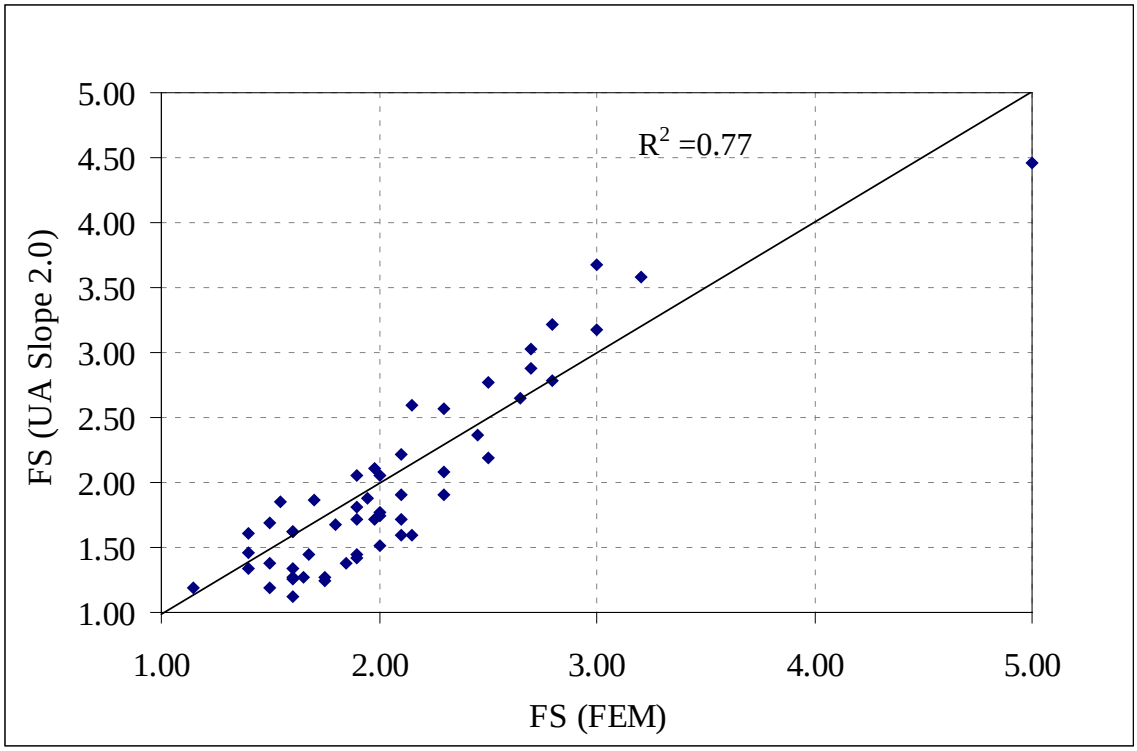

(a)

Figure 4.7: Validation of UA SLOPE 2.0 Program: (a) Comparison of FS (b) Comparison of the Net Force on Shaft

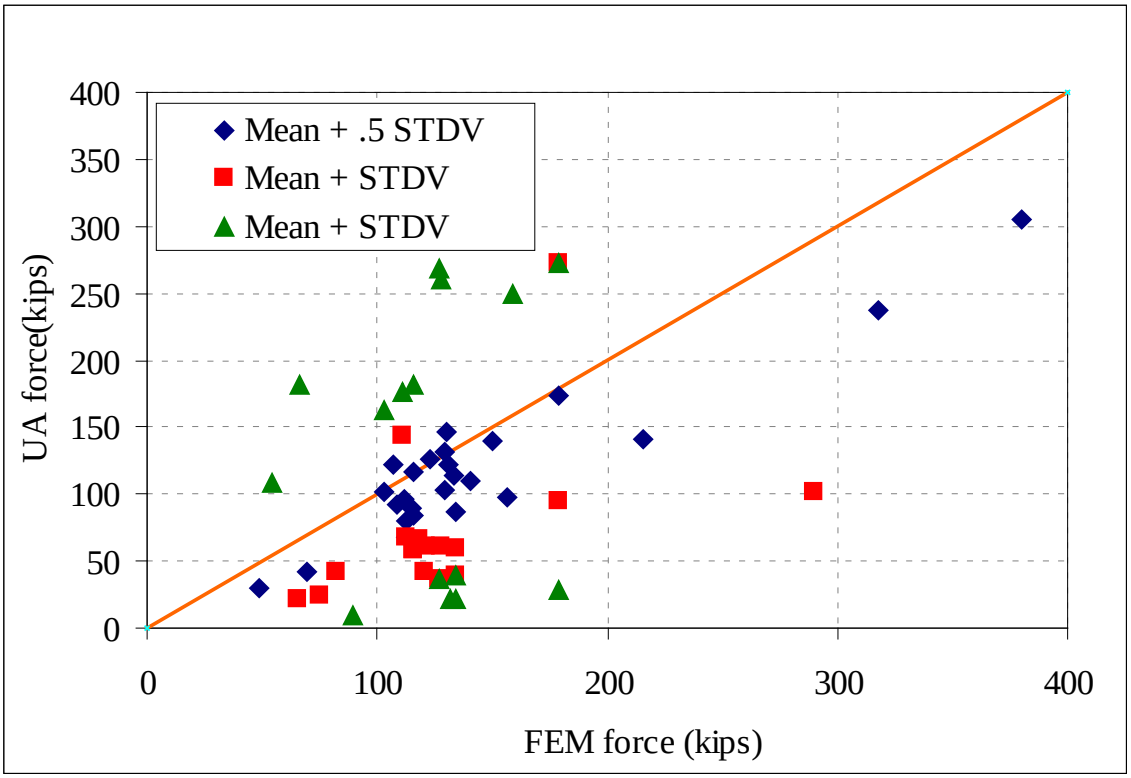

(b)

Figure 4.7: Validation of UA SLOPE 2.0 Program: (a) Comparison of FS (b) Comparison of the Net Force on Shaft, Continued

4.6 Validation of UA SLOPE 2.0 Program Using ATH-124 Project Data

For the purpose of verifying the validity of the proposed design methodology, a full scale field testing was implemented. A detailed explanation of the field work and the performed analysis for this case is provided in the following sections.

4.6.1 Site and Geotechnical Conditions

The failed slope at the State Route ATH-124, from station 107 + 40 to 108 + 60, was part of a test site where drilled shafts were installed and tested by controlled surcharge loading at the crest area of the failed slope. Extensive instrument sensors were installed both inside the constructed drilled shafts and on the slope for monitoring the performance and response of the drilled shafts and the slope during surcharge loading. A total of four drilled shafts were installed at the site, with three of them placed in a row, while the fourth placed as an isolated single shaft. The original intention of this load test program was to place sufficiently large surcharge load at the crest area of the slope to reactivate slope movement so that the interaction between the slope movement and the drilled shafts can be measured during the controlled loading. However, the actual surcharge load placed at the site was not sufficient enough to cause catastrophic failure of the slope; therefore, the measured response during the two stages of controlled loading was used for calibrating a site specific finite element simulation model of the drilled slope/shaft system at the ATH-124 site. With the finite element model of ATH-124 site created and calibrated using measured data, the finite element model was subsequently used to simulate the failure condition by increasing the surcharge load to induce very large slope and shaft movements to a state considered as a failure state. Thus, the testing at the ATH-124 site served the purpose of providing a set of real data to calibrate a finite element model with which to generate numerical simulation mimicking the ultimate slope failure condition for comparisons with the results computed with the UA SLOPE 2.0

program, in terms of global FS of the reinforced slope and the net forces on the drilled shaft.

The slope failure at ATH-124 site was first observed in the fall of 2004 with the evidence of sudden slope movement clearly visible in the form of tension cracks and scarps. The triggering mechanism for slope failure was attributed to a sudden drawdown of the water level in the adjacent Ohio River. Initial site investigation after slope failure included conducting eight soil borings for determining the site soil profile and for obtaining undisturbed Shelby tube samples for laboratory testing. In addition, five inclinometer casings were installed to monitor any subsequent slope movement and to delineate the location of the slip surface. The plan view of the site was previously shown in Figure 4.3. The State Rt. 124 was eventually relocated and the site was abandoned by ODOT. In June 2007, as part of this study, this site was investigated with four additional soil borings and laboratory testing. The laboratory tests of soil samples retrieved from the field included specific gravity, natural water content, direct shear test, CIU test, and UC test. For rock cores, RQD and unconfined compression strength of rock core were obtained. Three additional inclinometer casings were installed at the slope site. Based on the two site investigation reports, the simplified soil profile at the failed slope was determined and shown previously in Figure 4.4. The pertinent soil and rock properties, including strength parameters, are summarized in Table 4.1.

4.6.2 Determining the Slip Surface

The slip surface of the failed slope was determined from the inclinometer readings during the two years of monitoring after the occurrence of the first slippage in 2004. The four points defining the slip surface in Figure 4.4 were determined from inclinometer reading without ambiguity. However, the last point defining the exit point of the slip surface was determined by stability analysis using the computer code Gstable7 with STEDwin (Slope Stability Analysis System, Version2.004, Manual, 2003) and UA SLOPE 2.0 program. The angle of internal friction at the slip surface, associated with a factor of safety equal to one at a rapid drawdown water level condition, was determined to be 15.5^{o}. Figure 4.8 provides a photograph taken at the test site prior to the construction of the test drilled shafts.

Figure 4.8: A Picture Showing the ATH Site Condition Prior to Construction of Test Drilled Shafts

4.6.3 Construction of Drilled Shafts

Four drilled shafts were constructed at the failed slope site in two types of arrangement. One arrangement included a single isolated drilled shaft (labeled as Sh#4 in Figure 4.3), and the second arrangement involved a row of three drilled shafts (labeled as Sh#1, Sh#2, Sh#3 in Figure 4.3). The as-built properties and geometries of the drilled shafts are as follows: shaft diameter D = 2 ft and 8.6 inch (0.83 m), shaft length L = 50ft, rock socket length L_{Socket} = 15 ft, center to center shaft spacing S = 7.5 ft, S/D = 2.75. The 28 day compressive strength of concrete f'_c = 4570 psi, modulus of elasticity of concrete

was calculated from the above mentioned compressive strength and found to be equal to E_{conc} = 2.6 x 106 psi, steel section = Hp 10x42, the equivalent flexural modulus of the drilled shaft (EI) = 1.57389 x 10^{11} lb-in^2. The moment capacity of the drilled shaft is computed using the computer code LPILE (LPILE plus, version 5.0.7, Manual, 2004) as 14,000 kip-inch, while the shear capacity is computed as 500 kips. It should be noted that the distance between the three shafts in a row and the single isolated drilled shaft is 27 ft. All four drilled shafts were placed at the same offset (i.e., 35 ft) from the edge of the slope crest.

4.6.4 Instrumentation Layout

The movement of the slope and the constructed drilled shafts were instrumented with various sensors and inclinometer casings. The general layout of the instrumentation is shown in Figure 4.3. Altogether, four inclinometer casings were installed (INC#1, INC#2, INC#3, and INC#4) on the slope about two months prior to construction of the drilled shafts to establish baseline readings. INC#1 and INC#4 were located at the top of the slope, about 10 ft upslope from the location of the drilled shafts. The total length of INC#1 was 58 ft with about 20 ft into rock; and the total length of INC#4 was 54 ft, with 20 ft into rock. Inclinometer INC#2 was located between shaft #1 and shaft #2 to capture the possible effect of soil arching between the adjacent drilled shafts. It has a total length of 68 ft, with 30 ft into the rock. Inclinometer INC#3 was located 13 ft down slope from the drilled shafts and has a total length of 50 ft, with 15 ft into the rock.

Three piezometers (PZ#1, PZ#2, and PZ #3) were installed to observe the fluctuations of the ground water level. PZ#1 was installed in the upper third of the slope at the depth of 26 ft. PZ#2 was installed in the middle portion of the slope at the depth of 26 ft. PZ#3 was located near the toe of the slope at 24.5 ft below ground surface.

Each constructed drilled shaft was instrumented with conventional inclinometer casings (Shaft #1 with INC#5, Shaft #2 with INC#6, Shaft #3 with INC#7, and Shaft #4 with INC#8). In addition, a total of 30 vibrating wire based strain gages (Geocon Model 4000) were installed on the H-beams, i.e., 15 gages on the anticipated tension side (up-slope side) and 15 gages on the anticipated compression side (down-slope side) of the H-beams. The vertical spacing of the strain gages was 3-foot apart. Figure 4.9 provides a photograph of the H beams instrumented with strain gages and inclinometer casings ready for installation in to the drilled holes for the drilled shafts.

4.6.5 Application of Surcharge Loading

The surcharge load at the slope crest area was applied in two stages as follows. Stage 1 loading occurred between 11/19/2007 and 11/27/2007 with an equivalent of 750 psf uniform pressure covering an area of roughly 17 ft by 73 ft. Stage 2 loading occurred from 10/20/08 to 10/22/08 with additional 848 psf uniform surcharge pressure added to the existing surcharge load from Stage 1. Thus, the total surcharge load provides a roughly uniform pressure of 1,598 psf at the end of stage 2 loading. Figure 4.10 shows the photo taken after the total surcharge load was placed at the site. The description of different stage of works with the corresponding dates is provided in Table 4.3.

(a)

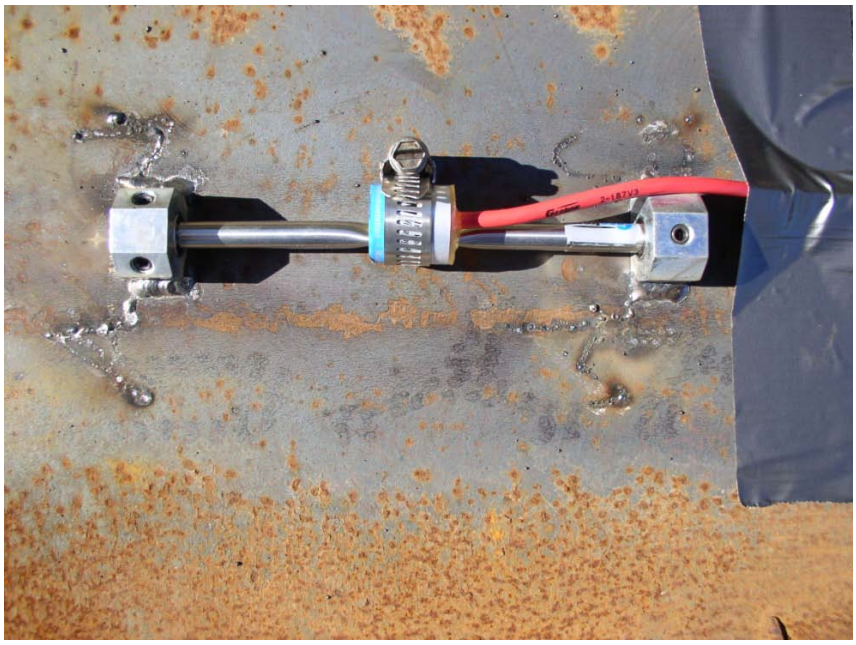

(b)

Figure 4.9: Pictures Showing the Strain Gages Mounted on H-Beams Prior to Construction of Drilled Shafts a) the Whole Beam b) a Strain Gage

Figure 4.10: A Picture Showing the Surcharge Load Placed at the Test Site

Table 4.3: Dates of the Critical Stages of Field Testing

No	Description	Date
1	Completion of drilled shafts construction	11/1/2007
2	Base line reading prior to the first loading	11/19/2007
3	Base line reading prior to the second loading	10/20/2008
4	Immediately after second loading	10/22/2008
5	Most recent reading	8/11/2009

4.6.6 Monitoring Results

The representative results from instrumentations and monitoring work are summarized as follows.

- Soil Movements:
  - The slope movement at the top of the slope after completing the second stage of loading was about 0.7 inches at the ground surface, and the maximum soil movement at the slip surface was about 0.4 inches, as can be seen from INC #1 reading in Figure 4.11-a. It also can be seen that the last reading indicated no significant additional movement at this location.
  - From INC#2 readings shown in Figure 4.11-b, the maximum slope movement within the arching zone was 0.48 inches after the first loading, while no significant soil movement can be seen after the second loading. The last reading showed an increase of the soil movement, on average, of less than 0.1 inch.
  - The maximum slope movement on the down-slope side of the drilled after the second loading was 0.4 inches, as provided by INC#3 reading shown in Figure 4.11-c. The major part of the soil movement was triggered by the first loading, as there was no significant movement caused by the second loading.

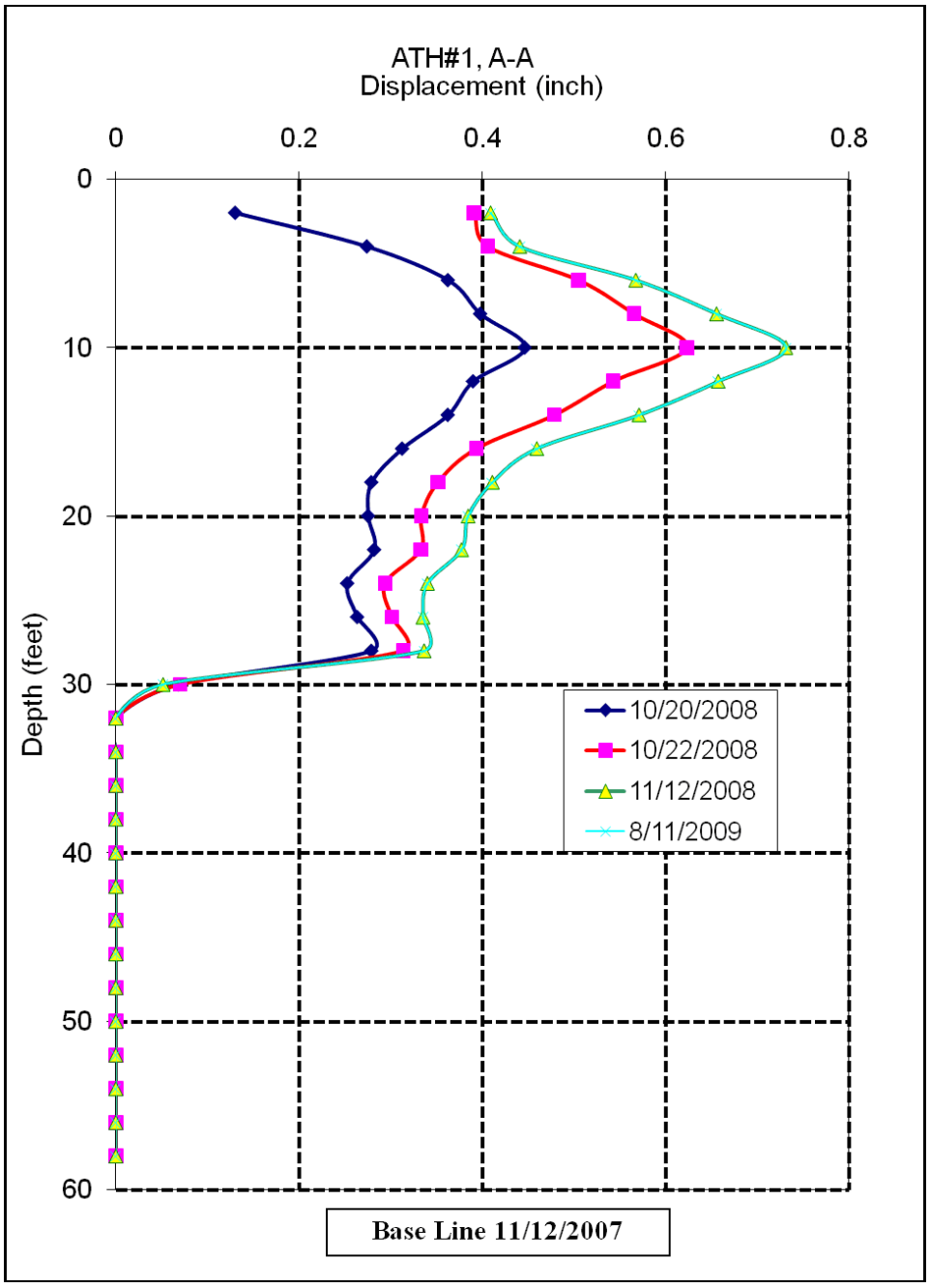

(a)

Figure 4.11: Measured Cumulative Slope Movements at Three Inclinometer Stations: (a) INC #1 at Upslope (b) INC #2 Immediately behind Drilled Shaft Down-slope (c) INC #3 near the Toe

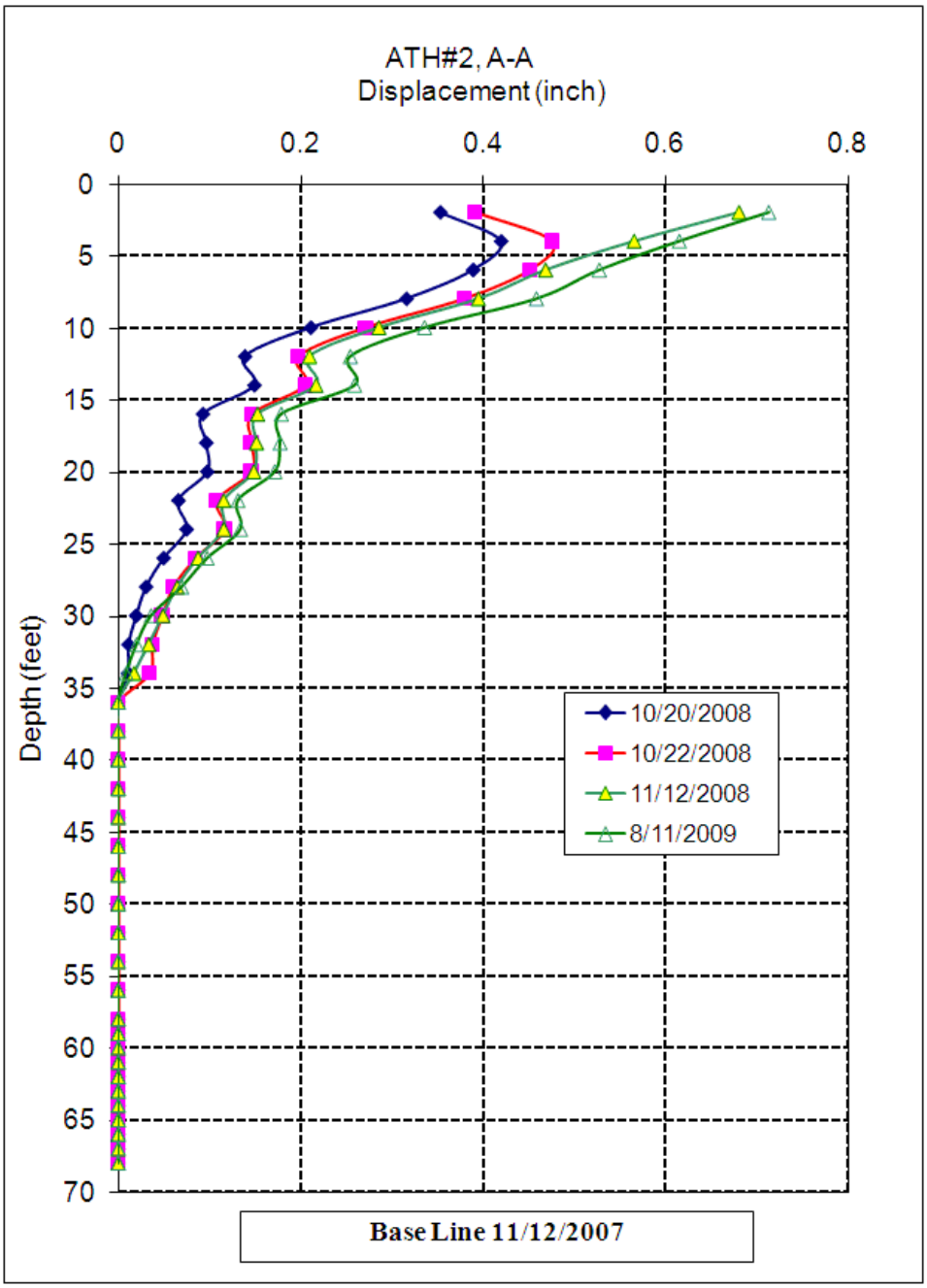

(b)

Figure 4.11: Measured Cumulative Slope Movements at Three Inclinometer Stations: (a) INC #1 at Upslope (b) INC #2 Immediately behind Drilled Shaft Down-slope (c) INC #3 near the Toe, Continued

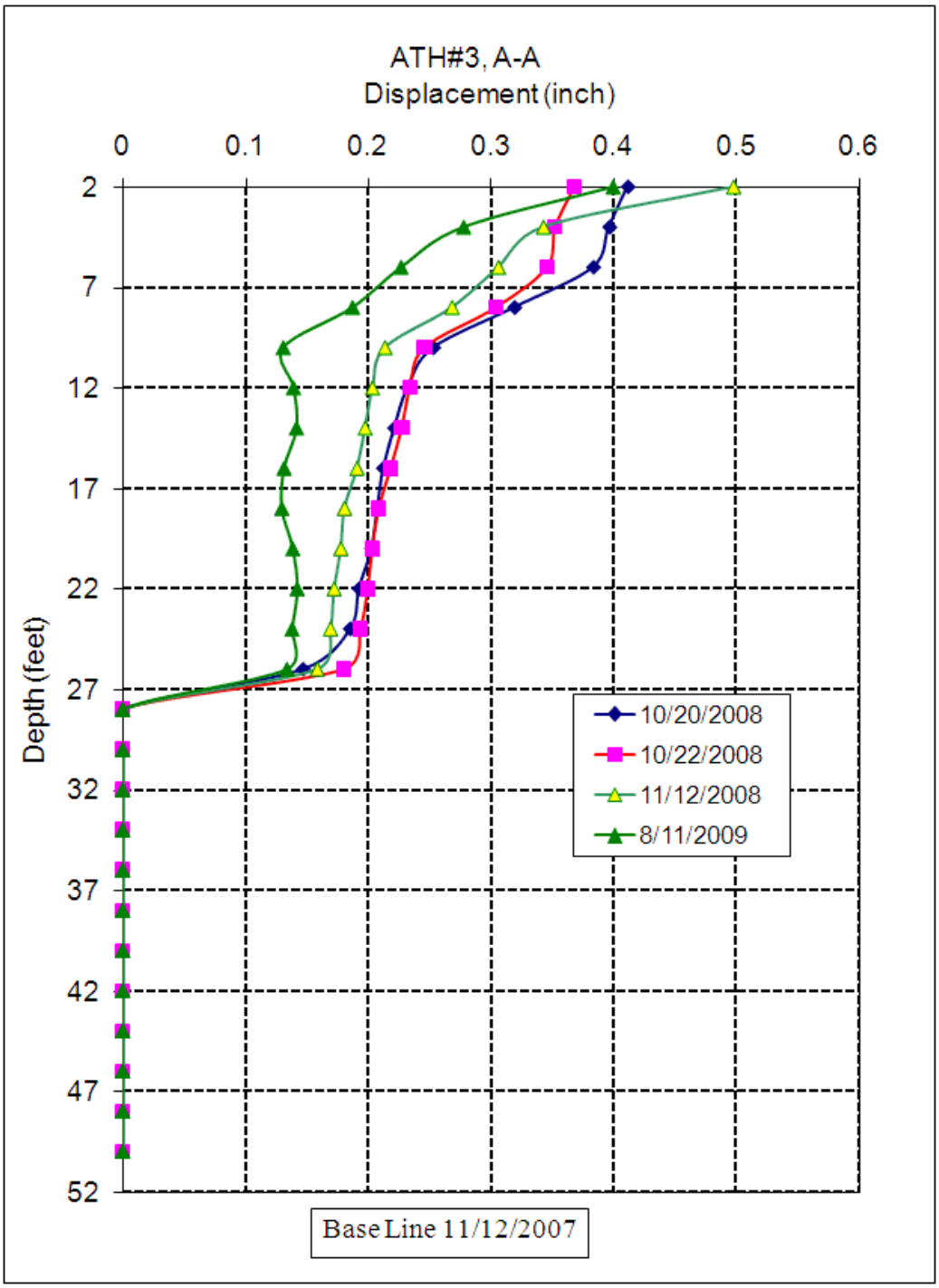

(c)

Figure 4.11: Measured Cumulative Slope Movements at Three Inclinometer Stations: (a) INC #1 at Upslope (b) INC #2 Immediately behind Drilled Shaft Down-slope (c) INC #3 near the Toe, Continued

- Drilled Shaft Deflections
  - The maximum deflection in Shaft #2 due to the total surcharge loading was 0.24 inches as shown in Figure 4.12-a. An average increase equals to 0.1inch in the deflection of shaft#2 can be seen from the last reading.
  - The maximum deflection at the top of Shaft #4 due to the total surcharge loading was 0.3 inches as shown in Figure 4.12-b. Generally the amount of deflection shown by the last reading indicated that the increase in the shaft deflection since the second loading was less than 0.2 inch.
- Bending Moments on Drilled Shafts
  - The maximum positive and negative moments in shaft #2 were 2,408 inch-kip and 801 inch-kip, respectively, as shown in Figure 4.13-a. The last reading shows a significant increase in the maximum moment only (5700 inch-kip).
  - The maximum positive and negative moments in shaft #4 were 1,605 inch-kip and 722.8 inch-kip, respectively, as shown in Figure 4.13-b. The last reading showed an increase in the moment on both the negative and the positive sides (-2500, 1400) inch-kip, respectively.

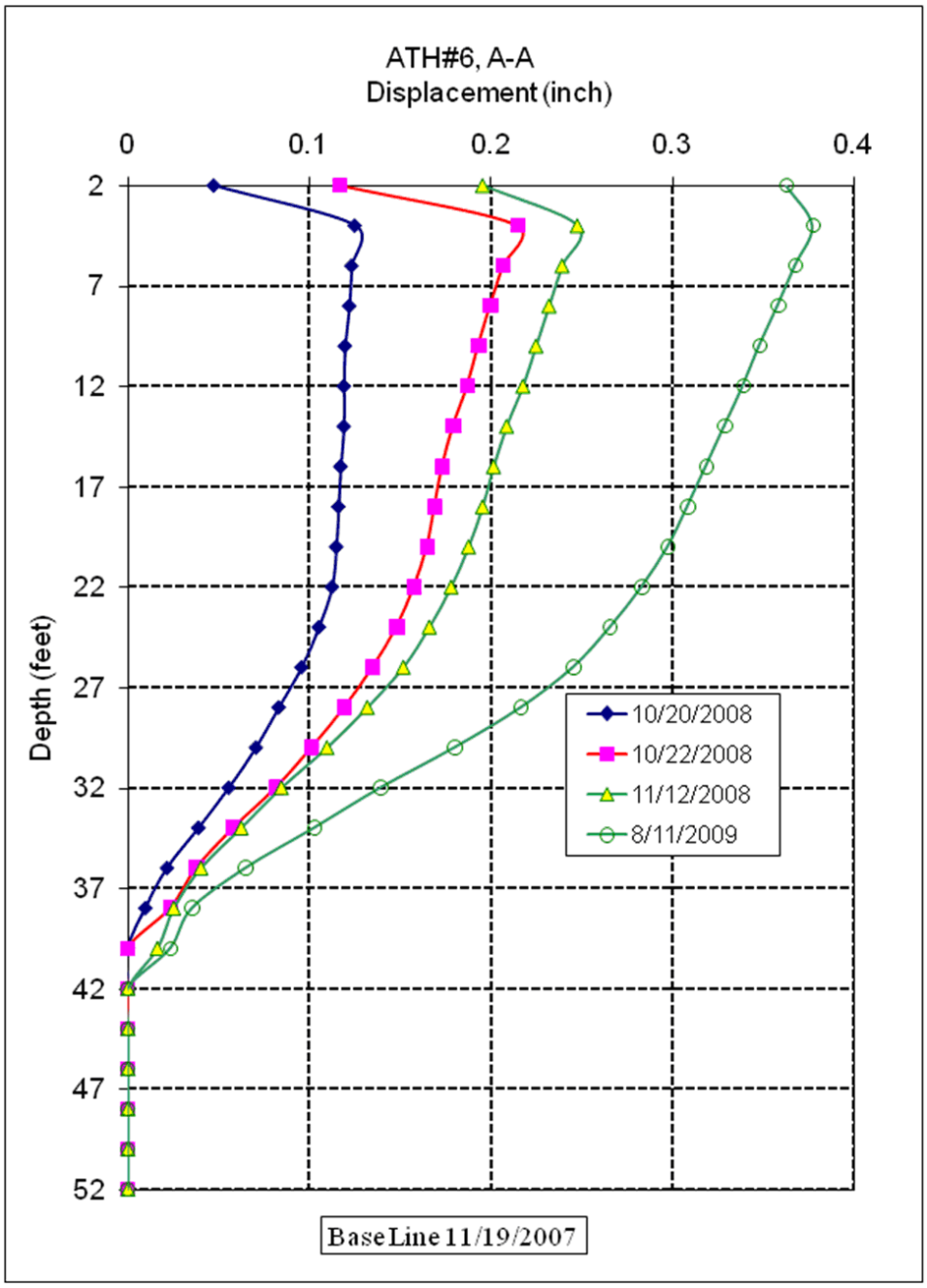

(a)

Figure 4.12: Measured Cumulative Deflections: (a) Shaft #2 (b) Shaft #4

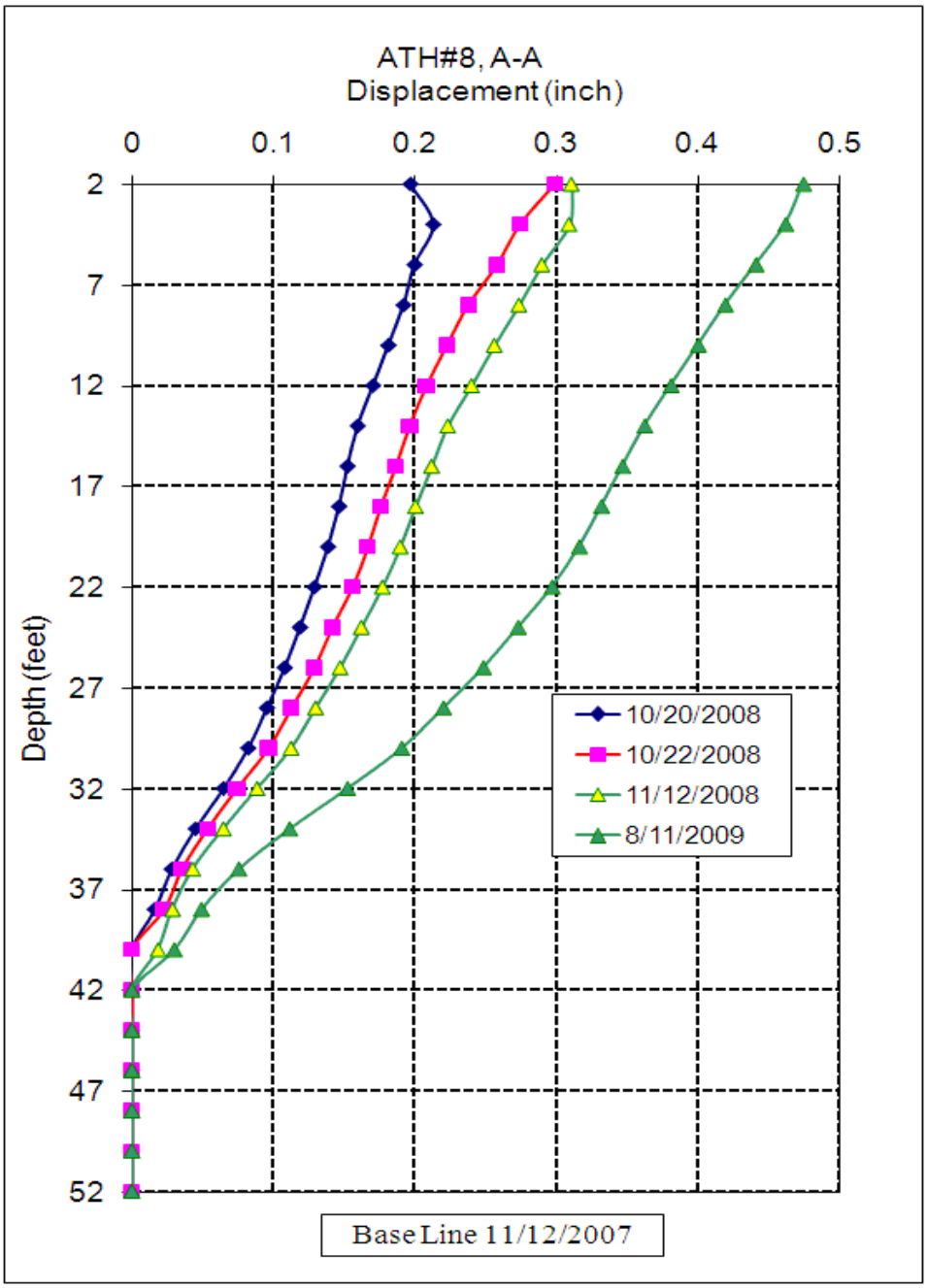

(b)

Figure 4.12: Measured Cumulative Deflections: (a) Shaft #2 (b) Shaft #4, Continued

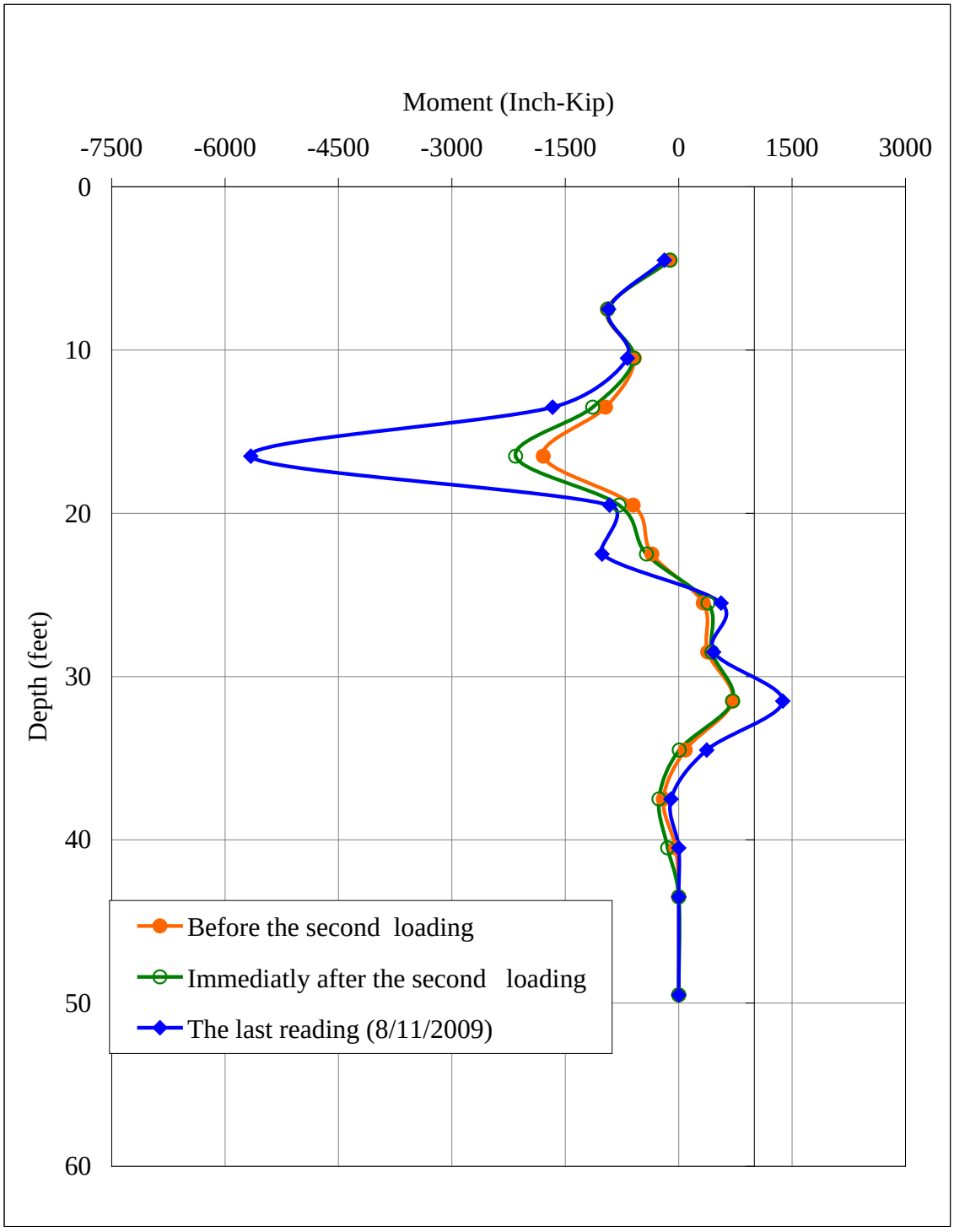

(a)

Figure 4.13: Measured Bending Moments in Shafts due to Surcharge Loading and Slope Soil Movement: (a) Shaft #2 (b) Shaft #4

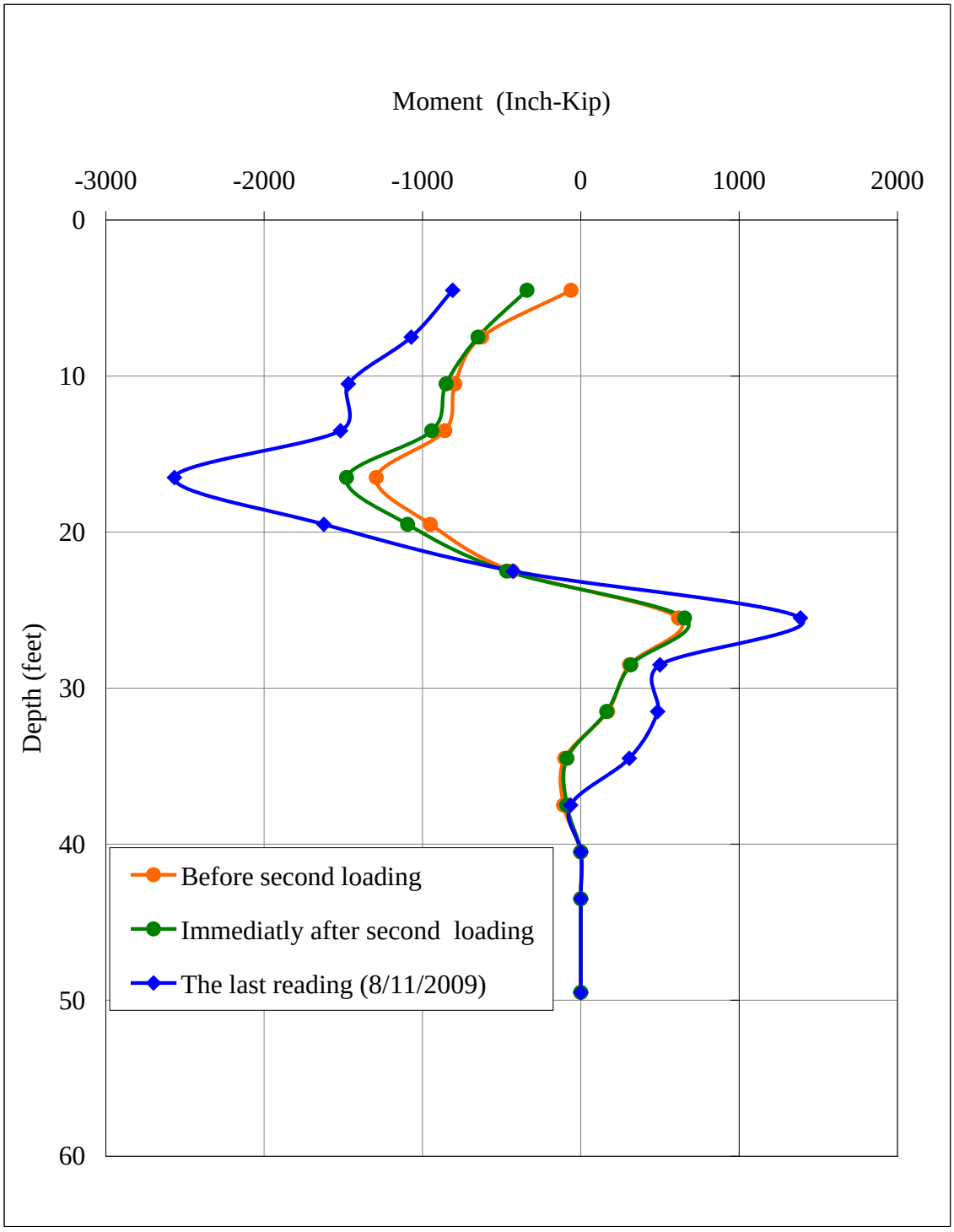

(b)

Figure 4.13: Measured Bending Moments in Shafts due to Surcharge Loading and Slope Soil Movement: (a) Shaft #2 (b) Shaft #4, Continued

4.6.7 Finite Element Simulations

A 3D finite element model to mimic ATH-124 site soil and geometry conditions as well as the placed surcharge loads was constructed using ABAQUS program (Version 6.7-1) to allow for modeling and further studying the drilled shaft-slope system of the study site.

4.6.7.1 Material Modeling

Soil was modeled as a linear elastic-perfectly plastic material which obeys Mohr-Coulomb failure criterion. The rock and the drilled shaft were modeled as elastic materials. The relevant material parameters used in the finite element model are summarized in Table 4. 1.

4.6.7.2 Modeling of Interfaces

Three types of contact interfaces in the finite element model were defined to account for three contact boundaries: soil-shaft interface, rock-shaft interface, and soil-rock interface. Each interface was defined by two interface interaction properties: 1) Normal interaction property to define the nature of the normal contact; and 2) Tangential interaction property to define the friction coefficient at the interface.

4.6.7.3 Load Simulations

The loads used in the model included the gravity load, the surcharge loads at the top of the slope, the hydrostatic water pressure along the failure surface, and the hydrostatic water pressure outside the slope to mimic the effects of the river water level. Tow loading steps were carried out: (a) the first step was defined as geostatic, in which the gravity load was created and the soil was considered in equilibrium with zero initial displacement, (b) the second step was defined by adding the surcharge loading. Pore water pressure was defined by the initial values of the hydrostatic pressure within the soil mass at each nodal point below the ground water table (GWT). There was no excess pore pressure generation during surcharge loading, as the permeability of the materials below the GWT was relatively high based on soil classifications.

4.6.7.4 Boundary Conditions

The boundary conditions of the finite element model are as follows: The bottom of the rock was totally fixed as depicted in Figure 4.14-a. The soil was restrained from moving horizontally in the transverse direction at the two sides as illustrated in Figure 4.14-b. To take advantage of symmetry, a single drilled shaft was modeled as shown in Figure 4.14-b. In essence, the boundary conditions at two vertical sides were considered to be planes of symmetry. The movement of front side and the back sides was prohibited in direction 1 (i.e., horizontal direction) as shown in Figures 4.14-a, and 4.14-b.

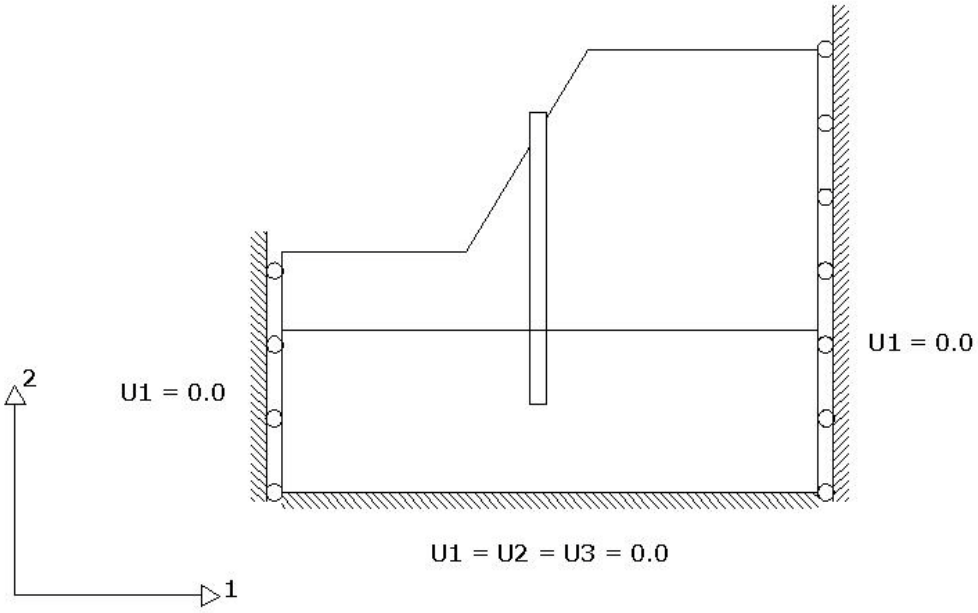

(a)

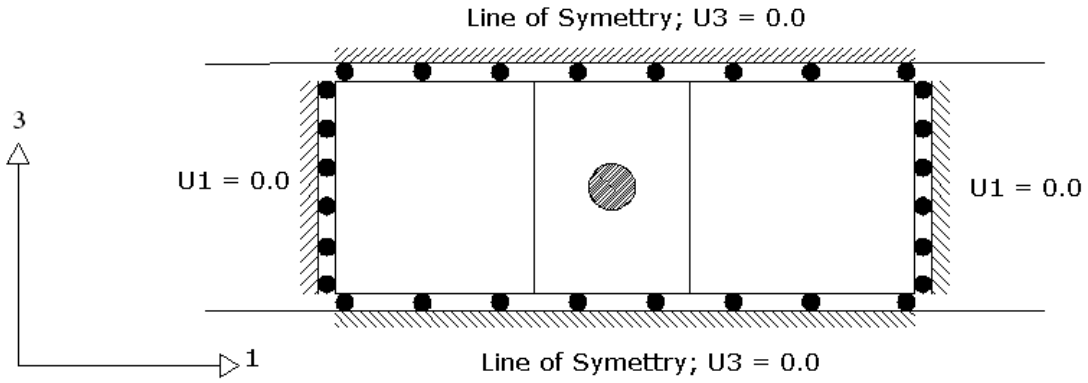

(b)

Figure 4.14: The Boundary Conditions of the FEM a) Side View b) Plan View

4.6.7.5 FEM Mesh

The FEM mesh generated for the problem is depicted in Figure 4.15. It is consisted of 85,913 hexahedral elements for soil body, and 31,431 similar hexahedral

elements for rock. The drilled shaft was modeled using 1,597 hexahedral elements. The mesh for the soil adjacent to the drilled shaft was much dense than that in the other regions.

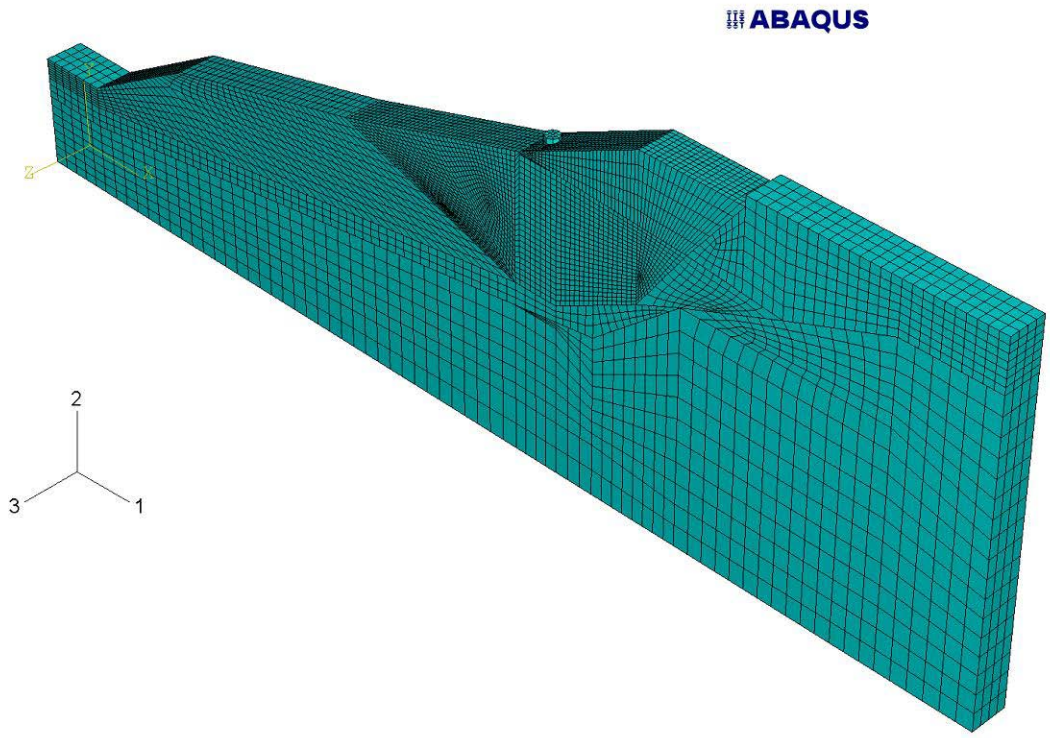

Figure 4.15: FEM Mesh of the ATH-124 Test Site

4.6.7.6 Single Shaft versus a Row of Shafts

The difference between the modeling of three drilled shafts in a row and a single isolated shaft is the choice of the spacing between the shafts and the specified boundary conditions. In the case of three shafts in a row, the width of the 3-D FEM model is 7.75 ft with S/D = 2.75, reflecting the spacing of adjacent drilled shafts, and the boundary

conditions at the sides being treated as planes of symmetry. The width for the FEM model of the single isolated drilled shaft was 20 ft, i.e., S/D =7.5, thus reflecting no effects from the adjacent drilled shafts.

4.6.8 FEM Analysis Results

The FEM analysis results, including soil movements, the deflections and moments of the drilled shafts, and the net soil reactions on the shafts, are compared with the measured for the single isolated shaft and the middle shaft in a row of three shafts.

The measured soil displacements at the top of the slope appeared to be in agreement with FEM numerical results, as can be seen from Figure 4.16. Finite element simulation results showed no major displacements in the arching zone as seen from Figures 4.17-a, 4.17-b. The same observation can be made for the slope movement on the down-slope side of the drilled shafts as shown in Figures 4.18-a, 4.18-b.

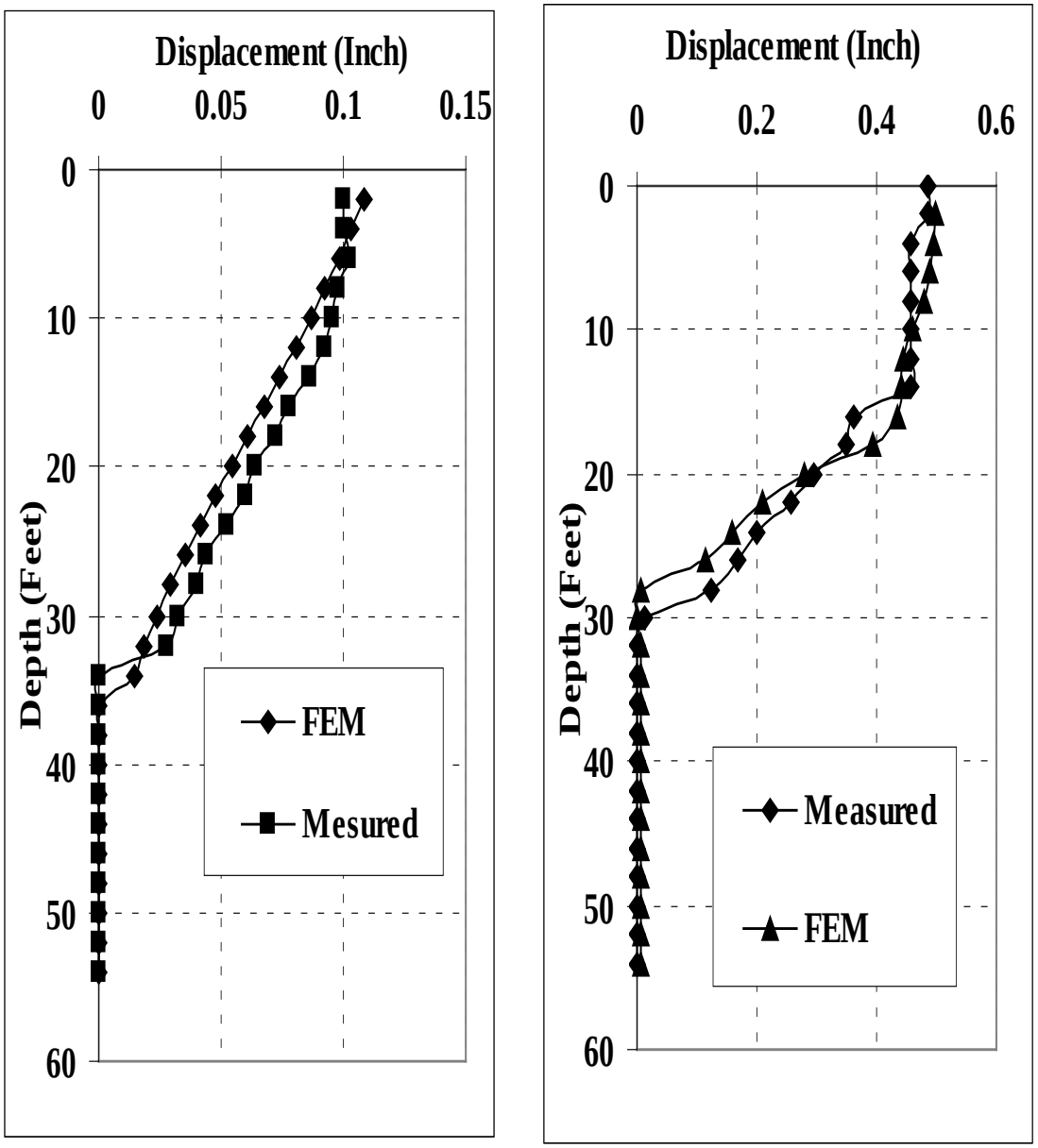

a b

Figure 4.16: Comparison between Measured and FEM Computed Ground Displacement at INC #1: (a) due to First Loading (b) due to Second Loading

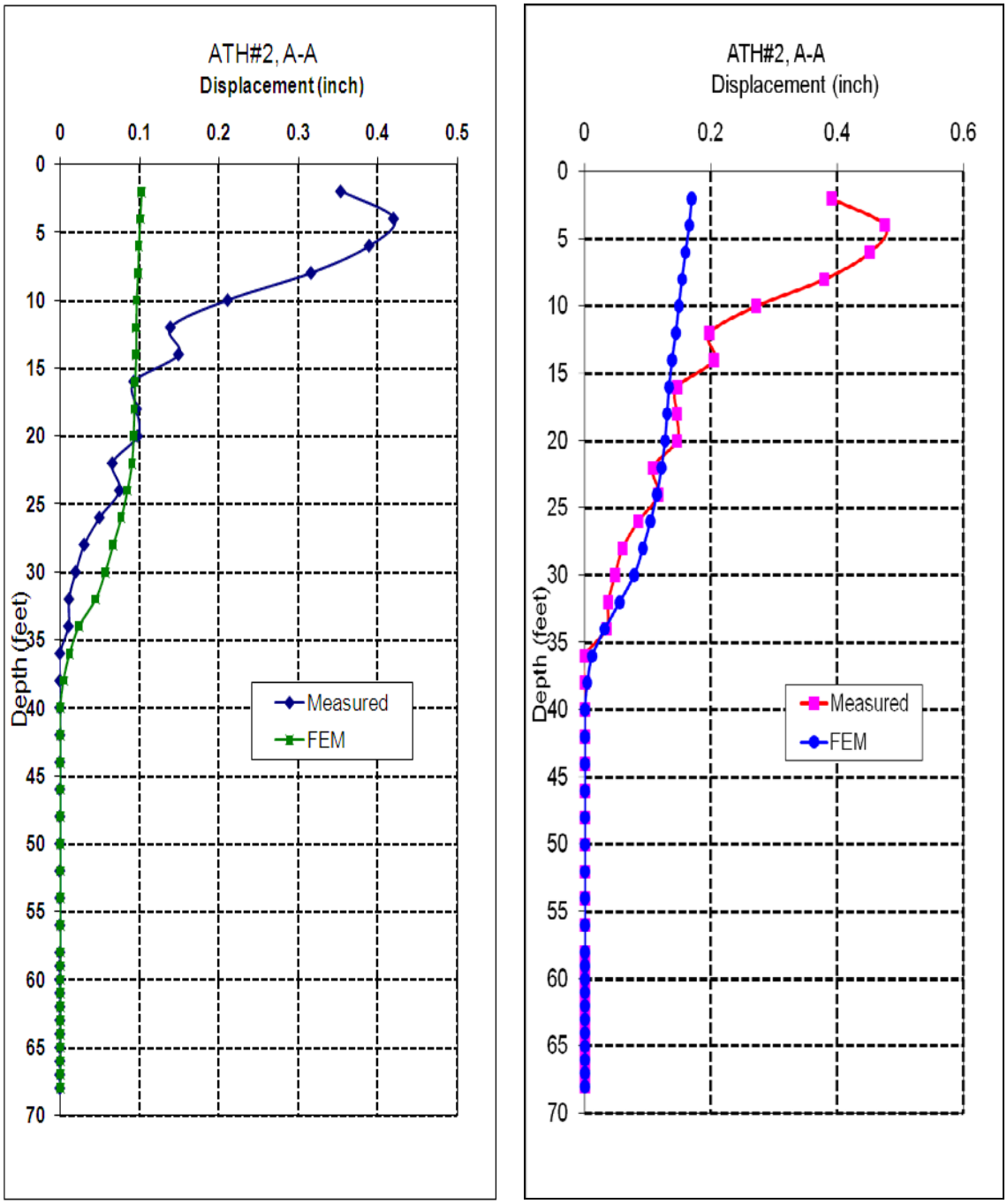

a b

Figure 4.17: Comparison between Measured and FEM Computed for INC #2 (a) due to First Loading (b) due to Second Loading

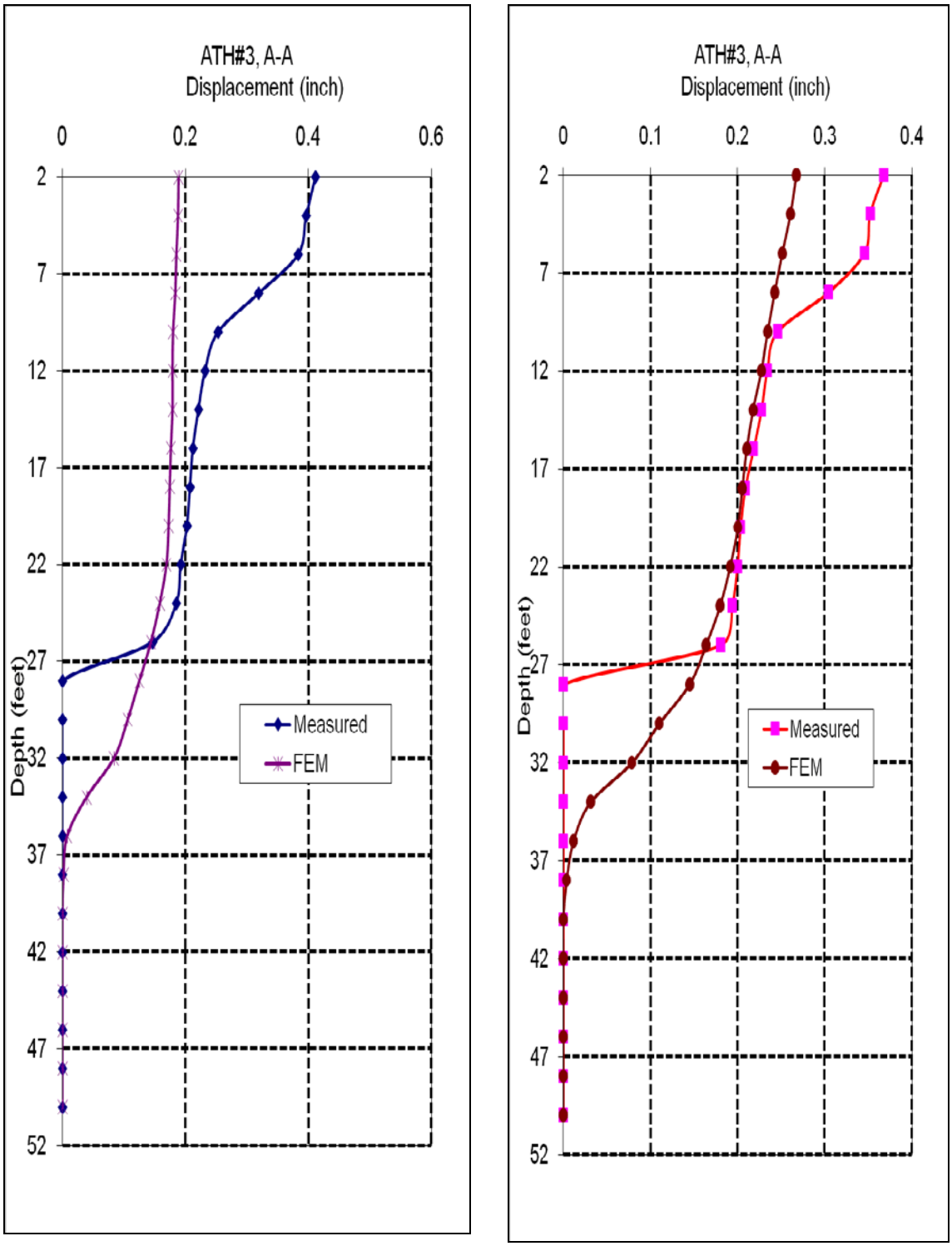

a b

Figure 4.18: Comparison between Measured and FEM Computed for INC #3: (a) due to First Loading (b) due to Second Loading

The shaft deflections obtained from the FE simulations match with the measured deflections both in the case of a single shaft and in the case of the middle shaft in a row of shafts at the different loading stages, as can be seen in Figures 4.19 and Figure 4.20 for Shaft #2 and Shaft #4, respectively. Although the shaft deflection above the slip surface was slightly over estimated and the shaft deflection below the slip surface was slightly under estimated by the FE analysis, the trend and the absolute values of the calculated and measured deflections were close to each other. Furthermore, the measured moments in both Shaft #2 and Shaft #4 for the two loading stages showed good agreement with the moment obtained from the FEM computations, as shown in Figures 4.21-a, 4.21-b and 4.22-a, 4.22-b, for Shaft #2 and Shaft #4, respectively.

Based on the comparisons between the FEM simulation results and measured data presented herein, it is reasonable to state that the site specific FE model for the ATH-124 load testing program is accurate enough to allow for additional simulations to exam the failure conditions when large slope movement is activated due to the placement of very large surcharge loads. It is noted that this failure condition can not be achieved in the field load testing program.

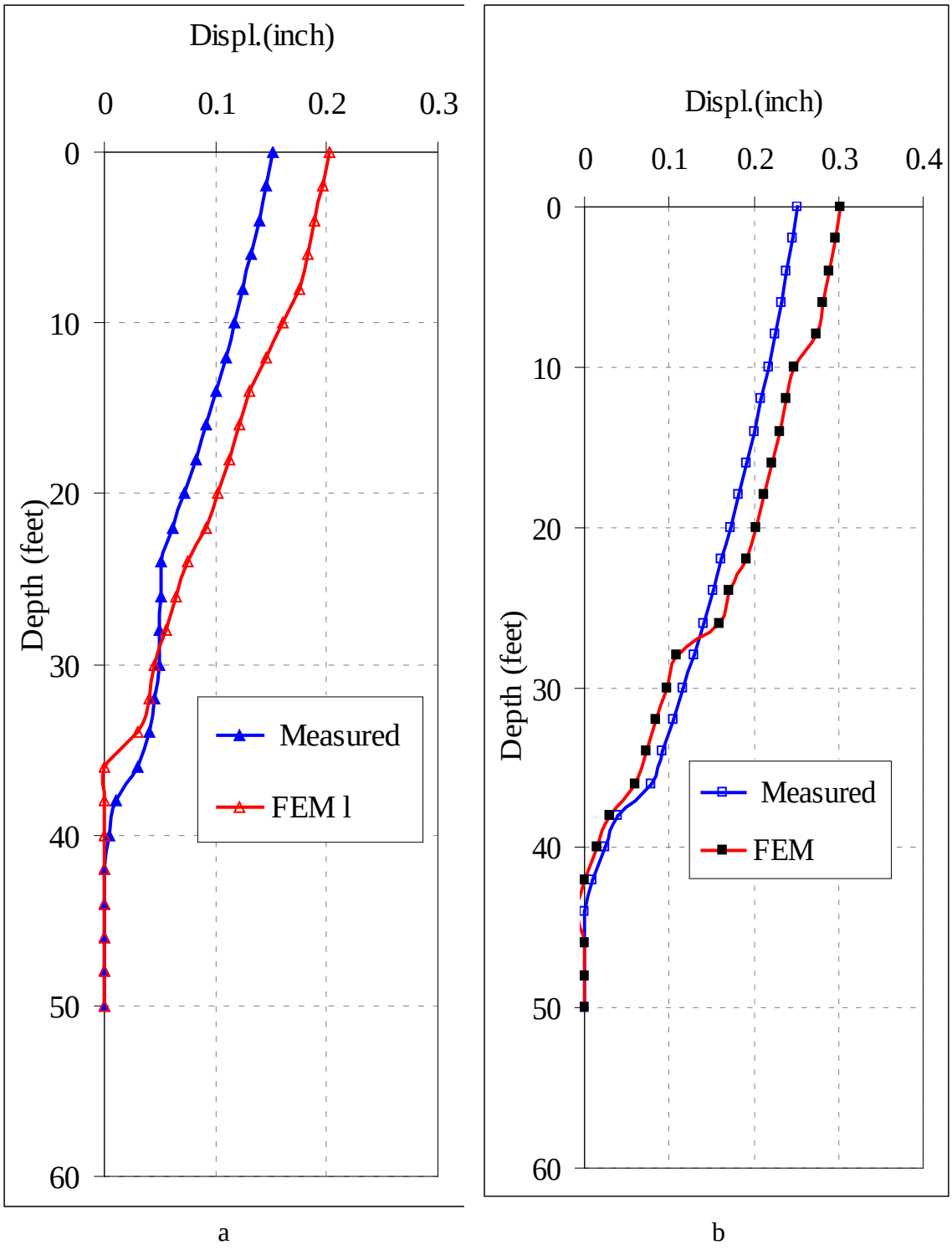

Figure 4.19: Comparison between Measured and FEM Computed Shaft Deflections for Shaft #2: (a) due to First Loading (b) due to Second Loading

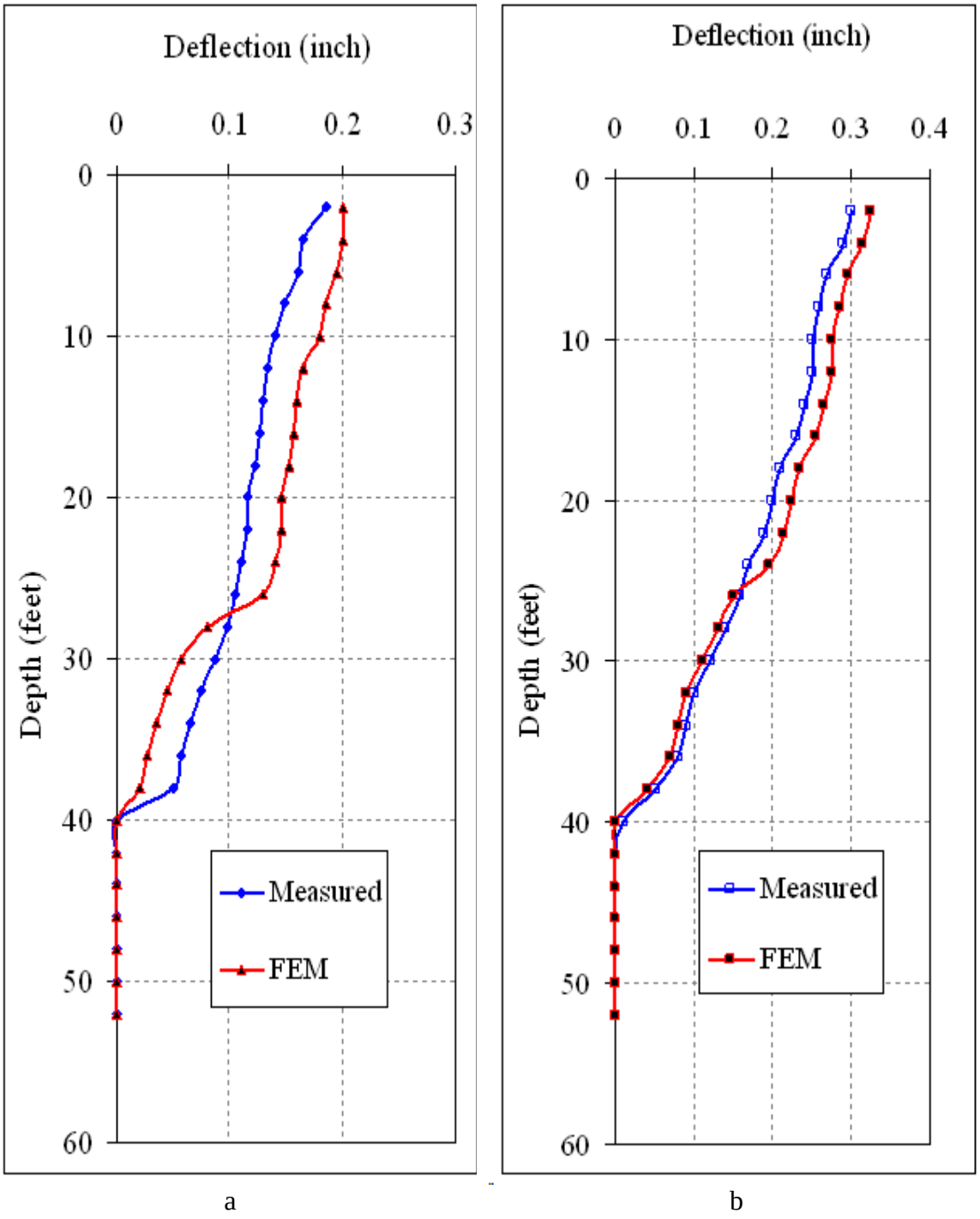

Figure 4.20: Comparison between Measured and FEM Computed Deflections for Shaft #4: (a) due to First Loading (b) due to Second Loading

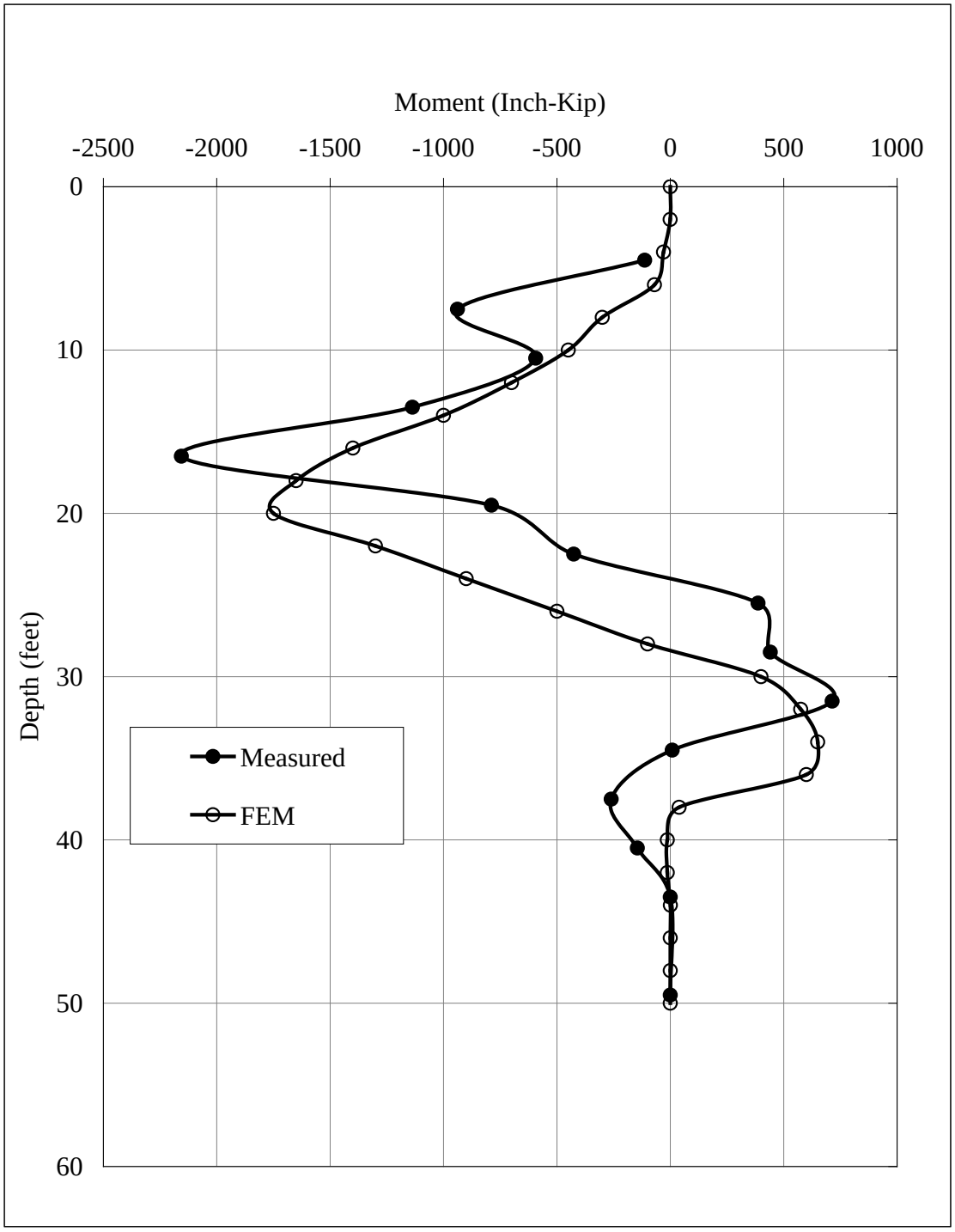

(a)

Figure 4.21: Comparison between Measured and FEM Computed Moments in Shaft #2: (a) due to First loading (b) due to Second Loading

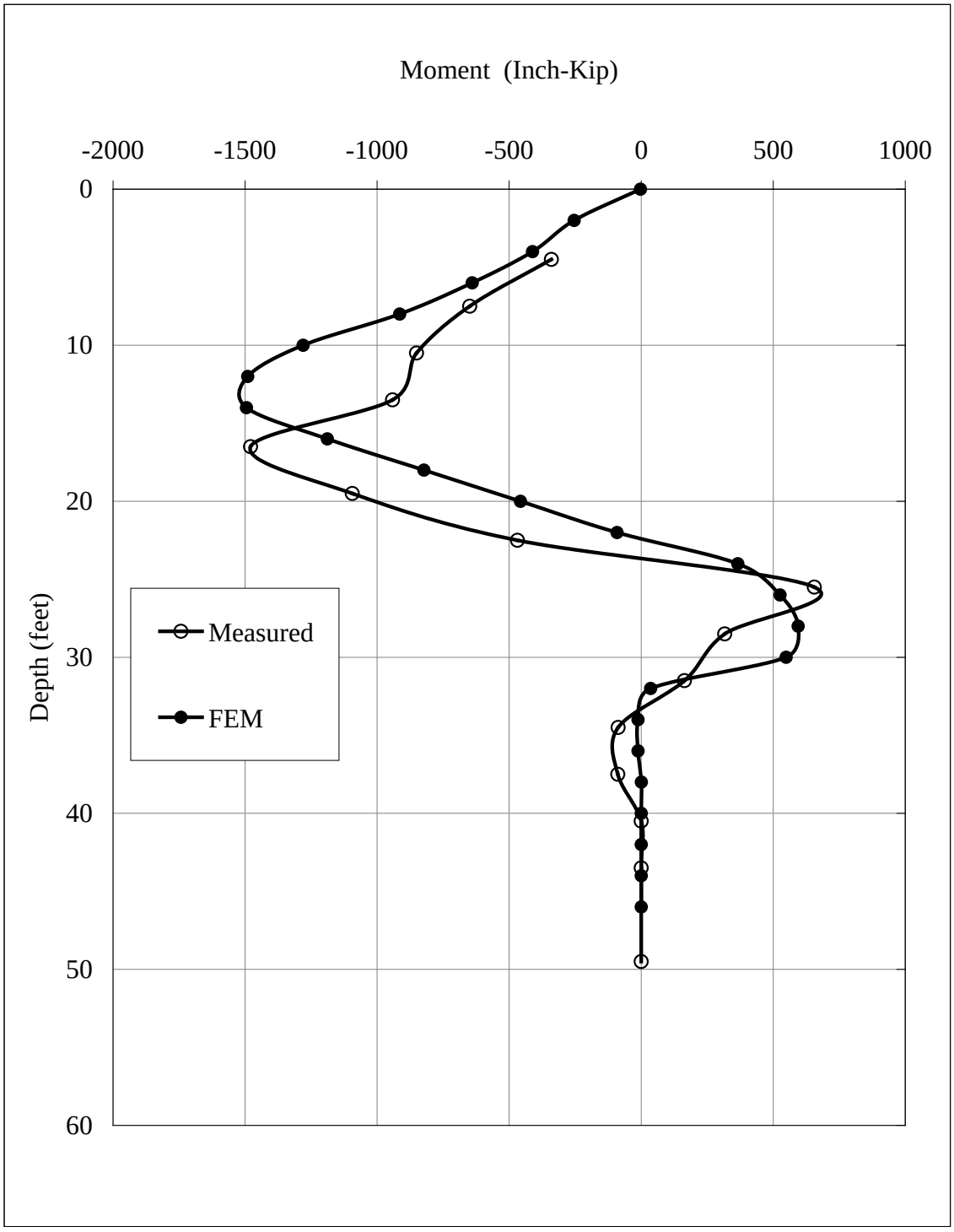

(b)

Figure 4.21: Comparison between Measured and FEM Computed Moments in Shaft #2: (a) due to First loading (b) due to Second Loading, Continued

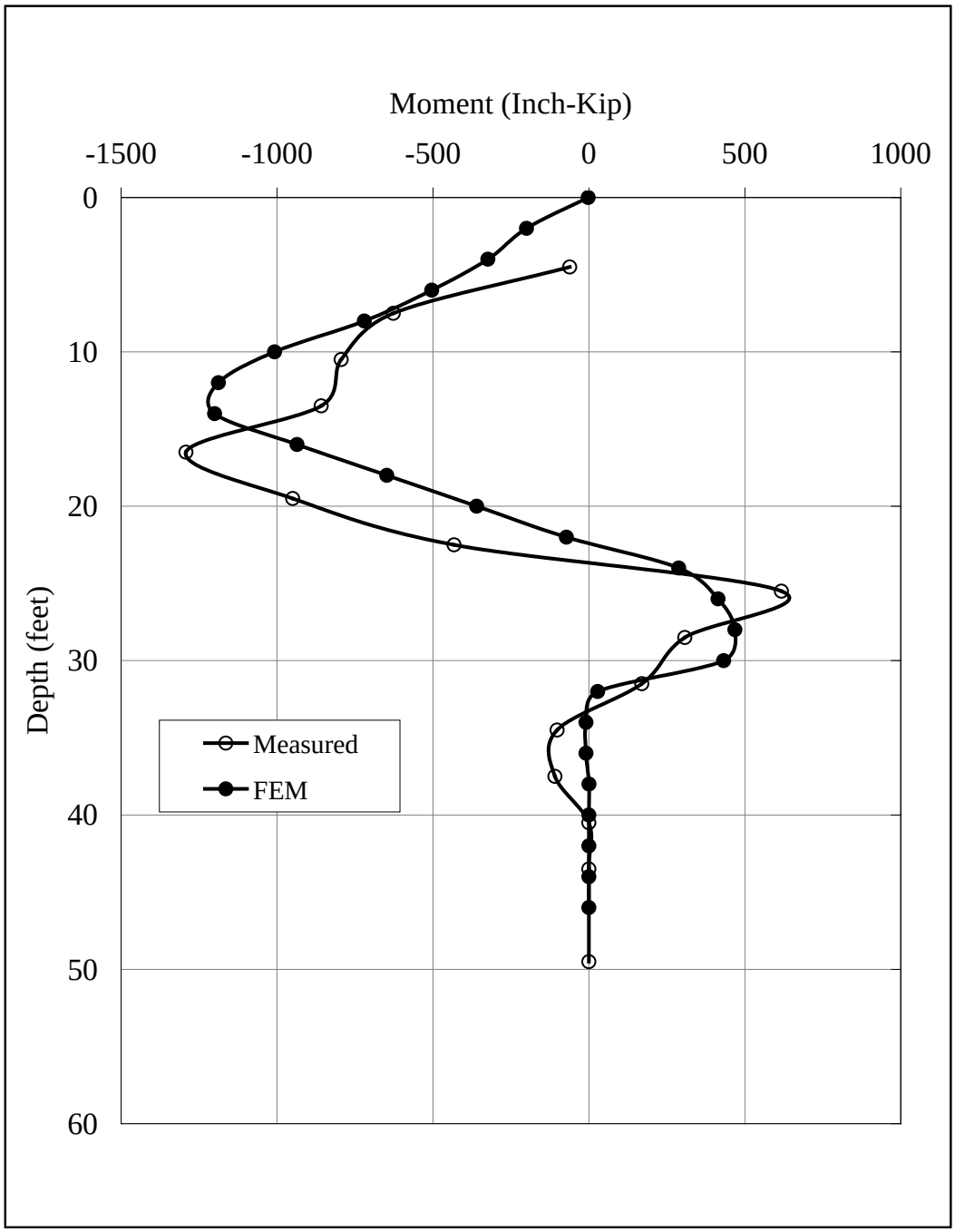

(a)

Figure 4.22: Comparison between Measured and FEM Measured Moments in Shaft #4: (a) due to First loading (b) due to Second Loading

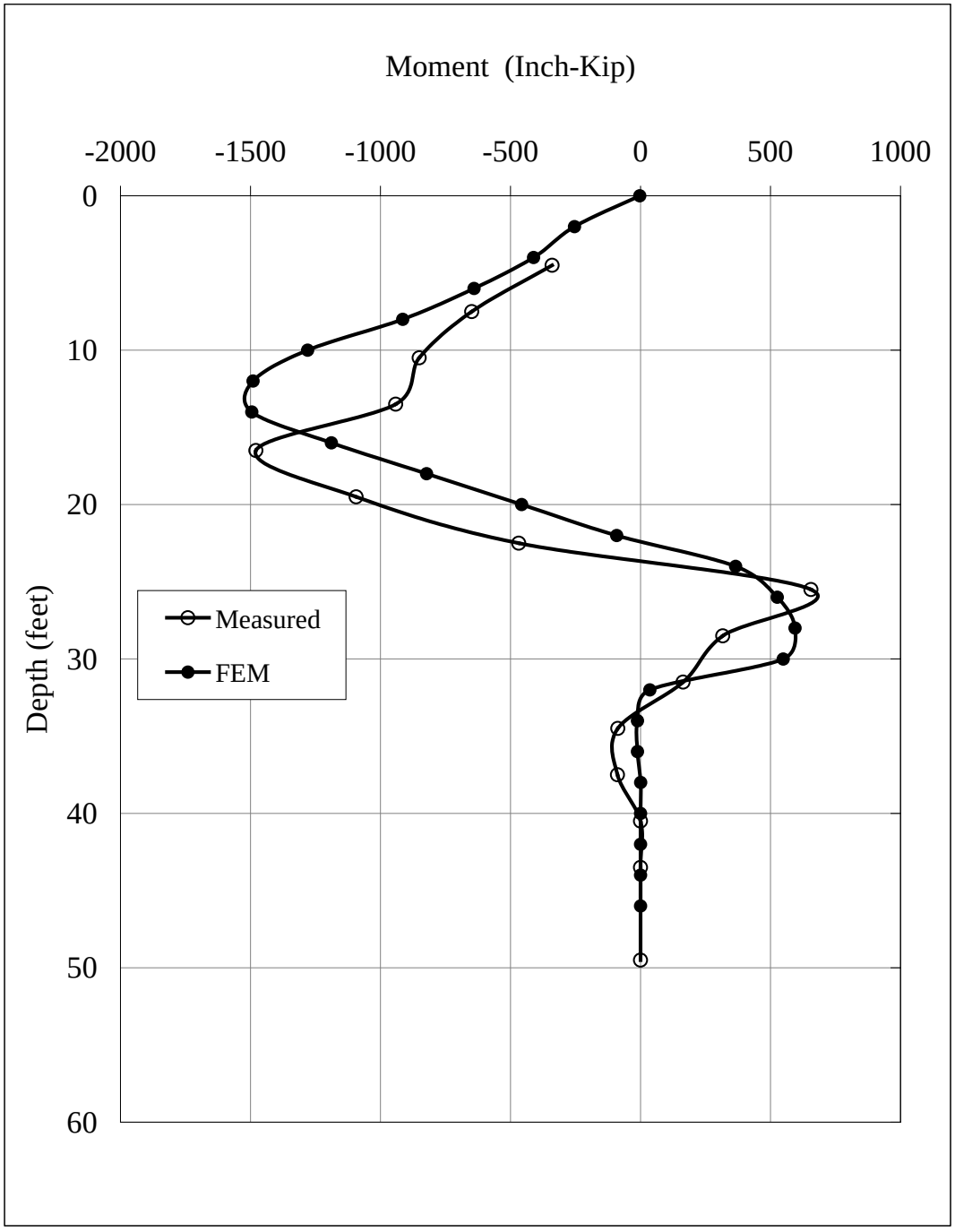

(b)

Figure 4.22: Comparison between Measured and FEM Measured Moments in Shaft #4: (a) due to First loading (b) due to Second Loading, Continued

4.6.9 Analysis for Surcharge Induced Slope Failure

After verifying the validity of the FEM model for the two loading stages, the established site-specific FEM model was used to simulate the large surcharge load induced slope failure conditions. In essence, the surcharge load was increased until no numerical convergence can be obtained, which means that a total plastic flow in the slope has occurred. The computed stress field at failure is shown in Figure 4.23. For the case of a single isolated shaft, the numerical divergence occurs when the surcharge load at the top of the slope reaches 3,237 psf. At that moment, the horizontal soil displacement at the top of the slope was 8 inches as shown in Figure 4.24, and the maximum shaft deflection was 4.5 inches at the top of the shaft as shown in Figure 4.25. The net force imparted on the single shaft at the failure condition was 98 kips. For the case of a row of drilled shafts, the numerical divergence occurs when the surcharge load reaches 4,282 psf. The corresponding shaft deflection was 3.8 inches as shown in Figure 4.25. The soil movement at the top of the slope was about 8.2 inches as shown in Figure 4.23. The internal moments and shear forces in the drilled shaft are shown in Figures 4.26 and 4.27, respectively. The net soil reaction for the single shaft (#4) and for the shaft within a row (#2) obtained from the finite element analysis at failure are depicted in Figure 28.

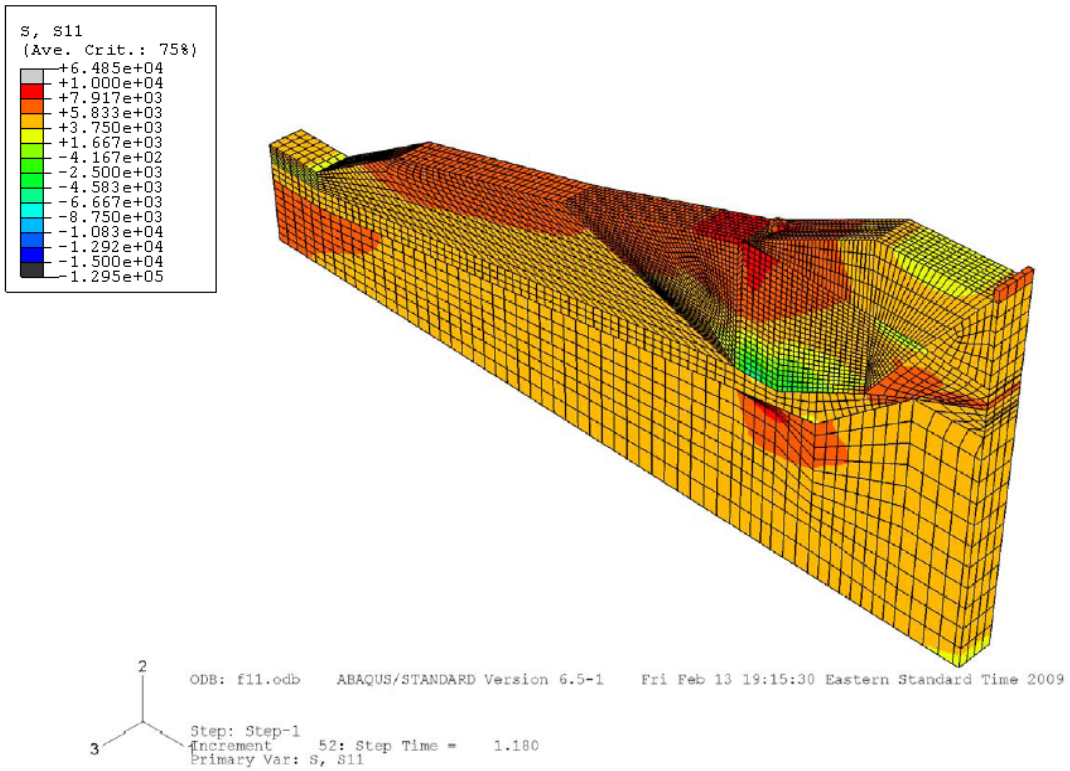

Figure 4.23: FEM Computed Stress Field at Failure Condition

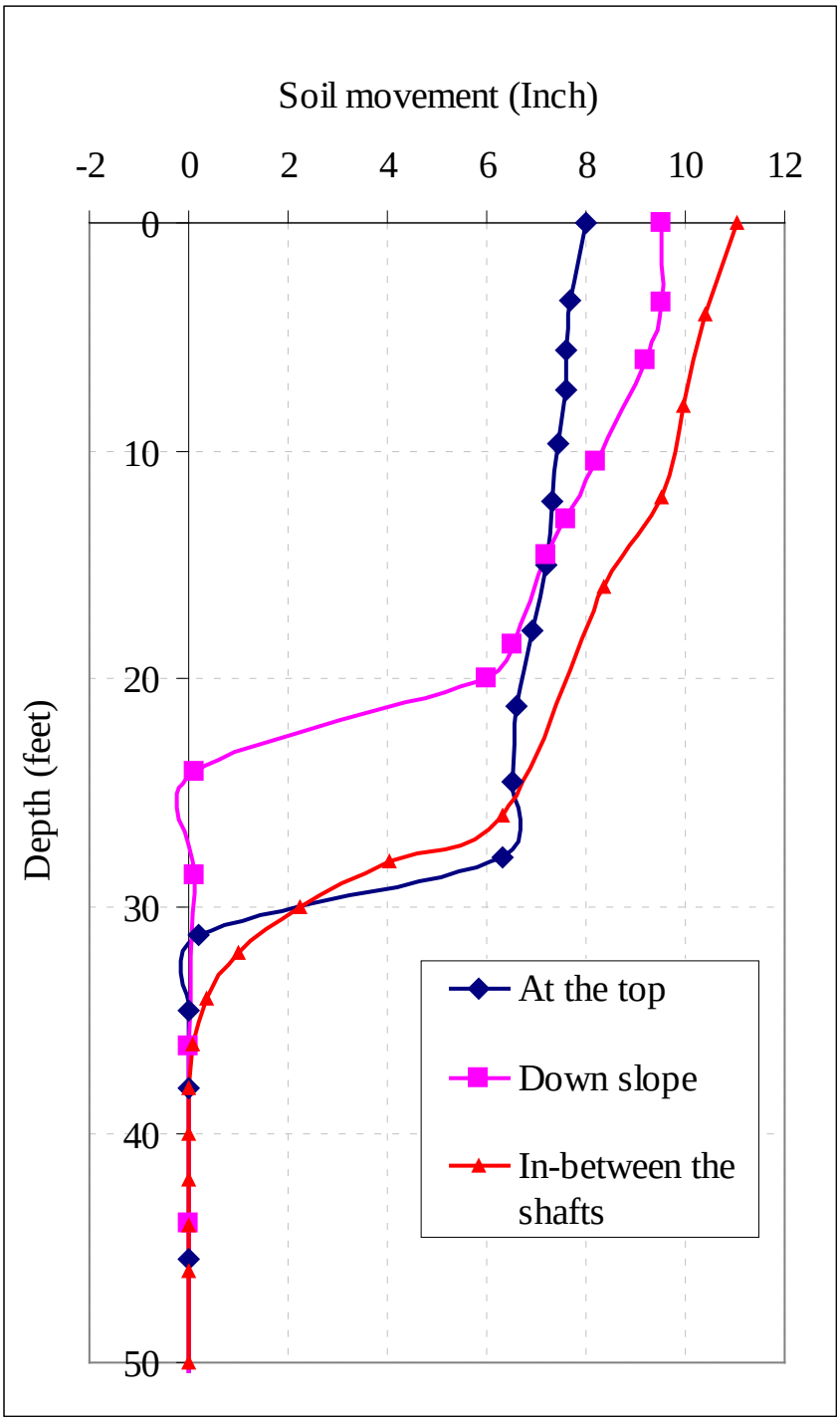

Figure 4.24: Computed Ground Movement Profiles due to Extreme Surcharge Loads

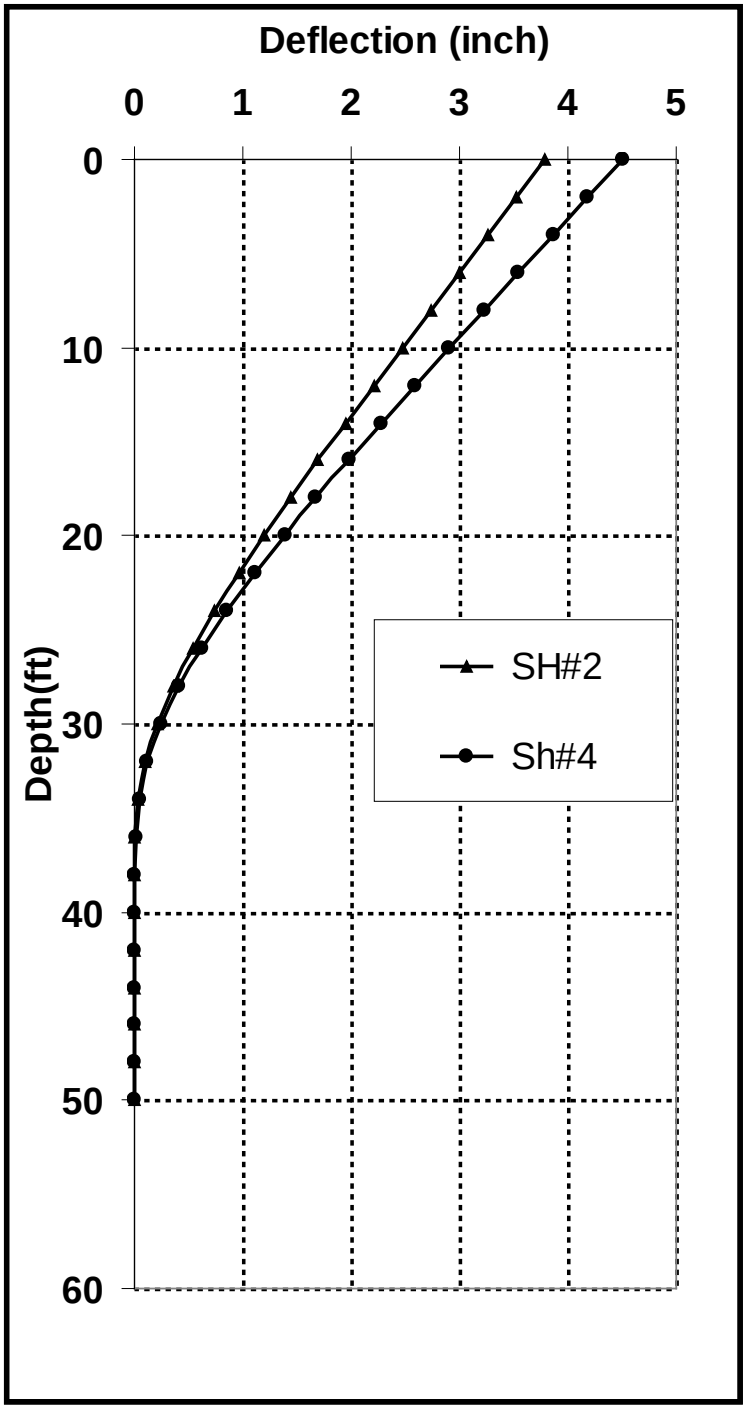

Figure 4.25: Computed Drilled Shaft Deflections at Extreme Surcharge Loads

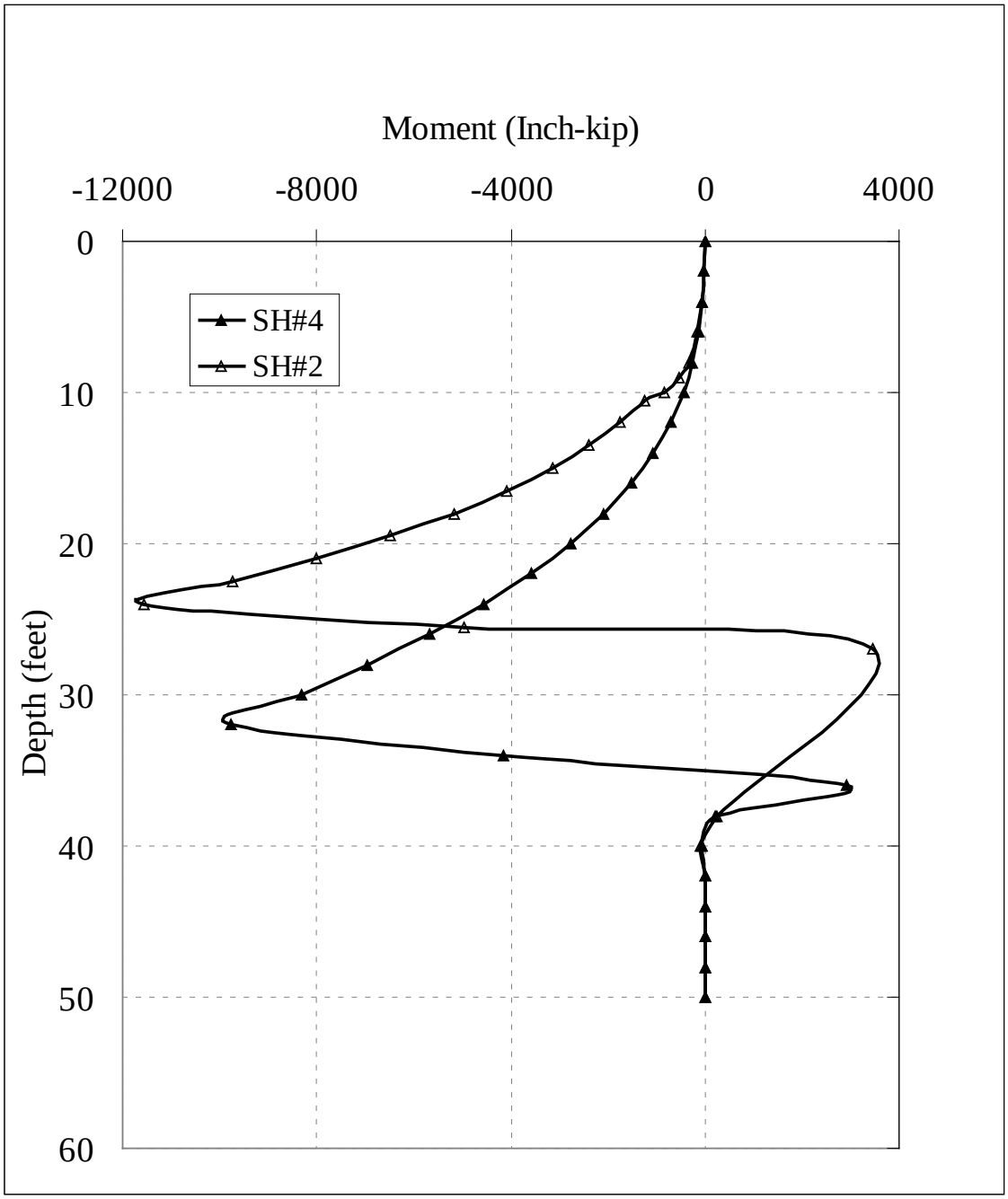

Figure 4.26: Computed Bending Moments in Drilled Shafts at Extreme Surcharge Loads

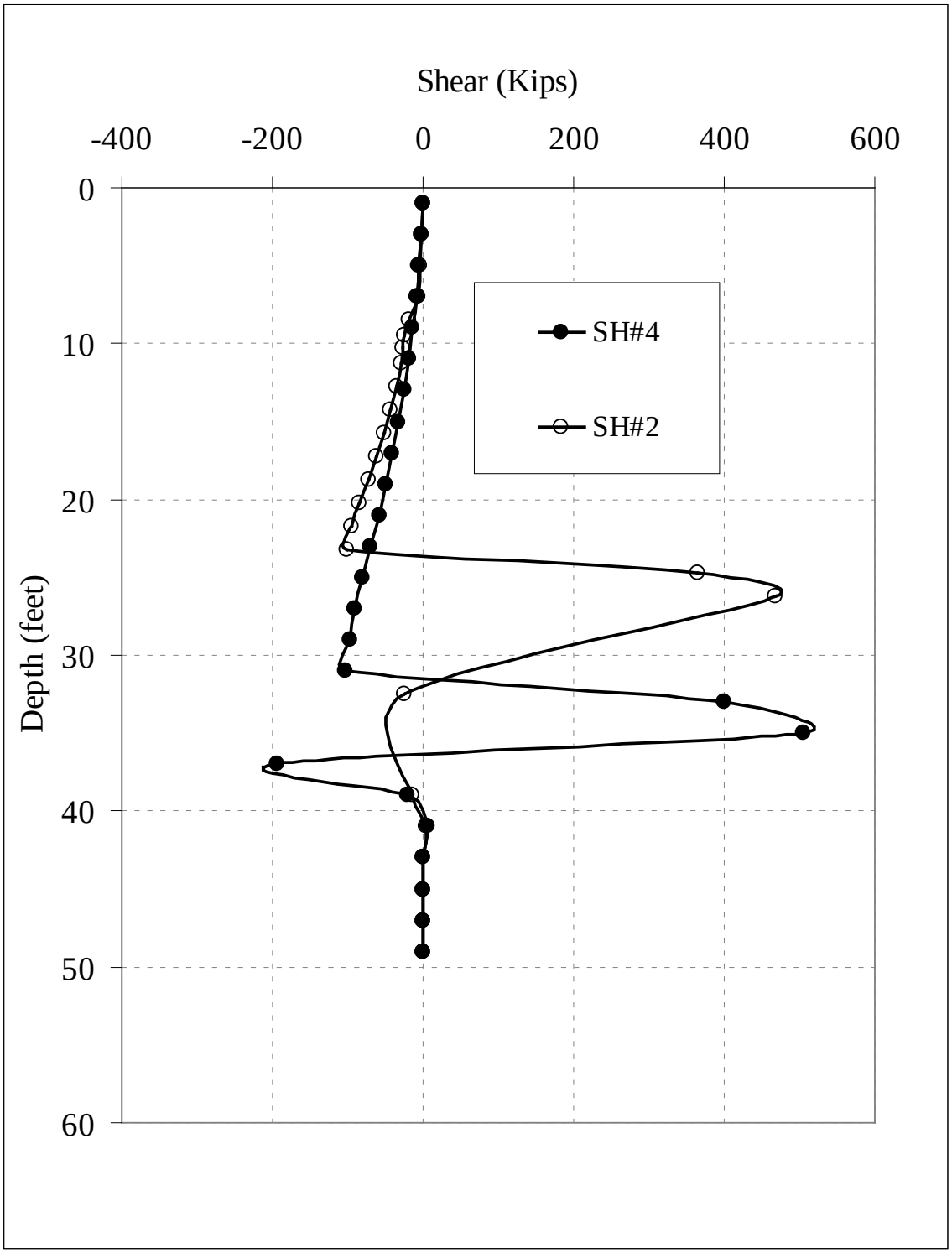

Figure 4.27: Computed Shear in Drilled Shafts at Extreme Surcharge Loads

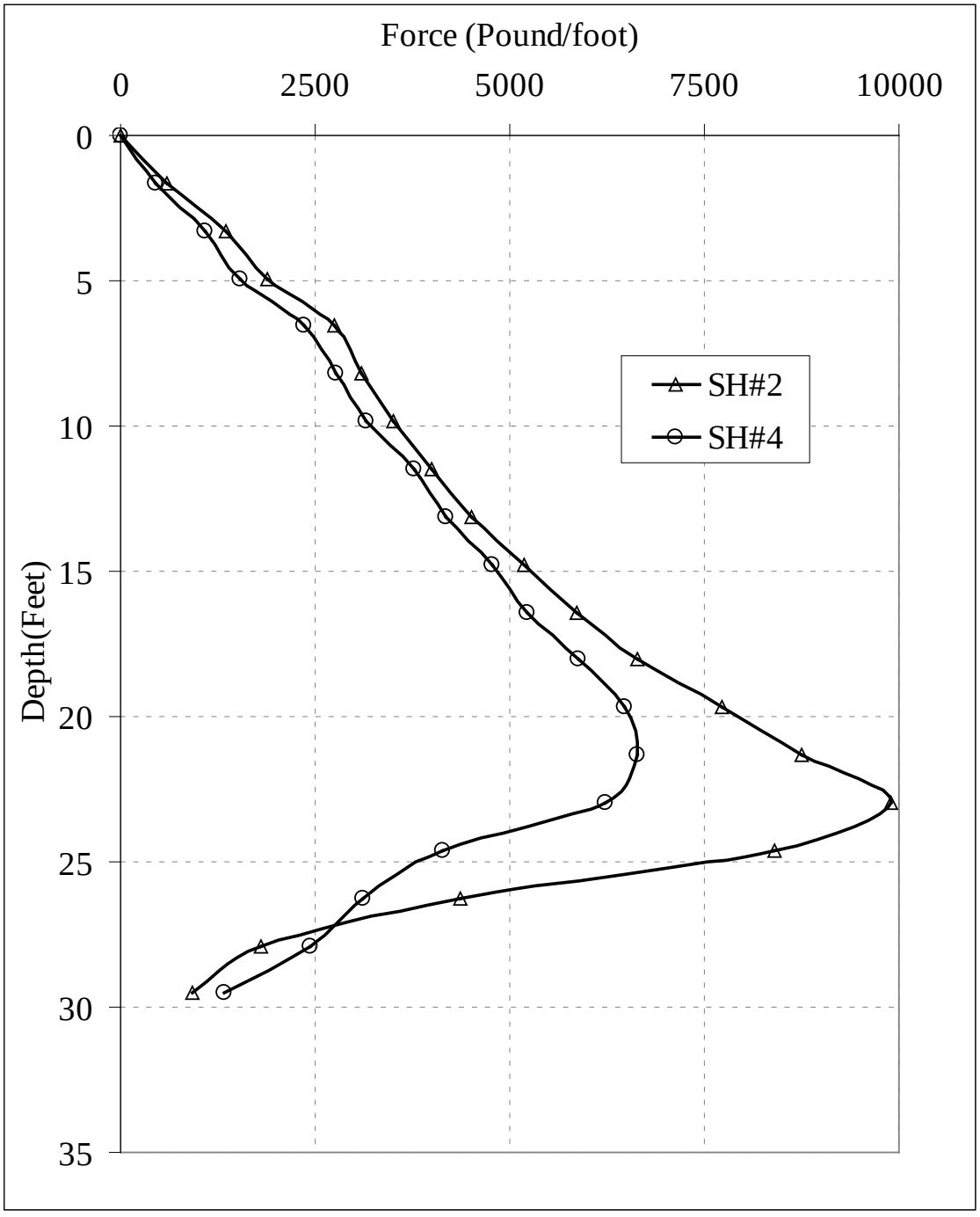

Figure 4.28: Computed Net Soil Reaction Force at Extreme Surcharge Loads

4.6.10 Global Factor of Safety

The global factor of safety (FS) of the slope was computed in finite element simulations for three different conditions by employing the strength reduction techniques. Specifically, the friction angle of the slip surface was incrementally reduced until the numerical divergence occurred in the finite element simulation. This was accomplished by reducing the tangent of the residual angle of internal friction $\tan(\phi_r)$ along the failure surface by a reduction factor RF until the displacement flow occurred. The smallest reduction factor which leads to numerical divergence is FS. The finite element analysis results for three cases are summarized as follows:

- Case 1: The slope reinforced with a row of drilled shafts but no surcharge load, FS = 1.7
- Case 2: The reinforced slope as in Case 1 but was subjected to the first loading, FS = 1.55
- Case 3 : The reinforced slope as in Case 1 but was subjected to both stages of loading, FS = 1.3

4.6.11 Factor of Safety of Drilled Shaft

The factor of safety of the drilled shaft can be determined as the ratio between the nominal moment capacity of the drilled shaft and the developed maximum moment in the shaft, or the ratio between the nominal shear capacity of the drilled shaft and the maximum shear force developed in the drilled shaft. The smaller of the two ratios is the

structural factor of safety of the drilled shaft. In the current case study, the structural FS of the drilled shaft is controlled by moment and equal to 5.7.

4.6.12 Comparisons with UA SLOPE 2.0 Predictions

The UA SLOPE 2.0 program was used to analyze the three cases cited in Section 4.6.10 where finite element simulation results were given. Table 4.4 provides a summary of comparisons for the FS and net force predicted by UA SLOPE 2.0 and those predicted by FEM simulations. The good match between the two methods indicated that UA SLOPE 2.0 program worked very well for complicated slope geometry and soil profiles.

Table 4.4: Comparison between FEM and UA SLOPE 2.0 Predictions for ATH-124 Load Test Site

Method	No Load		Load 1		Load 2	
	Shaft force (kips)	FS	Shaft force(kips)	FS	Shaft Force(kips)	FS
FEM	-	1.7	95.4	1.55	122.4	1.3
UA Slope 2.0	90.6	1.53	101.1	1.39	112.7	1.28

4.7 Summary and Conclusion

In this chapter, the method of slice stability analysis method for a slope, with or without the presence of a single row of spaced drilled shafts, was developed to incorporate the arching induced load transfer effect in a slope/shaft system. A PC based, user friendly computer program, UA SLOPE 2.0, was developed from the modification of earlier program, UA SLOPE developed by Liang (2002). The modifications of the computer program involved the adoption of the newly developed load transfer factor

through 3-D finite element simulation parametric studies wherein the strength reduction technique was used to facilitate reaching a failure state of a slope/shaft system. Based on the availability of UA SLOPE 2.0 for handling complicated slope geometry and soil profile conditions and composite non-circular type of failure surface, a step-by-step design procedure was outlined in this chapter. A design example was presented to demonstrate the application of UA SLOPE 2.0 program for the ATH-124 project site conditions. The validity of the developed method and the accompanied computer program, UA SLOPE 2.0, was established by excellent comparisons with 57 cases of 3-dimensional finite element simulation results using ABAQUS finite element program and the strength reduction technique. Furthermore, the actual load test data at the ATH-124 project site, together with the calibrated site specific finite element models were used to validate the accuracy of the UA SLOPE 2.0 program in a real case involving complex slope geometry, soil profiles, and composite non-circular failure surface.

It should be pointed that UA SLOPE 2.0 program has limitations. The main limitation is that it can only be used for design of a single row of appropriately spaced drilled shafts. The applicable range of S/D is between 2 to 4, as the load transfer factor was derived based on finite element parametric study in this range. In addition, the slope angle should not be greater than 60 degree. The value of cohesion is limited to 2500 PSF while the friction angle should not be greater than 55 degree. The contributions of the design methodology presented in this chapter, together with the accompanied UA SLOPE 2.0 program, can be enumerated as follows:

- It provides a practical, relatively simple, and yet accurate design methodology, based on the method of slice limiting equilibrium approach and FEM generated semi-

empirical equations, for the engineers to design an optimized slope/shaft system involving the use of a single row of spaced drilled shafts as a means for enhancing slope stability.

- The developed method includes consideration of both geotechnical and structural design requirements while providing the optimized design outcome with least construction cost.
- The developed method with the user-friendly UA SLOPE 2.0 program can be easily used for optimization of the design parameters related to the design of drilled shafts, i.e., shaft diameter, spacing between adjacent shafts, location of the shaft, and the slope angle if necessary.
- The developed method with the user friendly UA SLOPE 2.0 program is capable of handling complex slope geometries, soil profiles, general shape of failure surfaces, and different locations of the drilled shafts.
- The developed methodology is capable of estimating the design forces imparted on the drilled shafts for structural design of the drilled shaft.

CHAPTER V

INSTRUMENTATION AND MONITORING AT THREE ODOT PROJECT SITES

5.1 Introduction

As a part of this research, the research team has participated in instrumentation and monitoring of three ODOT slope stabilization projects, in which a single row of drilled shafts were used as a means for slope stabilization. These three slope stabilization projects are located in Jefferson County (JEF-152), Washington County (WAS-7), and Morgan County (MRG-376). The instrumentation installed at the sites was designed to monitor both drilled shafts and slope behavior so that the safety and the performance of the stabilizing drilled shafts as well as the stabilized slopes can be assessed. The main objective of this chapter was to provide succinct information about the three projects, including a summary of site conditions, the instrumentation layout, the construction plans, and the monitoring results. In addition, the UA SLOPE 2.0 program was used to re-analyze the stability of the drilled shafts stabilized slope. Observations regarding the performance of the stabilized slopes using single row of drilled shafts and adequacy of the drilled shaft structural capacity were presented for each project site.

5.2 JEF-152

In this section a detailed study for the project site JEF-152 is provided. The slope reconstruction, remediation (reinforcement using single row of drilled shaft and the selection of parameters of the slope/shaft system), instrumentation, and monitoring are explained.

5.2.1 Site Conditions

The 300 ft long failed slope was located on the Westside of State Road SR-152 from Station 54+50 to 57+50. The slope failure was considered mainly a translational landslide with a basal shear surface typically at the depth between 27 to 33 ft from ground surface. The slip surface was found to be along the shallow dipping mudstone basal rock and parallel to the ground surface. The triggering mechanism of the slope failure was attributed to rising ground water table. The pictures showing the landslide site under repair and after embankment restoration using drilled shafts are shown in Figure 5.1 and Figure 5.2, respectively.

Figure 5.1: JEF-152 Failed Slope under Repair

Figure 5.2: The Re-constructed JEF-152 West Embankment

5.2.2 Site Investigation and Soil Properties

As part of this research effort in quantifying the weak rock properties, pressuremeter test was performed in July 2005 on the rock at a depth of 26.5 ft. Based on pressuremeter test results, the average modulus of elasticity for the intermediate geo-materials encountered at JEF-152 site is 14 ksi and an unconfined compressive strength is 100 psi. Detailed pressuremeter test results along with interpreted results, such as rock mass modulus and unconfined compression strength test results can be found in Table 5.1. The p-y curves at a depth of 26.5 ft and 31.5 ft deduced from Briaud's method (The Pressuremeter, 1992) are shown in Figure 5.3. Table 5.2 provides a summary of the test results of the intact core specimens.

Table 5.1: Pressuremeter Test Results at JEF-152 Site

Sample	Depth (ft)	Limit Pressure (psi)	Q_u (psi)	E_m (psi)
1	26.5	710	100	15140
2	31.5	905	125	13300

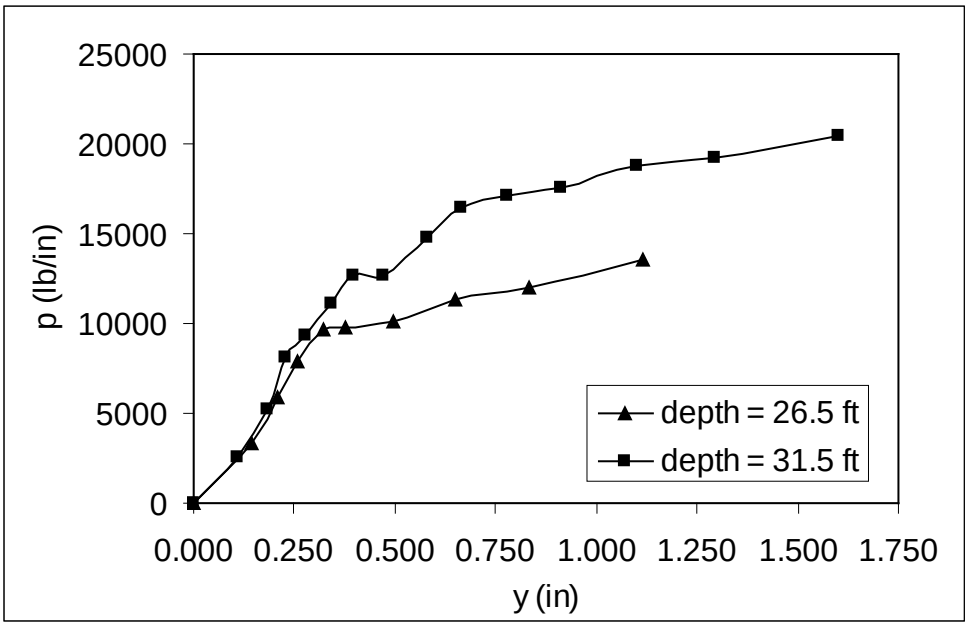

Figure 5.3: P-y Curves for JEF-152 Mudstone Deduced Using Briaud's Method

Table 5.2: Laboratory Test Results at JEF-152 Site

Sample	Top (ft)	Bottom (ft)	Q_u (psi)	E_i (psi)	Posson's Ratio
1	26.5	27	39	16700	N/A
2	27	27.5	21	4200	0.39
3	28	28.5	57	4460	0.43
4	29	29.5	56	4690	N/A
5	31.5	32	15	550	N/A
6	32	32.5	16	580	0.38

5.2.3 Drilled Shaft Properties and Instrumentation Plans

The failed slope was reconstructed and stabilized with a single row of circular drilled shafts. A total of 42 drilled shafts were installed at 40 ft off the centerline of the road pavement. The total shaft length was designed to be equal to 45 ft, including about 20 ft length of the shaft penetrating through the relatively firm weak rock layer. The diameter of the shaft is 3.5 ft and the center-to-center spacing between the adjacent shafts is 7 ft. The longitudinal steel reinforcement of the drilled shafts consists of 26 #11 bars. The nominal moment capacity of the drilled shaft, based on LPILE analysis, was 2,824 kip-ft.

The slope/shaft system at the site was instrumented and monitored. Two drilled shafts (shafts #20 and #21) as well as the ground of the slope were instrumented according to the instrumentation plan shown in Figure 5.4. Instruments inside each drilled shaft include nine vibrating wire pressure cells at 3 different levels (i.e., at 10 ft, 16 ft, and 22 ft from the top of the shaft.) At each elevation level, a total of three pressure cells (i.e., upslope side, down-slope side, and 45^{o} from upslope side) were installed. In addition to the pressure cells, sixteen vibrating wire strain gages were installed on each shaft at 8 different elevation levels (i.e., at the depth from shaft top = 13 ft, 16 ft, 19 ft, 22 ft, 25 ft, 27 ft, 29 ft, and 31 ft, respectively), with two strain gages at each level (i.e., the upslope side and down-slope side). Also, two inclinometer casings extended into the entire length of the drilled shaft were installed inside each drilled shaft to measure the shaft deflection due to the slope movement. For monitoring ground movement, two inclinometer casings were installed as follows: Inclinometer (INC#3) on the up-slope side of the drilled shaft

and inclinometer (INC#4) on the down-slope side of the drilled shaft. To measure the earth pressure, three earth pressure cells were installed between the drilled shafts at 3 elevation levels (i.e., at the depths of 10 ft, 16 ft, and 22 ft from the ground surface). A total of three vibrating wire piezometers were installed at 3 locations across the slope to monitor the ground water table level. Figure 5.5 shows a representative cross-section at station 56 + 00, along with the interpreted slip surface and layout of instrumentation plans. Figure 5.6 shows a schematic diagram of the instrumentation details along the shafts length for shafts #20 and #21. Locations of the pressure cells mounted on the drilled shafts and installed between the shafts are shown in Figure 5.7.

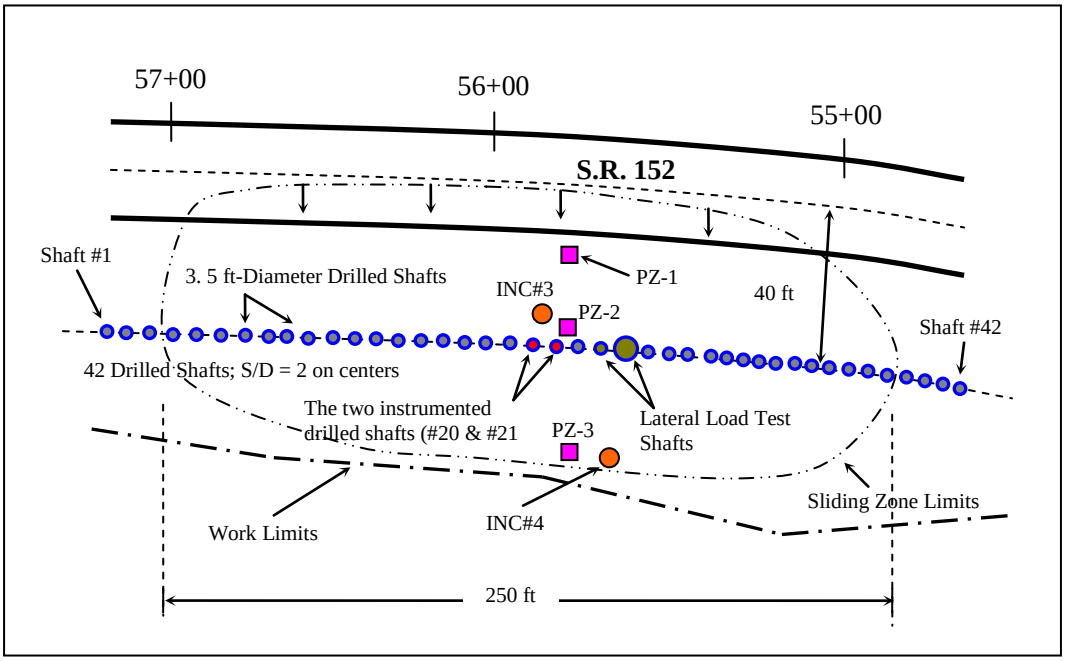

Figure 5.4: Plan View of the Instrumentation Details at JEF-152 Landslide Site

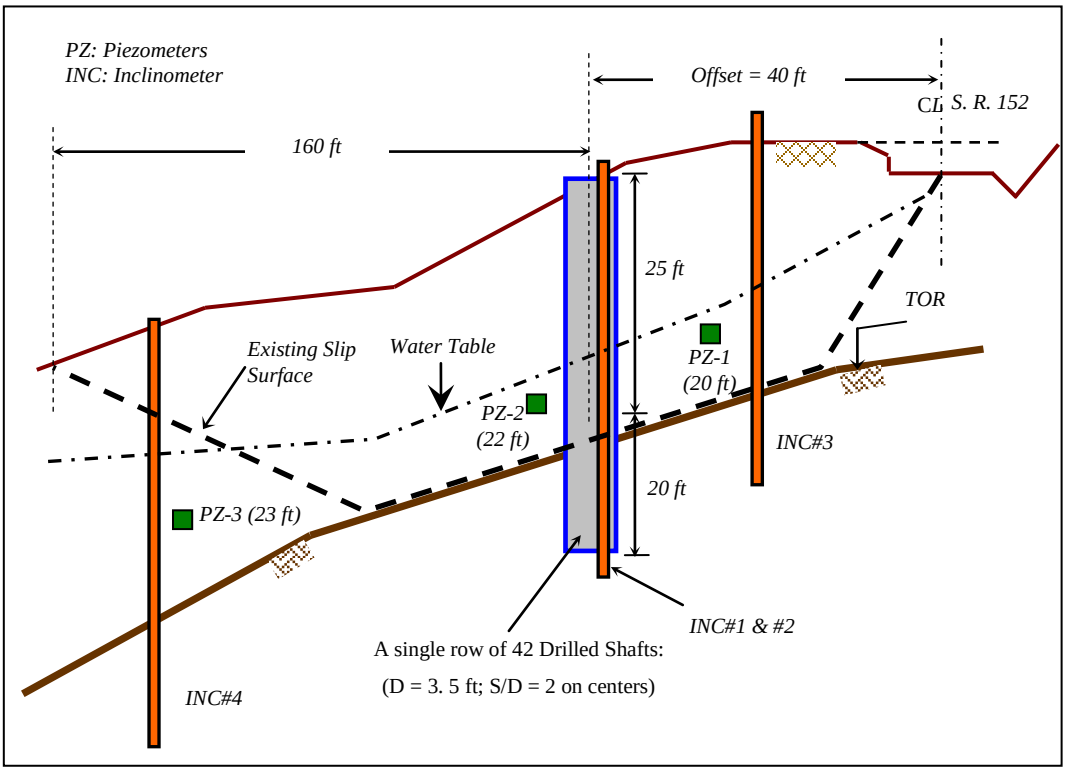

Figure 5.5: Representative Cross Section at JEF-152 Site

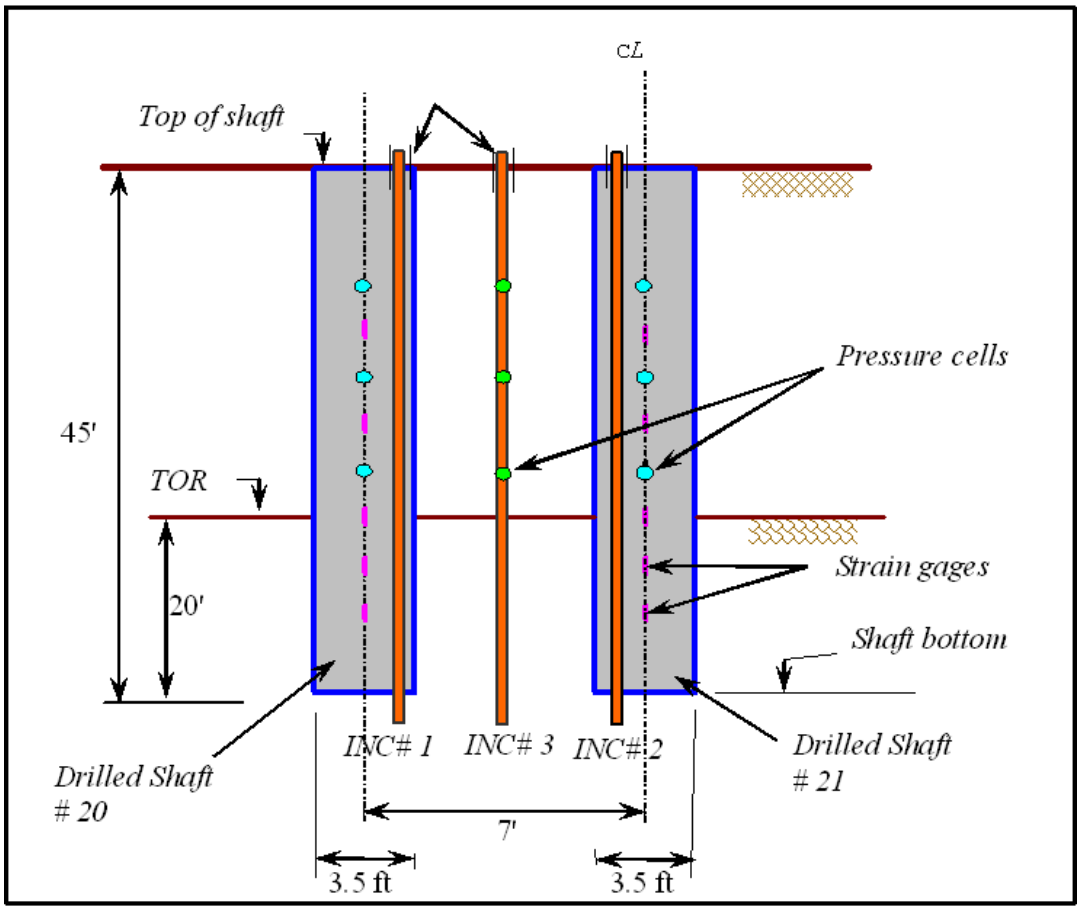

Figure 5.6: Schematic Diagram of Instrumentation Layout at JEF-152 Site

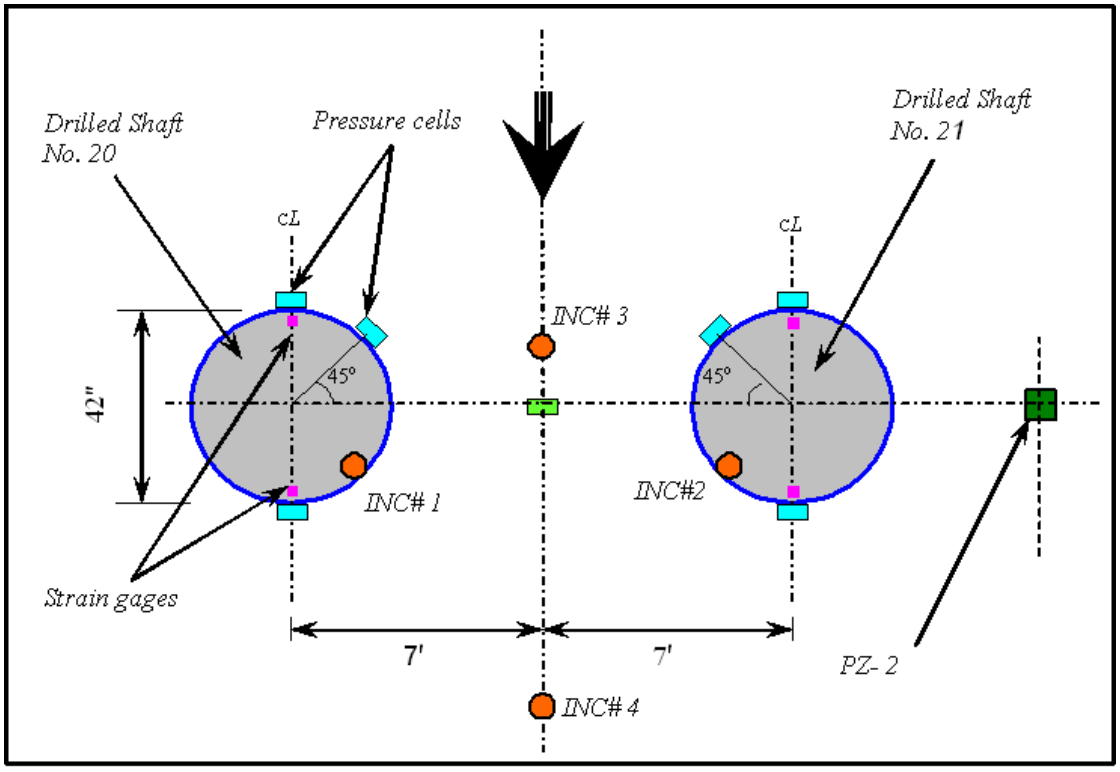

Figure 5.7: Schematic Diagram of Pressure Cells and Strain Gages at JEF-152 Site

5.2.4 Monitoring Results

The ground moments at the stabilized slope site were monitored by inclinometer (INC#3) on the up-slope side of the drilled shafts and inclinometer (INC#4) on the down-slope side of the drilled shaft near the toe of the slope. The complete set of figures showing the cumulative soil movements for INC#3 and INC#4 are presented in Figure 5.8 and Figure 5.9, respectively. The up-slope inclinometer readings show that the cumulative soil movement over the past three years at the slip surface location is less than 1.0 inch. It is noted that the large deflection measured at the top of the inclinometer casing down to 5 ft depth is due to the fact that this portion of casing is above the ground surface. It can be seen that the slope movement on the up-slope side of the drilled shafts

was relatively small over the three years of monitoring period. The cumulative soil slope movements taken from INC #4, as shown in Figures 5.9, indicates that there was no significant slope movement (less than 0.25 inch) on the down-slope side of the drilled shafts over the past three years.

The behavior of drilled shafts was monitored by inclinometer casings and the strain gages, as described in the previous section. The inclinometer readings are shown in Figure 5.10 for Shaft #20 (INC #1) and in Figure 5.11 for Shaft #21 (INC #2), respectively. As can be seen, the maximum cumulative deflection in shaft #20 (INC#1) in the direction of slope movement equal to 1.25 in. Similarly, the maximum deflection of the shaft #21 in the direction of slope movement is about 1.0 in. It should be noted that the drilled shafts were installed such that its head is 12.0 ft below the top of the inclinometer casing and 8.0 ft below the ground surface.

The profiles of the bending moment measured form the embedded strain gages are shown in Figure 5.12 and Figure 5.13 for Shaft #20 and Shaft #21, respectively. The maximum moment developed in shaft #20 was located near the rock surface and equal to 600 ft-kip. The maximum measured moment is Shaft #21 is 950 ft-kips. The maximum moment capacity of the as-built drilled shaft is 2,824 ft-kip. Therefore, it appears that the structural design of the drilled shaft is quite adequate.

The piezometer readings were used to determine the ground water table. The measured ground water level at the site is shown in Figure 5.14. All of the installed pressure cells, both in the soil and the reinforcing shafts, did not work properly. Therefore, the measured data from pressure cells is not presented in this dissertation.

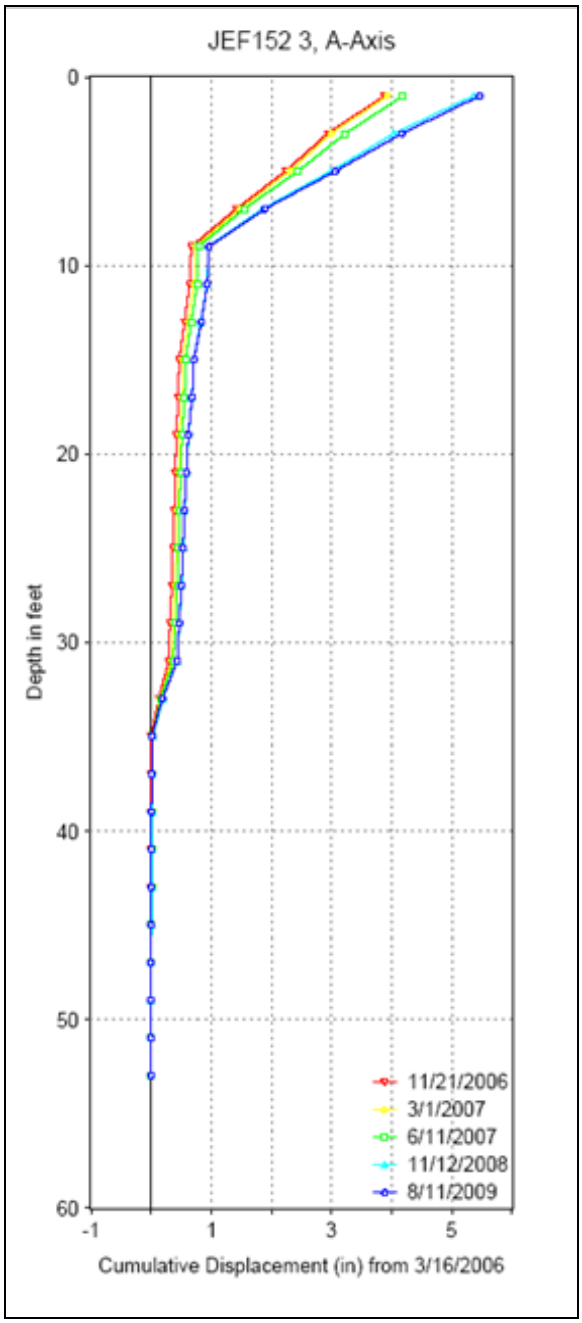

Figure 5.8: The Cumulative Soil Movement Up-Slope the Shafts (Inclinometer #3) at JEF-152

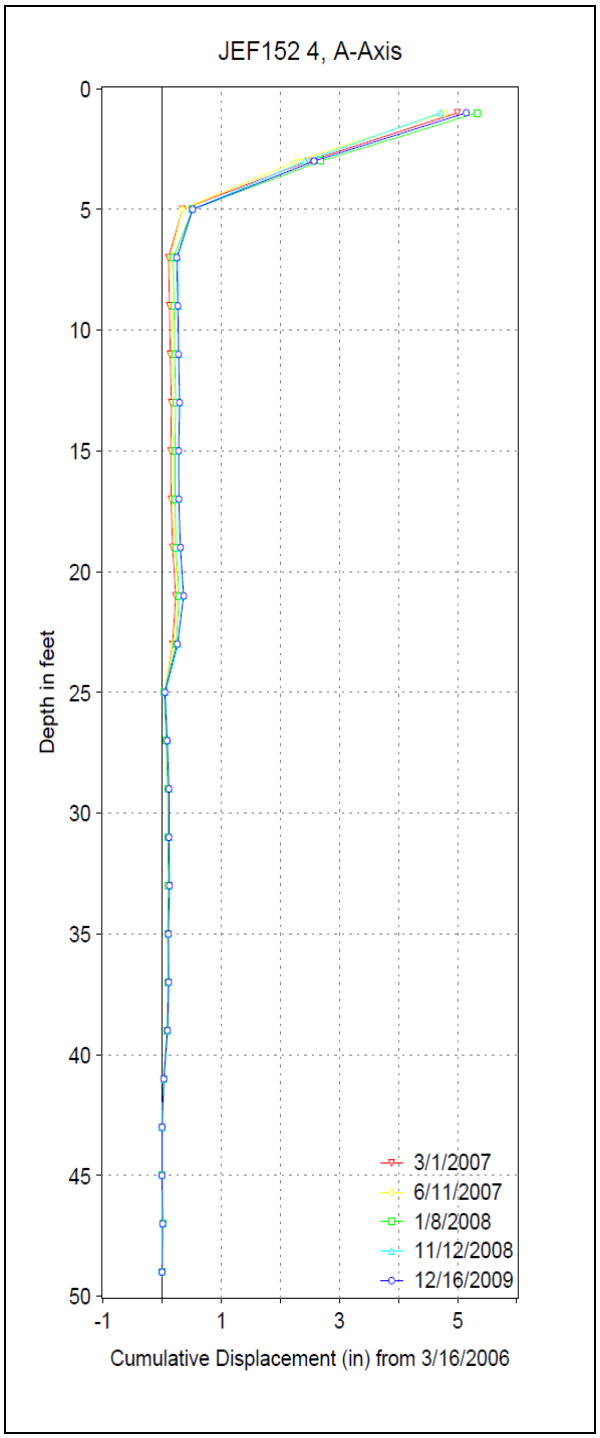

Figure 5.9: The Cumulative Soil Movement Down-slope the Shafts (Inclinometer #4) at JEF-152

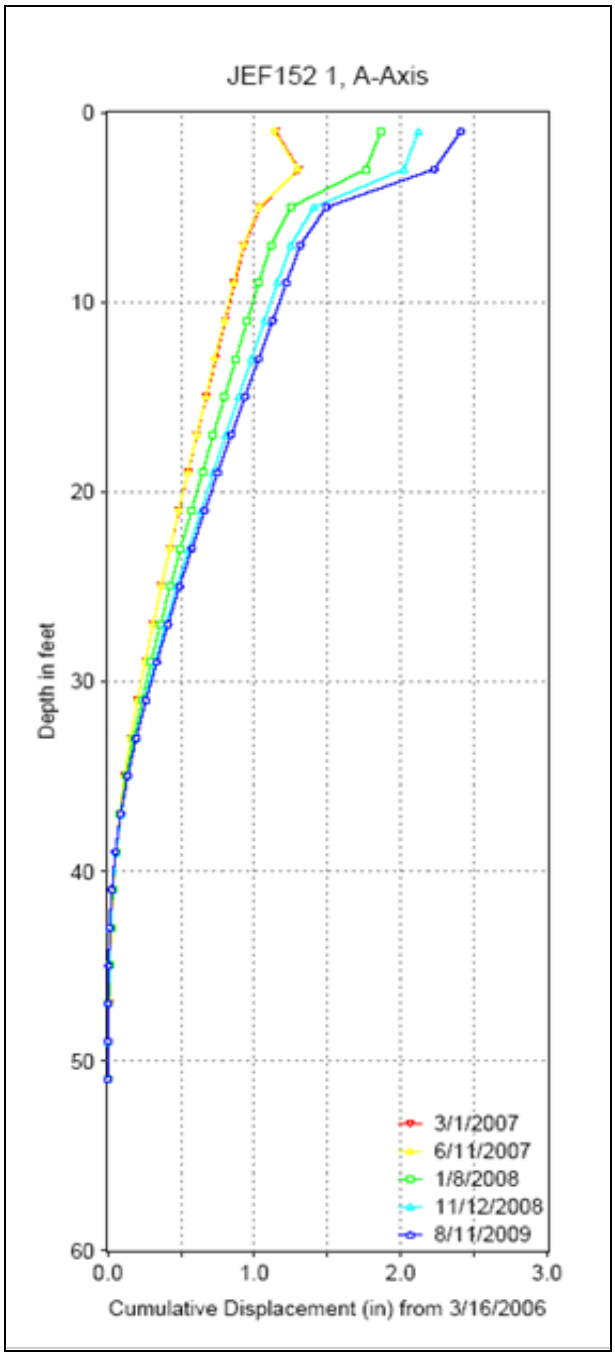

Figure 5.10: The Cumulative Deflection in Shaft #20 at JEF-152 (Inclinometer #1)

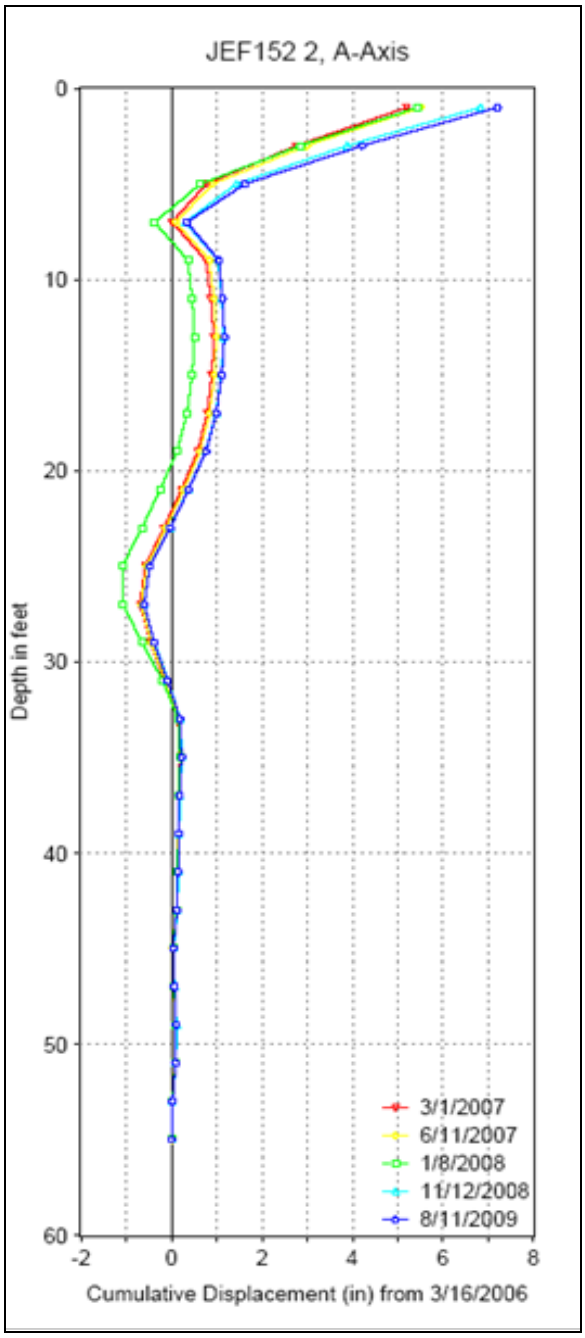

Figure 5.11: The Cumulative Deflection in Shaft #21 at JEF-152 (Inclinometer #2)

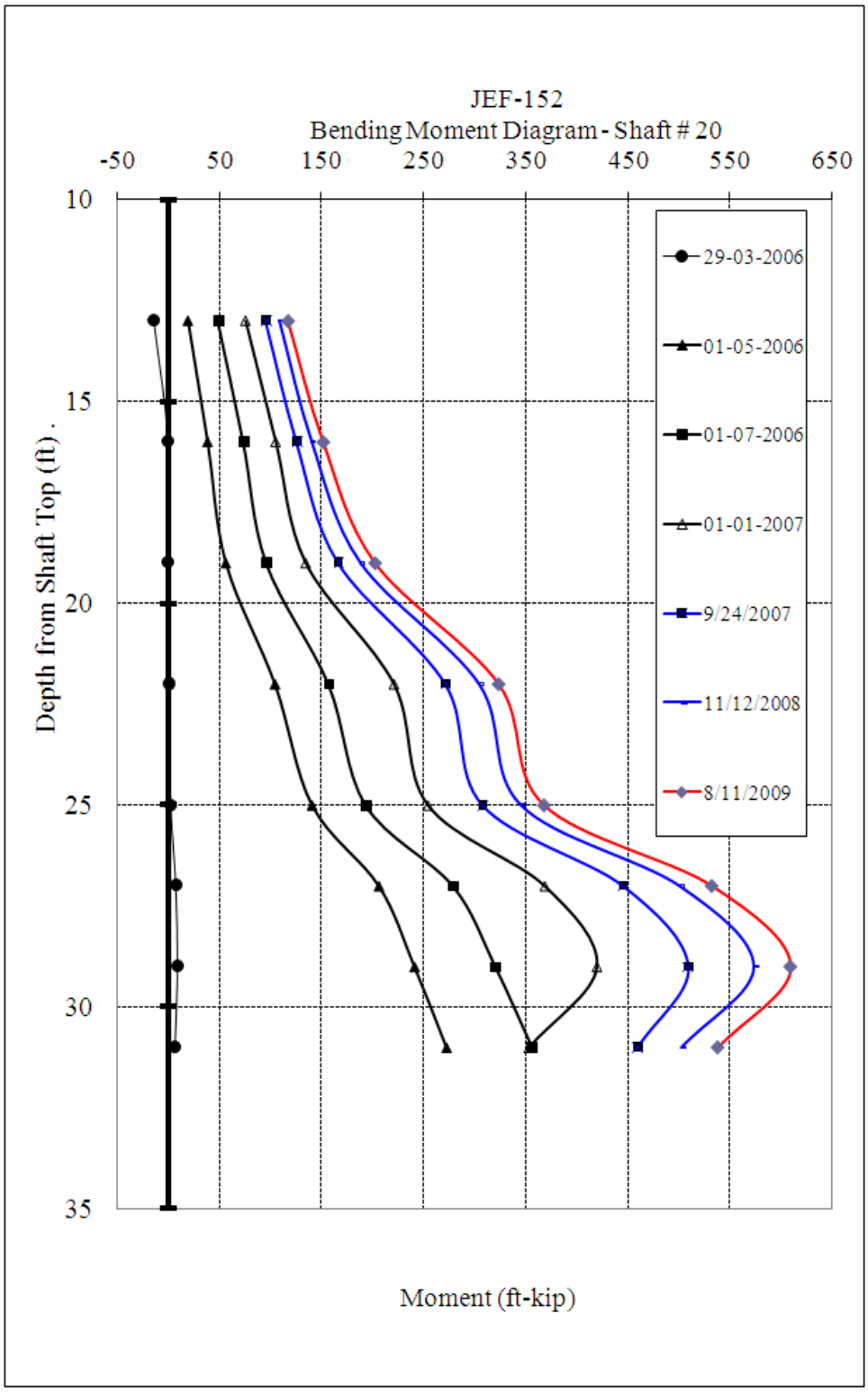

Figure 5.12: Measured Moments along Shaft #20 at JEF-152 Site

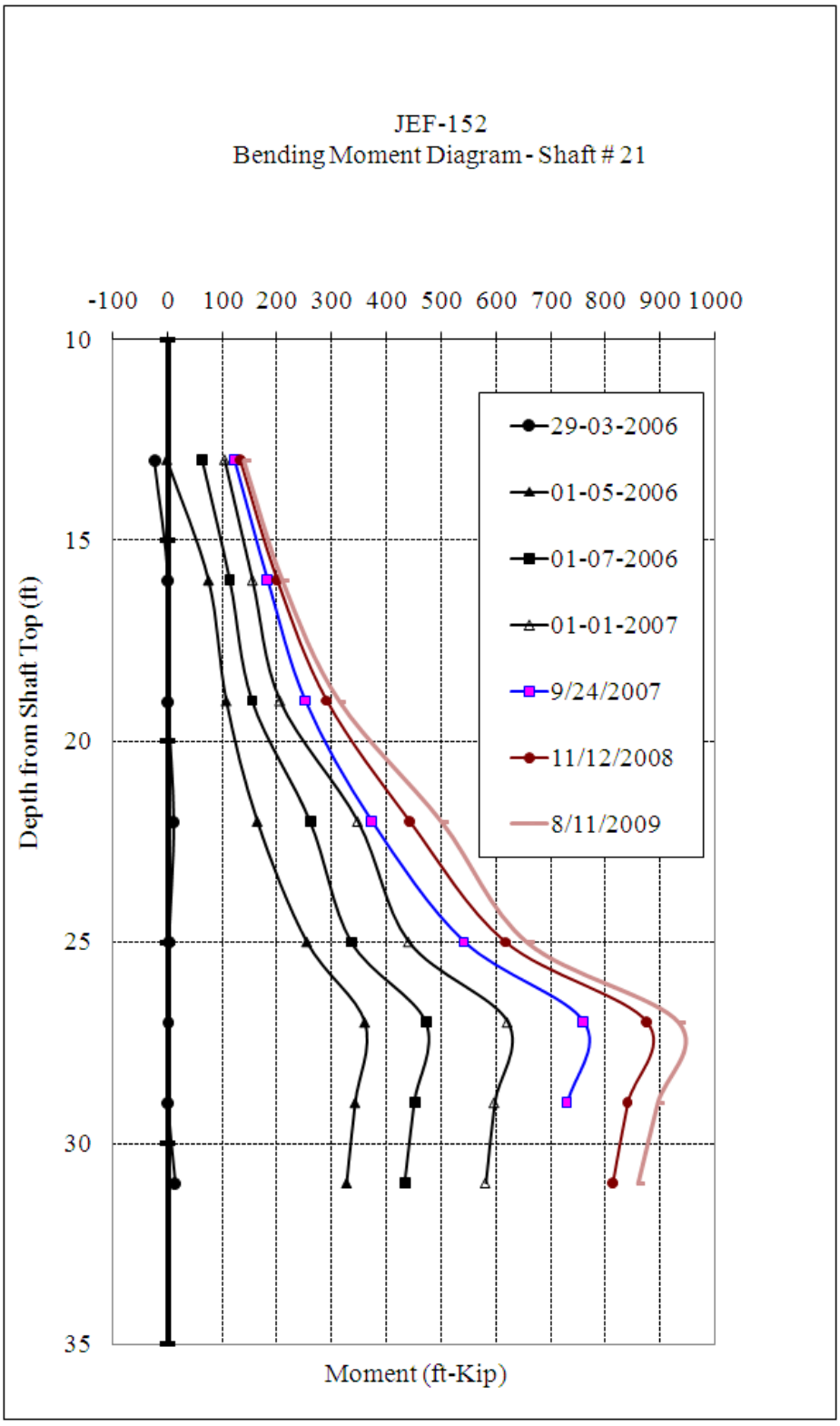

Figure 5.13: Measured Moments along Shaft #21 at JEF-152 Site

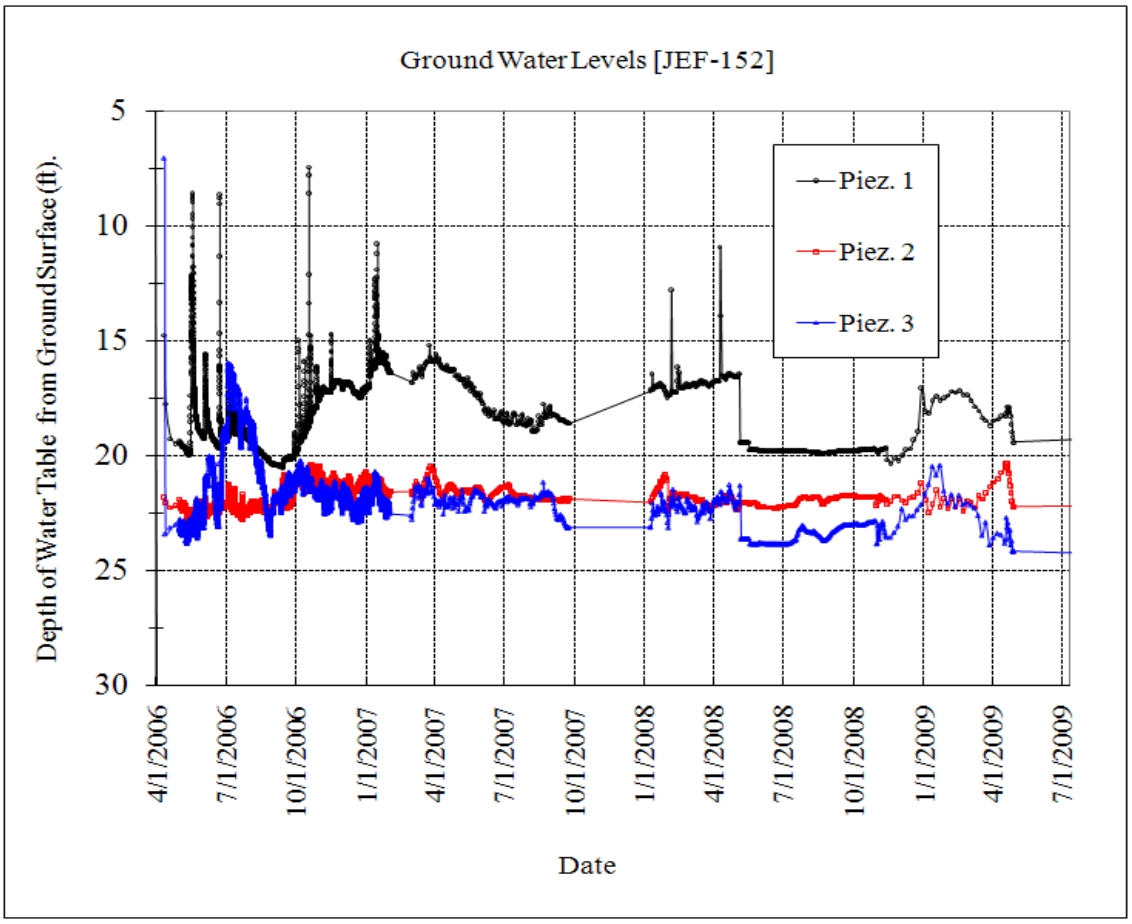

Figure 5.14: Measured Ground Water Table Depths at the JEF-152 Site

5.2.5 UA SLOPE 2.0 Analysis Results

The computer code UA SLOPE 2.0 is used for analyzing the slope/shaft system of the re-constructed JEF-152 site with the installed stabilization drilled shafts. The simplified slope profile and soil profile, shown in Figure 5.15, along with other input information summarized in the Table 5.3, was used for analysis. The soil layer No. 2 in Table 5.3 is used to represent the existing slip surface, where the residual friction angle of the thin soil layer was back calculated from the slope stability analysis using UA SLOPE 2.0 program. For the computed FS of 1.08 for the slope without the drilled shafts, the

strength parameters of layer No. 2 were found to be as follows: c =0.0 and ϕ =11^{o}. The factor of safety of the slope-shaft system, representing the as- built system, was found to be 1.24 by the UA SLOPE 2.0 program. The computed net force applied to the shaft was 102 Kips. The results of UA SLOPE 2.0 analysis for both cases, without shafts and with shafts are shown in Figures 5.16 (a) and (b), respectively

The maximum moment from this computed earth thrust, using LPILE program, is 1.6 x 10^4 in-kips, while the maximum computed shear force is 150 kips, and the corresponding shaft head deflection is 3.2 in.

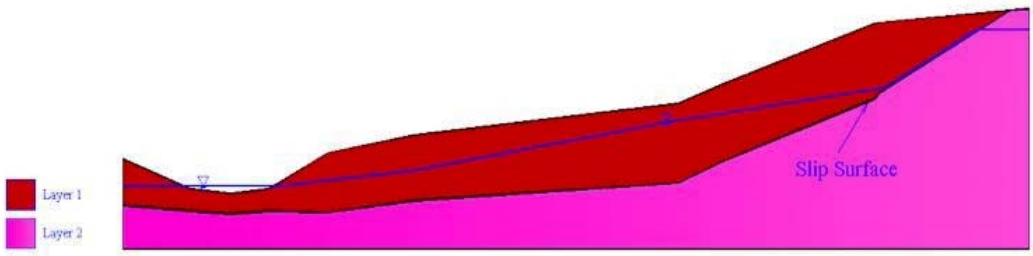

Figure 5.15: Simplified Slope Cross-Section Used in UA SLOPE Analysis

Table 5.3: Soil Properties Used in UA SLOPE Analysis for JEF-152 Site

Layer	c (psf)	ϕ (^{o})	γ (pcf)
Surface layer	100.0	20.0	125
Residual/Slip surface	0	11.0	125
Firm/Rock	500	26	140

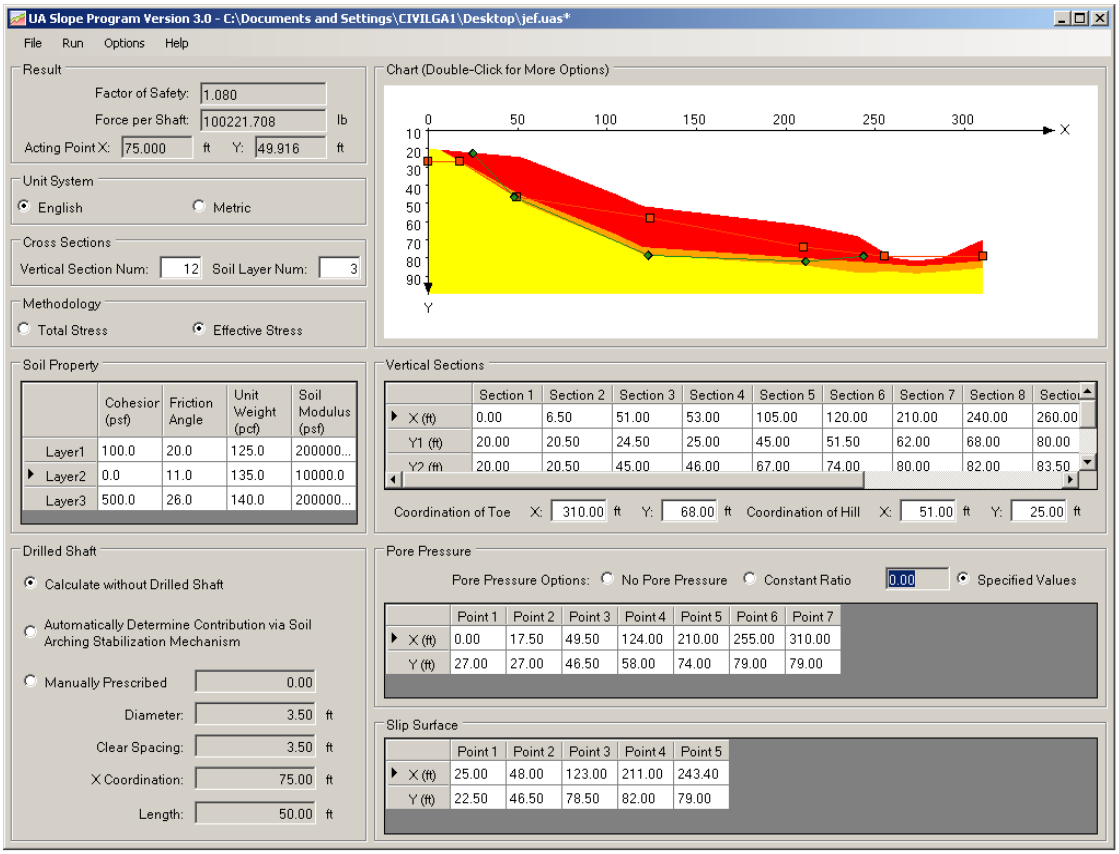

(a)

Figure 5.16: UA SLOPE 2.0 Analysis Results: a) without Drilled Shaft b) with Drilled Shaft

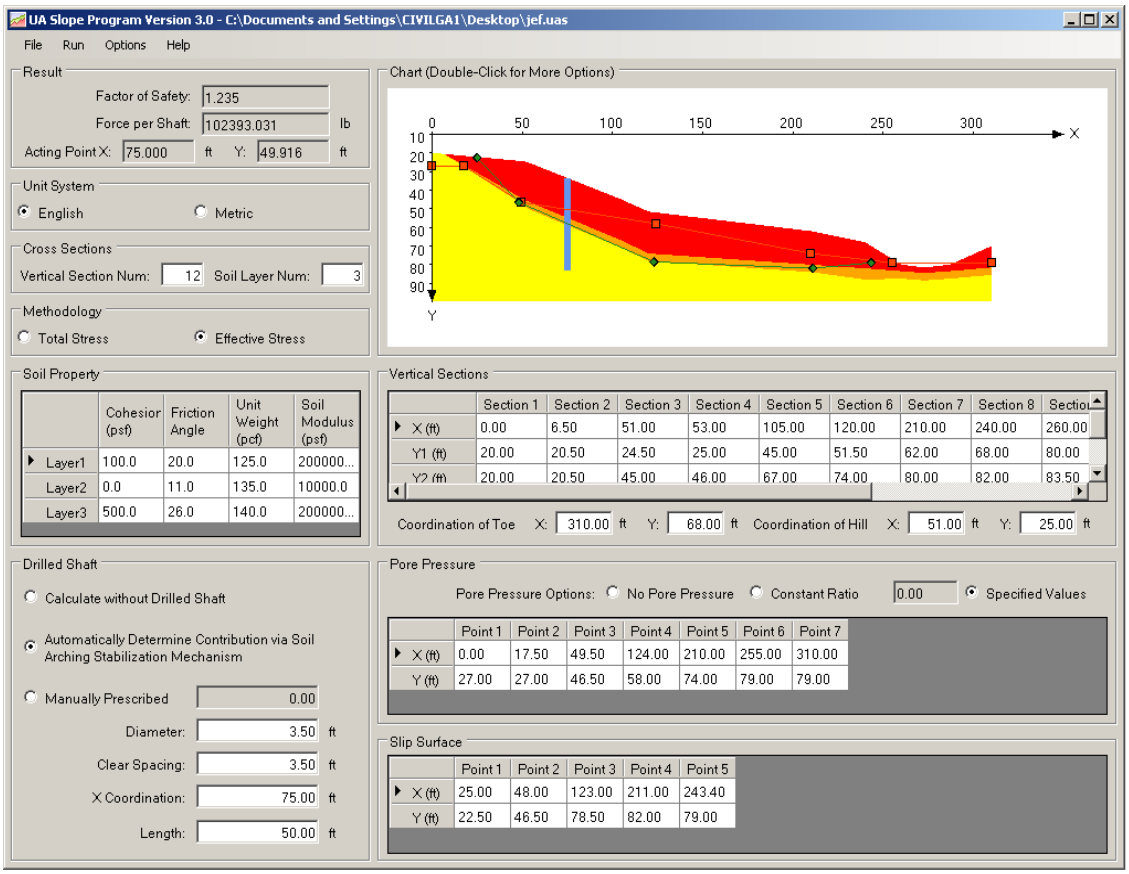

(b)

Figure 5.16: UA SLOPE 2.0 Analysis Results: a) without Drilled Shaft b) with Drilled Shaft, Continued

5.3 WAS-7

In this section a detailed study for the project site WAS-7 is provided. The slope reconstruction, remediation (reinforcement using single row of drilled shaft and the selection of parameters of the slope/shaft system), instrumentation, and monitoring are explained.

5.3.1 Site Conditions

The failed slope is located in Washington County at State Rout SR 7 on the edge of the Ohio River. The 1,100ft long slope failure (between Sta. 2528+00 and Sta. 2539+00) was large, deep seated block failure, with the block sliding along the bedrock surface and extending out into the river. The soil mass moved along a well-defined rupture surface at the depth of 50 ft. The slope failure was triggered by a rapid drawdown of the Ohio River occurred at the end of January, 2005, when runway barges were lodged in the Belleville Lock Dam. The water level dropped rapidly about 27 feet. In spring 2005, ample evidences of landslide movement along SR 7 were observed, including dropped and bowed sections of guardrail and cracks and drop-off in the pavement.

The failed slope was reconstructed and reinforced with a single row of drilled shaft. The restored embankment slope is shown in Figure 5.17.

Figure 5.17: The Restored Embankment at WAS-7 Site.

5.3.2 Site Investigation and Soil Properties

For site investigation, seven borings were drilled along the roadway and lower part of the slope. Borings along the roadway encountered from 10 ft to 11 ft of fill above the native soils, upon which the roadway was constructed. These soils appear to be of local native origin, containing many fragments of weathered sandstone and shale. This fill is composed of soils generally described as soft to stiff clayey gravel (A-2-6), sandy silt (A-4a), silty clay (A-6a and A-6b), and clay (A-7-6). The average soil in the fill is medium stiff silt and clay (A-6a).

A layer of colluvium, ranging in thickness from 7.5 ft to 27.5 ft was encountered next in the borings. The colluvium was encountered below the fill in the borings along the roadway, but was encountered just below the surface in the borings further down the slope. Colluvium is a loose deposit of rock debris accumulated through the action of gravity at the base of a cliff or slope. The colluvium is composed of soils generally described as stiff to hard silty and clayey gravel (A-2-4 and A-2-6), silty clays (A-6a and A-6b), and clay (A-7-6), with many fragments of weathered sandstone and shale. The average soil in the colluvium is very stiff silty clay (A-6b).

A layer of alluvium, ranging in thickness form 16.7 ft to 18 ft was encountered below the colluvium. The alluvium is composed of soils generally described as medium stiff to stiff sandy silt (A-4a), silt (A-4b), and silt and clay (A-6a), with very little to no coarse sand or gravel. The average soil in the alluvium is medium stiff silt and clay (A-6a).

A layer of residual soils, weathered directly off of the parent bedrock, was encountered beneath the alluvium or colluvium. This layer ranges in thickness from 3 to 16 ft. The residual soils are composed of material generally described as medium stiff to stiff sandy silt (A-4a) and silty clays (A-6a and A-6b). SPT blow-count refusal was encountered at the bottom of this layer, in materials composed of highly weathered sandstone and shale bedrock. Bedrock was encountered in all borings between elevations 586.4 ft and 596.0 ft, with an average elevation of approximately 591.6 ft. Bedrock is generally described as being composed of inter-bedded layers of sandstone, shale, siltstone, and mudstone. The RQD in the bedrock varied between 0% and 91%. The RQD of recovered shale, siltstone, and mudstone was 0%. One recovered sample of sandstone had an RQD of 91%, however, most sandstone samples had an RQD varying between 0% and 33%. No rock unconfined compression tests were performed. A cross-section of the landslide, on which the soil layers and types are illustrated, is shown in Figure 5.18. The pertinent soil properties for the soil layers are summarized in Table 5.4.

Field pressuremeter test was performed at this site in July 2005 on the rock at a depth of 32 ft. According to the pressuremeter results, the modulus of elasticity for the sandstone encountered at this site was 707 ksi and the un-drained shear strength was estimated as 578 psi. The p-y curve at a depth of 32 ft was deduced using Briaud's method as shown in Figure 5.19.

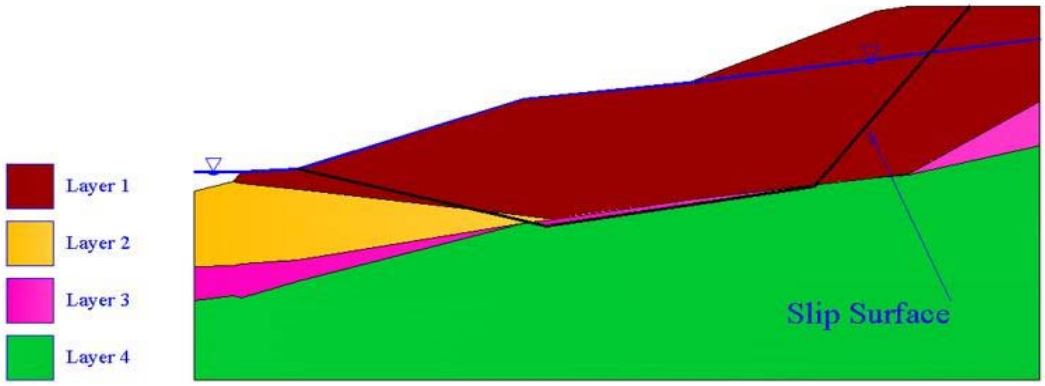

Figure 5.18: Representative Cross Section of WAS-7 Site

Table 5.4: Soil Properties for Each Soil Layer at WAS-7 Site

Layer No.	Description	ϕ (^{o})	c (psf)	γ (pcf)
1	Colluvium	22	50	100
2	Alluvium	24	100	110
3	Residuum	26	100	120
4	Soft Rock	12	0	125

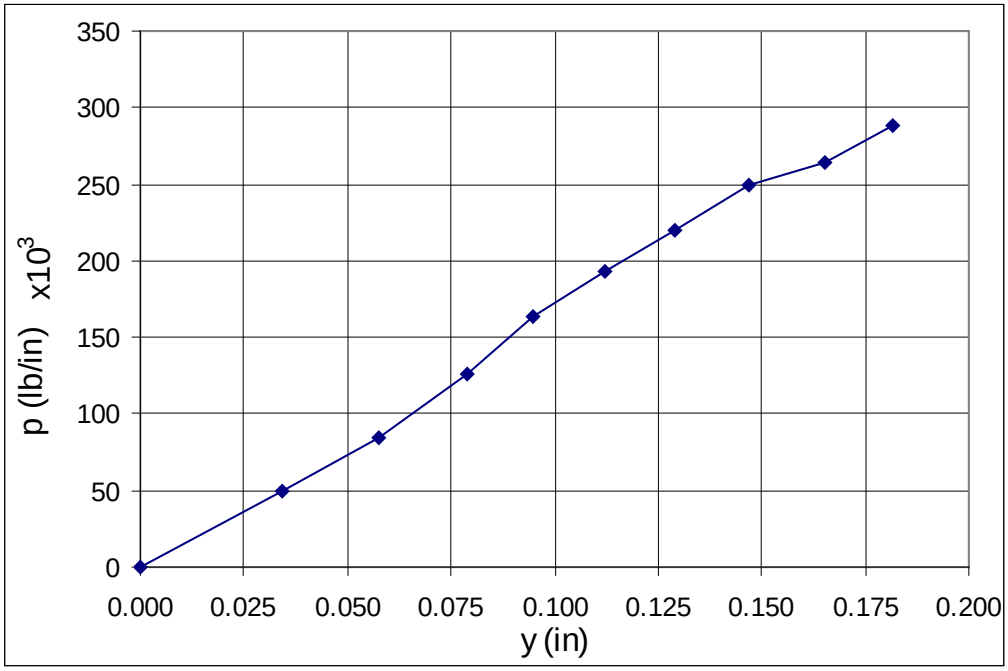

Figure 5.19: P-y Curve at Depth of 32 ft at WAS-7 Site

5.3.3 Drilled Shaft Properties and Instrumentation Plans

The slope was reconstructed and reinforced using a single row of circular drilled shafts. A total number of 128 drilled shafts were installed 100 ft off the centerline of the road pavement. The total shaft length was designed to be 40 ft. A portion of 10 ft length of the shaft penetrated down through the firm layer. The diameter of the shaft is 4 ft and the center-to-center spacing between the adjacent shafts is 12 ft. The steel reinforcement of the drilled shaft consists of 32 #14 bars. The nominal moment capacity of the drilled shaft was computed as 4,918 ft-kips.

The slope-shaft system at WAS-7 site was extensively instrumented and monitored. Two drilled shafts (shafts #53 and #54) as well as the surrounding soil mass on the slope were instrumented and monitored. Instrument inside each drilled shaft

included nine vibrating wire pressure cells at 3 different levels (i.e., depth from shaft top = 12.5 ft, 18.5 ft, and 24.5 ft). At each level, there were three pressure cells (i.e., upslope side, down-slope side, and 45^{o} from the upslope side). In addition to the pressure cells, sixteen vibrating wire strain gages were installed on each shaft at 8 different elevation levels (i.e., depth from shaft top = 11 ft, 14 ft, 17 ft, 20 ft, 23 ft, 26 ft, 29 ft, and 32 ft repectively). There were two strain gages at each level (i.e., upslope side and down-slope side). Also, two inclinometer casing extended for the entire shaft length were installed inside each drilled shaft to measure the shaft deflections. Instrument on the ground included three inclinometer casings (i.e., up-slope, between the shafts, and down-slope). In addition, three earth pressure cells were installed between the drilled shafts at 3 elevation levels (i.e., depth from ground surface = 12 ft, 18 ft, and 24 ft). Three vibrating wire piezometers were installed at 3 locations across the slope (i.e., at upslope location: depth = 28 ft, between the drilled shafts: depth = 27 ft, and down-slope location: depth = 25 ft). Figure 5.20 shows a schematic cross-section of the slope at Stat. 2532 + 75.0, with piezometers, inclinometer casing, and shaft location illustrated. Figure 5.21 shows a schematic diagram of the instrumentation details along the shaft length for shafts #53 and #54. Details of the pressure cells mounted inside the drilled shafts on the ground are shown in Figure 5.22.

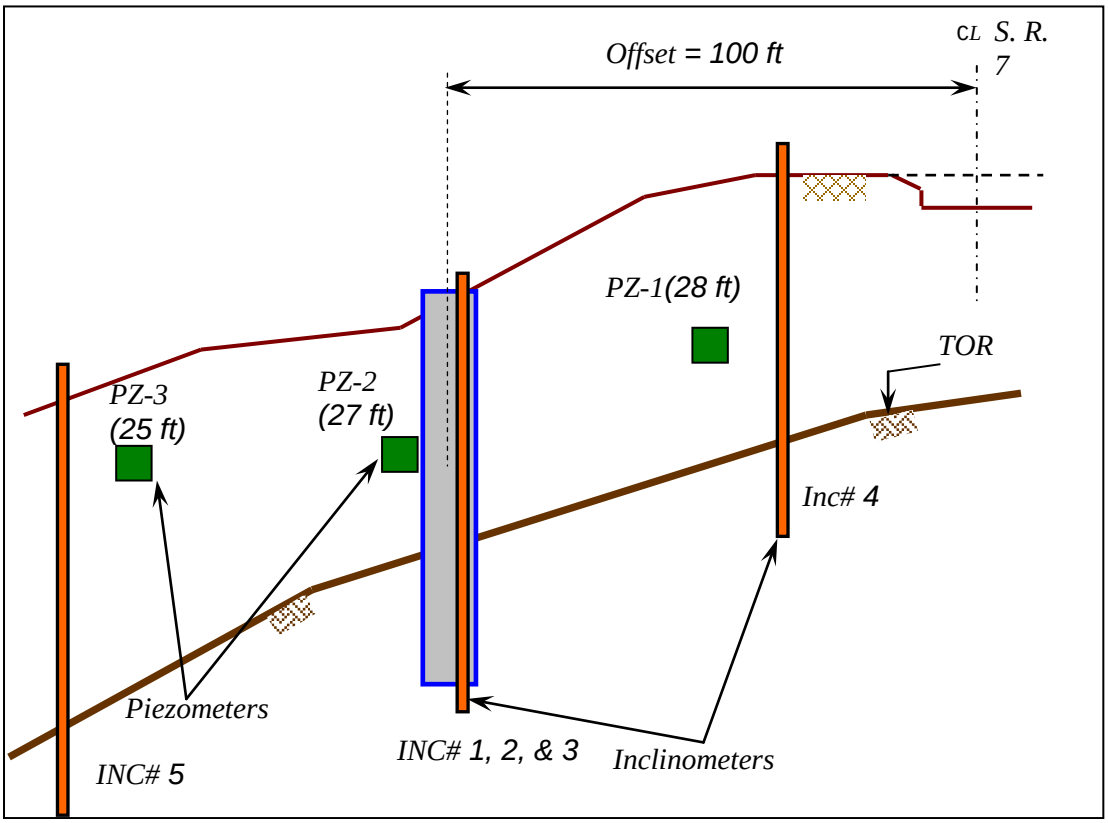

Figure 5.20: Cross-Section View of WAS-7 Site Showing Instrument Locations

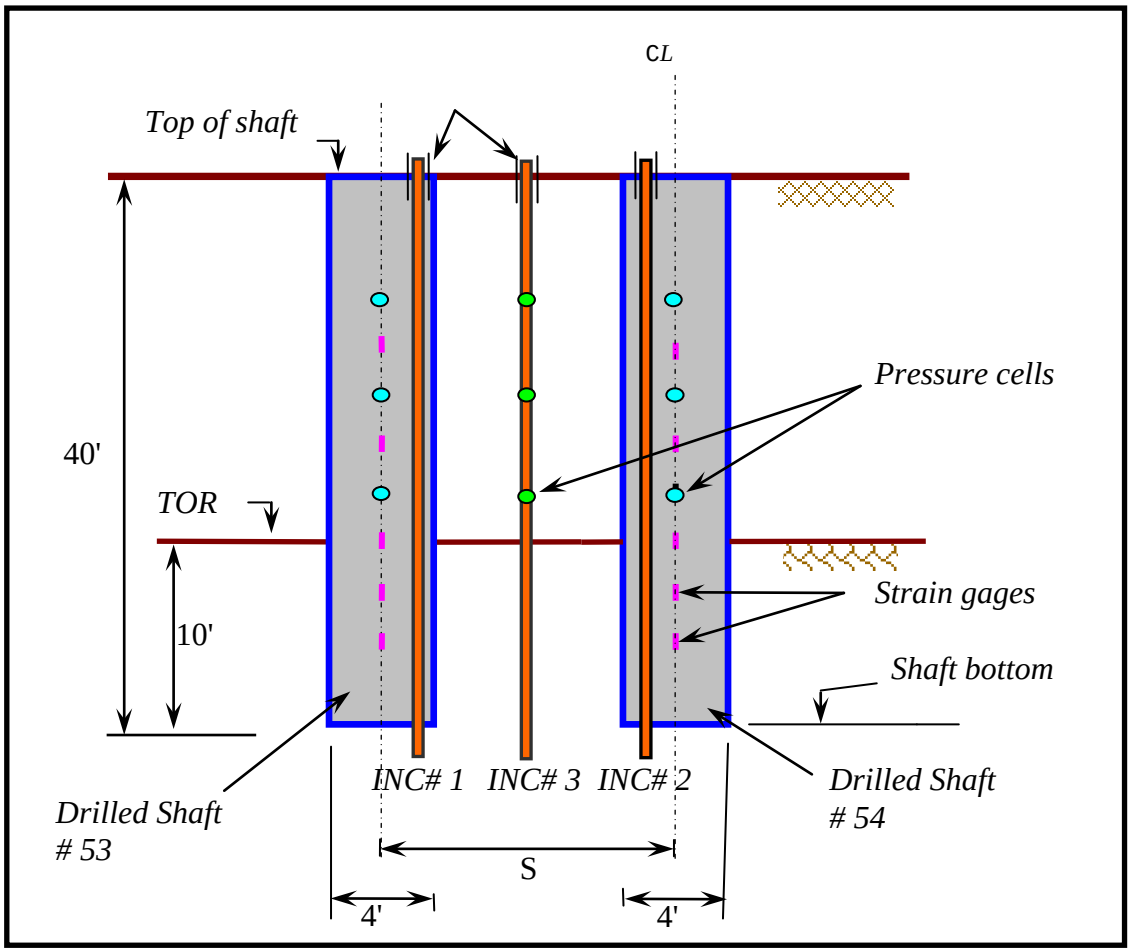

Figure 5.21: WAS-7 Instrumentation Plans (Cross-section 2)

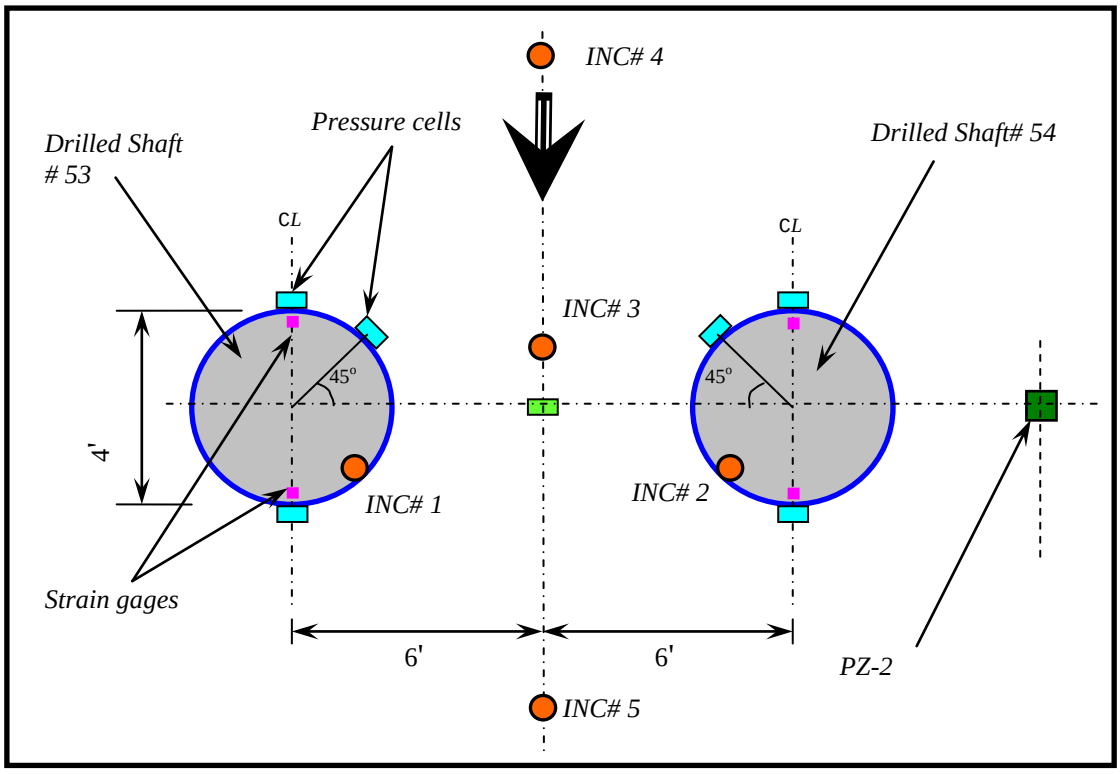

Figure 5.22: Plan View of Pressure Cell Locations Inside Drilled Shafts and on Ground at WAS-7 Site

5.3.4 Monitoring Results

The cumulative slope movements at the site obtained from the readings of inclinometer (INC#3) installed in the arching zone are shown in Figures 5.23. As can be seen, there was no significant soil movement in the arching zone. The cumulative soil movement (5 ft below top of casing) in INC#3 over the past three years was less than 0.25 in.

The up-slope and down slope inclinometer (INC#4, INC#5, respectively) readings are shown in Figure 5.24 and Figure 5.25. As can be seen, there was no major soil movement in the slope over the past three years.

The deflections of the two monitored drilled shafts (#53 and #54) are shown in Figure 5.26 and Figure 5.27 for shaft#53 and shaft#54, respectively. As can be seen from Figure 5.26 that the cumulative maximum deflection in shaft #53 (Inclinometer #1) in the direction of the slope movement, over the past three years, was less than 0.3 in. The reading of inclinometer #2 installed in Shaft #54 showed that there was no major cumulative deflection (the maximum was less than 0.2 in), as be seen from Figure 5.27.

The moment measured in Shaft #53 is shown Figure 5.28. The maximum measured moment is 225 ft-kip, while the shaft moment capacity is 4,918 ft-kip as estimated using the software LPILE. The moment measured in Shaft#54 is shown in Figure 5.29. The maximum moment measured in shaft #54 is 184 ft-kip.

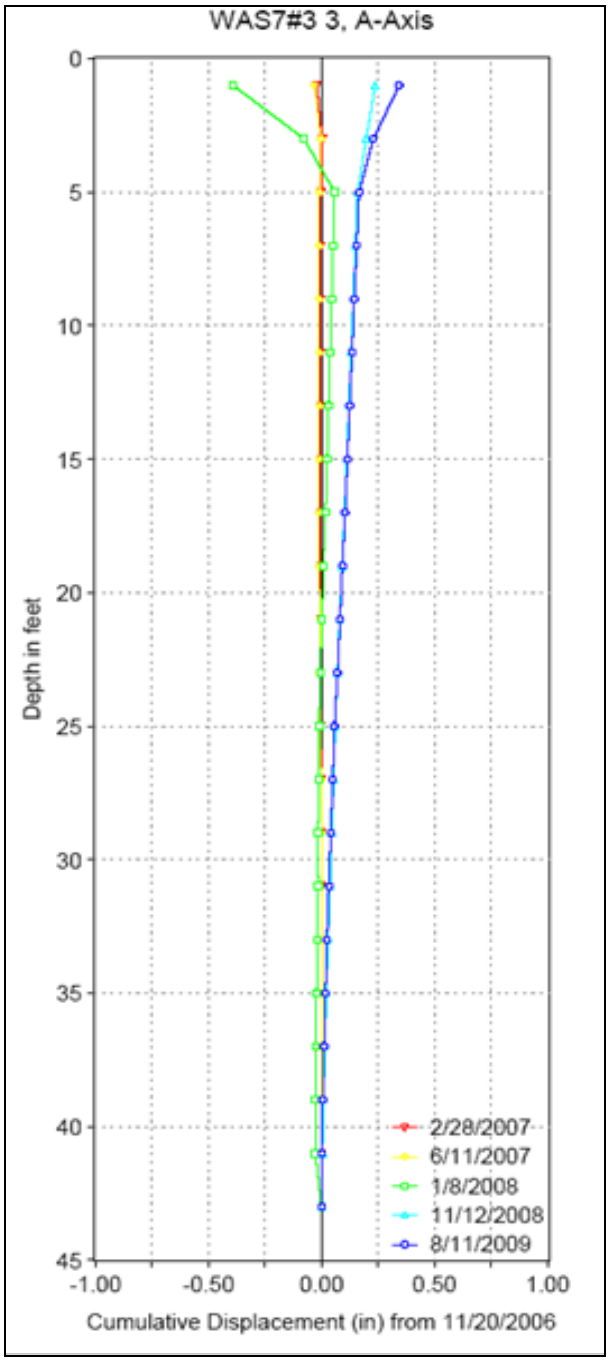

Figure 5.23: Cumulative Soil Movement (Inclinometer #3) In-between the Drilled Shaft at WAS-7 Site

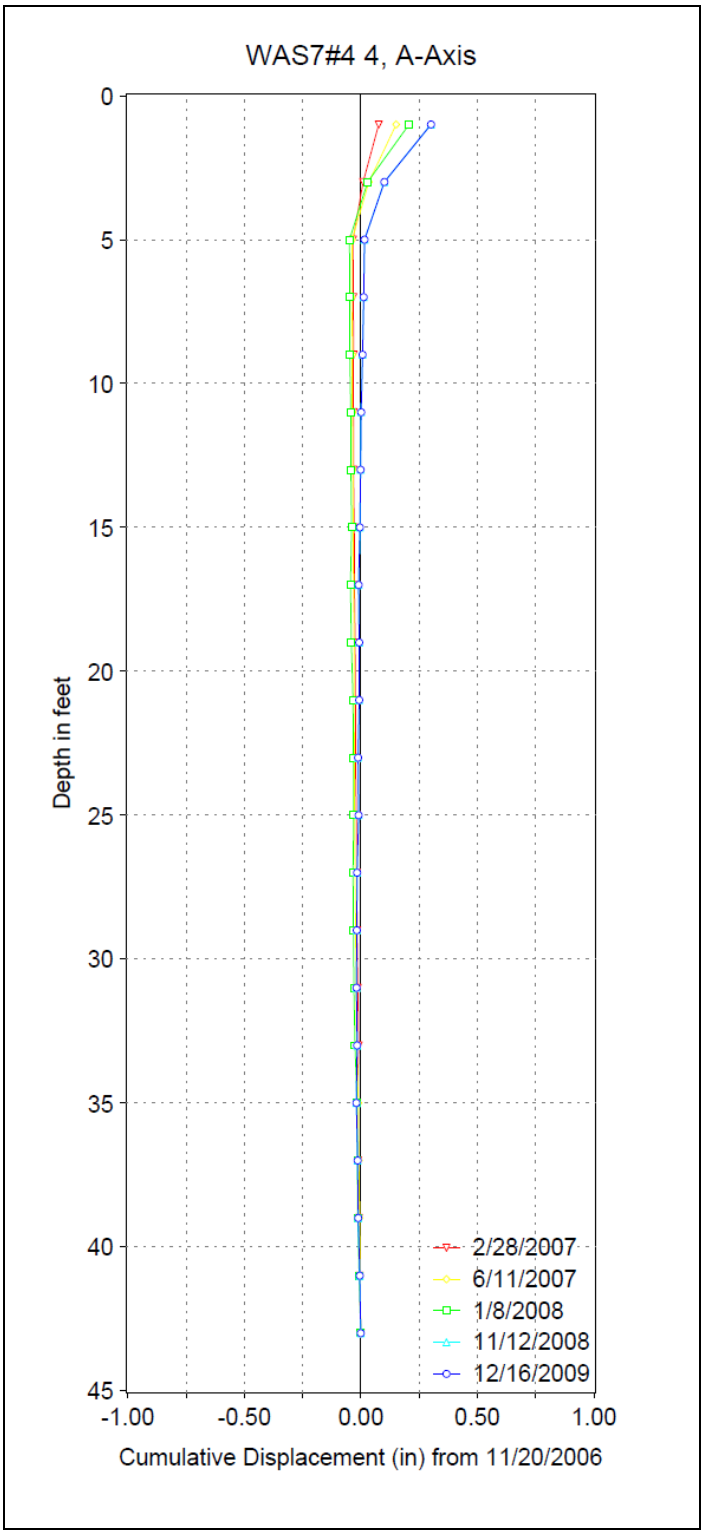

Figure 5.24: Cumulative Soil Movement at Upslope Side of the Drilled Shaft (Inclinometer #4) at WAS-7 Site

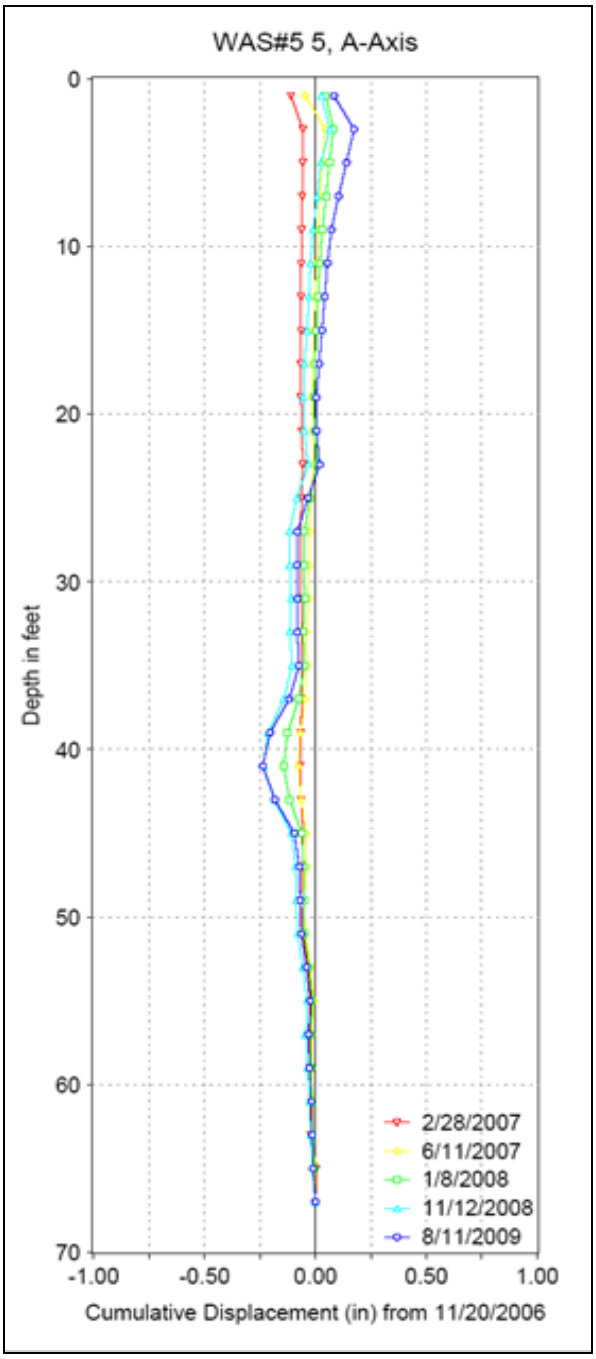

Figure 5.25: Cumulative Soil Movement at (Inclinometer #5) Down-slope Side of the Drilled Shaft at WAS-7 Site

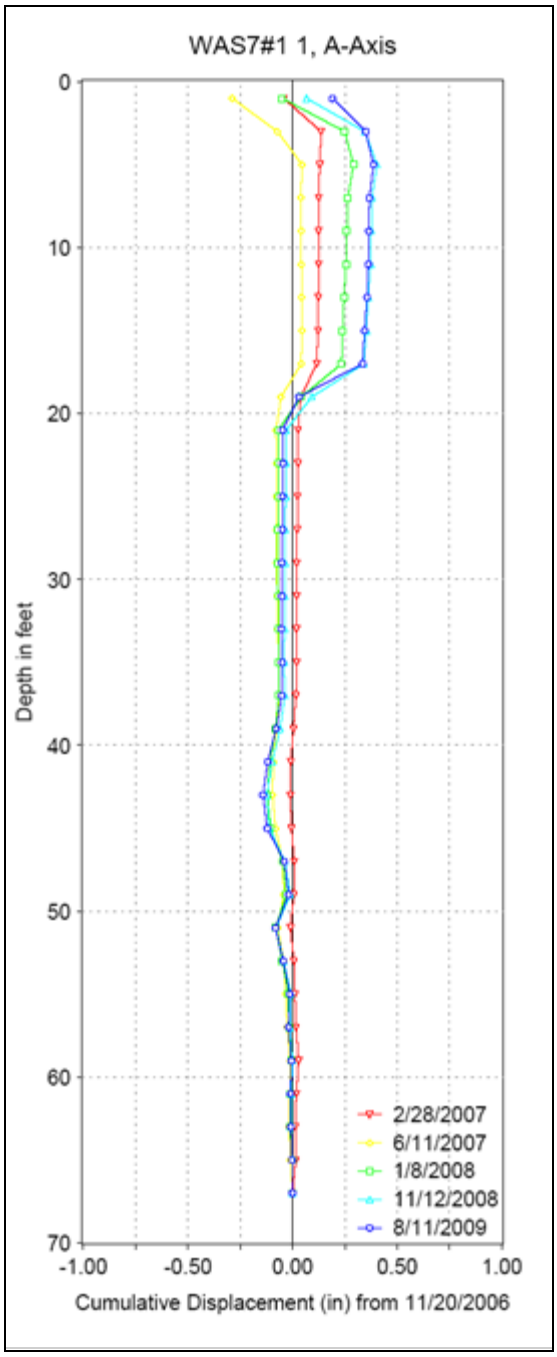

Figure 5.26: Cumulative Deflection in Shaft #53 at WAS-7 (Inclinometer #1)

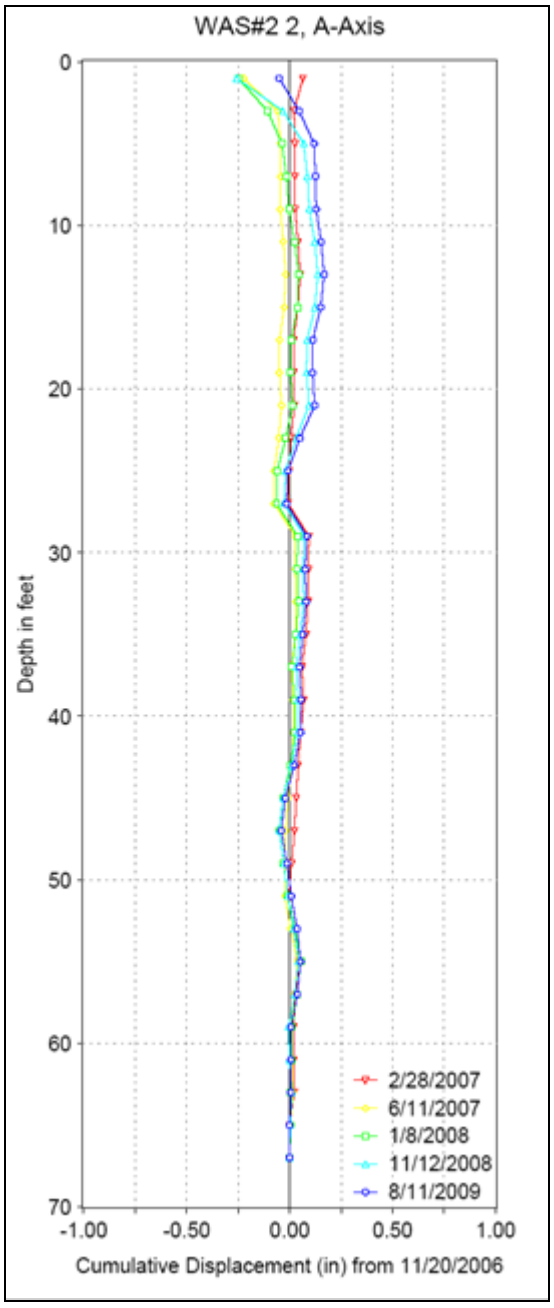

Figure 5.27: Cumulative Deflection in Shaft #54 at WAS-7 (Inclinometer #2)

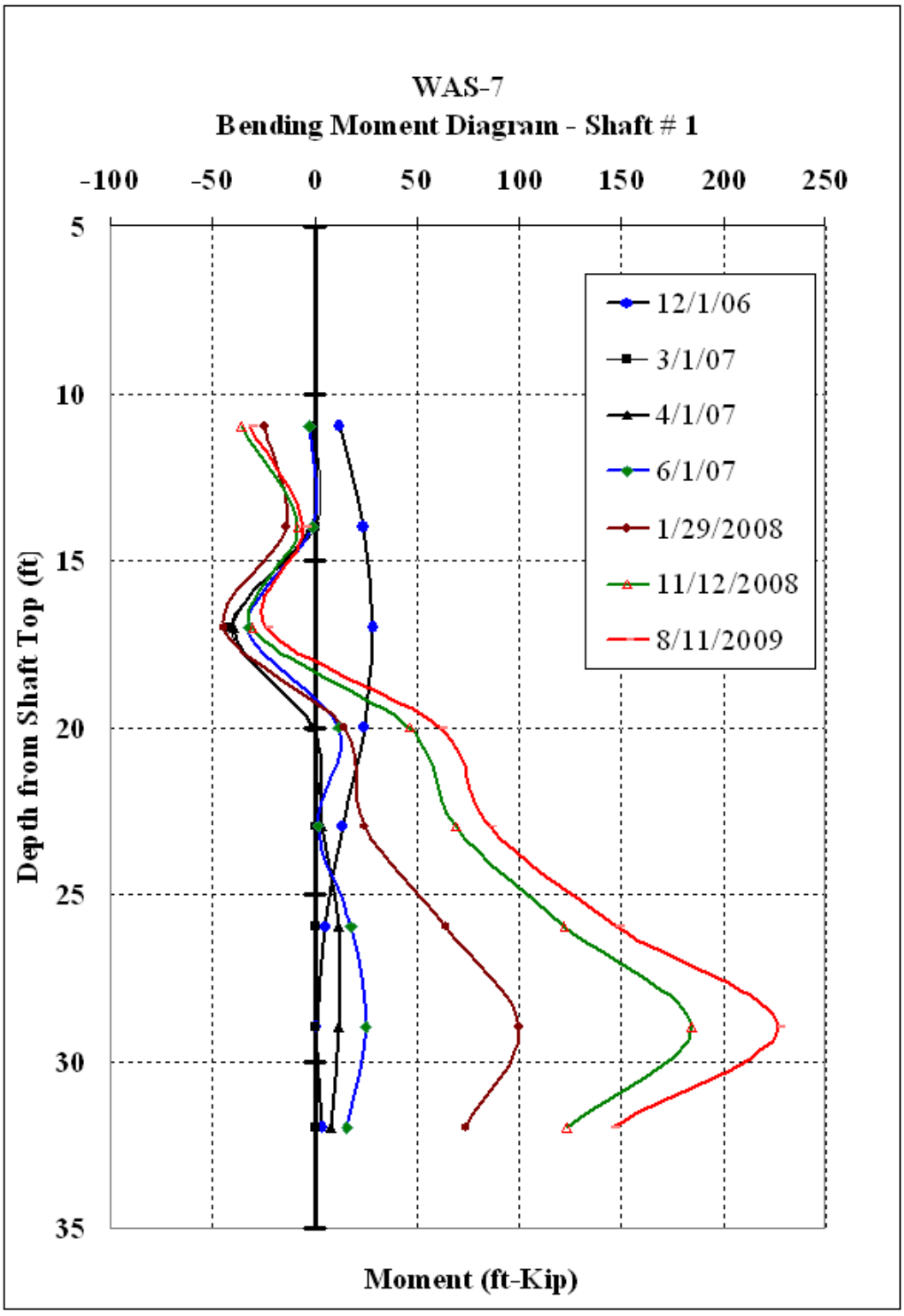

Figure 5.28: Moment Measurement from Shaft #53 at WAS-7 Site

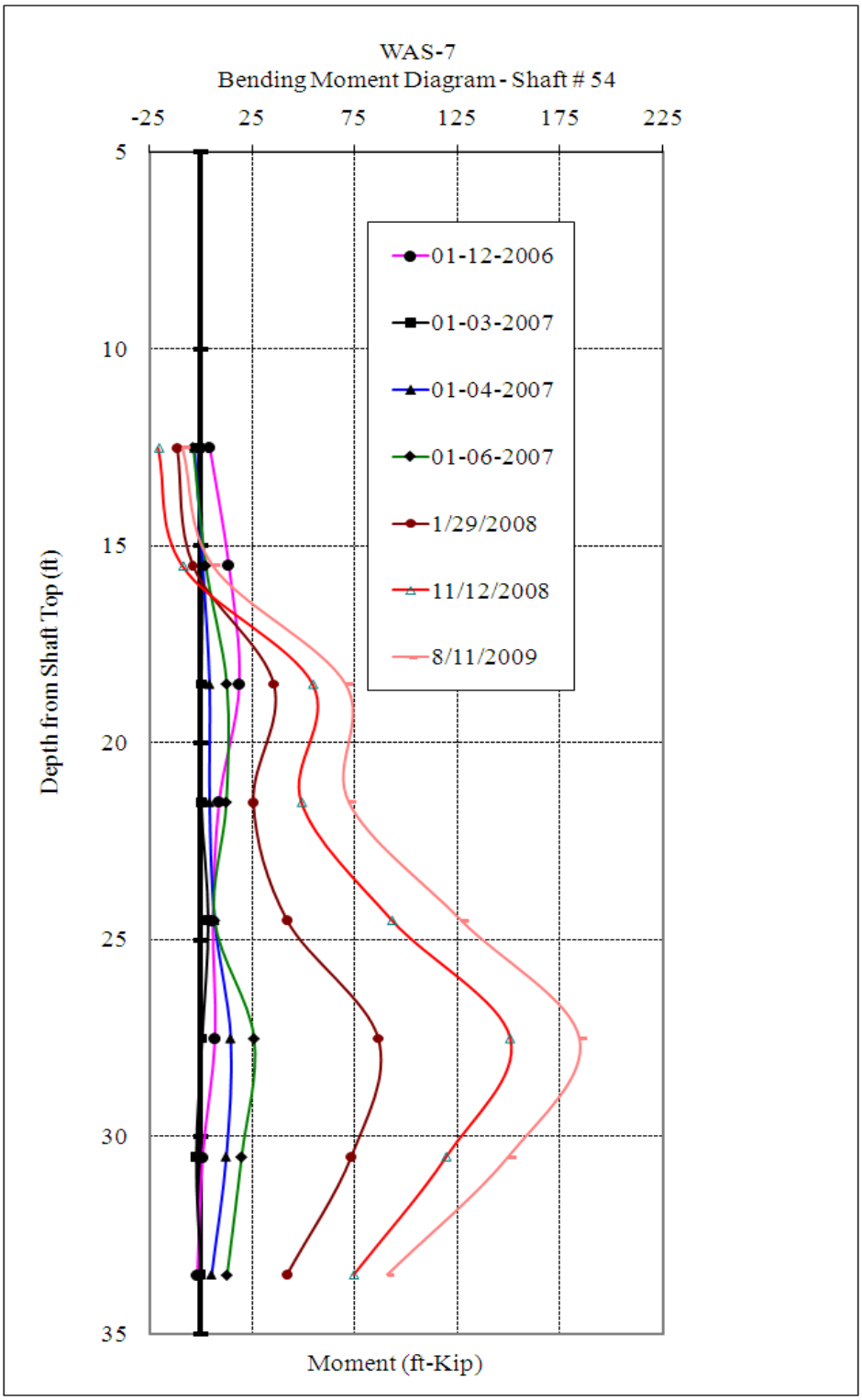

Figure 5.29: Moment Measurement from Shaft #54 at WAS-7 Site

The readings from piezometers were used to determine the elevation of ground water table. The fluctuations of the ground water levels at three piezometers locations are shown in Figure 5.30. All pressure cells at this site did not function properly; therefore, the recorded data from pressure cells are not presented herein.

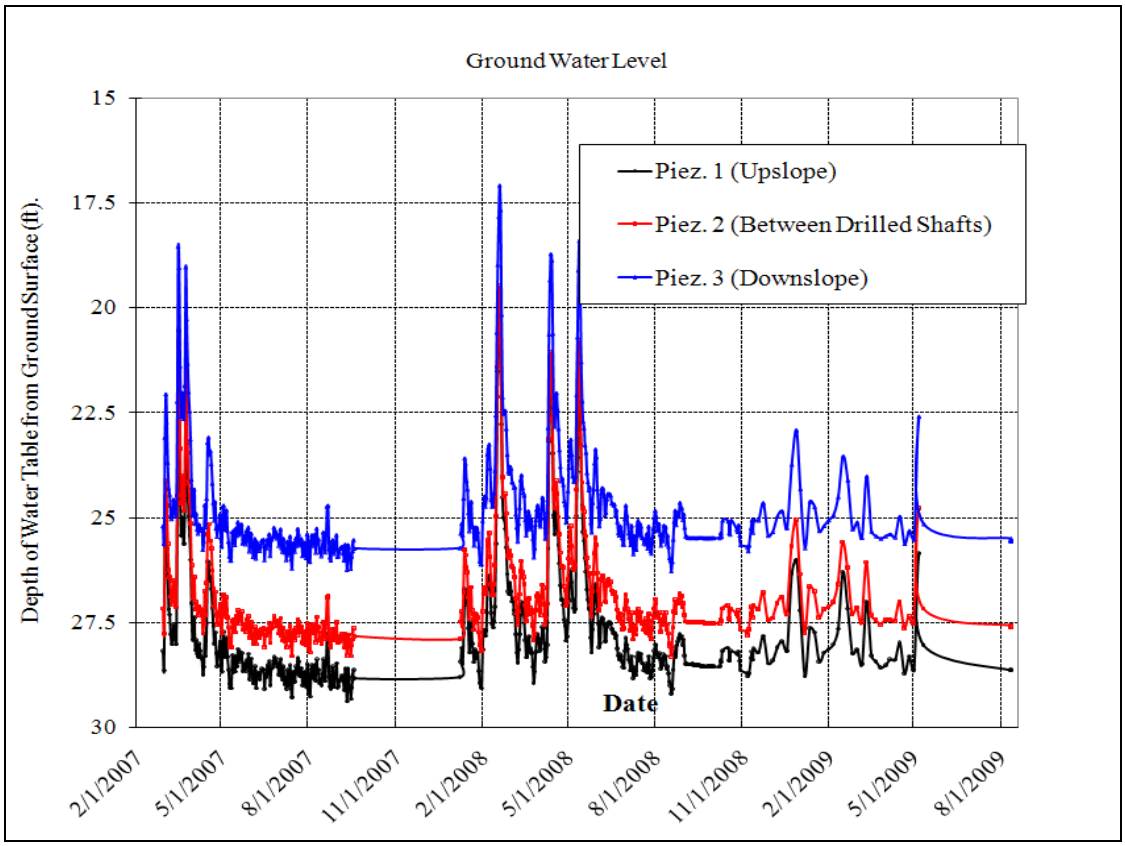

Figure 5.30: Ground Water Elevations at WAS-7 Site

5.3.5 UA SLOPE 2.0 Analysis Results

The computer code UA SLOPE 2.0 was used to analyze the re-constructed slope at the WAS-7 site. The simplified soil cross section and profile used in this analysis is shown in Figure 5.18. A total of four soil layers were used to represent the soil conditions at the site. The pertinent soil properties for the four soil layers are provided in Table 5.4.

The layer No. 4, labeled as soft rock, was used to represent the soil-bedrock interface where sliding occurred. The UA SLOPE 2.0 program was used to back calculate the residual friction angle of soil layer No.4. With the computed FS of 1.09, the back analyzed residual friction angle of layer No. 4 was 12 degree. The computed FS of the re-constructed slope with the installed drilled shafts at the WAS-7 site was 1.14. The results of UA SLOPE 2.0 analysis for both cases, without shaft and with shaft, are shown in Figures 5.31 (a) and (b), respectively. The net force on the shaft was 63 kips. The maximum moment from this computed earth thrust, using LPILE program is 2.3×10^3 ft-kips, while the maximum computed shear force is 610 kips, and the corresponding shaft head deflection is 2.6 in.

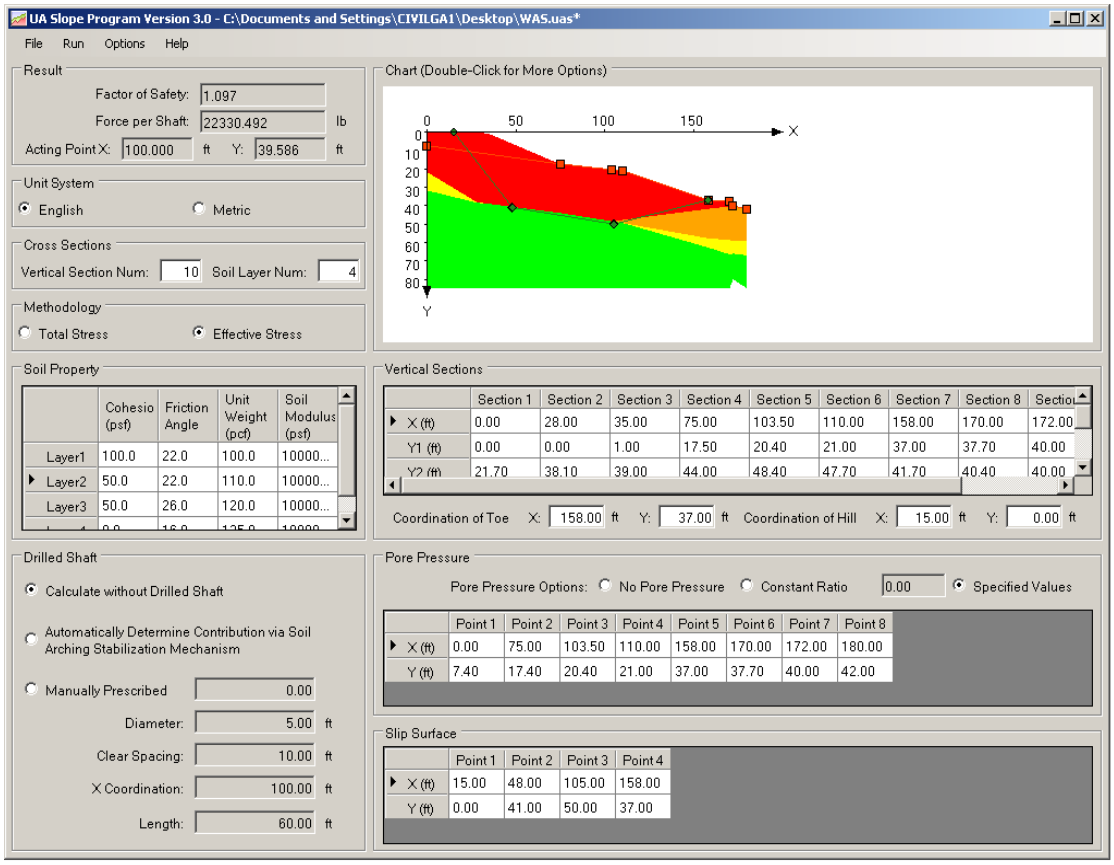

(a)

Figure 5.31: UA SLOPE 2.0 Analysis Results: a) without Drilled Shaft b) with Drilled Shaft

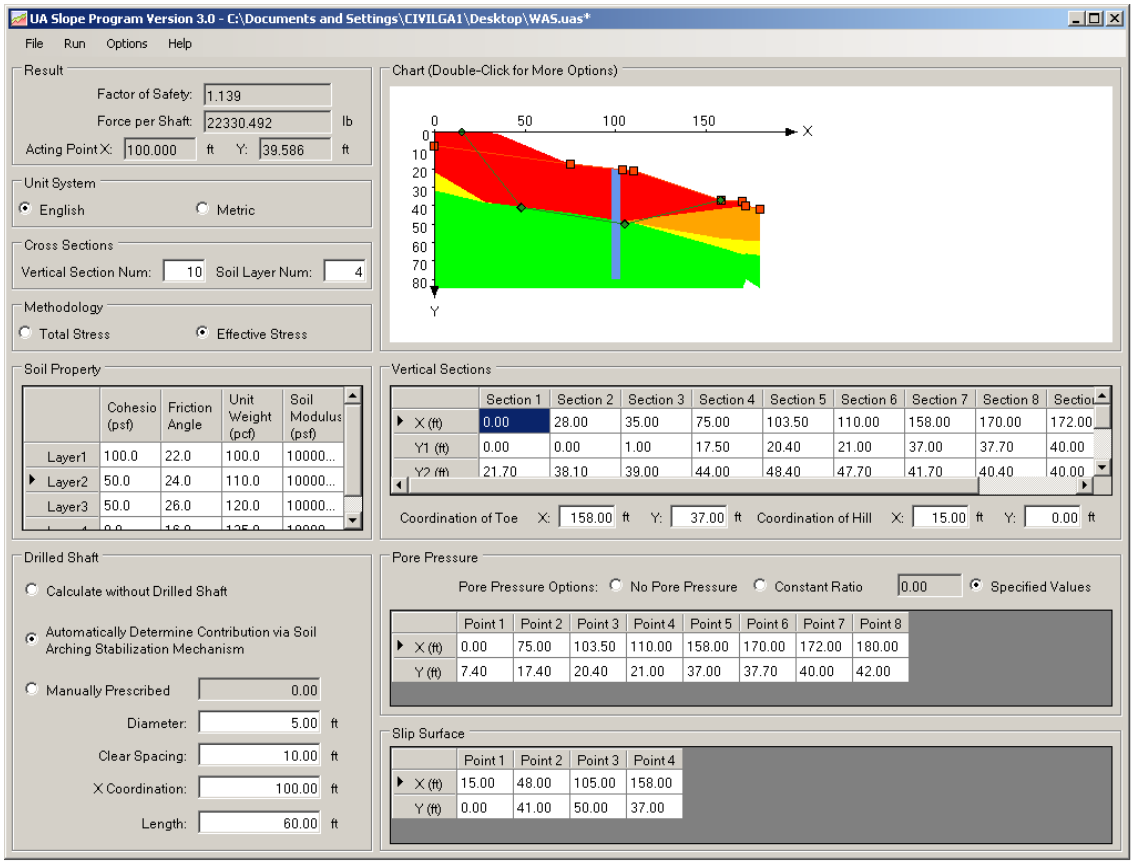

(b)

Figure 5.31: UA SLOPE 2.0 Analysis Results: a) without Drilled Shaft b) with Drilled Shaft, Continued

5.4 MRG-376

In this section a detailed study for the project site MRG-376 is provided. The slope reconstruction, remediation (reinforcement using single row of drilled shaft and the selection of parameters of the slope/shaft system), instrumentation, and monitoring are explained.

5.4.1 Site Conditions

This failed slope was located at State Route 376 which is aligned parallel with the Muskingum River. Evidences of the slope movements were observed at the site, such as pavement distress in a form of cracking and vertical drops. The average slope angle is 2.75(H):1(V) toward the river. The cross-section of the affected slope area at the MRG-376-1.1 site is shown in Figure 5.32. The affected area is approximately 150 ft long. Based on the site observations, the subsurface conditions and slope geometry, the slope failure appeared to be rotational in nature, passing the toe near the river.

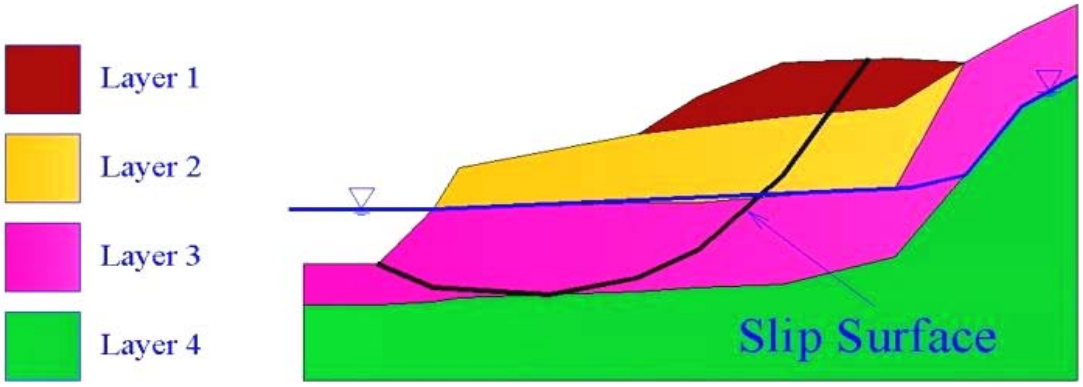

Figure 5.32: A Simplified Cross Section of MRG-376 Site

Based on Ohio Division of Geological Surveys (1997), the general regional geology of the bedrock in the area was of the Monongahela Group, representing the Pennsylvanian geologic period. This formation is typically identified as shale, siltstone, limestone, sandstone, and coal.

The failed slope was re-stored and stabilized with a row of drilled shafts and appropriate precast concrete lagging panels. Figure 5.33 shows the picture taken before the slope restoration began. Figure 5.34 shows the picture taken after the slope restoration was complete, while Figure 5.35 shows the picture of the rip rap placed at the toe of the restored slope.

Figure 5.33: A Picture Showing MRG-376 Site before Slope Repair

Figure 5.34: A Picture Showing the Restored Slope at MRG-376 Site

Figure 5.35: A Picture Showing the Rip Rap Placed at the Toe of the Restored Slope at MRG-376 Site

5.4.2 Site Investigation and Soil Properties

As part of site geotechnical investigation, ODOT drilling crew has advanced four borings along the affected alignment, as shown in Figure 5.36. As can be seen, three borings were along the downhill edge of the roadway (B-1 through B-3) while the remaining one boring was near the uphill edge (B-4). The subsurface elevations of the borings varied from 666.7 ft (B-2) to 667.7 ft (B-1) as determined by Canter Surveying. Asphalt pavement was observed at the surface of all four borings ranging in thickness from 0.7 ft (B-1, 3, and 4) to 1.0 ft (B-2). Groundwater was observed in all of the borings ranging in depth from 17.8 ft (elevation 649.5 ft) in B-3 to 34.0 ft (elevation 633.7 ft) in B-1.

Fill material was observed below the pavement in all of the borings to depth ranging from 7 ft in B-2 and B-3 to 7.3 ft in B-1. The fill was typically identified as clay (A-7-6), gravel with sand, silt and clay (A-2-6), gravel with sand (A-1-b) or gravel (A-1-a). Water contents of 19% - 21% and SPT N-values of 7 – 12 blows per foot were recorded in the clay fill. Water contents of 3 % - 16% and SPT N-values of 6 – over 50 blows per foot were recorded in the gravelly fill.

Below the fill, soils identified as silty clay (A-6b) or clay (A-7-6) were observed to depth ranging from 17 ft (B-3) to 24.5 ft (B-4) and described as moist and stiff to very stiff. Water contents ranged from 16% - 26% and SPT N-values varied from 10 – 24 blows per foot.

Softer cohesive soils were encountered below the aforementioned cohesive layer and identified as silt and clay (A-6a) or sandy silt (A-4a). These soils were described as

moist to wet and soft to medium stiff. Water contents varied from 22% - 32% and SPT N-values varied from 3 – 7 blows per foot.

Bedrock was encountered at depths ranging from 29.2 ft (B-3, elevation 638.0 ft) to 34.5 ft (B-1, elevation 633.2 ft). Approximately 10 ft of rock coring was performed in B-2 and the bedrock was identified as shale and described as gray, soft to moderately hard and thin to medium bedded with silty to sandy and weathered zones. No cores loss and a Rock Quality Designation (RQD) value of 40% were recorded in this coring interval.

An unconfined compressive strength of cohesive soil test (ASTM D-2166) was performed on a sample taken from B-3, at a depth of 10 ft – 11 ft. The visual description indicates clay with some sand and a little gravel, reddish-brown, moist, very stiff. About 0.9 inches was recovered from the sample. The unconfined compressive strength was 2.28 tsf and un-drained shear strength of 1.14 tsf. The pocket penetrometer reading was 2.25 tsf. The strain at maximum stress was 15% for a strain rate to failure of 0.99 %/min. The test was performed by FMSM Engineers.

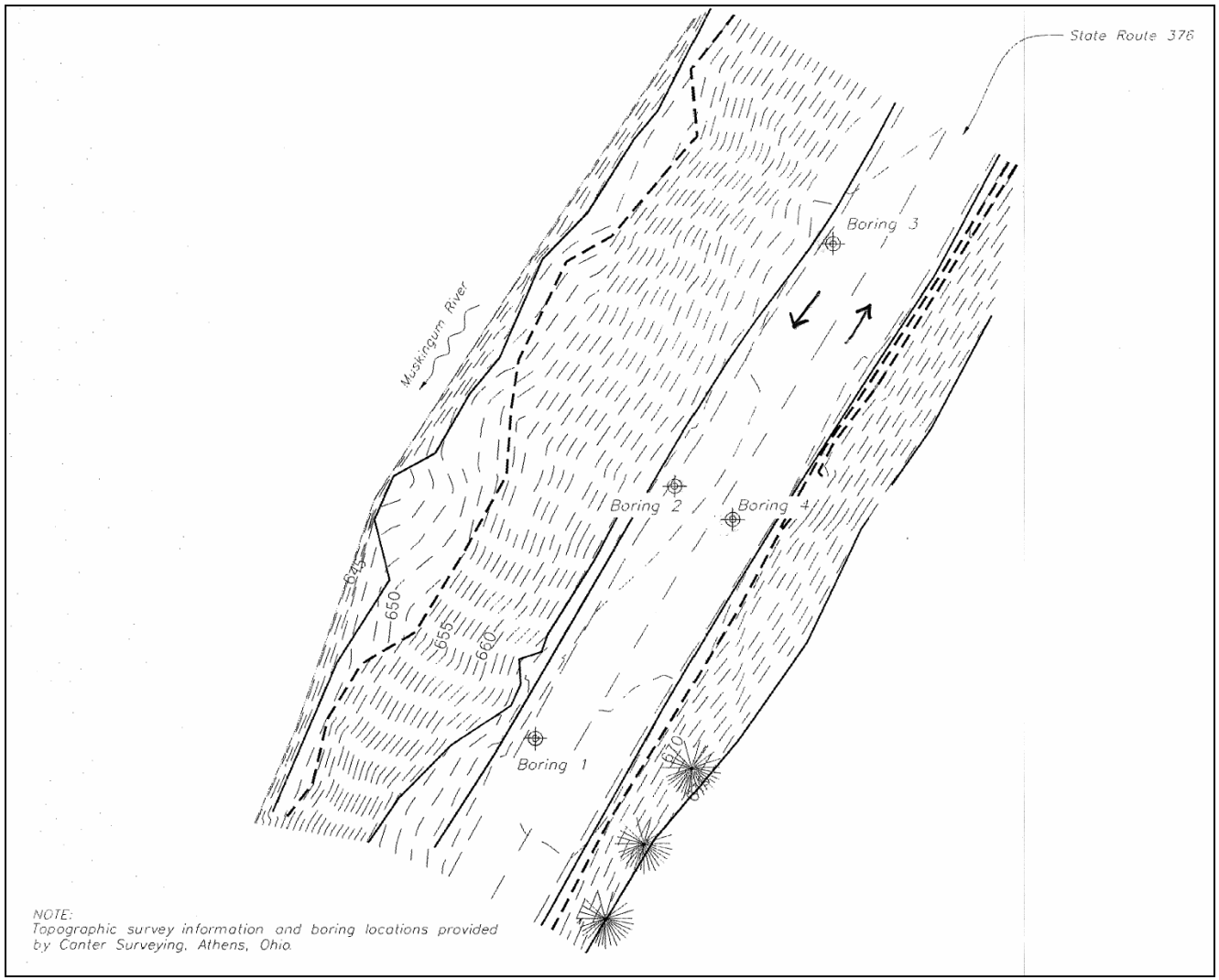

Figure 5.36: Locations of Four Soil Borings at MRG-376 Site

5.4.3 Drilled Shafts and Instrumentation Plans

The failed slope was reconstructed and stabilized with the use of a single row of drilled shafts, together with a lagging system and rip rap dump at the toe area of the slope. A total of 20 drilled shafts were installed with an offset of 20 ft off the centerline of the road pavement. The designed total shaft length was 43.6 ft, in which about 20 ft was considered to be rock socket. The diameter of the drilled shaft was 4 ft and the center-to-center spacing between the adjacent drilled shafts was 8 ft. The longitudinal steel reinforcement of the drilled shaft consists of a total of 28 #14 bars. The plan view of the installed drilled shaft location is shown in Figure 5.37. The nominal moment capacity of the drilled shaft was computed as 2,820 ft-kips.

The instrumentation at the MRG-276 site only included installation of inclinometer casings. A total of four inclinometer casings were installed at this site. Two inclinometer casings, each with a total length of 45 ft, were installed inside the drilled shafts (shafts #10 and Shaft #11). Two inclinometer casings, each 45 ft long, were installed in the ground in-between the drilled shafts (one was on the up-slope side of the drilled shaft and the other one was on the down-slope side of the drilled shaft). A schematic view of the inclinometer locations are depicted in Figures 5.38 and Figure 5.39 for top view and elevation view, respectively.

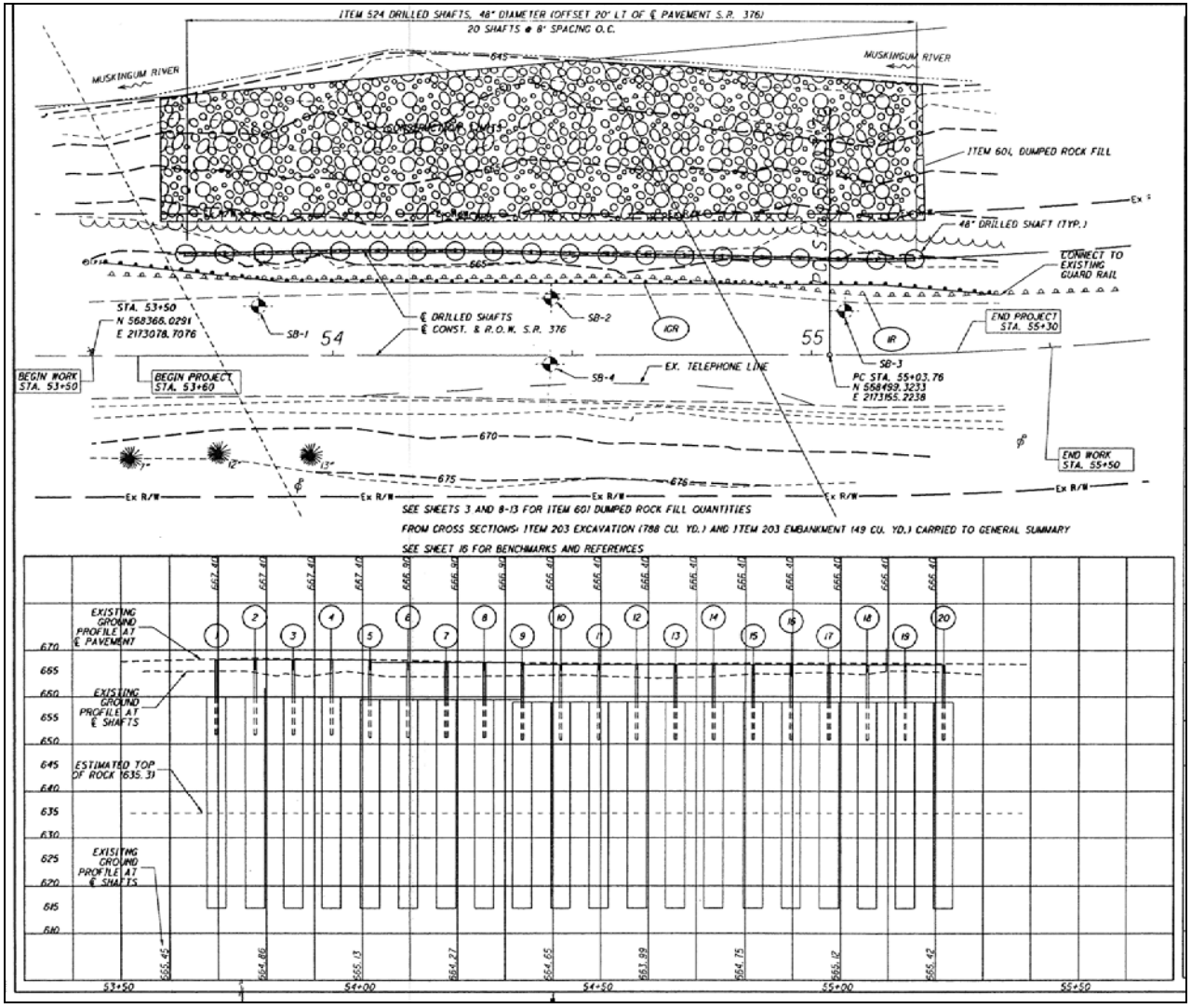

Figure 5.37: A Plan View Showing Drilled Shafts Location at the MRG-376 Site

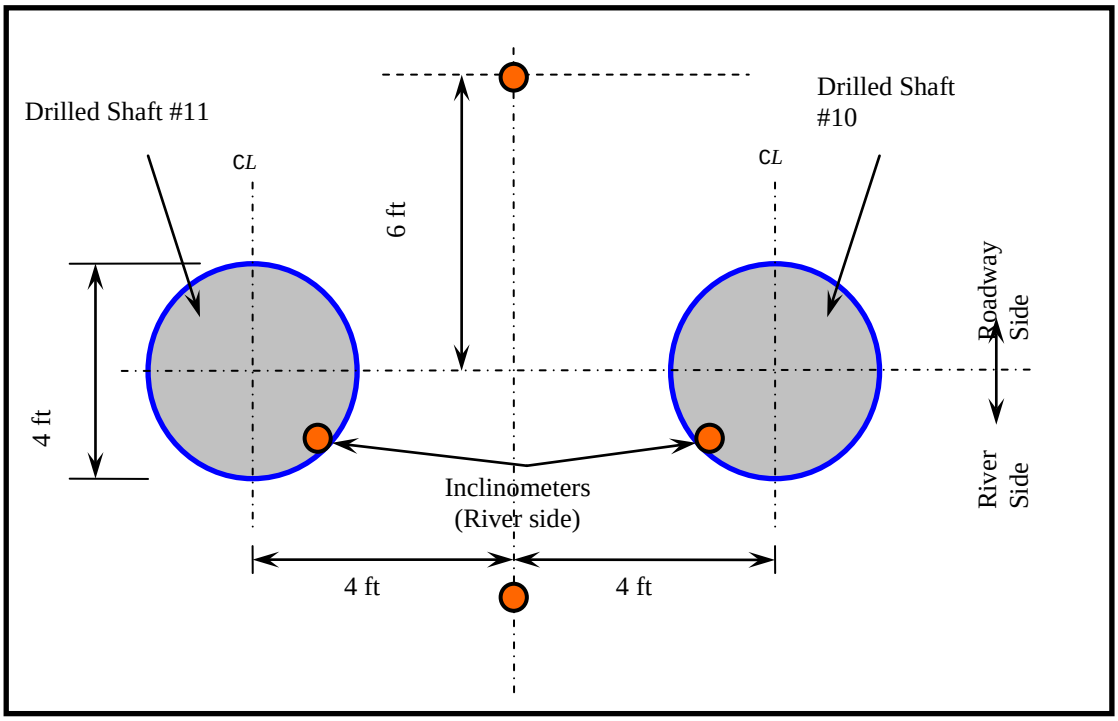

Figure 5.38: A Schematic Plan View of Inclinometer Location at the MRG-376 Site

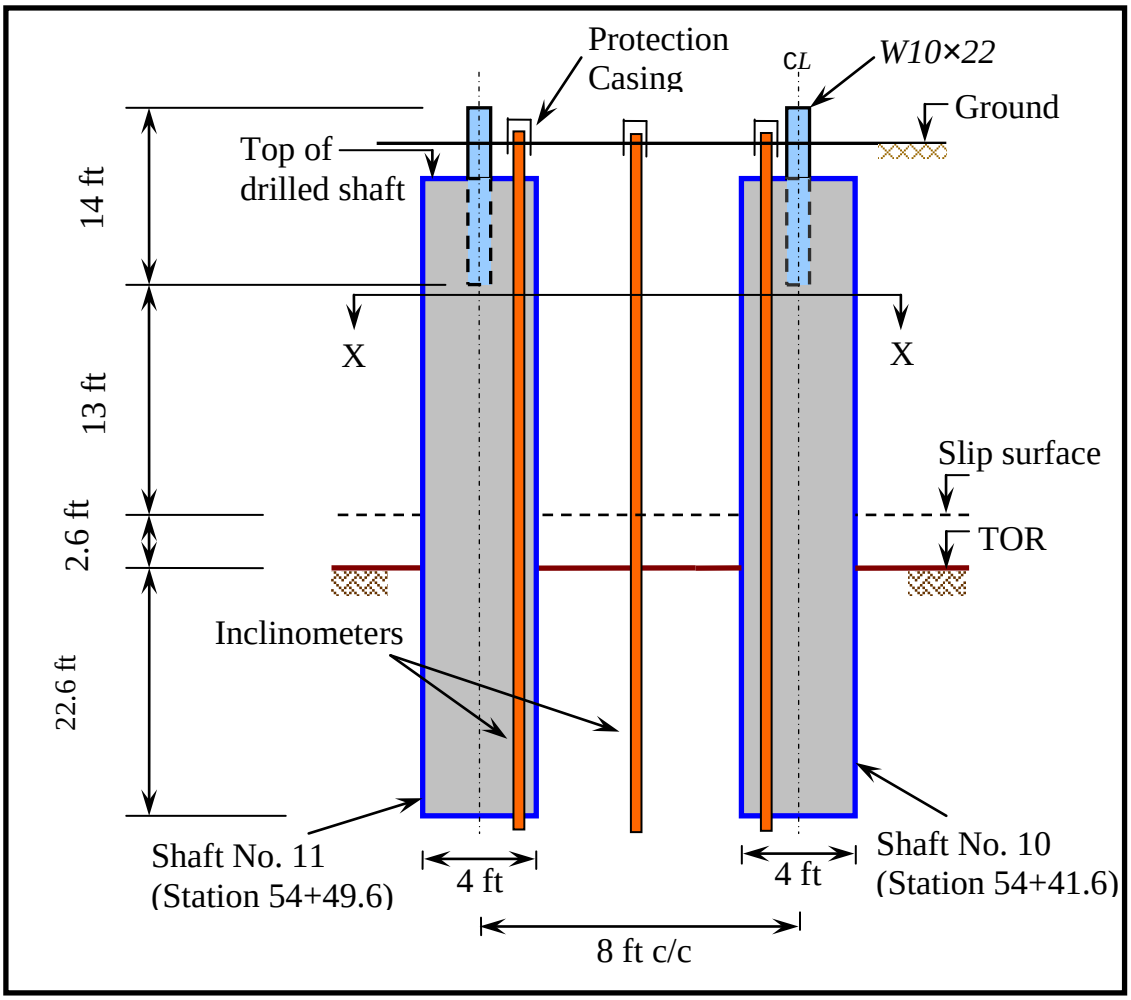

Figure 5.39: A Schematic Elevation View of Inclinometer Casing Location at the MRG-376 Site

5.4.4 Monitoring Results

The ground movements monitored by two inclinometer casings (INC #1 and INC #3) are shown in Figures 5.40 and Figure 5.41, respectively. As can be seen, the cumulative ground movement is less than 0.25 in.

The measured cumulative shaft deflection in shaft #10 (inclinometer #2) in the direction of the slope movement is shown in Figure 5.42. It can be seen that the drilled

shaft deflections were less than 0.25 in. The same observation can be made for drilled shaft # 11, as can be seen from inclinometer #4 readings depicted in Figure 5.43.

Based on both ground movement and drilled shaft deflection data, it can be concluded that the restored slope with the as-built stabilization structure was very stable over the last three years.

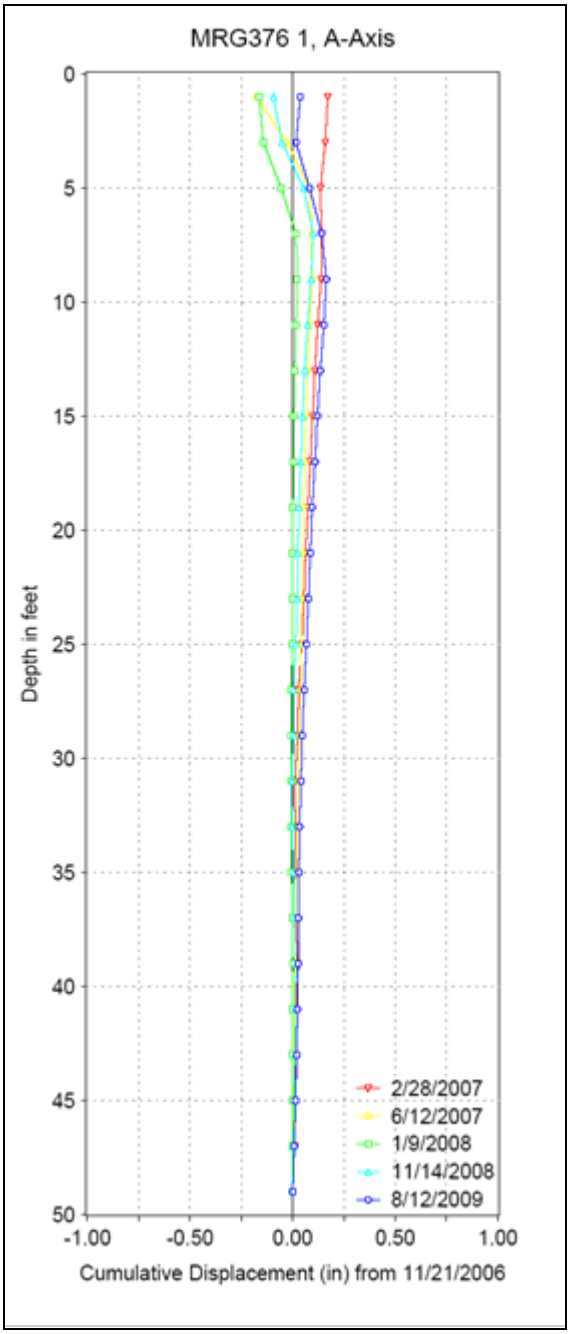

Figure 5.40: Cumulative Soil Movement Up-slope Side of the Drilled Shafts (Inclinometer #1) at MRG-376 Site

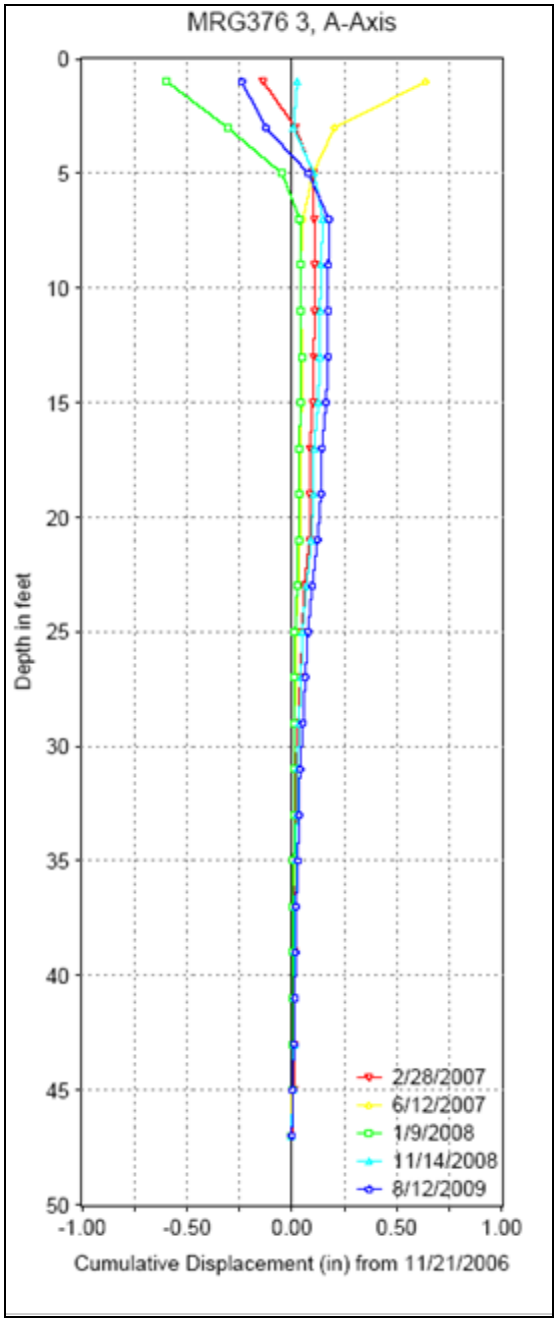

Figure 5.41: Cumulative Soil Movement within the Arching Zone (Inclinometer #3) at MRG-376 Site

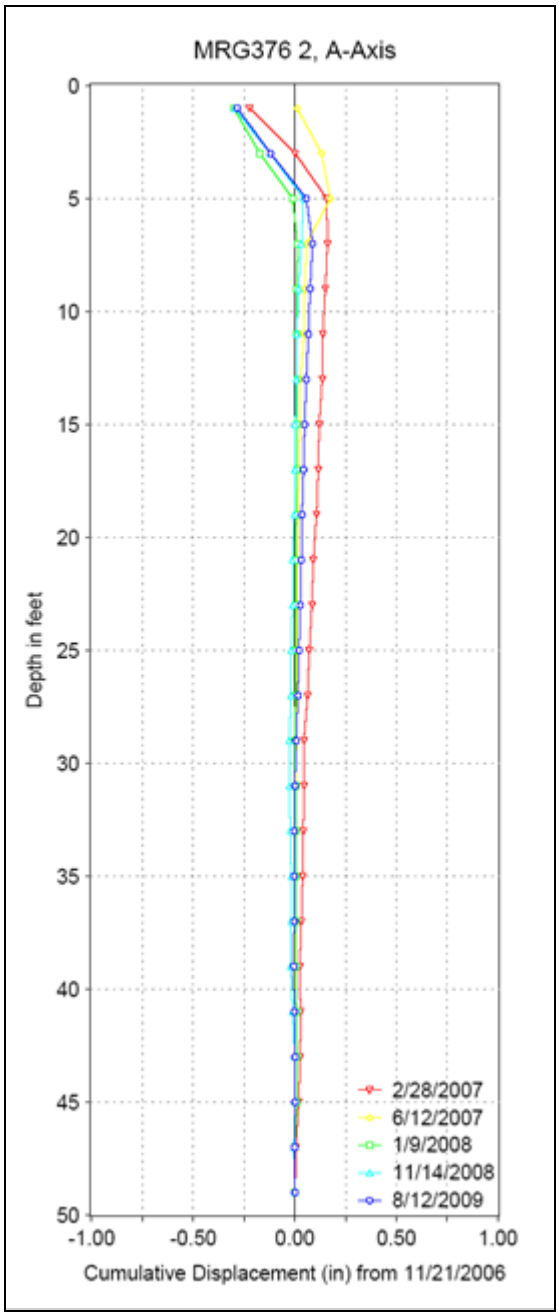

Figure 5.42: Cumulative Deflection of Shaft #10 at MRG-376 (Inclinometer #2)

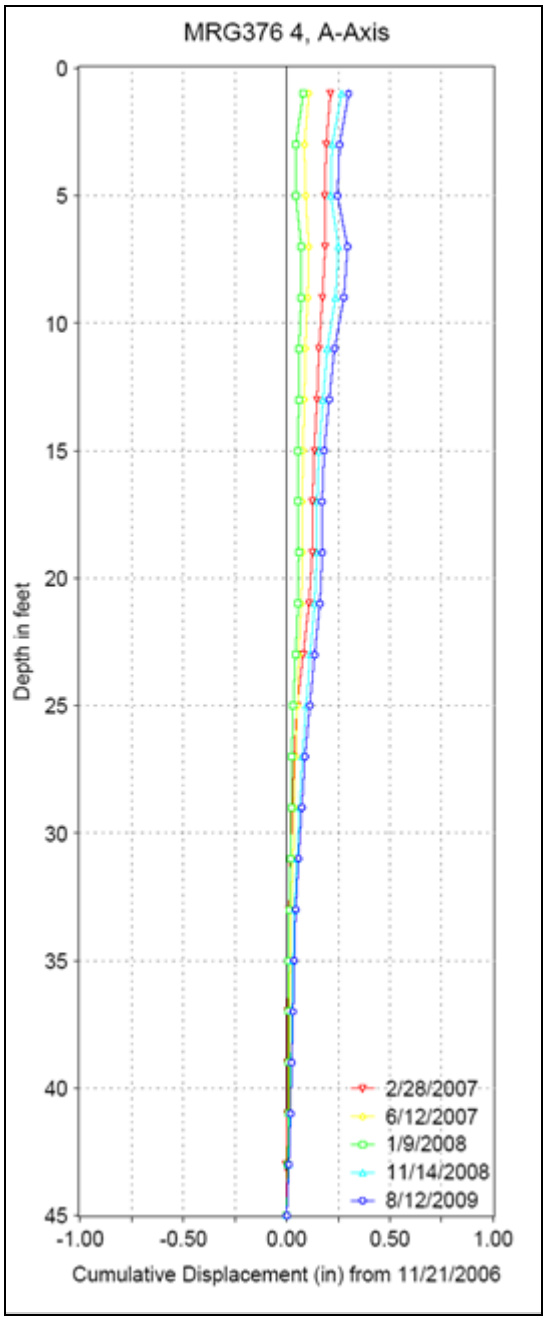

Figure 5.43: Cumulative Deflections of Shaft #11 at MRG-376 (Inclinometer #4)

5.4.5 UA SLOPE 2.0 Analysis Results

The computer program UA SLOPE 2.0 was used to analyze the re-constructed slope with the stabilization drilled shafts at the MRG- 376 site. It is noted that the computer program cannot model the lagging system. The simplified soil profile at the site is depicted in Figure 5.44. Since the slope had been already failed, the slip surface was considered to be a thin soil layer with the residual soil properties. The residual soil properties were obtained from the back analysis using UA Slope 2.0. The factor of safety of the slope/shaft system was found to be equal to 1.29 and the shaft force equal to 43.3 kips. The results of UA SLOPE 2.0 analysis for both cases, without shaft and with shaft, are shown in Figures 5.45 (a) and (b), respectively. The maximum moment from the computed earth thrust, using LPILE program is, 2.5 x 10^3 ft-kips, while the maximum computed shear force is 615 kips, and the corresponding shaft head deflection is 2.44 in.

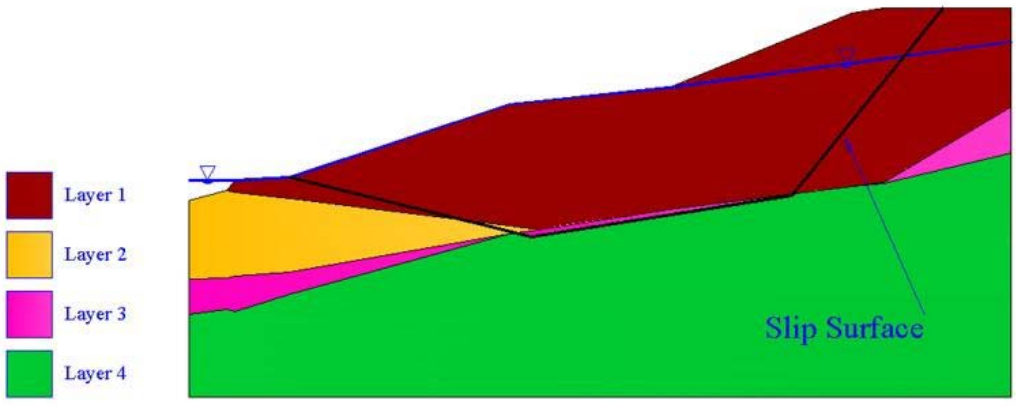

Figure 5.44: Simplified Slope Cross-Section Used in UA SLOPE 2.0 Analysis

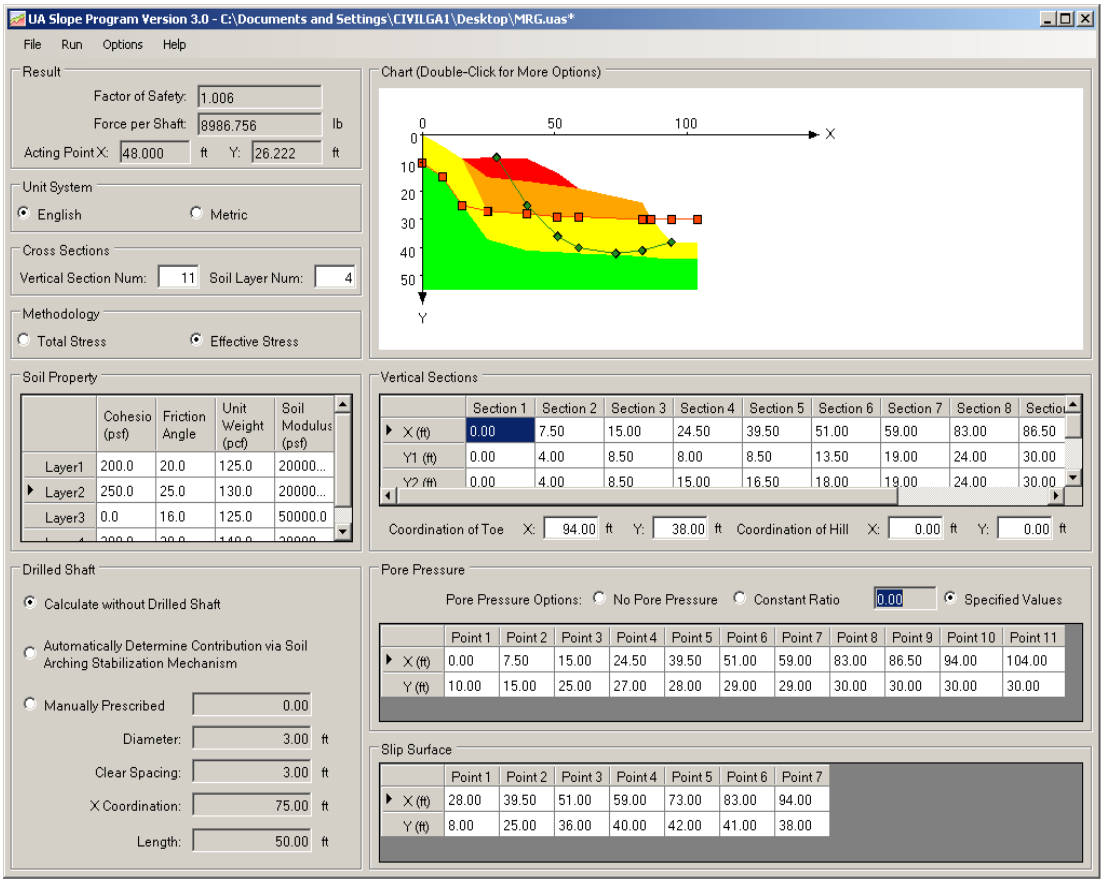

(a)

Figure 5.45: UA SLOPE 2.0 Analysis Results: a) without Drilled Shaft, b) with Drilled Shaft

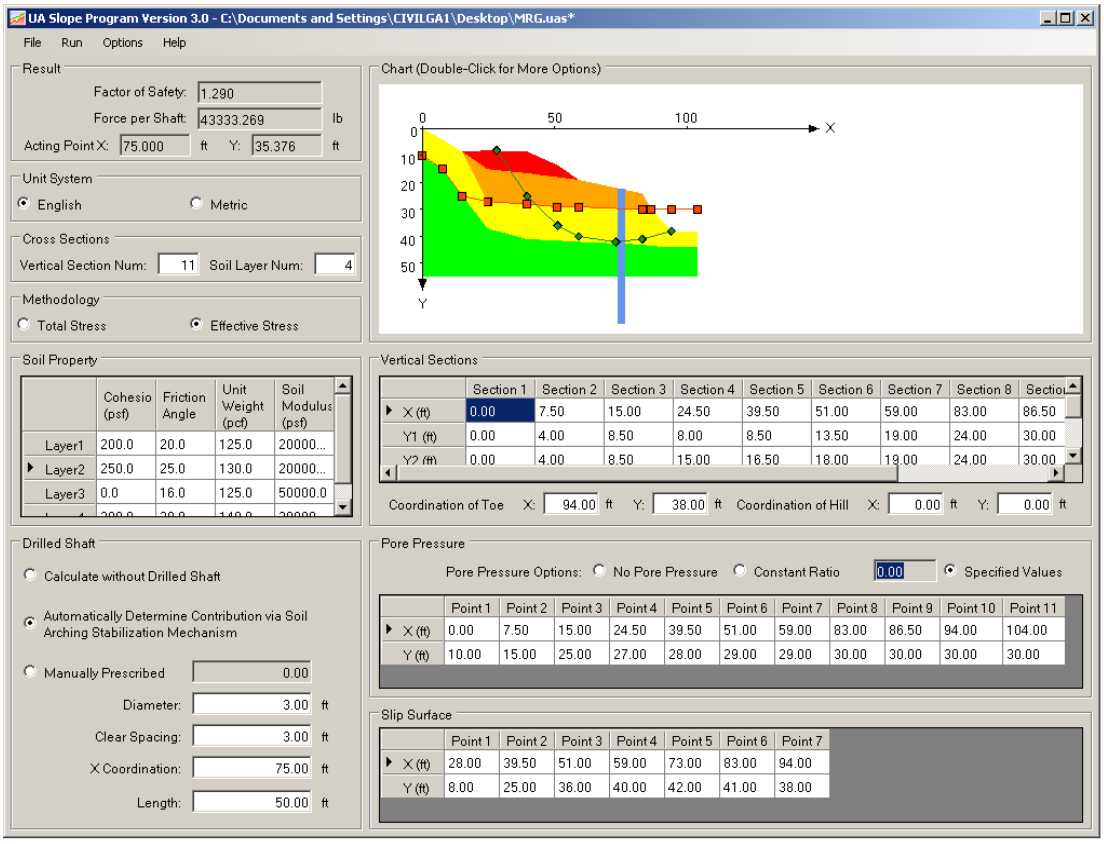

(b)

Figure 5.45: UA SLOPE 2.0 Analysis Results: a) without Drilled Shaft, b) with Drilled Shaft, Continued

5.5 Summary and Conclusions

Three ODOT slope repair projects were instrumented and monitored by the research team as part of this research project to gain important monitoring data on the performance of the as-built slope stabilization system over almost three years of service time after the slope stabilization work was completed. Three slope repair sites were selected by OGE engineers so that the site conditions and the slope stabilization schemes were fairly representative of the situations often encountered by ODOT in their slope restoration approach. All three slope stabilization projects used a single row of drilled shafts as the main slope stabilization means, with exception of MRG-376 site where a lagging system was employed as well.

The instrumentation plans for each studied project site were very comprehensive with intent to monitor not only the drilled shaft behavior but also the ground movements and ground water fluctuations. Drilled shafts were instrumented with inclinometer casings for deflection measurement and strain gages for finding moments on the shafts. Although earth pressure cells were also installed inside the drilled shafts to measure directly the earth pressure on the shaft; nevertheless, these pressure cells were found incapable of measuring the earth pressure accurately. As a result, there was no attempt to interpret the earth pressure cell readings. The slope movements at the restored landslide sites were typically monitored by inclinometer casings. In addition, ground water fluctuations were monitored with piezometers. Based on the monitoring results from three project sites, some observations can be made as follows.

The soil movements observed at the three study sites revealed the high efficiency of the single row of drilled shafts in facilitating slope stabilization. The soil movements, both on the up-slope and down-slope sides of the drilled shafts, over the past three years were in general very small such that it can be said that the slope was stable after the restoration work using drilled shafts.

The observed soil movements in between the adjacent drilled shafts were smaller than those observed by inclinometer in other locations, thus indicating that the driving soil stresses in this area was smaller than those in the other areas. This observed behavior is strong evidence on the development of soil arching in the drilled slope/ shaft system.

Defining the structural factor of safety as the ratio between the moment capacity of the drilled shaft and the measured maximum moment on the drilled shaft, then it is clear that the reinforcing structure of the as-built drilled shafts is quite safe.

Based on UA SLOPE 2.0 Analysis of the as-built drilled slope/ shaft system of each study site, the following observations may be made.

- Drilled shafts can be a practical and effective means for stabilizing landslides.
- The Geotechnical Factor of Safety was successfully enhanced by the drilled shafts for all three project sites: WAS-7, MRG-376, and JEF-152.
- The Structural Factor of Safety was very high due to the reinforcement used in the drilled shafts, not from the dimension (diameter) of the constructed drilled shafts.
- Using a smaller number of large-diameter drilled shafts can be more effective than using a larger number of small-diameter drilled shafts.

- For all studied landslide sites, the fixity of the drilled shafts was successfully achieved. In general, a minimum of rock socket length of 10% of total shaft length is recommended.
- The typical range for S/D is between 2 to 4. There was not much difference in the design between S/D of 2 and 3. Therefore, S/D = 3 can be effectively used.
- Backfilling and grading of the upper portion of the slope behind the shafts can exert an adverse effect on the overall stability of slope/shaft systems. Thus, it is recommended that careful monitoring be carried out during the construction when backfilling the slope to the designed grade.

CHAPTER VI

SUMMARY AND RECOMMENDATIONS

This chapter provides a summary of the work performed in this research and the conclusions related to optimal design of a slope/ shaft system with safe and most economical design outcome. The recommendations for implementation and future research are presented at the end of this chapter.

6.1 Summary of Work Accomplished

This research encompassed both theoretical and field work. The theoretical work consists of literature review, 3- dimensional finite element simulations, formulation of semi-empirical equation for arching effect, derivation of mathematic algorithms for the method of slice for the slope/ shaft system, the development of a PC based computer program UA SLOPE 2.0 for handling complex slope geometry and soil profile conditions in a slope/ shaft system, and numerical study of the ATH-124 field load testing program as well as case studies of three instrumented and monitored ODOT landslide repair projects. On the field work side, the UA research team carried out the work of instrumentation and long-term monitoring of three ODOT landslide repair projects. In addition, the UA team was responsible for carrying out a field load testing program at the

ATH-124 project site, with tasks including planning of site investigation, supervision of construction of drilled shafts at the project site, acquiring and installing all instrumentation sensors and inclinometer casings at the site, arranging the contractor to place surcharge loads for load testing, and completing both short-term and long-term monitoring of the instrumented project site. Specific contributions obtained from these theoretical and field works can be enumerated as follows.

- Literature review clearly supported the need for conducting this research, as there was no universally accepted method exist for design and analysis of a slope/drilled shaft system with assured safety and economy. It was observed that in the past, most of the design involving the use of drilled shafts tended to be ultra conservative, primarily due to a lack of adequate design procedure, thus costing the agency, such as ODOT, to spend excessive financial resource to fix landslides.
- Literature review also helped reveal the root cause of inadequacy of existing design method to be the inability to quantify the resistance provided by the drilled shaft in the slope stability analysis. As a result of using either plasticity theory or limiting passive resistance theory, the existing method of analysis tended to yield unrealistic value of F.S. of the slope/shaft system with the accompanied extremely high value of design earth thrust for structural design of drilled shaft. The method proposed by Liang (2002), which was adopted by ODOT as a preferred method, was shown to be fundamentally sound due to the fact that the drilled shaft effects were taken into account through the concept of arching and the reduction in the driving force in the slope stability analysis. Previous 2-dimensional finite element study by Liang and Zeng (2002) in quantifying the arching effect and in developing the load

reduction factor, however, was found to be deficient and required major improvement, particularly replacing 2-D finite element modeling with 3-D modeling approach.

- Detailed 3-D finite element simulations conducted in this research by both Yamin (2007) and this dissertation represented the first ever efforts in a true 3-dimensional finite element modeling of a slope/shaft system which in turn helped shed lights on the drilled shafts induced arching in a slope/shaft system. The differences between Yamin and the simulation techniques used in this work lie in the method used to activate slope movements in the simulation study. Yamin's approach employed the technique of placing surcharge load on the slope crest area, while the approach used in this research work utilized the strength reduction method. Both simulation study results were of importance in understanding the arching mechanisms. Nevertheless, the approach of this research work provided more benefits in that the F.S. of the slope/shaft system can be captured in the finite element simulations.
- The combined efforts of both Yamin and this work's 3-dimensional finite element simulations yielded detailed insight on the factors influencing the arching phenomenon in a slope/shaft system. This insight was not previously available in the literature. The insights gained from such an extensive and comprehensive numerical parametric study using the two different finite element modeling techniques added to the knowledge on optimum utilization of drilled shaft in a slope/shaft system.
- The method of slice for slope stability analysis was modified so that it can be used to compute the geotechnical F.S. of a slope/shaft system. The arching effects due to the installation of a row of spaced drilled shafts, as quantified through a

comprehensive 3-D finite element parametric study, were included in the modified method through the load reduction (or load transfer) factor. The UA SLOPE 2.0 computer program, coded in accordance with the modified method of slice theory, allows engineers to design drilled shafts for complex slope and soil conditions.

- In addition to the ability to compute geotechnical F.S. of the slope/shaft system, the UA SLOPE 2.0 program possesses the ability to compute the net earth force on the drilled shaft on the portion of the shaft above the slip surface. From this computed design force, the structural design of the drilled shaft can be accomplished by the use of LPILE program or its equivalent computer programs. It is noted that the computed design force is the working force under equilibrium conditions, which is different from the commonly adopted approach where the design force was taken as the ultimate soil reaction force as the soils around the shaft failed in a perfectly plastic failure condition. This first ever ability to compute the working net force on the drilled shaft represents the potential cost saving of drilled shaft construction, as the structural design of the drilled shafts can be based on realistic design force.
- The major contribution of this research consists of not only the development of improved theory and the accompanied computer program to solve a challenging design problem with no prior universally accepted solutions, but also the proof of the validity of the computer program via. excellent direct comparisons with 57 cases of 3-dimensional finite element cases. The favorable match between the UA SLOPE 2.0 predicted and finite element computed F.S. for more than 50 cases assured the applicability of UA SLOPE 2.0 program to a wide variety of slope conditions. In addition, a very good direct comparison between the predicted net force from UA

SLOPE 2.0 program and the finite element simulation results enabled the design engineer to proceed with structural analysis and design of drilled shaft with the realistic loadings.

- The step-by-step design procedure using the UA SLOPE 2.0 program for an optimized slope/ shaft system was presented in this dissertation. This represents the first ever documented procedure where the design of the drilled shaft stabilized slope was treated as an optimization process with an ultimate goal of achieving both targeted safety of the geotechnical system (including the structural components) and the economy of the construction cost.
- The field work involving the surcharge loading at the ATH-124 project site represents the first and the only controlled field experiment with a dedicated objective to understand the arching behavior in a slope/shaft system. The development of a specific finite element model of the ATH-124 testing program, together with the predictions made by the UA SLOPE 2.0 computer program, allowed for additional validation of the UA SLOPE 2.0 program based on the field testing data at the ATH-124 project site. The excellent predictions of the factor of safety of the slope/shaft system and the net design force on the shaft by the UA SLOPE 2.0 program confirmed the practical applications of UA SLOPE 2.0 for very complex soil profile and slope geometry conditions, which were not part of the 50 cases of finite element studies.
- The more than three years of long -term monitoring of instrument and sensors installed at the three ODOT landslide repair projects (MRG-376, WAS-7, and JEF -152) provided important knowledge base for the UA Research Team and gained

confidence of ODOT engineers on the safety of the design of the drilled shaft stabilization scheme at each project site. Not only each of the repaired slopes remained in excellent service conditions without displaying any significant post-repair slope movements, but the internal forces of the drilled shafts measured by the strain gages confirmed the structural adequacy of the as-built drilled shafts. The UA SLOPE 2.0 program was used to re-analyze the three landslide repair design.

6.2 Conclusions

The main conclusions of this study are summarized as follows.

- The existence of arching due to the presence of a single row of adequately spaced drilled shafts in a slope was ascertained from more than 150 cases of 3-dimensional finite element simulations and from field measured data at the ATH-124 load testing site.
- The arching behavior of the slope/shaft system was quantified into a set of semi-empirical equations through the use of the load transfer factor, which in turn, was incorporated into the method of slice slope stability analysis program, UA SLOPE 2.0 program, to facilitate computation of geotechnical FS and the net force on the drilled shaft in a complex slope/shaft system. The effectiveness of arching in a slope/shaft system is mostly influenced by the following factors: soil strength parameters, shaft location, shaft diameter, and shaft spacing.
- The design process involves the determination of the design parameters, including shaft location, shaft size (diameter and length), shaft spacing for optimum outcome; namely, finding the design providing the target global FS yet with the least load demand on the drilled shafts. The location of drilled shafts was also an integral part of the design parameter due to its influence on both achievable global FS and the required shaft length.
- The validity of the UA SLOPE 2.0 program was established by excellent comparisons between finite element simulation results and the UA SLOPE 2.0 predicted results, for both global FS and the net force on the drilled shaft. In addition,

the load test data at the ATH-124 project site was used to provide a calibrated and site specific finite element model, from which the finite element predictions and UA SLOPE 2.0 program predictions for both global FS and the net force were found to be in excellent agreement. The applicability of the UA SLOPE 2.0 program was therefore verified to the extent documented in this research work.

- The three ODOT landslide repair projects that were instrumented and monitored by the UA research team showed that the drilled shafts to be an effective means to restore the failed slope to its original slope geometry with enhanced global factor of safety. It was also observed that the post construction movements of the repaired slopes were within acceptable range and the measured forces on the drilled shafts were substantially below the structural capacity of the as-built structural elements.

6.3 Implementation Recommendations

The implementable outcome of this research was the development of a robust and user friendly PC based computer program UA SLOPE 2.0. This computer program, with necessary verification of its accuracy and range of applicability, can be used by the design engineer to analyze complex soil profile and slope conditions often encountered in real projects. The computer program can also be effectively used for the necessary iterative optimization design process to achieve the combination of best shaft location, shaft size, and shaft spacing, that would provide the target factor of safety for the geotechnical system (i.e., the drilled slope/ shaft) and the structural components (i.e., the drilled shafts) of the system but with the least construction cost.

6.4 Recommendations for Future Studies

The main development efforts of this study were concentrated on the design methodology for using a single row of spaced drilled shafts to stabilize an unstable slope. With the founding base of the developed methodology well established, the theory can be logically extended to develop the pertinent analysis and design methods for a wide array of slope stabilization methods as enumerated below.

- Extend the analysis method for the stabilization technique involving the use of stub piers – which essentially would cost less than the full length drilled shafts
- The feasibility of constructing rectangular shaped concrete shaft than the circular drilled shaft - the large aspect ratio rectangular reinforced concrete shaft could provide larger stabilization effects for a large and long translational landslide.
- The analysis of a massive landslide stabilized with multiple rows of drilled shafts
- The technical benefits of placing drilled shafts in different arrangements, such as in a staggered fashion or in an arched shape - these placement configurations tend to offer more global stabilization benefits than a straight row of spaced drilled shafts.
- Extend the design to allow for the use of combined drilled shafts and ground anchors
- Extend the design method to account for the seismic loads
- Extend the design method to root piles
- Extend the design method to the slope stabilization schemes involving the use of bio-engineering approach (i.e., plant roots) together with geosynthetics

REFERENCES

1. ABAQUS (2006). ABAQUS Standard User's Manual, Version 6.7-1, Hibbitt, Karlsson & Sorensen, Inc.

2. 1. AL-Bodour, W. (2009). "Development of Design Method for Slope Stabilization Using Drilled Shaft", Dissertation, The University of Akron.

3. Abramson, L., Lee, T., Sharma, S., and Boyce, G. (1996). Slope Stability and Stabilization Methods. John Wiley and Sons, Inc., pp. 381-340.

4. Adachi, T., Kimura, M. and Tada, S. (1989). “Analysis on the preventive mechanism of landslide stabilizing piles.“ 3rd International Symposium on Numerical Models in Geomechanics, pp. 691-698.

5. Bishop, A. W. (1955). “The use of the slip circle in the stability analysis of slopes.“ Geotechnique, Vol. 5, No. 1, pp. 7-17.

6. Bosscher, P. J. and Gray, D. H. (1986). “Soil arching in sandy slopes.” Journal of Geotechnical Engineering, Vol. 112, No. 6, pp. 626-645.

7. Bransby, M.F., and Springman, S. (1999). “Selection of load transfer functions for passive lateral loading of pile groups”, Computers and Geotechnics, Vol.24, pp. 155-184.

8. Briaud, J. L. (1992). The Pressuremeter. published by A. A. Balkema, Rotterdam, Netherlands.

9. Broms, B. B. (1964). “Lateral resistance of piles in cohesive soils." Journal of soil mechanics and Foundation Division, ASCE, Vol. 90, No. 2, pp. 27-63.

10. Bulley, W.A. (1965). “Cylindrical Pile Retaining Wall Construction-Seattle Freeway.” Paper presented at Roads and Streets Conference, Seattle, Washington.

11. Chen, C.-Y., Martin, G. R., (2002). "**Soil**-Structure interaction for landslide stabilizing piles." Computer and Geomechanics. J. Vol**.** 29:pp. 363-386

12. Christopher, M.,Geiger, G., Liang, R., and Yamin, M. (2007). “Design methodology for drilled shafts to stabilize a slope. “ First North American Conference, CD-form.

13. CurvExpert (1995). Manual, version, 1.3.

14. De Beer, E.E. and Wallays, M. (1972). “Forces Induced in Piles by Unsymmetrical Surcharges on the Soil around the Pile”. In Proc. 5th European Conf. On Soil Mechanics and Foundation Engineering, Vol 1, The Spanish Society for Soil Mechanics and Foundation, Madri

15. Duncan, J. M. (1996) “State of the art: limit equilibrium and finite-element analysis of slopes” Journal of Geotechnical Engineering, ASCE, Vol. 122, No. 7, pp577-596.

16. Dawson, E.M., Roth, W.H. and Drescher, A. (1999). “Slope stability analysis by strength reduction.“, Geotechnique, Vol. 49, no. 6, pp. 835-840.

17. Esu, F. and D’Elia, B. (1974). “Interazione terreno-struttura in un palo sollecitato dauna frana tip colata”, Rev. Ital di Geot. III, pp. 27-38.

18. Fellenius, W. (1936). “Calculation of the stability of earth dams. “ Proceedings of the Second Congress on Large Dams, Vol. 4, pp. 445-463.

19. Finn, W. D. (1963). “Boundary value problems of soil mechanics.“ Journal of soil mechanics and foundation division, ASCE, Vol. 89, No. SM5, pp. 39-72.

20. Fukumoto, Y. (1972). “Study on the behaviour of stabilization piles for landslides.” Journal of JSSMFE, Vol. 12, No. 2, pp. 61-73.

21. Fukumoto, Y. (1973). “Failure condition and reaction distribution of stabilization piles for landslides.” Proc., 8th annual meeting of JSSM, pp. 549-562.

22. Fukuoka, M. (1977). “The Effects of Horizontal Loads on Piles due to Landslides”. In Proc. 10th Spec. Session, 9th Int. Conf. Soil Mechs and Fndn. Eng., Tokyo, pp27-42.

23. Griffiths, D. V. and P.A.lane. (1999) "Slope stability analysis by finite elements". Geotechnique, Vol. 49, No. 3, pp. 387-40

24. Gudehus, G. and Schwarz, W. (1985). “Stabilization of creeping slopes by dowels.” Proc. 11th International Conference on Soil Mechanics and Foundation Engineering, San Francisco, Vol. 3, pp. 1679-1700.

25. GSTABLE7 with STEDwin (2003). Slope Stability Analysis System, version 2.004, manual.

26. Hassiotis, S., Chameau, J. L. and Gunaratne, M. (1997). “Design method for stabilization of slopes with piles.” Journal of Geotechnical and Geoenvironmental Engineering, Vol. 123, No. 4, pp. 314-323.

27. Hewlett WJ, Randolph MF. Analysis of piled embankments. Ground Engineering, London, England 1988, Vol. 21, No. 3, pp.12–18.

28. Hügel, H.M., Henke, S., Kinzler, S. (2008). “High-performance Abaqus simulationsin soil mechanics.”, Proceedings, Abaqus User’s Conference, pp. 1-15.

29. Ito, T. and Matsui, T. (1975). “Methods to estimate lateral force acting on stabilizing piles.” Soils and Foundations, Vol. (15), No. (4), pp. 43-59.

30. Ito, T., Matsui, T. and Hong, P. W. (1981). “Design method for stabilizing piles against landslide—one row of piles.” Soils and Foundations, Vol. 21, No. 1, pp. 21-37.

31. Ito, T., Matsui, T. and Hong, P. W. (1982). “Extended design method for multi-row stabilizing piles against landslide.” Soils and Foundations, Vol. 22, No. 1, pp. 1-13.

32. Janbu, N. (1973). “Slope stability computations in embankment-dam engineering.“ R. C. Hirschfeld and S. J. Poulos, Eds. New York: Wiley, pp. 47-86.

33. Jeong , S., Kim, B., Won, J., and Lee, J. (2003). "Uncoupled analysis of stabilizing piles in weathered slopes." Computers and Geotechnics J., Vol. 30, pp. 671-682.

34. Kellogg, CG. (1987). “Discussions—the arch in soil arching. Journal of Geotechnical Engineering.”, ASCE, Vol.113, No. 3, pp.269–71.

35. Liang, R. Y. (2002). Drilled Shaft Foundation for Noise Barrier Walls and Slope Stabilization, Final Report for Ohio Department of Transportation, Report Number FHWA/OH-2002/038.

36. Liang, R. Y. and Yamin, M. (2010) "Three Dimensional Finite Element Study of Arching Behavior in Slope/Drilled Shafts System", International Journal of Numerical and Analytical Methods in Geomechanics, Early Web Publication, DOI:10.1002/nag.851

37. Liang, R., and Zeng, S. (2002). “Numerical study of soil arching mechanism in drilled shafts for slope stabilization.” Soils and Foundations, Japanese Geotechnical Society, 42(2), pp. 83-92.

38. LPILE plus (2004), version 5.0.7, manual, Austin, Texas.

39. Morgenstern, N. R. (1982). “The analysis of wall supports to stabilize slopes.” In application of walls to landslide control problems, Edited by Reeves, R. B., ASCE, pp. 19-29.

40. Nethero, M. F. (1982). “Slide control by drilled pier walls.” In application to landslide control problems, Edited by Reeves, R. B., ASCE, pp. 61-76.

41. Offenberger, J.H. (1981). “Hillside stabilized with concrete cylinder pile retaining wall”. Public Works, Vol. 112, No. 9, pp. 82-86.

42. Poulos, H. G. (1995). “Design of reinforcing piles to increase slope stability.” Canadian Geotechnical Journal, Vol. 32, pp. 808-818.

43. Poulos, H. G. (1999). Design of slope stabilizing piles. Slope Stability Engineering, Yagi, Yamagami and Jiang ©.

44. Qianjun Xu *, Honglei Yin, Xianfeng Cao, Zhongkui Li (2009) "A temperature-driven strength reduction method for slope stability analysis" Mechanics Research Communications, Vol. 36 , pp. 224–231.

45. Reese, L. C., Wang, S. T. and Fouse, J. L. (1992). “Use of drilled shafts in stabilizing a slope.” Proc. Specialty Conference on Stability and Performance of Slopes and Embankments, Berkeley.

46. Reese, L. C., Wang, S. T., Isenhower, W. M., and Arrellaga, J. A. (2004). LPILE Plus 5.0 for Windows, Technical and User Manuals, ENSOFT, Inc., Austin, Texas.

47. Rollins, K. M. and Rollins, R. L. (1992). “Landslide stabilization using drilled shaft walls.” In ground movements and structures, Vol. 4, Edited by Geddes, J. D., Pentech Press, London, pp. 755-770.

48. Sommer, H. (1977). “Creeping slope in stiff clay.” Proc. Special Session No. 10, 9th International Conference on Soil Mechanics and Foundation Engineering, Tokyo, pp. 113-118.

49. Spencer, E. (1967). “A method of analysis of the stability of embankments assuming parallel interslice forces.“ Geotechnique, Vol. 17, No. 1, 11-26.

50. SPSS (2003). SPSS Base 12.0 User's Guide, SPSS Inc., USA.

51. Taniguichi, T. (1967) “Landslides in Reservoirs”. In Proc 3rd Asian Regional Conf. Soil Mech. and Fndns. Eng., Bangkok, Vol 1, pp. 258-261.

52. Terzaghi, K. (1936). “Stress distribution in dry and saturated sand above a yielding trap-door.” Proceeding, 1st International Conference on Soil Mechanics, Harvard University, Cambridge, Mass, Vol. 1, pp. 307-311.

53. Terzaghi, K. (1943). Theoretical Soil Mechanics, John Wiley and Sons, New York.

54. Ugai, K. (1989) " A method of Calculation of total Factor of safety of Slopes by Elasto-Plastic FEM.", Soils and Foundations, Vol. 29, No. 2, pp. 190-195.

55. Viggiani, C. (1981). “Ultimate lateral load on piles used to stabilize landslides.“ Proceedings, 10th International Conference on Soil Mechanics and Foundation Engineering, Stockholm, Vol. 3, pp. 555-560.

56. Wang, W. L., Yen, B. C. (1974). “Soil arching in slopes.” Journal of Geotechnical Division, ASCE, Vol. 105, No. GT4, pp. 493-496.

57. Yamin, M. and Liang, R. Y. (2010) "Limiting Equilibrium Method for Slope/Drilled Shafts System", International Journal of Analytical and Numerical Methods in Geomechanics, Early Web Publication, DOI:10.1002/nag.852.

58. Yamin, M. (2007). "Landslide Stabilization Using a Single Rock-Socketed Drilled Shafts and Analysis of laterally loaded Drilled Shafts Using Shaft Deflection Data. ", Dissertation, The University of Akron.

59. Zeng, S. , Liang, R. (2002). “Stability analysis of drilled shafts reinforced slope.” Soils and Foundations, Japanese Geotechnical Society, Vol. 42, No. 2, pp. 93-102.

60. Zienkiewicz, O. C., Taylor, R. L. (1973) "The Finite Element Method", Vol. 1, 1st edition, McGraw-Hill, New York.

61. Zeng, S. (2002). "Elastodynamic Solution for Multi-layered systems and Analysis Techniques for Drilled Shafts Stabilized Slopes", Dissertation, The University of Akron.